

THE LATE CENOZOIC GEOLOGY OF CAJON PASS;
IMPLICATIONS FOR TECTONICS AND SEDIMENTATION
ALONG THE SAN ANDREAS FAULT

Thesis by
Ray James Weldon II

In Partial Fulfillment of the Requirements
for the Degree of
Doctor of Philosophy

California Institute of Technology
Pasadena, California

1986

(Submitted June 14, 1985)

This thesis is dedicated to LiLi Mezger, without whose love and support this thesis would not have been successfully completed, and to my parents, Patricia McCreedy and Charles Weldon, who instilled in me my love for knowledge and dedication to excellence that led me to undertake this project.

ACKNOWLEDGMENTS

This thesis is the product of collaborative research by a number of people working on the San Andreas fault and the Transverse Ranges. I believe that the product of this collaborative effort is greater than the individual contributions, so it is inappropriate to acknowledge only specific contributions. Close cooperation, both in the lab and the field, with Kris Meisling, Les McFadden, Bob Reynolds, Doug Winston, Gene Humphreys, Joe Kirschvink and Kerry Sieh led to the results presented here. These, and several other people, are coauthors of the five papers that make up this thesis and two other manuscripts in preparation.

Each chapter acknowledges the contributions of specific individuals and the funding agencies that supported this work. In addition, I would like to acknowledge the efforts of my thesis committee. Kerry Sieh acted as principal adviser and participated in my early work in Cajon Pass. Joe Kirschvink supervised and participated in the paleomagnetic work on the Cenozoic sediments in Cajon Pass. Clarence Allen supervised the work Kris Meisling and I carried out in the San Bernardino Mountains. Lee Silver provided an inexhaustible source of knowledge and discussion on the tectonics and bedrock geology of southern California and helped date several key units. Arden Albee acted as my academic adviser.

In addition to these individuals, many students, faculty members and staff members at Caltech contributed to this project. Some of their efforts are individually noted in the appropriate chapters. Of particular note was Jan Mayne's assistance in drafting figures and maps and Dorothy Coy's guidance through the paperwork. Outside the Institute, Bill Bull, Mason Hill and Dick Crook made especially noteworthy contributions to my education as a geologist.

Finally, most of this thesis was written while I was supported as a part-time employee of the US Geological Survey, under the supervision of Tom Hanks. I especially appreciate Tom's and the Survey's patience and support that allowed me to complete this degree.

ABSTRACT

The geology in Cajon Pass, southern California, provides a detailed record of strike slip activity on the San Andreas fault, compressional deformation associated with the uplift of the central Transverse Ranges and an excellent Cenozoic record of syntectonic sedimentation. Age control was established in all of the sediments deposited since the late Early Miocene, using biostratigraphy, magnetostratigraphy, fission-track dating of volcanic ashes, radiocarbon dating, soil development, and the relative stratigraphic and geomorphic position of the units. Tectonic deformation and sedimentation styles varied through time, reflecting the evolution of the San Andreas fault zone within the Pacific - North American plate boundary. Particular attention was paid to determining rates of tectonic deformation and establishing the timing of changes in deformational and depositional styles in the area.

Progressive offset of radiocarbon-dated alluvial and paludal sediments have been used to determine the Holocene slip rate on the San Andreas fault in Cajon Pass. Four independent measurements of the slip rate yield an average of 24.5 ± 3.5 mm/yr. The similarity of the four values, which span different intervals of time up to 14,400 years ago, suggest that the slip rate has been constant during this period.

An excavation across the San Andreas fault provided some constraints on the timing of paleoearthquakes. Coupled with the historic record, this investigation indicates that the last earthquake associated with rupture on the fault in Cajon Pass occurred around 1700 AD. At least 2 earthquakes caused rupture on the San Andreas fault after 1290 AD and perhaps 6 earthquakes are recorded in the thousand year period before European settlement of southern California in the 1770s.

Downcutting and erosion into the western San Bernardino Mountains, during the last 700,000 years, has created Cajon Pass as it exists today. The downcutting was punctuated by at least four pulses of channel aggradation that provide stratigraphic markers throughout the area. They are dated at 0.5 ± 0.1 million, $55,000 \pm 10,000$, 17,000 to 6,000, and 2000 to 300 years ago. These aggradational periods were caused by order of magnitude increases in sediment production associated with changes in the climate from relatively wet to dry conditions.

The locus of the latest Pleistocene to early Holocene fill migrated upstream through time, with aggradation lasting only a few thousand years at any point in the drainage. Incision of the fill also migrated upstream, beginning long before the fill pulse reached the headwaters of the system. The fill terrace, or upper surface of the fill deposit, does not represent a time line or a surface down which water flowed everywhere at once. Thus, the use of a fill terrace as either a time or spacial reference line for tectonic studies, without accounting for the its transgressive character, can result in erroneous conclusions.

During the early to middle Pleistocene, prior to the erosion of Cajon Pass, the southern part of the area was uplifted and coarse fan deposits were shed across the northern part of the area onto the Mojave Desert. Some of these sediments were derived from distinctive sources in the San Gabriel Mountains southwest of the San Andreas fault zone. Matching these distinctive facies in the deposits with their sources established offsets across the fault zone and made it possible to tie the uplift northeast of the fault to activity on the San Jacinto fault as it passed by across the San Andreas fault. The fan deposits are dated by a combination of biostratigraphy and magnetostratigraphy.

The average slip rate across the combined San Andreas and San Jacinto faults is 37.5 ± 2 mm/yr during the Quaternary Period. The six determinations of the slip rate show no evidence for rate changes during the Quaternary Period. The slip rate on the San Andreas fault alone was determined by one offset to be 21 ± 7 mm/yr. The record of contemporaneous activity on the San Jacinto fault to the southeast requires that the San Andreas fault's rate be close to the upper limit of this range.

Contemporaneous activity on the San Andreas and San Jacinto faults is uplifting the high, eastern San Gabriel Mountains and deforming the San Andreas fault plane. The geometry of this deformation is such that uplift of the country on the northeast side of the San Andreas fault occurs. This hypothesis is supported by the northwest migration of the uplift at the slip rate on the San Andreas fault, and the style of surface deformation that is characteristic of folding over a steeply dipping lateral ramp at depth.

A kinematic model was constructed to determine the role of the San Andreas fault in the Pacific - North American plate boundary. The Quaternary slip rates determined for the San Andreas fault in Cajon Pass and the slip vectors associated with the geometry of the fault zone were combined with an assumption of rigid block motion away from the faults and published slip rates for the other major faults in southern California. The model produces internally consistent motions for all of the blocks. Vector sums of the slip rate across the Pacific - North American boundary yield only the relative plate motion if the path includes the western Transverse Ranges. The model solution indicates that the western Transverse Ranges are not part of the San Andreas system but are a left-step in a separate coastal system that currently accommodates about 1/3

of the Pacific - North American plate motion.

The southeastern San Bernardino Mountains are being uplifted because of a left step in the arcuate trace of the San Andreas fault. The western San Bernardino Mountains and the eastern San Gabriel Mountains are being uplifted by the deformation associated with the junction of the San Andreas and San Jacinto faults. Because the convergence in this area can be explained by local geometry, it is clear that southern California cannot be part of the Pacific plate, colliding at the plate rate into North America across the Transverse Ranges. Instead, southern California appears to be a sliver between the San Andreas system and the coastal system, and is rotating counterclockwise as it translates northwest, transferring the convergence to the coastal system.

The middle to late Quaternary uplift of the Cajon Pass area was the culmination of the uplift of the San Bernardino Mountains that began in the Miocene. Three distinct phases of uplift have been recognized, suggesting a long-term interaction between the strike-slip activity on the San Andreas system and the compressional tectonics of the Transverse Ranges. The San Bernardino Mountains began to take shape following a pervasive earliest Miocene unconformity. Broad, homogeneous basins, separated by mature uplands of moderate to low relief developed across the southwest-draining regional paleoslope. The earliest activity on the San Andreas fault is believed to be associated with this early extensional phase.

Late Miocene to early Pliocene, south-directed thrusting uplifted the "proto" San Bernardino Mountains, creating steep, south-facing relief along the San Andreas. During this time the San Gabriel fault was the most (and perhaps only) active trace of the San Andreas system. Thrusting

stopped as the San Andreas fault became active again, probably coincident with the beginning of the opening of the Gulf of California, 5 million years ago. Pliocene and earliest Pleistocene sedimentation took place in narrow east-west trending, structurally controlled basins created by the Mio-Pliocene thrusting.

Early to middle Pleistocene, north-directed thrusting across a shallow, south-dipping ramp uplifted the broad central plateau of the San Bernardino Mountains, and created the North Frontal fault system. During the middle and late Quaternary, this activity was largely replaced by south-directed thrusting and lateral ramping on steep, north-dipping planes along the San Andreas fault. This activity produced the tremendous relief and regionally-extensive north-dipping structural blocks in the San Geronio and Cajon Pass areas, and continues today. The structures and geomorphology of the range reflects its varied history; different parts of the range are as old as late Early Miocene and as young as the Holocene.

All three phases of uplift appear to be related to the southern Big Bend in the San Andreas fault system, which has existed since the Miocene. Contemporaneous and alternating periods of thrusting and strike-slip activity has created bedrock "flaps", displaced fault slivers and strand switching that are responsible for the complex geology associated with San Andreas fault through the Transverse Ranges. Recognition of these features with detailed field work will greatly expand our knowledge of the tectonics and seismic hazards associated with the San Andreas system in southern California.

<u>TABLE OF CONTENTS</u>	<u>Pages</u>
I. <u>CHAPTER ONE - INTRODUCTION</u>	1
Motivation.....	2
Organization.....	2
Previous and Contemporaneous Work.....	6
Present Study.....	6
Related, Unfinished Studies.....	10
Bibliography.....	13
II. <u>CHAPTER TWO - HOLOCENE RATE OF SLIP AND TENTATIVE RECURRENCE INTERVAL FOR LARGE EARTHQUAKES ON THE SAN ANDREAS FAULT, CAJON PASS, SOUTHERN CALIFORNIA</u>	17
ABSTRACT.....	18
INTRODUCTION.....	19
STRATIGRAPHY.....	23
Fluvial History.....	23
Lost Swamp Deposits.....	31
FAULTING.....	43
Faulting near Lost Swamp and Lost Lake.....	45
SLIP RATES.....	52
Case One.....	52
Case Two.....	55
Case Three.....	61
Case Four.....	62
Summary of Slip Values and Possible Problems.....	63
LOST SWAMP EXCAVATION.....	64
Stratigraphy.....	65
Fault Activity.....	71

<u>TABLE OF CONTENTS (Continued)</u>	<u>Pages</u>
DISCUSSION.....	80
Tectonic Implications.....	80
Seismic Implications.....	83
ACKNOWLEDGMENTS.....	89
APPENDIX - Worst Case Evaluation.....	90
REFERENCES.....	95
III. <u>CHAPTER THREE - THE CAUSE AND TIMING OF TERRACE FORMATION</u>	
<u>IN CAJON CREEK, SOUTHERN CALIFORNIA.....</u>	99
ABSTRACT.....	100
INTRODUCTION.....	102
STRATIGRAPHY.....	105
Qoa-e.....	109
Qoa-d.....	110
Qoa-c.....	116
Qoa-a.....	127
Cut Terraces and Tributaries.....	128
Qhf.....	134
PROFILES AND VOLUMES.....	138
Cajon Creek's Profile since the Onset of Qoa-c Deposi-	
tion.....	138
Volume Estimates.....	143
Comparison of Current and Holocene Sediment Supply Rates	149
DISCUSSION.....	152
Impact of Tectonics on the Alluvium.....	152
Climate Control.....	154
Correlation with other Drainages.....	165

<u>TABLE OF CONTENTS (Continued)</u>	<u>Pages</u>
Response to the Climate Change.....	166
Upstream Migration of the Fill.....	174
Long-term Storage and Preservation of the Fill.....	178
Distinguishing Qoa from Qhf Deposits.....	179
CONCLUSIONS.....	180
ACKNOWLEDGMENTS.....	183
BIBLIOGRAPHY.....	184
IV. <u>CHAPTER FOUR - PALEOMAGNETIC CONSTRAINTS ON THE UPLIFT</u>	
<u>AND RATE OF OFFSET OF THE CENTRAL TRANSVERSE RANGES</u>	
<u>ACROSS THE SAN ANDREAS FAULT SYSTEM, SOUTHERN CALIFORNIA</u>	191
ABSTRACT.....	192
INTRODUCTION.....	193
LATE CENOZOIC STRATIGRAPHY.....	197
Late Tertiary Sediments.....	198
Quaternary Stratigraphy.....	201
MAGNETIC STRATIGRAPHY.....	206
Technique.....	206
Quaternary Magnetostratigraphic Correlation.....	212
DISCUSSION.....	216
Slip Rate across the San Andreas System.....	216
Slip Rate North of the San Jacinto Fault.....	219
Slip Rate South of the San Jacinto Fault.....	225
Integration of the Slip Rates with the San Jacinto	
Fault's History.....	226
The Uplift of the Transverse Ranges.....	227

<u>TABLE OF CONTENTS (Continued)</u>	<u>Pages</u>
CONCLUSIONS.....	232
ACKNOWLEDGMENTS.....	233
BIBLIOGRAPHY.....	234
V. <u>CHAPTER FIVE - A KINEMATIC MODEL OF SOUTHERN CALIFORNIA.</u>	241
ABSTRACT.....	242
INTRODUCTION.....	242
PROBLEMS WITH PREVIOUS KINEMATIC MODELS.....	243
PROPOSED MODEL.....	252
UNCERTAINTIES IN THE MODEL.....	262
IMPLICATIONS.....	266
ACKNOWLEDGMENTS.....	272
REFERENCES CITED.....	273
VI. <u>CHAPTER SIX - THE LATE-CENOZOIC TECTONICS OF THE NORTH-</u> <u>WESTERN SAN BERNARDINO MOUNTAINS, SOUTHERN CALIFORNIA...</u>	280
ABSTRACT.....	281
INTRODUCTION.....	282
TECTONIC EVOLUTION.....	287
The pre-Middle Miocene Weathering Surface.....	293
Miocene Basins.....	293
The Crowder Formation.....	294
The Cajon Beds of the Punchbowl Formation.....	297
The Santa Ana Sandstone.....	299
Late Miocene to Early Pliocene Thrusting.....	300
The Squaw Paek Fault.....	300
The Cedar Springs Reverse Fault System.....	303

<u>TABLE OF CONTENTS (Continued)</u>	<u>Pages</u>
The Proposed Squaw Peak Thrust System.....	304
Early Pliocene to Early Pleistocene Basins.....	305
The Phelan Formation (Informal).....	308
The Old Woman Sandstone.....	309
The Santa Ana Sandstone.....	310
Pleistocene Thrusting.....	310
Geometry of the Thrust System.....	311
Constraints on Timing of Thrusting.....	315
The Pleistocene Victorville Fan Complex.....	316
Pleistocene Arching.....	320
The Pleistocene Cleghorn Fault System.....	320
Late Pleistocene Faults.....	322
DISCUSSION.....	325
Implications for thrusting across the San Andreas Fault	334
The Squaw Peak Thrust West of the San Andreas Fault....	337
Quaternary Uplift of the San Bernardino Mountains.....	339
CONCLUSIONS.....	343
REFERENCES CITED.....	346
 <u>VII. CHAPTER SEVEN - CONCLUSION: A SPECULATIVE HISTORY OF THE</u>	
<u>SAN ANDREAS FAULT IN SOUTHERN CALIFORNIA</u>	357
Introduction.....	358
The early San Andreas fault.....	358
Uplift associated with the San Gabriel phase of the San	
Andreas system.....	368
The Pliocene San Andreas fault.....	379
The Quaternary San Andreas fault.....	380

TABLE OF CONTENTS (Continued)Pages

The relationship of the San Andreas system to the Gulf of California.....	390
Implications of the model for seismic hazards.....	392
References Cited.....	394

<u>FIGURES</u>	<u>Pages</u>
1-1. Index Map of the central Transverse Ranges, southern California.....	3
2-1. Index map of southern California showing the major faults..	20
2-2. Geologic map of the study area, emphasizing the Quaternary geology.....	24
2-3. Schematic section through Cajon Creek.....	28
2-4. Airphoto mosaic of the Lost Lake area.....	32
2-5. Plane table map of the Lost Swamp area, showing the offset of the riser between Qt-3 and Qt-2, and the excavation site	37
2-6. The age and thickness of the Lost Swamp sediments.....	41
2-7. Schematic development of the Lost Lake - Lost Swamp area...	46
2-8. Topographic profiles across a flight of terraces.....	48
2-9. Offset of the channel into which Qoa-c was deposited.....	53
2-10. Slip rate on the San Andreas fault at Cajon Creek.....	56
2-11. Offset of the tributaries of Prospect Creek.....	59
2-12. Trench log of the excavation at the southeast end of Lost Swamp.....	66
2-13. Formation of a new, smooth scarp after an earthquake.....	73
2-14. Reconstruction of paleoscarps using the breccia deposits...	77
2-15. Models for the distribution of rupture associated with recent earthquakes to account for the recurrence intervals observed for the southern San Andreas fault.....	86
2-A. "Worst-case" estimates of the slip rate at Cajon Creek.....	91
3-1. Distribution of the late Quaternary sediments in the Cajon Creek area.....	103

<u>FIGURES (Continued)</u>	<u>Pages</u>
3-2. Schematic cross-section through Cajon Creek, showing the elevations and settings of the major alluvial units.....	106
3-3. Photographs of the fill deposits.....	111
3-4. Longitudinal cross sections through Qoa-d at Prospect and Cable Creeks.....	114
3-5. Longitudinal sections through Qoa-d and Qoa-c in Cajon Creek.....	117
3-6. Height of Qoa-c above Cajon Creek.....	120
3-7. The age of Qoa-c in Cajon Creek, plotted as a function of distance upstream.....	123
3-8. The height of Cajon Creek at the San Andreas fault during the last 15,000 years.....	129
3-9. Longitudinal valley profiles up two tributaries of Cajon Creek.....	132
3-10. Relative levels of Cajon Creek, constructed at 1000-year intervals for the last 17,000 years.....	140
3-11. Channel aggradation and degradation in Cajon Creek during the last 17,000 years.....	145
3-12. Comparisons of the record at Cajon Creek with two records of long-term climate change.....	160
3-13. The deposition of Qoa-c in Cajon Creek, represented by successive profiles.....	175
4-1. The geology of the western San Bernardino Mountains.....	195
4-2. Magnetic stratigraphy of the Phelan formation at Phelan Peak.....	199

<u>FIGURES (Continued)</u>	<u>Pages</u>
4-3. Magnetic stratigraphy of the Quaternary sediments in the western San Bernardino Mountains region.....	202
4-4. Typical demagnetization paths (stereonet and Zijderveld diagrams) of stable samples.....	207
4-5. Typical demagnetization paths (stereonet and Zijderveld diagrams) of unstable samples.....	209
4-6. Hopper car analogy of sedimentation in the Cajon Pass area	217
4-7. Quaternary slip rate across the San Andreas system northwest of the junction with the San Jacinto fault.....	220
5-1. The principal faults of southern California and the subdivisions of the Transverse Ranges used in this paper.....	244
5-2. The major blocks in southern California and the data used to calculate their velocities relative to North America...	247
5-3. Integration paths and slip vectors for the major blocks in southern California.....	255
5-4. Schematic representation of the active deformation in the Transverse Ranges.....	269
6-1. Index map of southern California.....	283
6-2. Simplified geologic map of the study area.....	288
6-3. Stratigraphy, age, and correlation chart for the late Cenozoic sedimentary rocks of the western San Bernardino Mountains.....	291
6-4. Interpretive paleotectonic reconstruction of the western San Bernardino Mountains: 17 to 9.5 my ago.....	295

<u>FIGURES (Continued)</u>	<u>Pages</u>
6-5. Interpretive paleotectonic reconstruction of the western San Bernardino Mountains: 9.5 to 4.5 my ago.....	301
6-6. Interpretive paleotectonic reconstruction of the western San Bernardino Mountains: 4.5 to 2.0 my ago.....	306
6-7. Interpretive paleotectonic reconstruction of the western San Bernardino Mountains: 2.0 to 1.5 my ago.....	312
6-8. Interpretive paleotectonic reconstruction of the western San Bernardino Mountains: 1.5 to 0.7 my ago.....	317
6-9. Schematic block diagrams across the central San Bernardino Mountains.....	328
6-10. Microseismicity beneath the central San Bernardino Mountains.....	332
7-1. Accumulation of slip on the San Andreas system in southern California.....	363
7-2. Paleogeography of the "proto" Transverse Ranges and their inferred offset across the San Andreas fault.....	370
7-3. Magnetic stratigraphy of the type Crowder Formation.....	375
7-4. Declination and Inclination of the Crowder Formation.....	377
7-5. Active deformation near the junction of the San Jacinto and the San Andreas faults.....	382
7-4. Major drainages developed into the southwestern escarpment of the San Bernardino Mountains.....	387

TABLES

1-1. Radiocarbon Dates.....	22
-----------------------------	----

PLATESIn Envelope

- Plate 1 - 1:24,000 scale map of the Cajon Quadrangle, Cajon Pass, southern California.
- Plate 2 - 1:24,000 scale map of a portion of the Silverwood Lake Quadrangle, along the Cleghorn fault.
- Plate 3 - 1:12,000 scale map of a portion of the Cajon Quadrangle, along the San Andreas fault, east of Cajon Creek.
- Plate 4 - 1:12,000 scale map of a portion of the Cajon and Devore Quadrangles, along the San Andreas fault, from Cajon Creek to Devore Heights.
- Plate 5 - 1:12,000 scale map of a portion of the Cajon Quadrangle, along the Squaw Peak fault.
- Plate 6 - 1:12,000 scale map of a portion of the Cajon Quadrangle, along the western edge of the San Bernardino Mountains.
- Plate 7 - 1:12,000 scale map of a portion of the Cajon and Devore Quadrangles, along the San Andreas fault, from Devore Heights to Cable Canyon.
- Plate 8 - Trench log of the excavation across the San Andreas fault at Lost Swamp.
- Plate 9 - Map of the late Quaternary stratigraphy of the Cajon Creek area.
- Plate 10 - Active deformation in the Cajon Pass area and its relationship to the trend of the San Andreas fault.
- Plate 11 - Magnetic stratigraphy of the Victorville Fan.
- Plate 12 - Simplified geologic map of the western San Bernardino - northeastern San Gabriel Mountains region.

CHAPTER ONE

INTRODUCTION:

MOTIVATION AND ORGANIZATION OF THE THESIS

Motivation

This thesis was undertaken to characterize the tectonic deformation and late Cenozoic sedimentation in the Cajon Pass - western San Bernardino Mountains region of Southern California (Fig. 1). The Holocene activity of the San Andreas fault was the early focus of my work and a summary of the results from that study is presented in Chapter 2. Detailed mapping (at scales of 1:10 to 1:12,000) of late Pleistocene and Holocene deposits along the fault revealed a number of offsets that were dated to yield the slip rate and recurrence interval of earthquakes on the San Andreas fault. The strip map and detailed site study approach employed in this early work proved to be less successful in studying faults less active than the San Andreas. Also, it was found that much of the deformation associated with the uplift of the mountains did not take place across faults at all, and the evidence commonly could only be found in unconformities and facies changes in the surrounding basins, often kilometers away. Thus, the latter part of this thesis emphasizes developing a detailed regional stratigraphy and a broader view, both spatially and temporally, of the deformation in the area. Some of the results of the latter approach are presented in Chapters 3 - 7. Together, these chapters provide a picture of the evolution of the Cajon Pass area during the late Cenozoic.

Organization

This thesis is written as five separate papers, Chapters 2-6, an introduction (this chapter) and a conclusion (Chapter 7). Each paper appears here with separate abstracts, introductions and bibliographies. With the exception of several of my maps that appear as plates that accompany this thesis, only the work that is of broad enough interest to be formally published is included here.

Figure 1-1 - Index Map of the central Transverse Ranges (modified from Fig. 1, Chapter 6), showing the major physiographic features, towns, faults, and Tertiary basins. The area enclosed in dots (1) has been mapped at scales of 1:12,000 or 1:24,000 and is presented in Plates 1-7. The area enclosed by the dashed line (2) was covered in conjunction with Meisling (1984) or mapped by Weldon (unpublished) and is not included in detail here. Plates 10 and 12, and several figures in Chapter 6 summarize these data. The Squaw Peak fault (SPF), Cajon Valley fault (CVF), Waterman Canyon (WC) fault, and the Wilson Creek fault (WCF) are abbreviated.

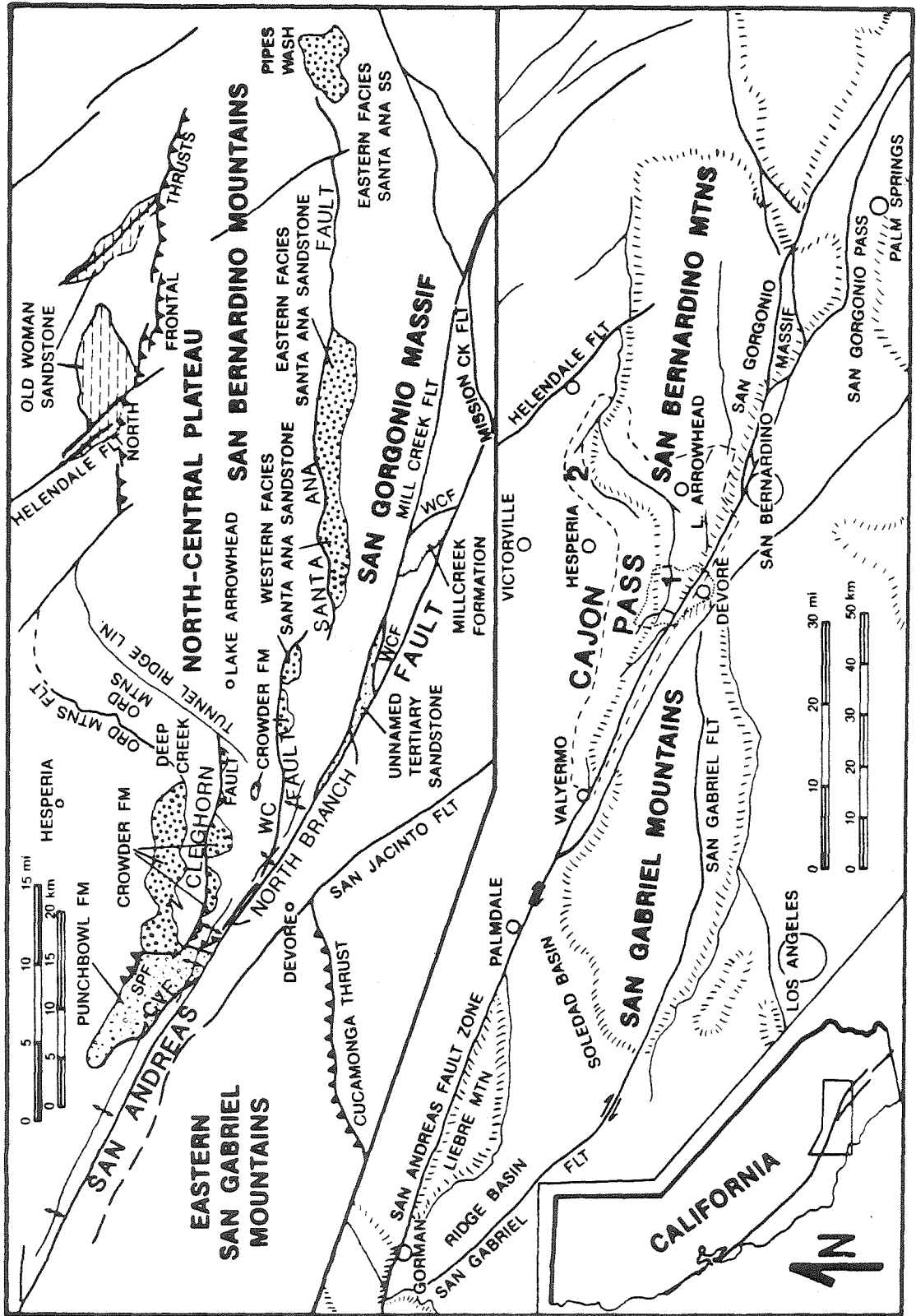


Figure 1-1

Chapter 2 discusses the Holocene slip rate and the recurrence interval of earthquakes on the San Andreas fault. Chapter 2 has been published as a paper in the June 1985 issue of the G.S.A. Bulletin. Chapter 3 addresses the formation of the late Quaternary alluvial deposits in the Cajon Creek area that were used to determine the activity on the San Andreas fault. The relative importance of climate, tectonics and baselevel in forming alluvial deposits in the Transverse Ranges is analysed in that paper. Chapter 3 has been submitted for Survey review and will be submitted to the Journal of Geology upon approval. In Chapter 4 the magnetic stratigraphy in the Plio-Pleistocene sediments north of the Transverse Ranges is used to determine the Quaternary rate of slip across the San Andreas fault and the uplift of the Cajon Pass area during the early and middle Pleistocene. Chapter 4 is in Survey review and will be submitted to the Journal of Geophysical Research. In Chapter 5 a kinematic model of Southern California is presented, based on the geometry and rates of deformation along the San Andreas fault (developed in Chapters 2 and 4) and the other major faults in Southern California. Chapter 5 is currently in review for publication in Tectonics. Chapter 6 presents a synthesis of work by K. Meisling and myself on the uplift of the San Bernardino Mountains and its implications for interaction between the San Andreas fault and the compressional tectonics uplifting the Transverse Ranges. Chapter 6 is in ARCO and Survey review, and will be submitted to the G.S.A. Bulletin for publication.

Chapter 7 is an attempt to weave a few threads through the separate papers. The conclusion also mentions some work not discussed in detail here and presents a speculative view of the relationship between the San Andreas fault, the Pacific-North American plate margin, the Transverse Ranges, and depositional styles in Cajon Pass.

Previous and Contemporaneous Work

Each chapter references the appropriate earlier work in the area, so no comprehensive review of the literature is included here. However, particular note is given to the efforts of several geologists, which form a background for much of my work. Levi Noble did some of the pioneer work in Cajon Pass, setting forth the stratigraphy and recognizing the problems involved in understanding the San Andreas fault and the Transverse Ranges (Noble, 1932; 1954). Tom Dibblee's maps (1965, 1967, 1975a, 1975b) were invaluable, and the maps and detailed late Cenozoic stratigraphy of Mike Woodburne and Dave Golz (1972), and John Foster (1980) were important foundations upon which much of my work in Cajon Pass was built.

Contemporaneous and, to a large degree, collaborative efforts by Kris Meisling along the northern range front of the San Bernardino Mountains (Meisling, 1984; this thesis, Chapter 6), paleontology by Bob Reynolds and colleagues at the San Bernardino County Museum (Reynolds 1983, 1984, 1985), soil studies with Les McFadden (McFadden and Weldon, 1984, in preparation), kinematic studies with Gene Humphreys (Chapter 5), paleomagnetic work with Doug Winston and Joe Krischvink (Weldon et al., 1984; this thesis, Chapter 4; in preparation), work with Kerry Sieh along the San Andreas fault (Chapter 2), and structural and stratigraphic work of John Matti (in review; in preparation) and Peter Sadler (1981; 1982; Sadler and Reeder, 1983) led to many of the insights in this thesis. These, and other workers are involved in a concerted effort to understand the Central Transverse Ranges. Most of these researchers are coauthors on the papers that make up this thesis.

Present Study

The San Andreas fault is currently the most important tectonic element in the southwestern United States, and despite intensive investigation there

are many unanswered questions about its activity, evolution, and relationship to other tectonic elements of the Southwest. The work carried out for this thesis answers some of these questions and raises many new questions that must be addressed. As discussed in Chapter 7, more work must be done to understand the early history of the San Andreas fault and its relationship to other structures, particularly those offshore and in the Transverse Ranges.

The initial goal of this thesis was to determine the recurrence interval and slip rate on the San Andreas fault in Cajon Pass. The average recurrence interval was shown to be similar to that determined from earlier studies at Pallett Creek (Sieh, 1978; 1984), and the slip rate, 24.5 ± 3.5 mm/yr, was found to be less than half of the rate between the North American and Pacific plates (Chapter 2). Later work focused on determining longer term rates (Chapter 4) and understanding the interaction of the San Andreas fault with the other tectonic elements in Southern California.

Using Plio-Pleistocene deposits it was possible to demonstrate that the San Andreas and San Jacinto faults have had a combined slip rate of 37.5 ± 2 mm/yr, and that the San Andreas southeast of their junction has accumulated slip about two and a half times as fast as the San Jacinto fault (Chapter 4), the same relationship that apparently exists today. The uplift of the northeast San Gabriel Mountains and the westernmost San Bernardino Mountains is due to contemporaneous activity on the San Andreas and San Jacinto faults.

The fact that the San Andreas and San Jacinto faults together accommodate only two-thirds of the motion between the Pacific and North American plates led to the kinematic model presented in Chapter 5. The activity associated with the San Andreas fault system is consistently 20 - 25 mm/yr

less than the plate rate throughout south and central California. The difference can be explained by a coastal system that is offshore except in the western Transverse Ranges, which are being uplifted by a left step in that system. The kinematic model provides a better tectonic basis for characterizing the uplift of the different parts of the Transverse Ranges. The conventional view of Southern California's being part of the Pacific plate, colliding at the full plate rate into North America across the central Transverse Ranges is certainly incorrect.

The geology in the San Bernardino Mountains reveals a long history of north-south compressional deformation associated with the San Andreas fault beginning in the late Miocene (Chapter 6). The superposition of at least three stages of compressional deformation has created the mountains that exist today. The record in the San Bernardino Mountains suggests that the San Andreas fault existed during the Miocene and that the geometric complexities that are causing compression and uplift in the area today have existed at least periodically since the beginning of the fault's activity.

In Chapter 7 a model is presented for the evolution of the San Andreas fault (based on the data in Chapters 2, 4, 5, and 6) beginning about 20 Ma, that is consistent with the slip history in central California (Huffman, 1972; Dickinson et al., 1972). The San Andreas fault system has accommodated an increasing fraction of the transform motion between the Pacific and North American plates during this period. Contemporaneous or alternating periods of compression and lateral activity in the San Bernardino Mountains indicate that the San Andreas fault system has always been geometrically complex. The switching of activity between different strands of the system appears to be related to compressional activity and may occasionally be due to physical displacement of the surface expression of the fault from the lower litho-

spheric trace. This mechanism may be responsible for slivering of the fault zone and bedrock offsets that are less than the total offset across the fault.

Unraveling the tectonic history required detailed understanding of the timing and distribution of the late Cenozoic sediments. A stratigraphy was constructed from detailed mapping and by establishing time control in many units throughout the area. The late Quaternary units were dated by C-14, soil development, geomorphic position, and occasionally, offset by faults with known slip rates. The Miocene through middle Quaternary sediments were dated by a combination of relative stratigraphic position, fossils, fission track dates and magnetostratigraphy.

Each period was characterized by deposits that reflect the tectonic style and, probably, the climate at the time. The middle Miocene was represented by broad homogeneous basins filled with braided stream deposits in a generally extensional setting. These were replaced by latest Miocene and Pliocene syntectonic deposits, characterized by rapid facies changes in narrow, tectonically controlled basins. The early to middle Quaternary deposits are generally thick fan conglomerates and rare playa deposits shed off the rapidly uplifting mass of the central Transverse Ranges. Rapid facies changes and variations in clast lithologies reflect lateral and vertical deformation in the mountains that affect the availability of local clast types. Facies changes, clast variations and angular unconformities within these units yield considerable insight into the activity within the range (Chapters 4 and 6).

The late Quaternary sediments consist of fluvial deposits in the maturing uplifted areas and fan deposits peripheral to the range. These sediments reflect both tectonic and climatic change during the late Quaternary

and, due to the climatic control, appear to be correlatable with similar deposits throughout the Transverse Ranges (Chapter 3). Formations in the field area are exclusively lithostratigraphic and the well-dated Quaternary units were found to be extremely time transgressive. Once time lines were established in units, it was found that formations separated by major structural unconformities overlapped in age in different parts of the area. Deformational and depositional events, therefore, migrated through the area producing laterally extensive deposits or structural styles that could be erroneously interpreted as widespread synchronous events. The importance of migrating depocenters and deformation in the well-dated sediments suggests that this is a widespread problem in studying tectonically active regions and this problem likely exists in the older sediments as well.

Related, Unfinished Studies

Several related studies were carried out in the Cajon Pass - western San Bernardino Mountains area that were not completed in time to be included in this thesis. Several of these studies are referenced in the text as papers in preparation. Included in this group is a paper on the Crowder and Phelan formations (Weldon et al., in preparation). This paper formally separates the Miocene Crowder Formation from the Pliocene Phelan formation and discusses the age, distribution and significance of these formations.

Another paper in preparation establishes a soil chronosequence in Cajon Pass based on the ages of directly dated surfaces (McFadden and Weldon, 1984; in preparation). Correlations based on soil development with dated deposits were very important in mapping the Quaternary deposits. This study also revealed that soil development proceeds at different rates through time, separated by process thresholds (McFadden and Weldon, 1984). The understanding of the processes and thresholds in soil development will

help in applying the chronosequence beyond the Cajon Pass area.

Clast types were described in many late Cenozoic deposits along the San Andreas fault, and results of some of this work were used in Chapters 4 and 6. Understanding the distribution of distinctive clast types within deposits along the San Andreas fault aids in deciphering the tectonic history, but the variability, due to facies changes, provenance variation, and clast recycling makes understanding even a single basin very difficult. Variation within a Tertiary basin, like the Punchbowl, Phelan or Crowder formation is generally greater than the average difference between basins, so arguments about correlations usually revolve around properties whose range within the basins being compared is unknown, or the presence or absence of key clast types. While clast studies hold tremendous potential in the area, erroneous assertions have been made, based on misidentified clasts. For example, the incorrect assignment of Pelona Schist debris to the Punchbowl (Yerkes, 1951) and the Crowder (Ramirez, 1982) led to the incorrect conclusion that these deposits were shed north instead of south. It is beyond the scope of this thesis to address the problem of clast distribution in the late Cenozoic deposits along the San Andreas fault, and the clast-type information collected during the course of my mapping has not been systematically organized or included.

Much of the study area is underlain by bedrock, to which little attention was paid during the early part of this work. In retrospect, this was an error; many of the major conclusions of Chapters 4, 6 and 7 evolved from relationships first seen in the bedrock. In particular, reactivation of older structures, especially low-angle thrusts, have a major impact on subsequent deformation. The recognition of the importance of low-angle structures in uplifting the range and deforming the San Andreas fault first

came from relationships seen in the bedrock (Chapter 6). The recognition that the Cajon Pass area was uplifted by broad warping, instead of as offset across faults exposed at the surface, came from mapping the broad bedrock antiform parallel to the San Andreas fault in the western San Bernardino Mountains (Chapter 4, Plate 1). While I did not map the bedrock in sufficient detail to adequately characterize its history, I recommend that future studies, even those focusing on active deformation, pay more attention to bedrock deformation than I did.

Reading the erosional history of Cajon Pass led to many insights in this thesis. Old geomorphic surfaces and the local lack of deposits yielded many clues about the geologic history. The area is rich in evidence about the timing of downcutting and periods of local and regional stability. A useful contribution to the geology of the area would be a paper focusing on the erosional history, integrating the scattered record.

Finally, seven geologic maps are included with this thesis as plates 1-7. The maps are not part of the individual papers because of the difficulty in publishing geologic maps. Many of the figures that appear in the text are derived from these maps and several other maps that are not included in this thesis. The maps include most of the Cajon 7 1/2' Quadrangle and portions of the Devore and Silverwood Lake Quadrangles. Portions of the Phelan Peak 7 1/2' quadrangle to the west of Cajon Pass and parts of the San Bernardino North and Harrison Mountain 7 1/2' quadrangles to the east were also mapped but are not included here. Some of the results are integrated into the larger scale plates and are simplified in figures in Chapters 4, 6, and 7. However, the 7 1/2' scale maps were too incomplete to present formally at this time.

BIBLIOGRAPHY

- Dibblee, T. J. Jr., 1965, Geologic map of the Cajon 7 1/2 minute Quadrangle, San Bernardino County, California, U. S. Geol. Survey Open-file map 65-42, 1:24,000.
- Dibblee, T. J. Jr., 1967, Areal Geology of the western Mojave Desert, California, U. S. Geol. Survey, Prof. Paper 522, 153 p.
- Dibblee, T. J. Jr., 1975a, Late Quaternary uplift of the San Bernardino Mountains on the San Andreas and related faults, in San Andreas fault in southern California, Crowell, J. C., ed., Cal. Div. Mines and Geol. Spec. Rept. 118, p. 127-135.
- Dibblee, T. J. Jr., 1975b, Tectonics of the western Mojave Desert near the San Andreas fault, in San Andreas fault in southern California, Crowell, J. C., ed., Cal. Div. Mines and Geol. Spec. Rept. 118, p. 155-161.
- Dickinson, W. R., Cowan, D. S., and Scheickert, R. A., 1972, Test of New global tectonics: Discussion, Amer. Assoc. Petro. Geol. Bull., v. 56, p. 375-384.
- Foster, J. H., 1980, Late Cenozoic tectonic evolution of Cajon Valley, southern California, Ph. D. Dissertation, University of California, Riverside, 235 p.
- Huffman, O. F., 1972, Lateral displacement of upper Miocene rocks and the Neogene history of offset along the San Andreas fault in central California, Geol. Soc. Amer. Bull., v. 83, p. 2913-2946.
- Matti, J. C., in review, Distinctive megaporphyritic monzogranite offset 160 km by the San Andreas fault, southern California: a new constraint for palinspastic reconstructions, submitted to Geology 1985, 18 p.
- Matti, J. C., Morton, D. M., and Cox, B. F., Geologic framework of the south-central Transverse Ranges, southern California: distribution

and nomenclature of faults in the San Andreas zone and associated fault systems, in preparation.

McFadden, L. D. and Weldon, R. J., Rates and process of soil development in Cajon Pass, southern California, in preparation.

McFadden, L. D. and Weldon, R. J., 1984, The recognition of a new threshold of soil formation in soils at Cajon Creek, southern California, in Abstracts with Programs, 97th Annual Meeting, Geol. Soc. Amer., v. 16, p. 588.

Meisling, K. E., 1984, Neotectonics of the north frontal fault system of the San Bernardino Mountains: Cajon Pass to Lucerne Valley, California, Ph. D. Dissertation, Calif. Inst. of Technology, Pasadena, Cal., 394 p.

Noble, L. F., 1932, The San Andreas rift in the desert region of southeastern California, Carnegie Inst. Washington Yearbook, v. 31, p. 355-363.

Noble, L. F., 1954, The San Andreas fault zone from Soledad Pass to Cajon Pass, California, Cal. Div. Mines and Geol. Bull., v. 170, Ch. 4, p. 32-48.

Ramirez, V. R., 1982, Hungry Valley Formation: Evidence for 220 km of post Miocene offset on the San Andreas fault, in Tectonics and sedimentation along the San Andreas system, eds., Andersen, D. W., and Rymer, M. J., Pac. Sect. S. E. P. M., p. 33-44.

Reynolds, R. E., 1983, Paleontologic salvage, Highway 138 Barrow Cut, Cajon Pass, San Bernardino County, California, San Bernardino County Museum Association, Redlands, for State of California Dept. of Trans. Distr. VIII, San Bernardino, 205 p.

Reynolds, R. E., 1984, Miocene faunas in the lower Crowder Formation, Cajon Pass, southern California: A preliminary discussion, in San Andreas

- Fault - Cajon Pass to Wrightwood, Hester, R. L. and Hallinger, D. E., eds., Pacific Section, AAPG, Volume and Guidebook 55, p. 17-21.
- Reynolds, R. E., 1985, Tertiary small mammals in the Cajon Valley, San Bernardino County, California, in Geologic investigations along Interstate 15 - Cajon Pass to Manix Lake, California, Reynolds, R. E., ed., Field trip guide for the 60th meeting, west. Assoc. Verte. Paleon., p. 49-58.
- Sadler, P. M., 1981, Structure of the northeast San Bernardino Mountains, Report and Open-File Maps submitted to Cal. Div. Mines and Geol. in response to RPF-SMPI.
- Sadler, P. M., 1982, Provenance and structure of late Cenozoic sediments in the northeast San Bernardino Mountains, in Late Cenozoic stratigraphy and structure of San Bernardino Mountains, Guidebook 6, Sadler, P. M. and Kooser, M. A., eds., in Geologic Excursions in the Transverse Ranges, Cooper, J. D., ed., Cal. State Fullerton, California, p. 83-91.
- Sadler, P. M. and Reeder, W. A., 1983, Upper Cenozoic quartzite-bearing gravels of the San Bernardino Mountains, southern California; recycling and mixing as a result of transpressional uplift, in Tectonics and Sedimentation along faults of the San Andreas system, Anderson, D. W. and Rymer, M. J., eds., Pacific Section, SEPM, Los Angeles, CA, p. 45-57.
- Sieh, K. E., 1978, Prehistoric large earthquakes produced by slip on the San Andreas fault at Pallett Creek, California, Jour. Geophys. Res., v. 83, p. 3907- 3939.
- Sieh, K. E., 1984, Lateral offsets and revised dates of large prehistoric earthquakes at Pallett Creek, southern California, Jour. Geophys. Res., v. 89, p. 7641-7670.
- Weldon, R. J., Winston, D. S., Kirschvink, J. L., and Burbank, D. W., 1984, Magnetic stratigraphy of the Crowder Formation, Cajon Pass, southern

California, in Abstracts with Programs, 97th Annual Meeting, Geol. Soc. Amer., v. 16, p. 689.

Weldon, R. J., Reynolds, R. E., Winston, D. S., Meisling, K. E., Kirschvink, J. L., and Burbank, D. W., Age, distribution, and significance of the Crowder and Phelan formations, central Transverse Ranges, southern California, in preparation.

Woodburne, M. O. and Golz, D. J., 1972, Stratigraphy of the Punchbowl Formation, Cajon Valley, southern California, Calif. Univ. Publ. Geol. Sci., v. 92, 57 p.

Yerkes, R. F., 1951, The geology of a portion of the Cajon Pass area, California, MA Thesis, Claremont Graduate School, 97 p.

CHAPTER TWO

HOLOCENE RATE OF SLIP AND TENTATIVE RECURRENCE INTERVAL
FOR LARGE EARTHQUAKES ON THE SAN ANDREAS FAULT,
CAJON PASS, SOUTHERN CALIFORNIA

by

Ray J. Weldon II and Kerry E. Sieh
Division of Geological and Planetary Sciences
California Institute of Technology
Pasadena, California 91125

ABSTRACT

Detailed mapping of the San Andreas fault zone, where it crosses Cajon Creek in southern California, has revealed a number of late Quaternary deposits and geomorphological features offset by the fault. Radiocarbon dating of these alluvial and swamp deposits has provided a detailed chronology with which to characterize the activity of the San Andreas fault.

Four independent determinations of the slip rate on the San Andreas fault yield an average rate of 24.5 ± 3.5 mm/yr for the past 14,400 years. The similarity of the four values, which span different intervals of time from 5900 to 14,400 years ago, suggest that the slip rate has been constant during this period. The sum of the Holocene slip rate on the San Andreas (24.5 mm/yr) and the Quaternary rate on the San Jacinto (10 mm/yr) faults southeast of their junction is the same as the Holocene slip rate on the San Andreas farther northwest (34 mm/yr). While the slip rate confirms that the San Andreas fault is accumulating slip faster than any other fault of the plate boundary, a large fraction of the plate boundary's rate of slip (about 20 of 56 mm/yr) cannot be accounted for on major faults in southern California.

An excavation has provided evidence for at least two and perhaps as many as four earthquakes that caused rupture on the fault between 1290 and 1805 A.D.; it has provided evidence for six earthquakes in about the last 1000 years. Both lines of evidence suggest an average recurrence interval for large earthquakes of about 1-1/2 to 2 centuries. Combined with the historic record, this investigation indicates that the last major earthquake at Cajon Creek was probably near the beginning of the 18th century.

Models consistent with the record at Cajon Creek and data from other localities along the San Andreas fault have been constructed to estimate the timing and rupture length for future earthquakes on the San Andreas fault.

INTRODUCTION

This paper addresses the late Quaternary rate of slip on the San Andreas fault and provides evidence for the recurrence interval of large earthquakes at Cajon Creek (CC, Fig. 1), about 60 miles east of Los Angeles. Progressive offset of radiocarbon dated, late Pleistocene and Holocene deposits and landforms by the San Andreas fault yields a set of slip rates spanning the last 14,400 years. An excavation provides evidence for the timing of recent earthquakes. The study area, which is southeast of the junction of the San Andreas and San Jacinto faults (CC, Fig. 1), provides data for comparing the activities of these two major faults in southern California.

Fourteen radiocarbon (^{14}C) dates (Table 1) were obtained from charcoal, peat and aragonitic gastropod shells collected from alluvial deposits and a swamp developed on several terraces formed by Cajon Creek and its major tributary, Lone Pine Creek. Horizontal offsets were measured on terrace risers, buried channels, small streams incised across the fault, and landslides. Vertical offsets were determined by comparing the levels of geomorphological surfaces across the fault after restoring the lateral motion.

The key to determining the slip rate and the tentative recurrence interval was to integrate the landforms and deposits into a coherent history of interaction between the faulting and the depositional and erosional processes active in the area. The fluctuation of Cajon Creek

Figure 2-1 - Index map of southern California showing the major faults.

The study area, Cajon Creek, is indicated by CC. Other localities mentioned in the text are Wallace Creek (WC), Mill Potrero (MP), Pallett Creek (PC), and Indio (I). Los Angeles (LA), San Bernardino (SB), Santa Barbara (S), Bakersfield (B), and the Salton Sea (SS) are indicated for location reference.

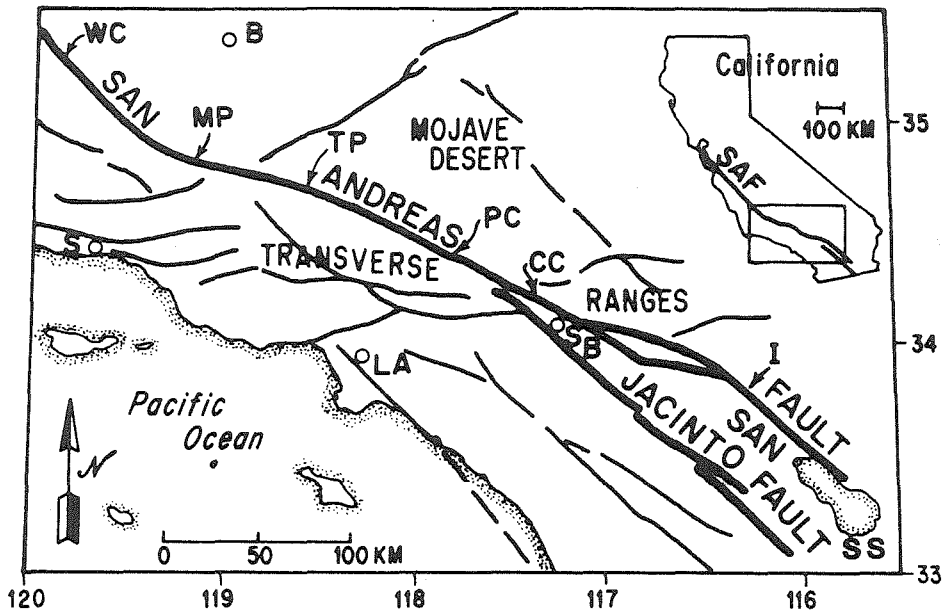


Figure 2-1

TABLE ONE

SAMPLES	¹⁴ C AGE (BP)	¹³ C (0/00)	CORR.-MEAN (BP)	DENDRO AGE (BP)	COMMENTS
CP-1 UM-1812	2,405 ± 110	-23.74	2,425	2510 ± 230	Low grade peat, collected by augering to the base of the peat at the southeast end of Lost Swamp.
CP-2 UM-1813	5,345 ± 85	-10.44	5,582	6345 ± 270	Aragonitic gastropod shells, separated from augered clay at the southeast end of Lost Swamp.
CP-3 UM-698	550 ± 60	-25.9	536	580 ± 80 [1290 - 1450 A.D.]	Small chunks of charcoal from the peat unit, Lost Swamp trench.
CP-4 UM-699	295 ± 29	-29.1	229	185 ± 40 [1725 - 1805 A.D.]	Charred log from the upper colluvium, Lost Swamp trench; dated a sample of the outermost rings.
CP-8 UM-700	5,450 ± 90	-11.1	5,676	6545 ± 200	Aragonitic gastropod shells, separated from the middle of the lake clay, Lost Swamp trench; same unit as CP-9.
CP-9 UM-702	4,480 ± 60	-20.0	4,561	5225 ± 230	Organic residual, separated from the middle of the lake clay, Lost Swamp trench; same unit as CP-9.
CP-10 UM-703	6,490 ± 50	-26.0	6,474	7380 ± 220	Organic residual, separated from lake clay about 50 cm from the base of the clay, augered from the Lost Swamp trench; same unit as CP-11.
CP-11 UM-701	7,100 ± 140	-10.8	7,331	8150 ± 550	Aragonitic gastropod shells, separated from lake clay about 50 cm from the base, augered from the Lost Swamp trench; same unit as CP-10.
D-1 UM-752	1,700 ± 40	-22.6	1,739	1705 ± 180	Small chunks of charcoal from the base of Qoa-a river deposits of Cajon Creek at Pitman Canyon.
D-2 UM-770	14,350 ± 130	-24.3	14,360	14,780 ± 1000	Small chunks of charcoal from the base of Qoa-c river deposits of Cajon Creek below Blue Gut.
CC-1 UM-753	1,050 ± 45	-23.6	1,073	990 ± 90	Small chunks of charcoal from the middle of Qoa-a river deposits of Cajon Creek about 100 meters south of the San Andreas fault.
CC-2 UM-767	50 ± 50	---	---	----	Small chunks of charcoal and wood collected 1/2 meter from the top of Qbf deposited on Qt-5 by Pink River where it enters Cajon Creek.
CC-3 UM-768	12,760 ± 80	-23.3	12,787	13,160 ± 1000	Large chunk of charcoal from the colluvium interfingering with the middle of Qoa-c deposits of Cleghorn Canyon where it enters Cajon Creek.
CC-4 UM-769	13,400 ± 300	-23.0	13,432	13,825 ± 1000	Small chunks of charcoal from the Qoa-c river gravels of Cleghorn Canyon where it joins Cajon Creek.

UM refers to University of Miami sample numbers and UM refers to University of Washington numbers. This includes all dates from this area; the gaps in sequences are samples collected but not considered important enough to date.

1 Reported ¹⁴C ages use Libby's half-life (5568 years), assume $\delta^{13}C = -25\text{‰}$ and have 1 sigma counting errors.

2 All ages are at 95% confidence level. For the last 2000 years we used Stuiver (1982) and Klein et al (1982). Where the corrections are not exactly the same we expanded our limits to include both reported values. Between 2000 and 7240 ¹⁴C years ago we used Klein et al (1982). For older samples, we recalculated the ¹⁴C age using a half-life of 5730 and assign error limits of ± 1000, as recommended by Klein et al (1982), to assure 95% confidence.

3 The corrected mean reported in Radiocarbon (Johnston and Stipp, 1980) is not correct.

4

Dendro corrections yield the multiple calendric ages of 1525 - 1570, 1605 - 1685 and 1725 - 1805 A.D. Other dates and inferences from the trench strongly support the 1725 - 1805 A.D. possibility (see text).

5

No $\delta^{13}C$ analysis was run for this sample. Since it is the same material as CP-2 and CP-8, we used the average of their $\delta^{13}C$ values.

6

This sample is 91 years beyond the corrections of Klein et al (1982). Since the corrections vary in a systematic manner we extrapolated to correct this date. We felt it was necessary to approximately correct for the 800 year real age versus ¹⁴C age difference that all samples in this age range exhibit.

7

This obviously does not date the deposit (~ 5900 years old) and has probably been introduced by man's activity.

between periods of deposition and erosion resulted in the major deposits and landforms which preserve both the offsets across the fault and the radiocarbon samples that date them. Even where local activity on the fault is directly responsible for the formation of deposits or landforms it has been possible to relate them to the more general history of Cajon Creek. As with any geologic history, extrapolations and scenarios must be constructed from the data to interpret the observations. These inferences are critical to determining the slip rate and dating paleoearthquakes, so considerable detail has been included.

STRATIGRAPHY

Fluvial History

Cajon Creek is a south-flowing stream that drains about 200 square km between the San Gabriel and the San Bernardino Mountains (Fig. 2). Paleontologic (C. Repenning, written communication, 1982) and paleomagnetic (Meisling and Weldon, unpublished) data indicate that during the middle Pleistocene the Cajon Creek area was part of a north-flowing alluvial fan system. Capture from the south appears to have begun about 500,000 years ago (Weldon et al., 1981). This capture occurred as the San Andreas fault laterally juxtaposed the low San Bernardino basin against the higher and more easily eroded late Cenozoic sediments north of the fault (Weldon and Meisling, 1982). Rapid and extensive downcutting of Cajon Creek and its tributaries has eliminated most of the record of the evolution of the drainage since the onset of capture and the latest Pleistocene.

The oldest extensive deposit preserved within the present south-flowing drainage system is an alluvial unit called Qoa-d (Fig. 2). It

Figure 2-2 - Geologic map of the study area emphasizing the Quaternary geology. The location of more detailed maps are indicated by boxes.

EXPLANATION FOR FIGURE 2



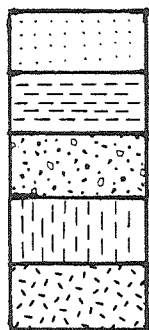
-- Fault, solid where certain, dashed where inferred, dotted where buried, and a thrust where barbed.



-- Depositional contact, dashed where inferred.



-- Fold hinge, arrows indicate sense of dip.



-- Holocene alluvium: includes Qal, Qal-0, Qoa-a, and, locally, Qhf (see text and more detailed figures)

-- Qoa-c: latest Pleistocene alluvium, 14.8 to 12.4 ka.

-- Major landslides and, locally, colluvium.

-- Qoa-d: late Pleistocene alluvium, about 55 ka.

-- Qoa-e: middle Pleistocene alluvium, about 500 ka.

Qm

-- Man-made fill.

Tp

-- Punchbowl Formation (Cajon facies).

grd

-- granodiorite, underlies the Punchbowl Formation.

gn-c

-- gneiss, granodiorite to tonalite, and Crowder Formation, these rocks underlie the San Bernardino Mountains.

gn-s

-- gneiss, overlain by latest Cretaceous San Francisquito Formation (?); relation to gn-c not clear.

Tu

-- unnamed Tertiary (?) conglomerates and sandstone, overlain and faulted against quartz monzonite; only outcrops between the North Branch and the San Andreas Faults.

psg

-- Pelona Schist: "green facies", mainly albite - epidote - chlorite schist; only outcrops between the Punchbowl and San Andreas Faults.

psb

-- Pelona Schist: "blue facies", mainly micaceous quartzofeldspathic schist: underlies much of the San Gabriel Mountains southwest of the Punchbowl Fault.

is up to 85 m thick, predates many of the minor tributaries of Cajon Creek and grades into thick colluvial slopes on the hillsides. The inferred age of this unit is about 55 ka, based on its lateral offset of 1.3 to 1.4 km by the San Andreas fault (see the distribution of Qoa-d near Prospect Creek, Fig. 2) and on the assumption that the slip rate of 24.5 mm/yr (determined below) can be extrapolated into the past. Removal of the lateral offset of Qoa-d approximately restores the geomorphic surface associated with Qoa-d, indicating that less than 20 meters of vertical slip have accompanied 1.3 km of horizontal slip.

Incision that postdates the deposition of Qoa-d established the modern channels of Cajon Creek and its major tributaries, which have since been offset about 1-1/4 km. This "inner gorge" is recognized in most of the major drainages in the area and appears to represent a regional climatic event (Weldon, 1983). Several strath terraces produced during this incision are only locally preserved within the inner gorge and add little to the fluvial or tectonic history. The incision probably had ended by 25 ka, and certainly was complete by 14.8 ka, when the deposition of Qoa-c (the next youngest deposit) began. The 25 ka estimate is based on the observation that the large landslide near Pitman Canyon (Fig. 2) buries a topography more deeply incised than the modern topography. The landslide's offset of about 615 m and the slip rate of 24.5 mm/yr are used to estimate its age.

The oldest alluvial deposit in the inner gorge is Qoa-c (Fig. 3). Six radiocarbon samples have been dated from this unit, throughout the Cajon Creek drainage, and three are from the study area. The oldest (D-2) is 14.8 ka and is from near the base of the deposit, about 1.5 km downstream from the San Andreas fault crossing. Two others, 13.8 and

Figure 2-3 - Schematic section through Cajon Creek. The section is parallel to the San Andreas fault south of the fault with Qt-2, Qt-3, Qt-4 and Lost Swamp added from Lone Pine Canyon. Radiocarbon dates, from up and down the creek and from Lost Swamp, are in approximate stratigraphic position (boxes). The abandonment ages of Qt-1, Qt-3, Qt-5 and Qt-6 (dates without boxes are extrapolations) are based on relating the stratigraphy to geomorphic events (see text). Notice that Qoa-c and Qoa-a extend below the current level of Cajon Creek and indicate earlier periods of deeper incision.

SCHEMATIC SECTION THROUGH CAJON CREEK

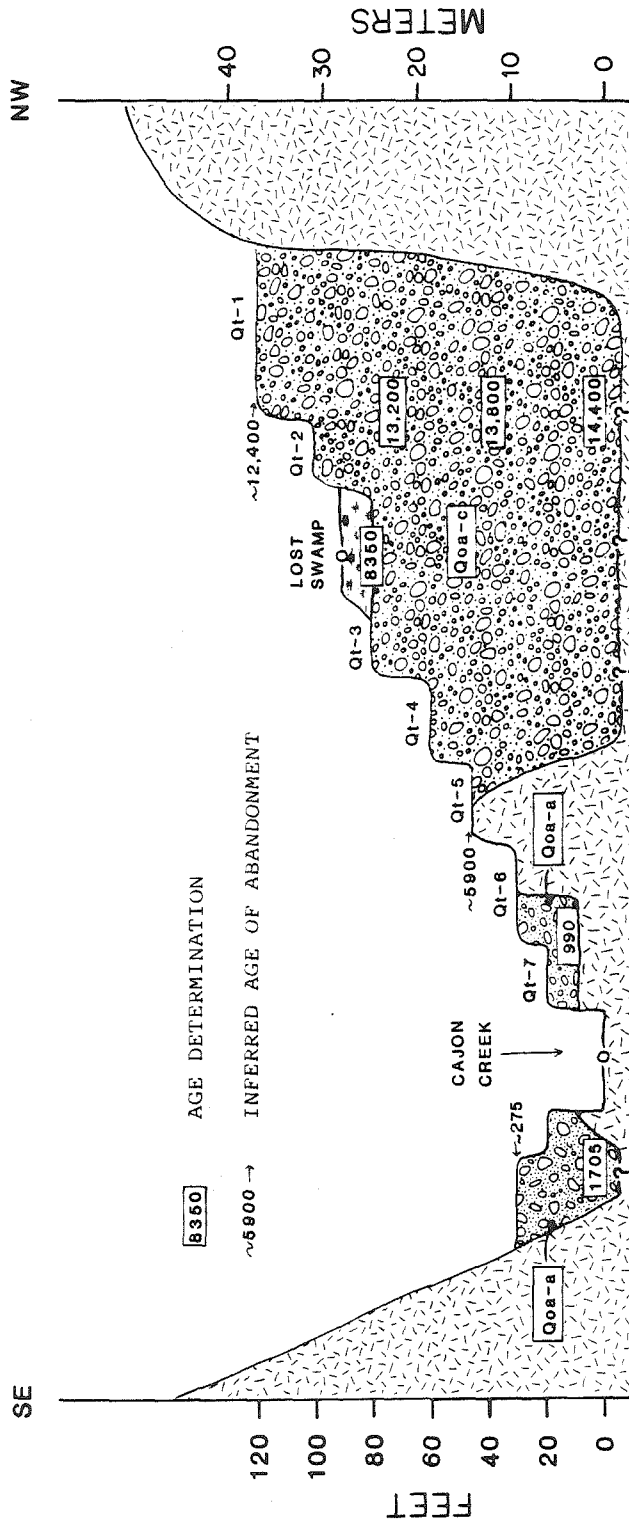


Figure 2-3

13.2 ka (samples CC-3 and CC-4), are from the mouth of Cleghorn Canyon, about 1.5 km upstream of the fault crossing (Fig. 2). Extrapolating the sedimentation rate between the 2 samples at Cleghorn Canyon to the top and bottom of the deposit indicates that the unit was formed between 14 and 12.4 ka. The apparent decrease in age of the deposit's base upstream is confirmed by three other samples outside the area discussed here (Weldon, unpublished). At the fault the creek is inferred to have started aggrading about 14.4 ka and to have finished depositing Qoa-c by about 12.4 ka.

At the junction of Cajon Creek and Lone Pine Canyon seven fluvial terraces, designated from the highest and oldest, Qt-1, to the lowest and youngest, Qt-7, have been recognized (Fig. 3,4). Qt-1 is a fill terrace and represents the depositional surface of unit Qoa-c. Qt-2 through Qt-5 are terraces cut into Qoa-c or into bedrock. Qt-3 is the best developed of these cut terraces and is the only one that can be mapped a significant distance up and down Cajon Creek. The peats and clays of Lost Swamp (discussed below) rest on Qt-3 and constrain the abandonment of this important terrace to about 8350 B.P.

Qt-5 is the youngest and lowest terrace preserved above the surface of the latest fill, Qoa-a. After the abandonment of Qt-5, at about 5900 B.P. (the details of this date are discussed below), Cajon Creek and its tributaries incised below their current level. By about 1705 B.P. (sample D-1) Cajon Creek was again at its modern level and was beginning to deposit Qoa-a (Fig. 3), and by about 990 B.P. (sample CC-1) 6 meters of fluvial sediments had accumulated. Extrapolating the rate of fill between the two dates would indicate that the Qoa-a fill culminated at about 275 B.P., forming the fill terrace Qt-6. Twelve

meters of incision have subsequently occurred, punctuated by the cutting of at least one mappable strath terrace (Qt-7).

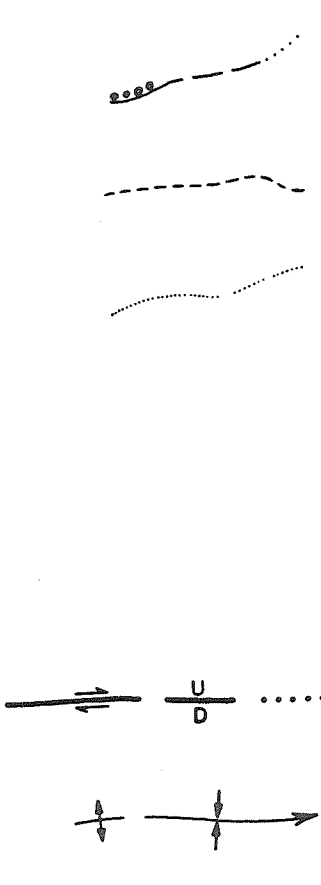
The preserved history of the river contains substantial gaps. The incision that postdated Qoa-d could have eroded minor deposits that may have been formed between 55 and 15 ka. Qoa-c buries the geomorphic history of the last 40 meters of the post Qoa-d incision, just as Qoa-a buries the last 12 m of the post Qoa-c incision (a time span of at least 4,000 years). Detailed study of the Quaternary history of Cajon Creek and its tributaries up and downstream of the area discussed here suggests that the fluvial units at the fault crossing are typical of the overall creek (Weldon, unpublished). It is therefore unlikely that there are any deposits or surfaces in the gaps that can affect the interpretation of the activity of faulting.

Lost Swamp Deposits

Southeast of Lost Lake and northeast of the main trace of the San Andreas fault is a small swamp here named Lost Swamp (Fig. 4, 5). The swamp deposits overlap Qt-2 and Qt-3 and owe their existence to a combination of lateral and vertical faulting. Auger holes and an excavation revealed, from top to bottom, colluvium (near the shore), peat, lake clay and colluvium resting on Qoa-c alluvium; the ages and thicknesses of these units at the excavation are shown on Fig. 6. Samples CP-10 and CP-11 are organics and aragonitic gastropod shells, respectively, from near the base of the lake clays. Roots, worms and other biologic activity make the organic date a minimum age and the presence of Paleozoic(?) marbles and carbonate-rich facies of the Pelona Schist in the drainage requires that the shell date represent a maximum age. Therefore, the outer limits of CP-10 and CP-11 bracket the actual age of the clay and

Figure 2-4 - Airphoto mosaic of the Lost Lake area. Stratigraphic and geomorphic units are annotated in white. The northwest trending terrace risers between the terraces cast shadows on the northeast side of the river and are brightly illuminated on the southwest side. The offsets of Pink River, Qt-3 (near Lost Swamp) and Qt-5 (at Cajon Creek) are well illustrated, as is the contrast between the fault and the sinuous river terraces. The younger terraces are less well defined, both in width and level, and are more numerous near the junction of Lone Pine and Cajon Creeks.

EXPLANATION FOR FIGURE 4

- 
- Depositional contact; solid where certain, dashed where inferred or uncertain and dotted where buried; contains circles for a distinct basal conglomerate.
 - Limit of present drainage.
 - Geomorphic contact, dashed where inferred or uncertain; designates the edge of a surface where it is not a geologic contact; where two surfaces meet it is the edge of the upper one (top of riser). Note that a geomorphic contact can cross a geologic contact where a geomorphic surface is developed across more than one geologic unit.
 - Fault, solid where certain, dashed where inferred and dotted where buried.
 - Fold hinge, with direction of plunge; arrows indicate syncline or anticline.

QUATERNARY UNITS

- | | | |
|-----------|-----|---|
| 1982 A.D. | Qal | -- Current alluvium. |
| | Qhs | -- Active swamp; underlain by sediments that span most of the Holocene. |
| | Qhf | -- Fanglomerates; locally includes material deposited continuously since the Pleistocene. |
| | Qc | -- Colluvium (where distinguished), commonly transitional into Qhf or Qoa. |
| | Qm | -- Man-made fill (where distinguished). |

QUATERNARY UNITS (Continued)

1938 A.D.	Qal-0	-- Alluvium deposited by the 1938 flood (where distinguished).
200 B.P.	Qt7	-- Youngest strath mapped.
275 - 1705 B.P.	Qoa-a (Qt6)	-- Holocene alluvium; Qt6 is the surface formed by the top of the Qoa-a deposit.
5900 B.P.	Qt5	-- Youngest strath recognized above the Qoa-a fill.
	Qt4	-- Strath terrace, probably underlies Lost Lake.
8350 B.P.	Qt3	-- Only Holocene strath widely recognized outside the Lost Lake area; Qt3 underlies most of Lost Swamp.
	Qt2	-- Oldest strath between Qoa-a and Qoa-c.
12.4 to 14.8 ka	Qoa-c (Qt1)	-- Latest Pleistocene alluvium; Qt1 is the surface of the deposit.
	Q1s	-- Landslide.
53 - 57 ka	Qoa-d	-- Mid-Wisconsin alluvium.
500 ka	Qoa-e	-- Old red alluvium; deeply weathered with, locally, several meters of brick red soil.

PRE-QUATERNARY UNITS

Mid to late Miocene	Tp	-- Punchbowl Formation (Cajon beds) - buff to pink, continental arkosic sandstone and conglomerate.
Late Cretaceous to Eocene (?)	Ksf	-- San Francisquito Formation. Marine sand and siltstone overlying gn. Has a coarse basal conglomerate of mainly local clasts (indicated by small circles).
> Mid Tertiary	Psb	-- Blue facies, Pelona schist; low grade metasedimentary marine (?) rocks; only occurs southwest of the Punchbowl fault.

- > Mid Tertiary Psg -- Green facies, Pelona schist; low grade, albite-epidote-chlorite metavolcanics and calcareous metasediments only occurs northeast of the Punchbowl fault
- > Late Cretaceous gn -- Undifferentiated gneiss. Heterogeneous, generally tonalitic, foliated and locally banded rocks. Consists of at least two distinct terranes (not distinguished here).

Figure 2-5 - Plane table map of the Lost Swamp area, showing the offset of the riser between Qt-3 and Qt-2 and the excavation site. The Qhf deposits were laid down by streams from the north that were isolated by the incision of Pink River below Qt-5. While Qhf was being deposited the depression overflowed down the gully buried by the powerline tower fill (Qm); this gully is graded to the Qt-5 level in Pink River. Hill 2769 is too high to be a portion of Qt-2 and is an eroded remnant of Qt-1, around which the Lost Swamp depression drained until the abandonment of Qt-5. Lost Lake drains either into Lost Swamp or down Qt-3 depending on the relative heights of the beaver dams at the two sites.

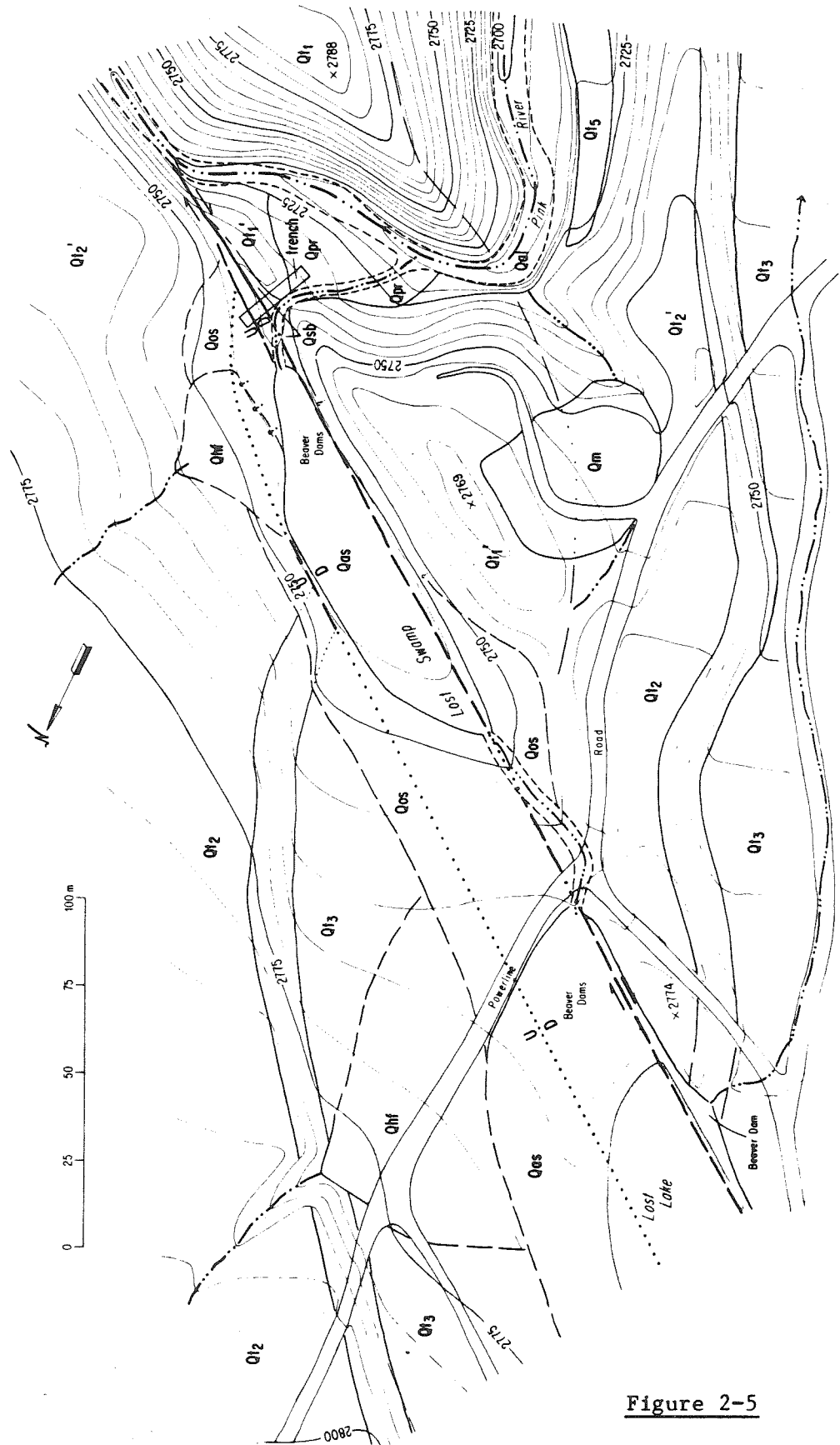


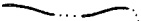



Figure 2-5

EXPLANATION FOR FIGURE 5

	Contact, geologic and geomorphic, solid where certain, dashed where inferred and dotted where buried.
	Current alluvial contact.
	Minor stream; active or abandoned channel.
	Fault, with arrows and symbols indicating sense of motion; solid where certain, dashed where inferred and dotted where buried.

Units

Qal	--	Present-day alluvium
Qas	--	Modern swamp deposits; peat or lake clay depending on the depth of water.
Qm	--	Man made fill (here, a powerline tower pad)
Qos	--	Old swamp deposits (where distinguished); peat or lake clay deposited in Lost Swamp before Pink River captured the area.
Qhf	--	Holocene fanglomerate; dominantly pink sand deposited from the north before Pink River captured the drainage and cut off flow across the terraces.
Qt5	--	Terrace of Pink River, cut into Qoa-c gravels deposited by Lone Pine Creek.
Qt4-2	--	Terraces cut by Lone Pine Creek into Qoa-c gravel.
Qt1	--	Fill terrace surface on Qoa-c gravel.
Qt'2-1	--	Eroded remnant of a higher terrace; no longer associated with a geomorphic surface but high enough that it's clearly not a younger terrace.

the average of the mean ages, 7770 B.P., is the best estimate (Fig. 6).

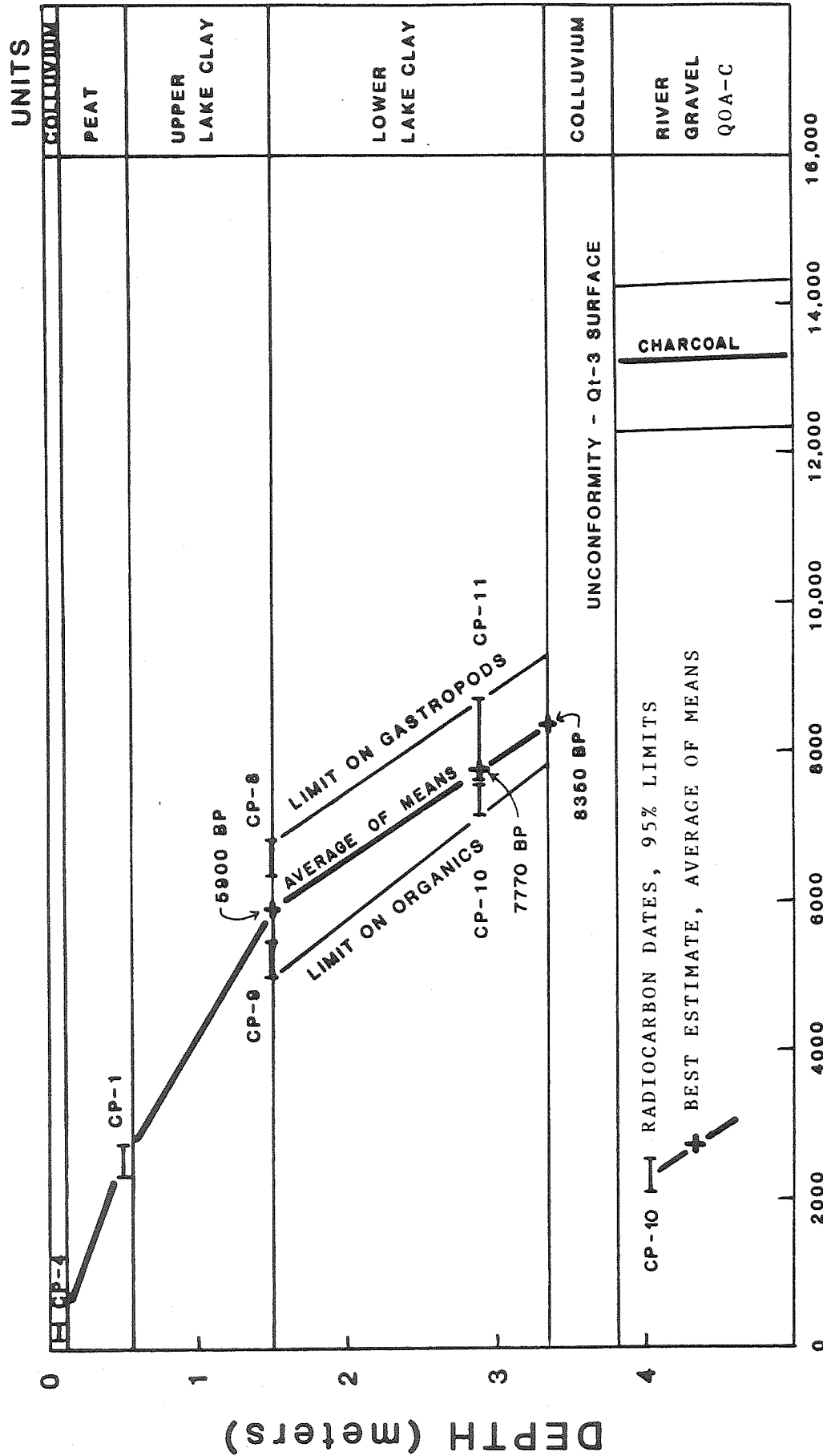
Samples CP-8 and CP-9 are gastropods and organic matter, respectively, collected at the boundary between progressively finer and more organic-rich clay above and clay with a fine gravel and pink sand component below. As with CP-10 and CP-11, CP-8 and CP-9 bracket the age of the boundary which is estimated to be about 5900 B.P. (see Fig. 6). CP-2, another sample of gastropod shells from this level collected from auger holes northwest of the excavation, is the same age as CP-8 (Table 1). In Figure 6, the best estimates of the ages of the two dated levels in the lake clays (average of the mean ages) and the outer limits of the gastropods and organics, are extrapolated to the base of the clays, yielding a best estimate of 8350 B.P., with limits of +950 and -500 years, for the onset of paludal sedimentation.

Sample CP-1 yielded an age of 2510 ± 230 B.P. for the base of the peat which overlies the lake clays with a gradational contact. It is clear from Fig. 6 that the upper meter of the clay was deposited at a rate similar to the overlying peat and much more slowly than the lower 1.8 meters of clay. This indicates that the peat, and ultimately the colluvium, are a continuation of the deterioration of the lake into a swamp that began about 5900 B.P.

The event that caused the change in the character of sedimentation in Lost Swamp was the integration of a number of small streams that drained the hills to the north into Pink River (Fig. 7). This capture event culminated when Qt-5 was abandoned, dramatically lowering the local base level (Fig. 7e). This isolated Lost Swamp from surface drainage to the north and overflow from the Lost Swamp depression ceased. The abandoned outlet has been partially buried by a powerline tower pad but can

Figure 2-6 - The age and thickness of the Lost Swamp sediments. Radio-carbon dates are plotted according to depth to determine the age of important stratigraphic boundaries. Gastropods and the organic residue from the lake clay were dated to assure bracketing the actual age of the sediments (see text). The average of the mean ages are used to determine the best estimate of the top and bottom of the lower lake clay and the 95% confidence levels of the shells and organics yield the limits. The sedimentation rate for the upper lake clay is about the same as the peat and is much slower than that of the lower clay. The lower clay includes sediments derived from the hills to the north by streams that were cut off about 5900 B.P. The upper lake clay only has debris from around the depression.

AGE OF LOST SWAMP



YEARS (BP)

Figure 2-6

still be seen grading to the Qt-5 level (Fig. 5). When the streams carrying pink sand and gravel from the hills to the north were captured by Pink River, Lost Swamp lost its major source of sediment and water. Since that time, the sedimentation rate has been fairly constant, reflecting input from the surrounding slopes of the depression.

In summary, the sediments under Lost Swamp record the formation of a lake beginning at about 8350 B.P. At about 5900 B.P. surface flow into the lake ceased, causing the lake to begin deteriorating into a swamp.

FAULTING

To determine the slip rate on the San Andreas fault it is necessary to establish the width of the zone of displacement and the number of fault strands that are involved. There are two faults other than the San Andreas with major geologic displacement in the study area. South of the San Andreas is a major zone, called the Punchbowl fault by Dibblee (1975a), that locally juxtaposes two distinct facies of the Pelona Schist (Fig. 2) and is inferred to have about 48 km of right-lateral offset (Dibblee, 1975a). It joins or is truncated by the San Andreas near Pitman Canyon (Fig. 2). The Punchbowl fault does not appear to offset any Quaternary units in this area and its sinuous trace suggests that more recent activity has deformed it.

East of Cajon Creek, a major fault runs parallel to and about 250 m north of the San Andreas fault. This fault has been mapped for about 10 km to the southeast, where it joins or is truncated by the San Andreas fault (Weldon, unpublished; Morton and Miller, 1975). As the rock types found between these two faults are similar to those found between the North and South Branches of the San Andreas fault to the southeast

(Dibblee, 1975b), this fault is here proposed to be the northwest continuation of the North Branch of the San Andreas fault. The North Branch dips steeply northeast and currently exhibits dominantly normal dip slip motion, as do many faults in the western San Bernardino Mountains that trend southeast or east (Weldon, unpublished mapping). The North Branch offsets several units that are also offset by the San Andreas fault, so a comparison of their activities can be made. The height of northeast facing scarps across Qoa-d and the surface of the large landslide to the southeast (Fig. 2) suggest a vertical slip rate of less than 1/2% of the lateral slip rate on the San Andreas fault. Locally, evidence for a small component of right-lateral motion is found on the North Branch but it is less than the normal component and cannot be a significant fraction of the lateral slip rate on the San Andreas proper.

A complicated zone of faulting wraps around the southwest edge of the San Bernardino mountains north of the North Branch (Fig. 2). Most of these faults are inactive and those that are active produce only minor displacements of Qoa-d. Like the North Branch the active faults are dominantly normal and cannot be accommodating a significant fraction of the total slip of the San Andreas system. A fault mapped south of the San Andreas is also dip slip and offsets Qoa-d about 10 m (Fig. 2). The San Andreas fault is the only fault that has accumulated significant lateral offset since the deposition of Qoa-d. So, the rates determined in this study are inferred to be representative of the fault southeast of its junction with the San Jacinto fault.

The similarity of the offsets of features that are mapped right up to the fault zone with those that are extrapolated from up to several hundred meters away argues against significant distributed shear extend-

ing beyond a few meters of the mapped faults. The trench excavated into Lost Swamp and several other exposures of the San Andreas reveal undisturbed Qoa-c gravels within a meter of the edge of the fault zone (e.g. Fig. 12). These observations suggest that the fault is accumulating slip across a very narrow zone and that distributed shear is not a significant problem, so the slip rate can be determined from the offset of very minor features.

Faulting Near Lost Swamp and Lost Lake

The depression occupied by Lost Lake and Lost Swamp contains critical data for several of the slip rate values and for the tentative recurrence interval for earthquakes on the San Andreas fault, so a detailed description of its setting is included. A key point in understanding the history of the depression and matching the terraces across the fault zone is the angle at which the river intersects the fault. If the trends of the terrace risers indicate the flow direction of the creek that they bounded, Lone Pine Creek formed Qt-2, Qt-3 and Qt-4 while flowing about S25E, intersecting the fault near Lost Lake at a 30° angle (Fig. 4 and 5). Because the terraces dip downstream, 3° to 3-1/2° SSE, the surface expression of the fault descends at 2-1/2° to 3° to the southeast as it crosses a terrace tread and only rises at the terrace risers. This "sawtoothed" traverse is schematically represented by profile a-c on Fig. 8. The width of the terrace treads relative to the height of the risers causes this "saw-toothed" traverse to have very little net elevation change along the fault zone between the northwest end of Lost Lake and the southeast end of Lost Swamp, on the southwest side of the fault. This creates the false impression that a series of asymmetric troughs and ridges, not terrace treads and risers, are

Figure 2-7 - Schematic development of the Lost Lake - Lost Swamp area.

The area shown is the central 2/3 of Fig. 4. The reconstruction demonstrates the progressive offset and erosion of the terraces and the development of the Lost Lake depression. Before the drainage from the north was consolidated into Pink River considerable erosion obscured the older terraces' locations. Since the consolidation the terraces have remained unchanged.

Figure 2-8 - Topographic profiles across a flight of terraces. While the figure is schematic, the angle between the terrace risers and profile a-c is the same as the angle between the San Andreas fault and the terraces near Lost Lake. The "step" topography of a flight of terraces becomes "saw-toothed" if the profile is not perpendicular to the flow direction of the stream.

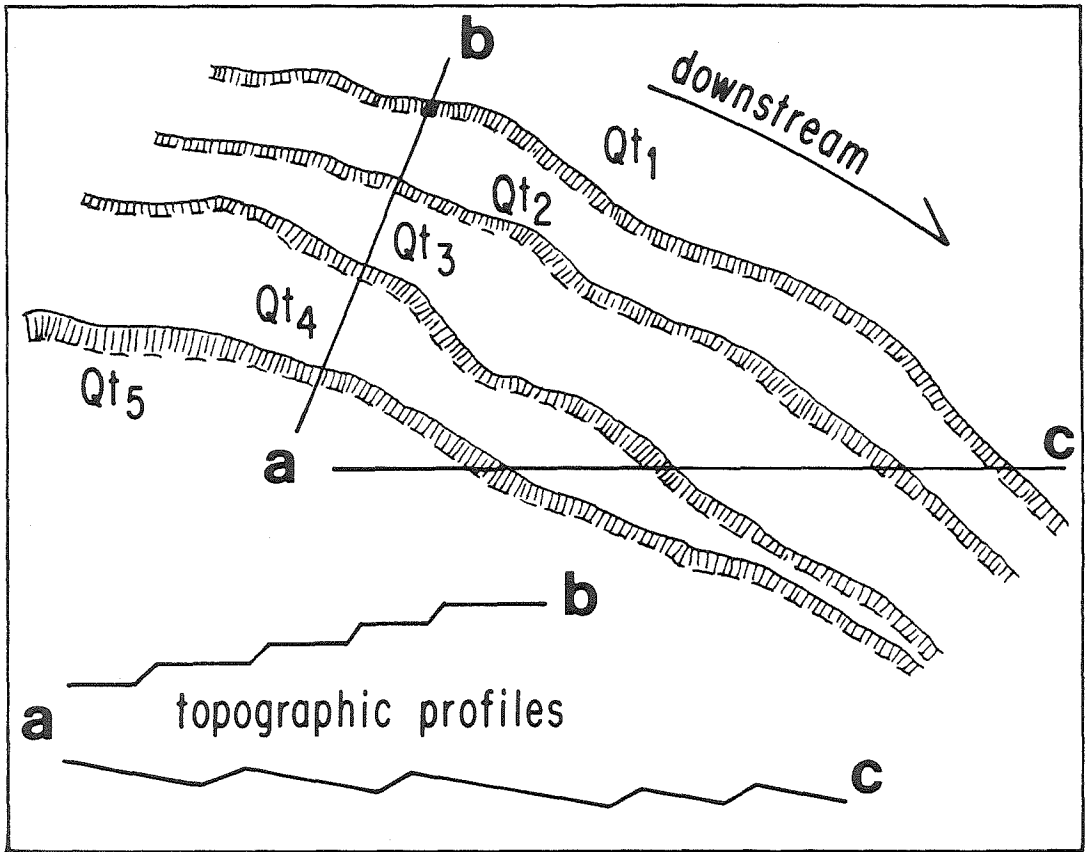


Figure 2-8

encountering the fault.

The "troughs and ridges" impression is enhanced by the fact that overflow from the depression necessarily occurs at the base of the risers (the low points in the "saw-toothed" profile, Fig. 8). Erosion, caused by overflow from the depression has accentuated the "troughs" but did not cause them. Coincidentally, the elevations at the bases of the risers above Qt-4, Qt-3 and Qt-2 are all within 2 meters and the depression drained out each of these three outlets before Pink River captured Lost Swamp. This delicate balance still exists for Lost Lake, which during the last four years has drained across Qt-3 or into Lost Swamp, depending upon which beaver dam across the two sills was higher (see Fig. 5).

Once the terrace treads and risers are recognized, it is easy to match the terraces across the fault zone and to measure the offsets on their risers. The riser representing the northeastern edge of Qt-4 generally follows the fault trace and is offset several times (Fig. 4). The northeastern edge of the higher and older terraces cross the fault only once, near Lost Swamp. Therefore, the Qt-4 riser enters and leaves the depression from the southwest side of the fault and the older ones enter the depression from the north side and leave to the southwest. The offset of each of the terraces is most easily established by working back through time. The obvious 145 m offset of the Qt-5 riser cut by Cajon Creek is first restored (Fig. 7e). This also restores the inner channel of Pink River, which was set by incision below the Qt-5 level (see the remnants of the Qt-5 level above Pink River, Fig. 5).

It appears that Lone Pine Creek, when it occupied the Qt-4 level here, abutted the northern trace of the fault zone for about 400 meters.

This commonly occurs today where streams are subparallel to the fault (see, for example, where Lone Pine Canyon crosses the fault, Fig. 2). A 70 meter portion of Lost Lake appears to extend northeast of the fault zone (Fig. 4), suggesting that Qt-4 actually crosses the fault zone here. In Fig. 7d, 175 m of offset have been restored to create a smooth riser for Qt-4 across the fault zone. This proposed offset is consistent with other tentative offsets of Qt-4 (e.g., near where Lone Pine Canyon crosses the fault, Fig. 4) and is bracketed by the well-documented offsets of Qt-5 and Qt-3 (that will be discussed below). Regardless of whether Qt-4 is offset exactly 175 meters, most of the depression northwest of Lost Swamp is certainly underlain by the Qt-4 surface.

The Qt-3 riser crosses the fault zone and is offset about 200 meters (Fig. 4 and 5). Fig. 7c restores the slip that has accumulated since the Qt-3 riser was established. Both traces of the fault were active by this time, beginning to create the closed depression that Lost Swamp and Lost Lake occupy today. The depression was formed by a combination of lateral juxtaposition of higher terraces, Qt-1, Qt-2 and Qt-3, downstream of lower ones, Qt-2, Qt-3 and Qt-4, and dip slip displacement on both traces, depressing the block in between. Reconstruction of the Qt-1, Qt-2 and Qt-3 surfaces across the whole fault zone indicates that the southern trace has had a greater amount of net vertical slip than the northern one. This also deepens the depression because the terraces dip south-southeast. Lost Swamp is underlain by both Qt-2 and Qt-3 but as the riser cannot be found between the two faults it is not clear how much of the swamp is on each.

Due to the burial of the terraces between the two traces it is not possible to determine directly which fault trace has had more offset,

but inferences can be made about their relative timing. In Lost Swamp the northeastern trace appears to be buried by a fan of pink sand and gravel that predates the formation of Pink River, about 5900 B.P. (see Fig. 5 and the stratigraphy section), so it cannot be very active now. This strand is quite prominent at the northwestern end of the depression, so it may still be active northwest of Lost Lake. Near Lost Swamp the southwestern fault trace is certainly now the most active and has been for the last 5900 years.

SLIP RATES

Using the history of faulting and the Quaternary stratigraphy developed above, four separate groups of offsets can be related to dated deposits. This yields four independent estimates of the average slip rate during the past 14,400 yrs. Each of the four estimates is discussed separately and the results are summarized below.

Case 1

The oldest slip rate is based on the offset of the channel into which Qoa-c was deposited. The eastern edge of the channel can be mapped about 150 meters west of the modern channel (Fig. 2), across Lone Pine Creek and Pink River, across the railroad cut and into the fault about 40 m south of the railroad tracks (Fig. 9). The eastern edge of the old channel on the northeast side of the San Andreas fault is defined by the outcrops of Tub (an unnamed Tertiary(?) sandstone). Because the fault has produced virtually no vertical offset since the deposition of Qoa-d and the minor vertical displacements of Qoa-c can be directly attributed to local geometric constraints in the fault, the channel edge, where it crosses the level of Cajon Creek, is used as the "piercing

Figure 2-9 - Offset of the channel into which Qoa-c was deposited. The heavy dots indicate the eastern channel edge at the level of Cajon Creek. As there has been virtually no vertical offset since the deposition of Qoa-c the edge of the channel wall at a particular level can be used as a piercing point. Contacts and units are the same as Figures 2 and 4.

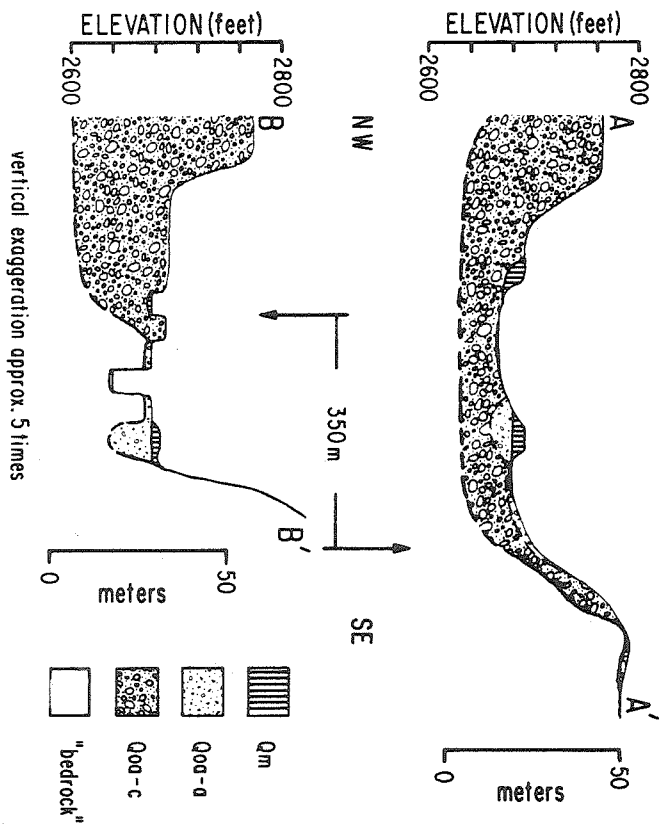
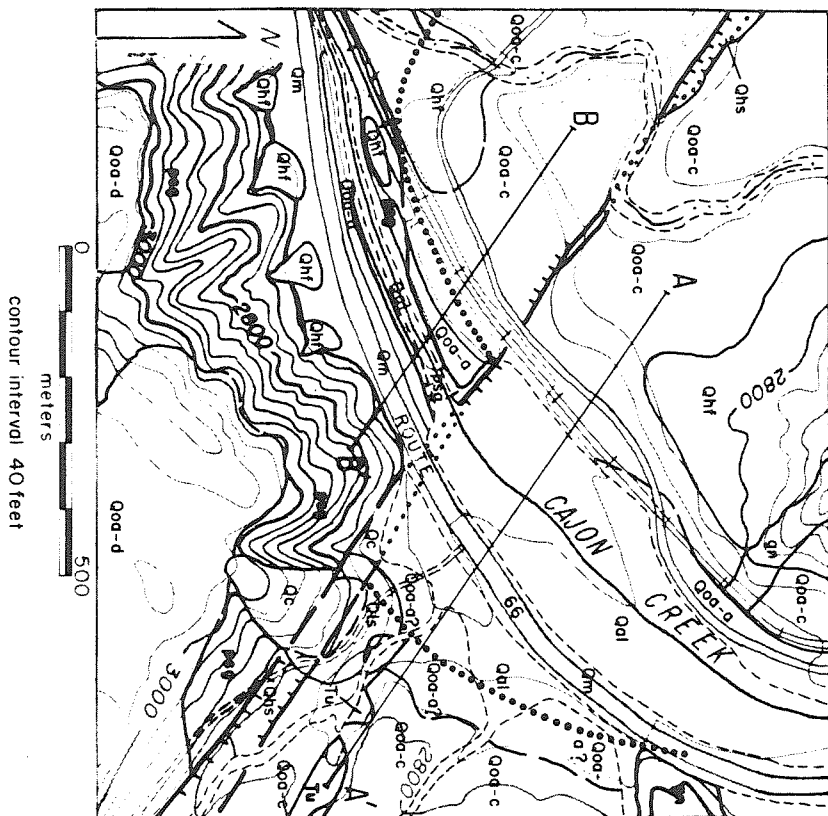


Figure 2-9

point" (see the cross sections, Fig. 9). The two piercing points are offset 350 ± 30 m across the fault (Fig. 9).

If the channel edge was preserved as the Qoa-c alluvium buried it, the age of Qoa-c at the level of the current creek can be used to calculate the slip rate. As discussed in the stratigraphy section, Cajon Creek aggraded above its current level at the San Andreas fault 14.4 ± 1 ka, preserving the channel edge that records the offset since that time. The distance of $350 \text{ m} \pm 30 \text{ m}$ in 14.4 ± 1 kyr yields a rate of 24 ± 4 mm/yr. The best estimate and a box representing the uncertainty in the age and the measurement are plotted as Box 1 on Fig. 10.

Case 2

The second estimate is based on the offset of streams and terraces incised into Qoa-c. Extrapolating the rate of fill indicated by the ages of samples CC-3 and CC-4 to the surface of Qoa-c suggests that the Qoa-c fill event culminated at 12.4 ± 1 ka. Small bedrock hills and delicate ridges protruding from the fill and the lack of notches or benches at the level Qt-1 (the surface of the Qoa-c deposit) indicate that the Qt-1 surface is the result of filling without significant lateral cutting. Therefore, Cajon Creek probably began to incise immediately after the Qt-1 level was reached and the estimate of 12.4 ± 1 ka can be used to date the onset of incision of the Qoa-c deposits.

Near Lost Lake, Lone Pine Creek abandoned Qt-1 (the fill terrace surface of Qoa-c) and produced a strath terrace, Qt-2, about 7 m below Qt-1 (Fig. 4 and 7). Subsequent erosion has obscured the exact location of the riser at the fault. The small hill (2769 on Fig. 5) immediately southwest of Lost Swamp is too high to be part of Qt-2. It is an eroded remnant of Qt-1. This interpretation is consistent with the trend of

Figure 2-10 - Slip rate on the San Andreas fault at Cajon Creek. The points represent the best estimates of the offsets and ages and the boxes represent 95% confidence limits. Each box represents independent offset features, radiocarbon dates and geologic assumptions. The points are not in the center of the boxes due to the asymmetric limits on some of the ages and measurements. The heavy line represents the best estimate of the slip rate at Cajon Creek and the lighter lines are the limits on the rate, constrained to touch each box. The starting point for each line is 180 years ago, the best estimate for one-half recurrence interval after the last earthquake (see text for details).

SLIP RATE ON THE SAN ANDREAS FAULT AT CAJON CREEK

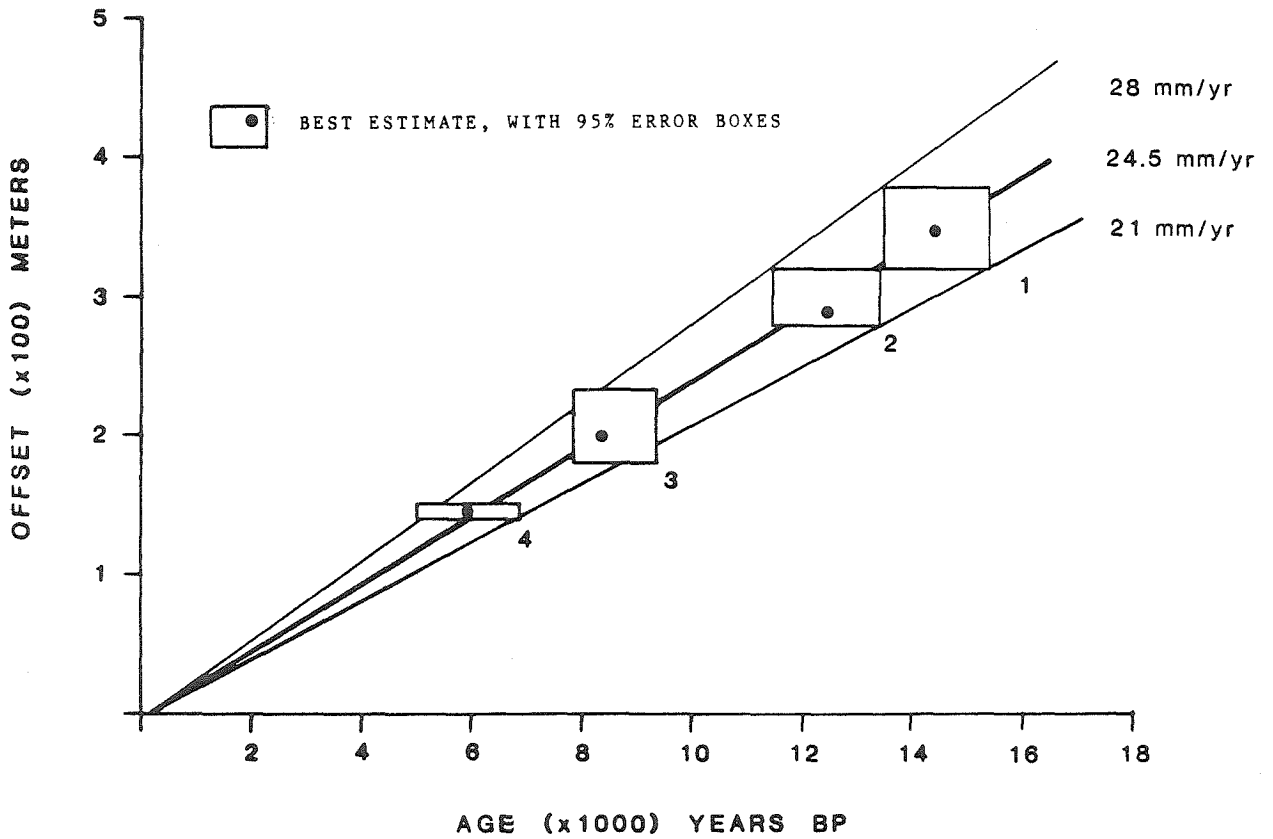
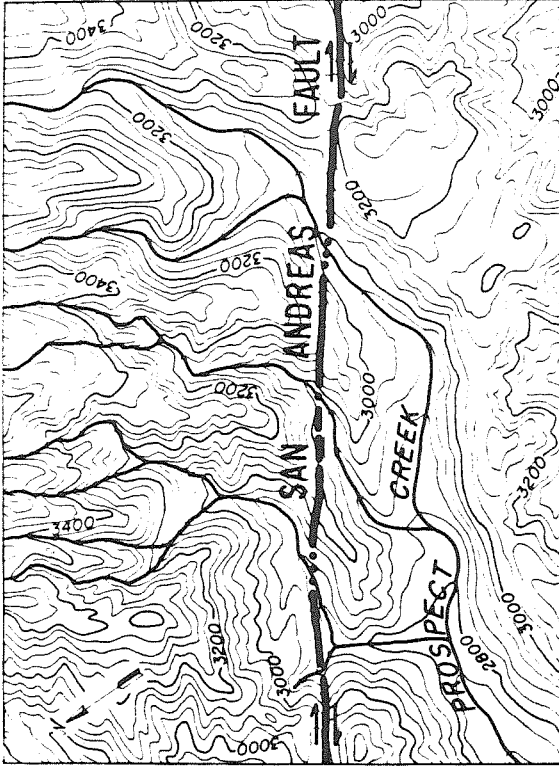


Figure 2-10

the riser between them to the southeast and allows the intersection of the riser and the fault to be located within 20 meters (Fig. 4 and 5). On the northeast side of the fault the riser between Qt-1 and Qt-2 has been completely eroded. However, the riser affected the development of the streams that eroded it and they can be used to locate its original position. Those streams that flowed only on Qt-1 were free to flow straight south across the fault zone and those that dropped down to Qt-2 were forced to flow to the west of the Qt-2 riser (Fig. 7). As offset accumulated, the streams on Qt-2 were forced to flow farther and farther to the northwest, around the higher, relatively northwest-moving Qt-1 terrace to the southwest across the fault (Fig. 7b). The divide between streams flowing south, straight across Qt-1, and those forced to flow southwest, west and, ultimately, northwest can still be located (note stream paths on Fig. 4 and 7); it is offset about 300 meters.

A more precise measurement can be made to the southeast where all three branches of Prospect Creek show total deflections of 290 ± 10 m (Fig. 11). While these tributaries are not directly incised into Qoa-c at the fault, Prospect Creek is a tributary of Cajon Creek and it is inferred that these incisions were initiated by the onset of incision represented by Cajon Creek's abandonment of the Qt-1 surface on Qoa-c. Because the incision of Qoa-c by Cajon Creek may have taken some time to propagate up Prospect Creek to the fault and the approximately 300 m offset of the Qt-2 riser may not have begun to accumulate until some time after the initial abandonment of Qt-1, it is possible that the offset values are a bit too low. However, due to the greater precision and number of the Prospect Creek offsets 290 m is used for the "best estimate" and 20 m is arbitrarily added to the maximum limit to allow

Figure 2-11 - Offset of the tributaries of Prospect Creek. The 290 meter offset of each of the streams is inferred to have begun when Cajon Creek (and its tributaries) incised after the deposition of Qoa-c. The matches are both based on the westernmost stream, which has a deeply incised channel on both sides of the fault. The 200 meter restoration is based on the "inner gorge" offset that probably relates to renewed incision following Qt-3.



contour interval 40 feet
0 500 meters

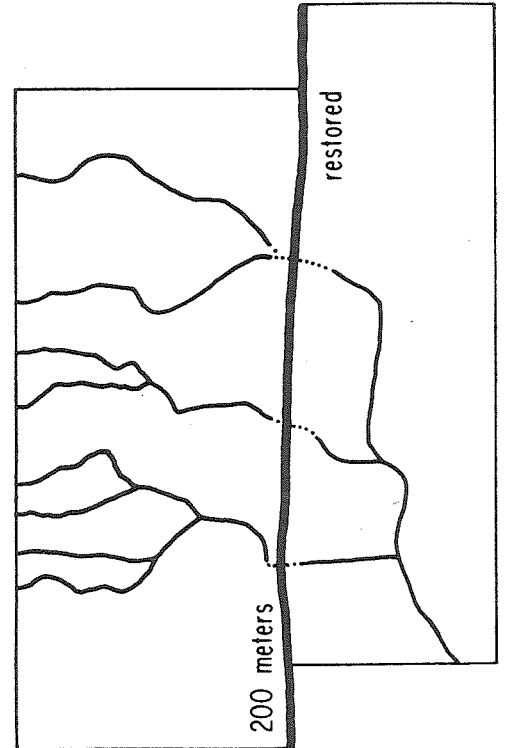
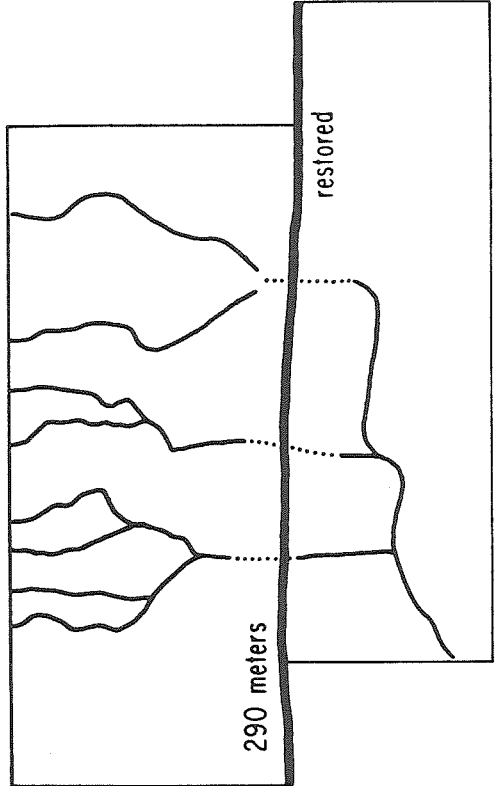
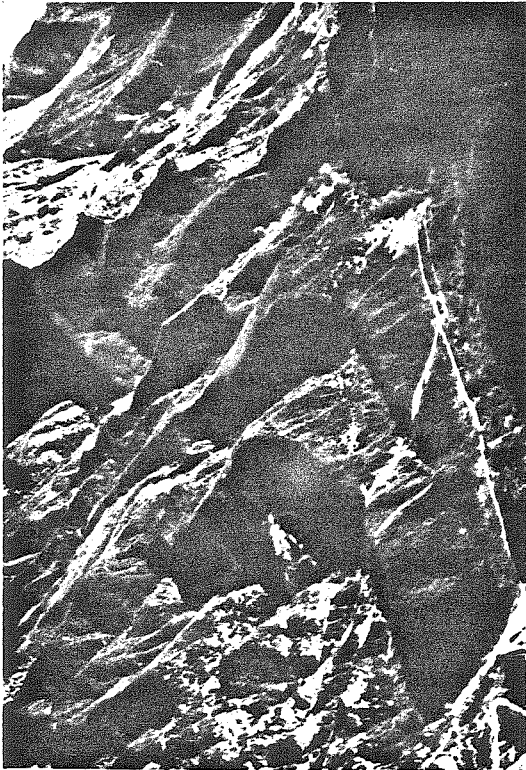


Figure 2-11

for the possibility that the features measured do not quite show the total offset of Qoa-c. The distance 290 ± 10 m divided by 12.4 ± 1 kyr yields 23 ± 2 mm/yr. The best estimate plus the limits of the age and measurements are plotted on Figure 10 as Box 2.

Case 3

The most pervasive cut terrace in the Cajon Creek drainage is Qt-3. The timing of the abandonment of this surface by Cajon Creek and its tributaries can be dated by the Lost Swamp sediments, which sit on Qt-3. Several offsets can be related to the incision of this surface and allow a calculation of the slip rate since its abandonment about 8350 B.P. At the northwest end of the study area, Sheep Creek North is incised into Qt-3 and has since been offset approximately 190 m (Fig. 2). Near Lost Lake the Qt-3 riser of Lone Pine Canyon crosses the fault at Lost Swamp with 180 to 235 m of offset (Figs. 4 and 5).

The three tributaries of Prospect Creek may also indicate approximately 200 m of offset associated with the abandonment of Qt-3. All three streams exhibit an "inner" separation of about 200 meters within the overall 290 m offset discussed in Case 2 (Fig. 11). The height of the well developed Qt-3 surfaces at the mouth of Prospect Creek, at about the level of the inflection in downcutting, points to the abandonment of Qt-3 as being responsible for this event. Finally, Pink River was set into its current position on both sides of the fault at this time (Fig. 7c). All of these observations lead to the conclusion that about 200 meters of slip have accumulated since the abandonment of Qt-3. The uncertainty of the measurement at Lost Swamp, 180-235 m, is used for this event.

The age of the Qt-3 terrace can be determined from the onset of sedi-

mentation in Lost Swamp. When Qt-3 was abandoned, a major precursor of Pink River drained across Qt-1, Qt-2 and Qt-3 into the Lost Swamp depression, depositing a fan of pink sand on the north shore of the swamp (Fig. 4 and 5). The channel of this stream is preserved where the stream descended from Qt-2 to Qt-3 northeast of Lost Lake. Sediment deposited by this stream could begin accumulating as soon as Lone Pine Creek left the Qt-3 level, so the age of the basal Lost Swamp sediments should closely date the beginning of the 200 meter offsets associated with this event. The age of the base of the lake clay is 8350 ± 500 B.P. (see Fig. 6 and the Stratigraphy section), so a slip rate of 24 ± 5 mm/yr is calculated. The best estimate of 200 m in 8350 years and the uncertainties are expressed in Figure 10 as Box 3.

Case 4

The consolidation of all of the minor streams draining the hills to the north of Lost Lake into Pink River cut off the supply of sediment and water to Lost Swamp and provided the youngest dated offset. As discussed above, the culmination of this capture occurred about 5900 B.P. (Fig. 7e), with the incision below the Qt-5 terrace level, and 145 ± 5 m of slip have accumulated since then, measured by the offset of the inner channel of Pink River and the Qt-5 riser on the northwest side of Cajon Creek (Figs. 4 and 7).

The cutoff of the supply of sediment from the hills to the north is recorded in the deposits under Lost Swamp by the change in the character of the lake clay at about 5900 B.P. (Fig. 6). The best estimate of the timing, 5900 ± 900 B.P., and offset distance, 145 ± 5 m, yields a rate of 25 ± 4 mm/yr. This value and the uncertainties are plotted as Box 4 on Figure 10.

Summary of Slip Values and Possible Problems

The San Andreas fault in this area accumulates slip in discrete increments associated with major earthquakes. At any given time, except for immediately after an earthquake, there is a certain amount of potential slip that has accumulated but has not yet been manifested as offset across the fault. A channel or terrace riser can probably form at any time, so the offset measured on these features may misrepresent the total slip by as much as the displacement produced by a single earthquake event. In general, this requires an additional uncertainty be added to the offsets. However, given many offset features, it is most likely that the average offset feature formed in the middle of the time between earthquakes. Taken as a group, the measured offsets should accurately represent the displacement at a time $1/2$ the average recurrence interval after some earthquake. So, if many features are measured and dated with respect to a point in time midway between earthquakes, the average slip rate calculated for that point in time should be the most accurate measure possible. As discussed below, the last earthquake occurred much longer ago than one-half the average time between earthquakes. Therefore, it is necessary to subtract the amount of time since $1/2$ the average recurrence interval after the last earthquake from the ages of the offset features to determine the slip rate most accurately. This value is estimated from the observations in the excavation at Lost Swamp to be about 180 years and has been accounted for graphically by drawing the slip rate lines through zero offset 180 years ago (Fig. 10). The line through all of the "best estimates" has a slope (the slip rate) of 24.5 mm/yr. The limiting rates are determined by lines required to touch each box, yielding the error of ± 3.5 mm/yr.

The data summarized in Figure 10 embody many assumptions and details that are necessary to estimate slip rates as accurately as possible. Depositional rates within units such as Qoa-c are assumed to be constant, terrace risers, streams, and other features used to measure offset are inferred to have had smooth paths across the faults, and changes in sedimentation in the swamp and erosion by the streams are assumed to be related to recognizable events in the overall fluvial history of the area. It is possible that some of these assumptions are imperfect and it is worth considering how deviations from the assumptions and possible errors might affect the slip rate. However, the details are extremely tedious and are not included in the body of this paper. A detailed reconsideration of each of the cases discussed above has been included in the data repository. The individual cases combine to constrain the slip rate between 20 and 28 mm/yr averaged over the last 14,400 years because each case requires maximums or minimums that overlap in that range. Only completely eliminating several of the cases or calling upon non-uniform slip rates between the cases can invalidate this conclusion. If several of the "worst cases" turn out to be true, then only the inference of a very constant slip rate is weakened, not the average rate itself.

LOST SWAMP EXCAVATION

The low point between Pink River and Lost Swamp was excavated to confirm the stratigraphy in the swamp (originally inferred from auger holes), to sample the critical units for radiocarbon dating, and to gain insights into the timing of recent earthquakes. The northwestern wall of the excavation was unmappable because of the substantial flow of

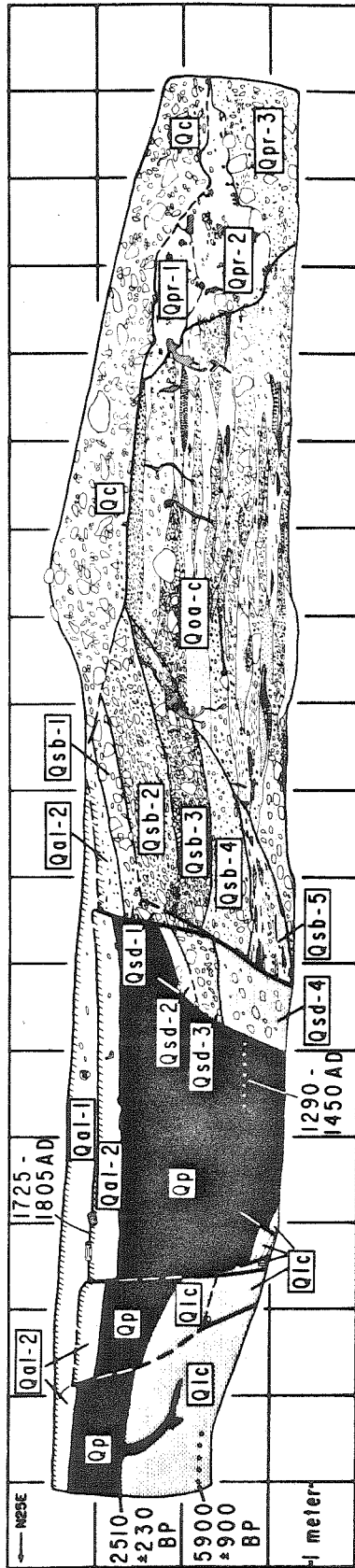
water out of the swamp, but the southeast wall dried out and is represented as Fig. 12.

Stratigraphy

Eight major stratigraphic units were exposed in the excavation wall. The youngest material exposed is colluvium (Qc) currently being shed into the small creek that drains Lost Swamp (Fig. 5). Most of the top of the exposure southwest of the swamp is capped by this unit (Fig. 12). The next youngest unit is fine-grained alluvium derived mainly from Qt-2 to the east (Fig. 5). This alluvial wedge is prograding onto the swamp and reached the trench site several hundred years ago. This unit has been subdivided into Qal-1 and Qal-2, separated by what is interpreted as a rapidly buried ground level or O-horizon, 5-10 cm thick. A radio-carbon date at the base of Qal-1 yielded an age of 1725 to 1805 A.D. (see note, Table 1, CP-4). There is another buried O-horizon below Qal-2 that preserves the transition from peat to alluvial deposits and represents the regressive margin of the swamp.

The next oldest unit is a series of breccia deposits off the San Andreas fault scarp into the swamp to the northeast. It is subdivided into five members, Qsb-1 through Qsb-5, from top to bottom. The breccias were not directly datable but they underlie Qal-2 and are inferred to be less than about 1000 years old. This age is based on the fact that the breccia rest upon the scarp formed during the last 24 meters of offset on the San Andreas fault (Fig. 5; for an analogous situation, see Fig. 7b where material cannot be shed north from Qt-1 onto Qt-2 until offset has created the northfacing scarp). The slip rate determined above therefore indicates that they are less than about 1000 years old. Perhaps related



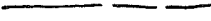



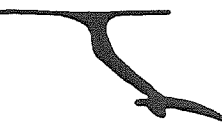

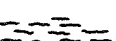
Figure 2-12 - Trench log of the excavation at the southeast end of Lost Swamp. The geomorphically evident main trace occurs 7 meters from the northeast end of the excavation. The faults at the northeast end of the excavation appear to be dominantly dip slip. No faulting is observed southwest of the main trace of the fault. The buried ground surface (with the wood on it) between Qal-1 and Qal-2 represents the surface before the last earthquake. The wedge-shaped units between Qoa-c and the fault are breccia shed off paleoscarps that have been buried and eroded (see Figure 14).



Ray Weldon, John Hopeck, Lili Mezger

Figure 2-12 (Also Plate 8)

EXPLANATION FOR FIGURE 12

	Fault; solid where certain and dashed where uncertain.
	Major depositional contact; solid where certain and dashed where approximate.
	Minor depositional contact within a major unit; solid where certain and dashed where approximate.
	Ground surface; active or buried O-horizon.
	Ground squirrel burrows.
	Rocks; most clasts larger than about 5 cm were mapped on the log in the field.
	Major fissure.
	Manganese oxide stains.
	Calcareous coating or laminations.

Units

Qc	--	Colluvium being shed into Pink River and the creek that drains Lost Swamp (up which the excavation was cut).
Qal-1	--	Recent fine grained alluvium and colluvium shed into Lost Swamp from the east; sole unfaulted unit in the swamp; capped by an O-horizon.

EXPLANATION FOR FIGURE 12 (Continued)Units

- Qal-2 -- Similar to Qal-1 but faulted and separated from Qal-1 by a buried O-horizon; Qal-2 becomes coarser to the southwest and probably contains some debris off the scarp.
- Qsb-1 -- Transitional between Qal and Qsb2-5; has coarse debris off the scarp and some fine grained debris from the east.
- Qsb2-5 -- Scarp breccia; reworked material derived from Qoa-c off the scarp.
- Qsd-1 -- Like Qsb units but completely within the fault zone.
- Qsd-2-4 -- Scarp deposits completely within the fault zone and containing peaty or clayey matrices; probably breccia shed into the swamp.
- Qp -- Massive, poorly sorted organic-rich sandy clay; referred to as the "peaty unit" in the text.
- Qlc -- Relatively organic-free lake clay; contains heterogeneously distributed sand, silt, gastropod shells and rare pebbles.
- Qpr1-3 -- Channel fill of Pink River; generally pink, conglomeratic, moderately well-sorted sand that is locally cemented by CaCO₃.
- Qoa-c -- Late Pleistocene river gravels and sand deposited by Lone Pine Creek; the size and sorting of individual units is illustrated by the size, spacing and regularity of the pebbles and sand grains.

to these breccias are the deposits within the fault zone, Qsd-1 through 5 (Fig. 12). These units have clay or organic-rich matrices so each may represent a scarp breccia that actually was deposited in the swamp or lake. Unfortunately, these units are completely within the fault zone so they cannot be confidently related to the other units in the trench.

The next oldest unit, partly overlapping in age with the scarp breccia, is a poorly sorted, massive peaty unit, Qp. Its deposition was initiated about 2510 B.P. (CP-1) and was terminated at the trench site by the deposition of Qal-2 several hundred years ago. Augering indicates that Qp is typically less than a meter thick in this part of the swamp but it has been thickened by progressive downdropping during deposition adjacent to the San Andreas fault (Fig. 6 and 12). Small pieces of charcoal from a depth of 2 m in the middle of the fault zone (Fig. 12) yielded an age of 1290-1450 A.D. (CP-3). The peaty unit overlies about 3 m of massive black to grey lake clay. As discussed above, five radiocarbon dates from the clay indicate that its deposition began about 8350 B.P. (Fig. 6).

At the southwest end of the trench, beneath the colluvium is calcium carbonate cemented Pink River alluvium (Qpr, Fig. 12). The source can be identified by the presence of pink sand and clast types characteristic of the Punchbowl formation that Pink River drains. Calcium carbonate-rich springs and water flowing out of Lost Swamp have cemented Pink River sediments into the fan shaped deposit preserved today (Qpr, Fig. 5).

Underlying the Pink River alluvium, the colluvium and the scarp breccia is Qoa-c alluvium. These gravels are the source of the scarp breccia shed into the swamp and of the colluvium. The well-defined contacts between interbedded sands and gravels in Qoa-c indicate that the

fault zone extends less than a meter to the southwest of the geomorphically evident main trace (the southernmost trace on Figure 12). This is in contrast to the zone of faulting extending 6 meters into the swamp to the northeast of the main trace.

Fault Activity

Qal-1 does not appear to be broken by any fault; it seems to fill the depression formed by the latest rupture event. However, the massive character of Qal-1 makes detection of a minor break in a single exposure difficult. A small charred log was found at the base of Qal-1 and a sample (CP-4) from the outer rings was dated. The ^{14}C age fell in a range that yields the multiple calendrical ages: 1725-1805 A.D., 1605-1685 A.D. and 1525-1570 A.D. Because of the age of CP-3 (1290-1450 A.D.) in Qp, 2 meters and at least one earthquake below Qal-1, the oldest possible age, 1525-1570 A.D., is considered very unlikely and the youngest age, 1725-1805 A.D., is considered most likely. If the unit containing the log, Qal-1, really does postdate any faulting, it follows that the 1857 San Andreas event did not produce ground rupture as far southeast as Cajon Creek. This conclusion is consistent with historic records from this area (Agnew and Sieh, 1978).

Unit Qal-2 is certainly faulted by the main trace and two subsidiary traces at the northeast end of the trench (Fig. 12). The porous, rooty organic-rich zone that separates Qal-1 and Qal-2 appears to be offset the same amount as Qal-2 and probably represents the ground surface at the time of the latest rupture. The displacement of the alluvial-peat contact is the same as Qal-1. Because the alluvial-peat contact is almost horizontal, the southwest side down separation across these faults probably represents a vertical component of offset. Longer term offset

of this nature would also explain the greatly thickened peaty unit (Qp) within the fault zone.

The flat surface of the swamp and the contacts between Qal-1, Qal-2 and Qp suggest that there was sufficient sediment input to quickly refill the depression in the swamp produced by the latest rupture on the fault. The vertical component of the latest earthquake deformed the flat swamp surface, creating a narrow depression that was rapidly filled (Fig. 13). Today, felled wood around the margin of the swamp disintegrates rapidly, so the presence of a well-preserved log lying on the buried swamp surface at the base of Qal-1 suggests that the log fell to the ground during or immediately before or after the last earthquake and was rapidly buried before it could deteriorate. If this is the case, the date of the log should be very similar to the date of the latest earthquake.

The thickness of the Qp unit mimics the offset of Qal-2 but records much greater displacement. At the northeast end of the excavation, Qp has a thickness of about 60 cm, typical of the swamp outside the active fault zone. Faulting and warping thickens Qp to the southwest, so Qp probably reaches its maximum thickness adjacent to the northeastern fault in the main fault zone. Small chunks of charcoal (CP-3) that form a discrete layer yielded an age of 1290-1450 A.D. This is remarkable because a sample of peat (CP-2) at the peat-clay contact and only 1/2 meter below the swamp surface (outside the fault zone) yielded an age of 795-385 B.C. (2510 ± 230 B.P.). Clearly, Qp, within the fault zone, is being dropped relative to the swamp outside the fault zone and is being thickened by rapid sedimentation that appears to keep the surface of the narrow depression close to the level of the swamp.

Several important conclusions can be inferred from these observa-

Figure 2-13 - Formation of a new smooth scarp after an earthquake. This is based on the deformation and deposition resulting from the last earthquake. The faults are all southwest-side down but result in a deposit that forms a surface graded to the swamp level (to the north). The relative height difference of the swamp and the scarp is reduced, which causes sediments to be deposited on the lower part of the scarp, progressively burying the fault and scarp as more earthquakes occur. The units and contacts are the same as those in Figure 12.

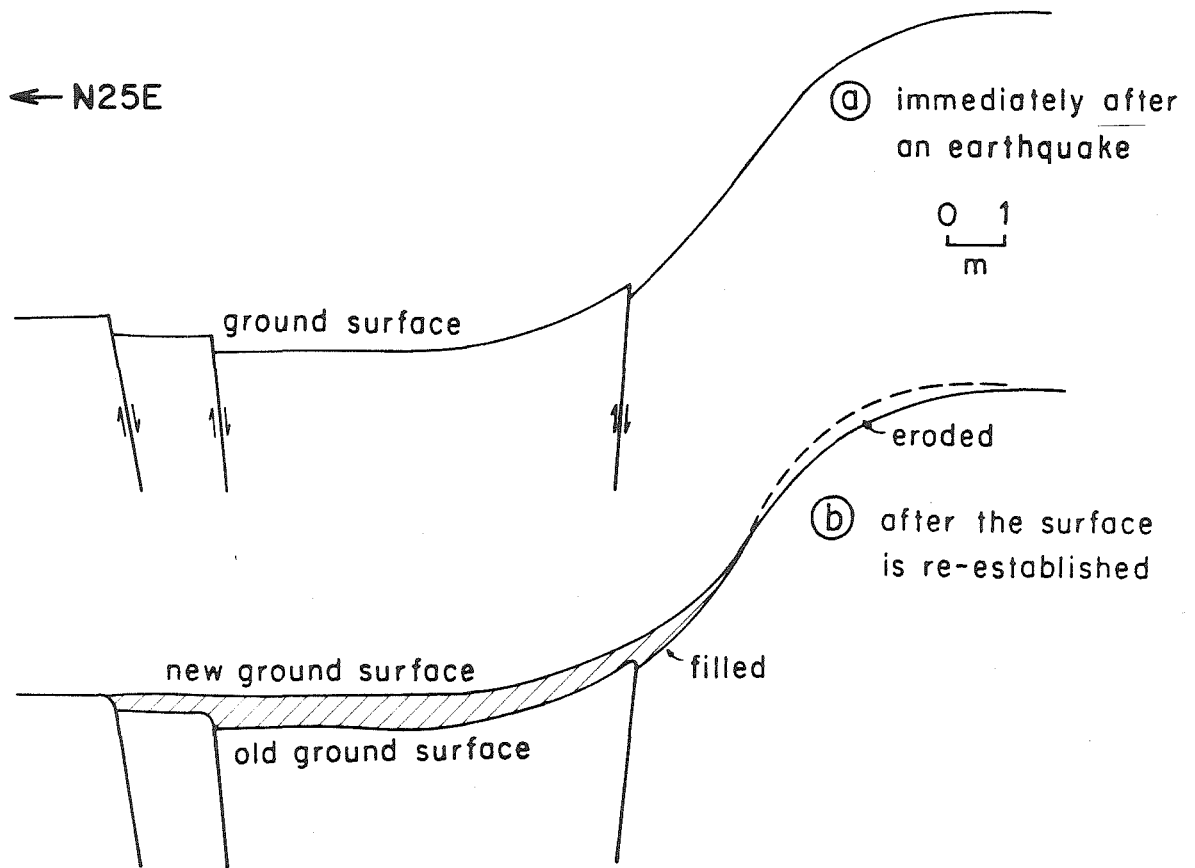


Figure 2-13

tions. First, there must have been at least two and perhaps as many as four events between the deposition of the charcoal in Qp and the burial of the log in unit Qal-1, a time span of at most 515 years (1290-1805 A.D.). This follows from the fact that Qp at the level represented by the charcoal is downdropped far more than Qal-2, which has been affected by one event. A minimum of two events is supported by the observation that at least two fault traces that offset the upper part of Qp (above the charcoal) do not break Qal-2 (Fig. 12). The suggestion of as many as four events is based simply on the depth of the charcoal layer; if the vertical offsets associated with the previous events were similar to the last one (50 cm), it would take three or four events to drop the charcoal layer to its current depth with respect to the swamp. Implicit in this calculation is the assumption that the swamp did not aggrade significantly between 1290 and 1805 A.D.; this is likely because only 50 cm of peat were deposited outside the fault zone in the last 2510 years (Figs. 6 and 12).

If each downdropped swamp surface could be identified, each earthquake could be recognized and, perhaps, dated. The contact between Qal-2 and Qp represents a buried ground surface that does not appear to be offset more than the contact between Qal-1 and 2 and simply represents the point at which the regressive shoreline of the swamp passed the site of the exposure. Unfortunately, Qp, below Qal-2, is too massive to allow recognition of old swamp surfaces that have been tectonically downdropped and buried.

Although these paleosurfaces are not recognizable within the peat, they can be identified in the scarp breccias southwest of the San Andreas fault. Between the San Andreas fault and the well-bedded Qoa-c gravels

there are at least five distinct, wedge-shaped, nested scarp breccias, Qsb-1 through 5. As discussed above, these sediments must be younger than about 1000 years old because of their position on the scarp southwest of the San Andreas fault. In Figure 14 each of the surfaces has been reconstructed up to the crest of the ridge between Lost Swamp and Pink River. Two things are evident: the surfaces reflect a progressive retreat of the scarp from the fault and the height of the Qoa-c ridge-crest relative to the swamp has decreased dramatically (even more so if significant erosion of the crest has occurred). Because the level of the swamp outside the fault zone has risen only 50 cm in the last 2510 years and the breccia that are shed onto the swamp are less than 1000 years old, more than 2 meters of vertical motion have occurred since the earliest breccia was deposited (Fig. 14). The relative height between the ridge and the swamp has been decreased to the point that material is not being transported down the scarp and the scarp is actually being buried by the Qal units that are derived mainly off the high ground to the east of the swamp and not off the scarp (Fig. 5). This is illustrated by the fact that the lowest point on the surface of the excavation northeast of the fault is where Qal-1 and 2 lap up on the scarp (Fig. 12).

The scarp breccia began forming off the scarp when the Qoa-c gravels first emerged from behind Qt-2 to face the depression of Lost Swamp (Fig. 5). The breccia were deposited across the fault and interfingered with the alluvium that is burying the swamp from the southeast. Depending on the position of the Qp-Qal contact through time, a breccia unit may interfinger with Qp where the scarp reaches the active swamp. At the site of the excavation the scarp is sufficiently stable that no breccia is shed across the fault anymore. At some point in time breccias

Figure 2-14 - Reconstruction of paleoscarps using the breccia deposits.

Smooth surfaces representing paleoscarps are drawn from the breccia contacts to the top of the scarp. The scarp decreases in height and retreats from the fault. Because the level of the swamp away from the fault has not changed significantly since the onset of deposition of the breccia (about 1000 yrs ago), at least 2-1/2 meters of vertical offset have accompanied the last six earthquakes. The units and contacts are the same as on Figure 12.

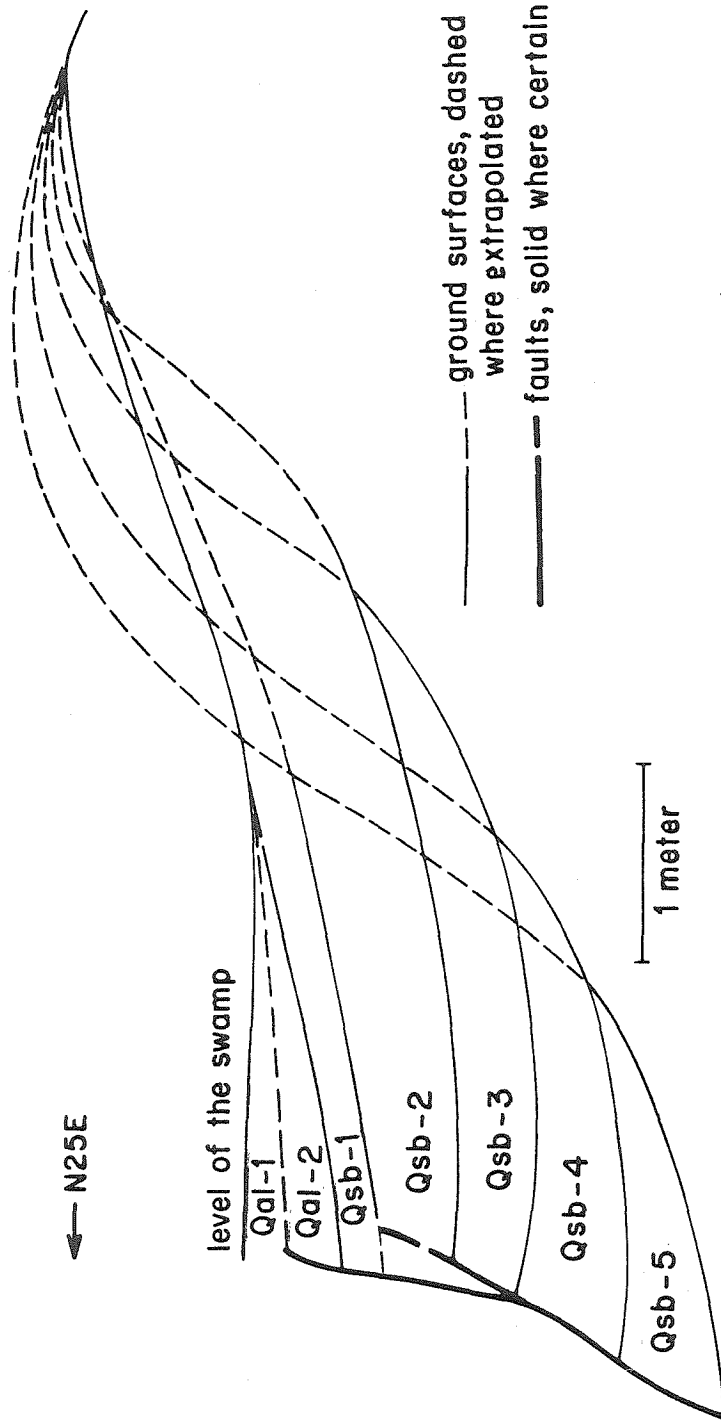


Figure 2-14

did interfinger with both the peat and clay. The Qsd units appear to be breccias like the Qsb units but have either clayey or peaty matrixes. Unfortunately, these units are completely within the fault zone so their relationship to either side is uncertain. Perhaps a trench in the active swamp would reveal relationships that would allow each breccia, and therefore each earthquake, to be directly dated; such an exposure would require draining the swamp.

If each scarp breccia represents an individual earthquake there have been six earthquakes in about the last 1000 years, five represented by the scarp breccias and the event between Qal-1 and 2 which did not produce much breccia because the scarp was so low. If six events have produced 24 m of offset, the average lateral offset per event has been 4 m on the main fault and the average recurrence interval has been $1 \frac{2}{3}$ centuries.

The interpretation that at least 2 and perhaps as many as 4 earthquakes have occurred in 515 years or less, is consistent with this recurrence interval. Also, there are several places in the mapped area where approximately 4 m of offset can be measured on young geomorphic features (Weldon and Sieh, unpublished data). Four meter offsets of several small streams and steep slopes that postdate the abandonment of Qoa-a suggest that the last event occurred after the onset of the current pulse of incision by Cajon Creek and was associated with about 4 m of slip. As discussed earlier, the best estimate of the culmination of the Qoa-a fill event is 275 B.P. This, coupled with the most likely age of the last rupture in the swamp and the historic record, indicates that the last earthquake was in the early 18th century.

DISCUSSIONTectonic Implications

To determine the best estimate of the slip rate a line has been drawn through all of the individual cases on Figure 10. As discussed above, the slip rate lines are required to pass through zero offset 180 years ago, the best estimate of 1/2 recurrence interval after the last slip event. This yields an average rate of 24.5 ± 3.5 mm/yr, at a 95 % confidence level of the ages and offsets. The individual best estimates are all close to the 24.5 mm/yr line, suggesting that the fault is accumulating slip at a relatively constant rate. There is no suggestion of any change in the average rate during the last 14,400 years, and the time periods between data points is sufficiently long to mask any evidence of the discreteness of the slip events.

While the evidence from the excavation (which suggests a recurrence interval of 1-1/2 to 2 centuries) indicates the periodicity in which the fault accumulates slip, the slip rate observations allow a long-term perspective that trenching does not permit. Suggestions of very long periods of quiescence, perhaps followed by exceptionally large or numerous large earthquakes on some parts of the San Andreas fault can be tested using the slip rate data. Any unusually active or quiescent period is limited at Cajon Creek to less than the time between the data points on Fig. 10 (a few thousand years).

The constant slip rate on the San Andreas fault over the last 14,400 years, south of the junction with the San Jacinto fault, makes it very unlikely that the two faults have alternately assumed the dominant role in the San Andreas system, as suggested by Sharp (1981). Further, the slip record at Cajon Creek strengthens the hypothesis that data repre-

senting time spans of only 100's to 1000's of years from excavations and the historic record are adequate for characterizing the longer-term activity of the fault.

There are very few published late Quaternary slip values for the southern San Andreas with which to compare our results. At Wallace Creek in the Carrizo Plain (WC, Fig. 1), the rate is approximately 34 mm/yr (Sieh and Jahns, 1984). Rust (1982) reports rates between 45 and 47 mm/yr near Three Points (TP, Fig. 1) and suggests that these values are minima because a large number of secondary traces exist nearby. At Pallett Creek (PC, Fig. 1) the slip rate documented for the period 260 A.D. to the present is a mere 9 mm/yr (Sieh, 1984). However, the geometry of the fault zone near the site allows that the actual rate across the zone is probably greater. Keller et al. (1982) report that the average slip rate on the San Andreas fault since the late Pleistocene near the southeast end of the Indio Hills (I, Fig. 1) is between 10 and 35 mm/yr, with 23 to 35 being the preferred value. The ages of the units are based on soil development, desert pavement development and geomorphic criteria, which yield the wide range of possible slip values.

Unfortunately, it is difficult to construct a consistent story that incorporates all of these values. In particular, the rates determined by Rust (1982), especially if they are minima as he reports, seem too high. A long-term minimum rate of 45 mm/yr is impossible for the San Andreas fault both north and south of his site. One possibility is that his rates are based on smaller offsets (~ 40 and ~ 100 m) than any of the other determinations (except for Pallett Creek which is not representative of the total zone). If the fault has had a recent period of high activity, the slip rate values from all sites could agree.

The simplest story that can be constructed for the San Andreas fault system is that the San Andreas fault southeast of the junction with the San Jacinto has a slip rate of ~ 25 mm/yr and north of the junction has a rate of ~ 35 mm/yr. This hypothesis is supported by the long term evidence for about 10 mm/yr on the San Jacinto fault (Sharp, 1981), which seems required if the faults are concurrently active, and is consistent with the measured values of annual slip in the creeping zone of the San Andreas to the north (Lisowski and Prescott, 1981).

If the late Quaternary rate of slip between the North American and Pacific plates in California is close to the 2-3 Ma average of 56 mm/yr, determined by Minster and Jordan (1978), the sum of all the active deformation associated with the boundary should be close to this value. In central California, summing the San Andreas rate (34 mm/yr, Sieh and Jahns, 1984) and the San Gregorio-Hosgri rate (6-13 mm/yr, Weber and Lajoie, 1977) yields a value only 9 to 16 mm/yr less than the total rate across the plate boundary. Activity in the Basin and Range province (~ 7 mm/yr, Thompson and Burke, 1973) may contribute to the extra, but Minster and Jordan (1984) demonstrate that the direction and magnitude are not appropriate to account for the total difference. The deformation associated with the San Gregorio-Hosgri system and the Basin and Range does not extend as far south as the latitude of Cajon Pass and the total on the San Andreas system (San Andreas plus San Jacinto) does not appear to change, so there must be significant activity in southern California that cannot be accounted for by major recognized faults. Rates of north-south shortening of up to 23 mm/yr in the western Transverse Ranges (Yeats, 1983) may contribute to the total but the geometry is such that it is difficult to understand how this can add to the rate south of the

Transverse Ranges unless the region represents a connection between the San Gregorio-Hosgri system and major structures in the southern California borderland.

The active San Andreas system (the San Andreas and San Jacinto fault zones south of their junction) is currently accommodating about 2/3 of the plate motion in both southern and central California. Despite the fact that more than 20 mm/yr of the plate boundary total cannot be accounted for by a major fault (or faults) in southern California, there can be little doubt that the San Andreas fault proper is accumulating slip faster than any other fault in southern California. The lack of historic seismicity associated with the San Andreas fault south of the Transverse Ranges cannot be taken as evidence that it is no longer the major structure of the plate boundary, as several recent summaries have suggested (e.g. Crowell, 1981).

Seismic Implications

The interpretation of the Lost Swamp excavation suggests that 2-4 earthquakes occurred between 1290 and 1805 A.D. Also, it appears that six events have occurred in about the last 1000 years. These conclusions suggest a recurrence interval of about 1-1/2 to 2 centuries. Both the observations presented here and the historic records from San Bernardino (Agnew and Sieh, 1978) indicate that the 1857 earthquake was not associated with rupture on the San Andreas as far southeast as Cajon Creek. Additionally, the historic record does not contain an earthquake in the last 215 years that could have caused the observed 4 meter offsets that appear to represent the latest movement on the San Andreas fault near Cajon Creek. The combination of the most likely ages of the units in the excavation, the estimated timing of the incision of Qoa-a and the

historic record suggest that the last large earthquake produced by the San Andreas fault at Cajon Creek occurred during the early 18th century.

Cores from trees near Wrightwood (20 km NW of Cajon Creek) demonstrated that the 1857 earthquake produced rupture at least 20 km northwest of Lost Swamp (Meisling and Sieh, 1980). Therefore, the rupture probably terminated in the 20 km stretch northwest of Cajon Creek. If the location of the termination of the 1857 rupture is characteristic of previous earthquakes north of the Transverse Ranges, the record at Cajon Creek may represent the segment of the San Andreas fault southeast of the 1857 segment. Alternatively, the 1857 rupture may have been atypically short for earthquakes north of the Transverse Ranges, and the Cajon Creek record may otherwise be equivalent to the record at Pallett Creek (Sieh, 1978; 1984). The average recurrence interval (140 to 200 years, Sieh, 1984) and the timing of the previous event (1720 \pm 50 A.D., Sieh, 1984) at Pallett Creek supports the latter hypothesis.

The relatively short recurrence interval (less than 200 years) at both Pallett and Cajon Creeks seems to be at odds with what is known about the record to the north and south. At Wallace Creek in the Carrizo Plain, the recurrence interval appears to be from 250 to 450 years (Sieh and Jahns, 1984). If the long period of time since the last event on the southern part of the fault (this paper; Agnew and Sieh, 1978; Sieh, 1981) is typical, then longer recurrence intervals may be more characteristic of the two big bend regions of the San Andreas fault (the northern big bend is at MP and the southern one is north of Indio on Fig. 1) than of the relatively straight intervening segment. Alternatively, the record at Cajon Creek may be representative of the southern big bend and only the northern big bend has an average recurrence interval greater

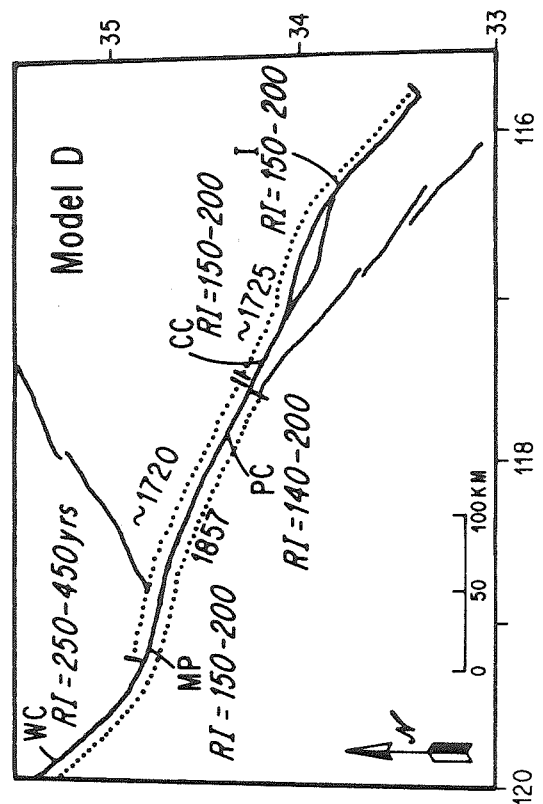
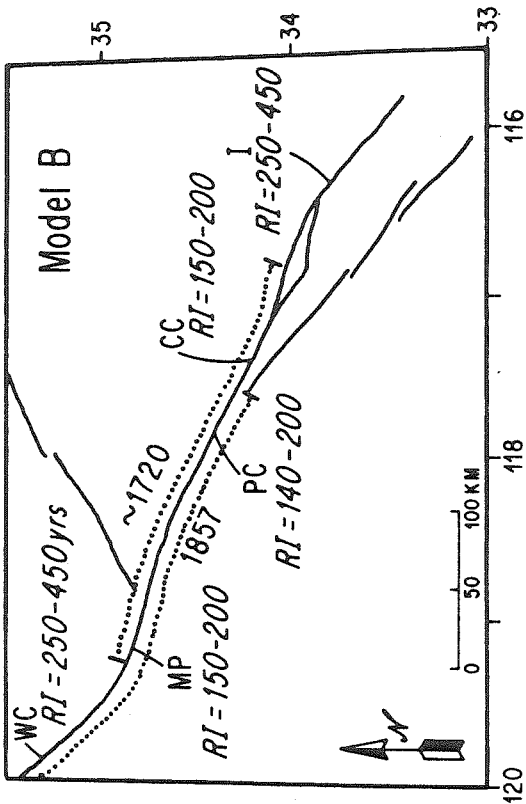
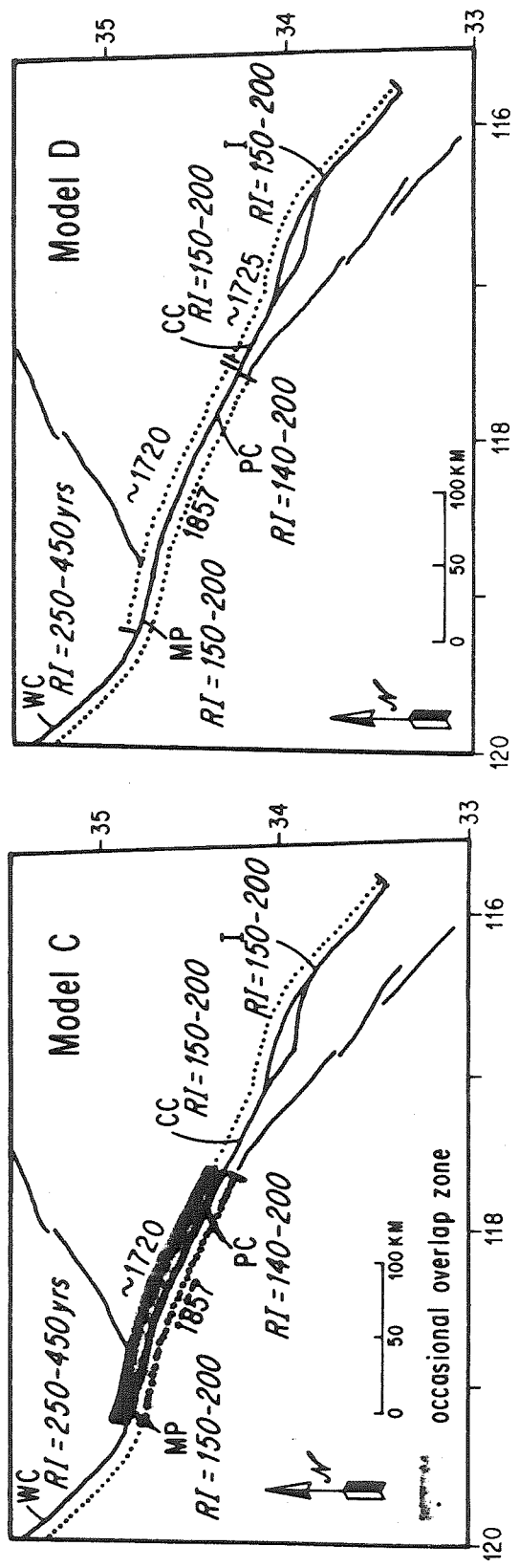
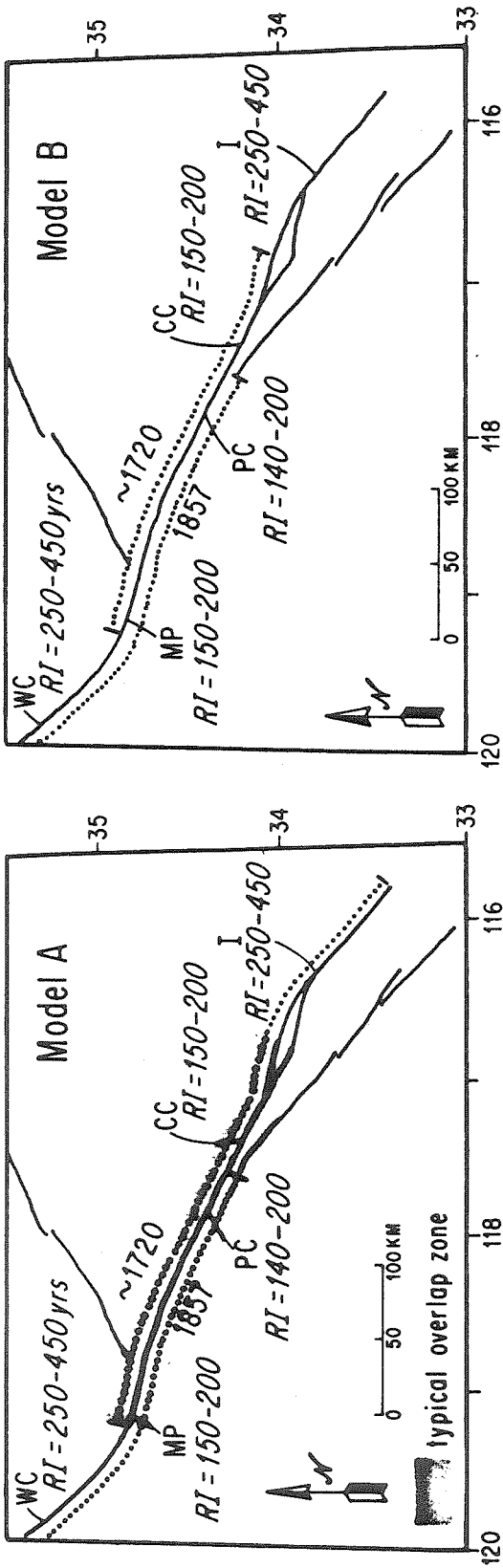
than 200 years.

Both of these hypotheses are consistent with what is known about the event before 1857. Apparently it occurred around 1720 and was associated with rupture at Cajon Creek, Pallett Creek (Sieh, 1984) and Mill Potrero (Davis, 1983) (Figs. 1 and 15). The event was associated with relatively minor deformation at Mill Potrero (Davis, 1983) and probably did not cause rupture at Wallace Creek (Sieh and Jahns, 1984), so it may have been an earthquake associated with rupture only between the bends, or one centered on the southern bend that ruptured through the straighter segments on each side.

The possibilities that the record at Cajon Creek and the other sites along the San Andreas fault suggest are summarized by four models in Fig. 15. In models A and B the southern big bend is assumed to have a recurrence interval similar to the northern big bend. In model A the higher average recurrence interval in between is explained by overlapping of events centered at each bend. The 1720 event was the last event on the southern bend and the 1857 event simply fell short of spanning the typical overlap zone, perhaps due to the relatively short time since the 1720 event. In this model the most likely next event would be a southern bend event, approximately 250 to 450 years after the 1720 event (about 1970 to 2170 A.D.), and would be associated with rupture from near the northern big bend to the southern end of the San Andreas fault.

In model B the shorter recurrence interval at Pallett and Cajon Creeks is due to extra events that rupture only between the bends. In this case the 1720 event was the last inter-bend event and the next event would most likely be a southern bend event from about Cajon Pass to the Salton Sea. In this model it would be expected about 250 to 450

Figure 2-15 - Models for the distribution of rupture associated with recent earthquakes to account for the recurrence intervals observed for the southern San Andreas fault. In models A and B the recurrence interval (RI) for the southern big bend region (near I) is assumed to be the same as that north of the northern big bend (WC). In models C and D the recurrence interval for the southern big bend region is the same as the record at Cajon Creek. In models A and C all events are inferred to be centered at the bends in the fault. In models B and D there are also events that rupture only the straight stretch between the bends. All of the models suggest that the most likely earthquake on the southern San Andreas would be one centered at the southern big bend. The timing and extent of rupture of the expected event varies with the model (see text).



1857 — Rupture associated with an earthquake

Figure 2-15

years after the last southern bend event. Because the timing of that event is unknown, it is not yet possible to estimate when the next event will occur. However, at least 215 years (the historic period) have passed since the last southern bend event.

In models C and D the southern big bend region is inferred to be represented by the record at Cajon Creek. In model C the record at Pallett Creek is caused by occasional overlap of events centered on either big bend. Events centered on either bend would rupture through the overlap zone only if sufficient time had passed since the previous event on the other bend. In this model the most likely next event would be a southern bend event that would rupture from the Salton Sea to Cajon Pass and through the overlap zone to the northern bend if it occurs long enough after the 1857 event. It would be expected to occur 150 to 200 years after 1720 (1870 to 1920 A.D.).

In model D the record at Cajon Creek is completely independent of the record to the northwest. In this case it is simply coincidence that the latest event at Cajon Creek appears to be the same as the prior event at Pallett Creek. For discussion it is assumed to be 1725 A.D. The shorter average recurrence interval at Pallett Creek relative to Wallace Creek would require extra events at Pallett Creek that do not reach either Wallace Creek or Cajon Creek; the 1720 earthquake would be such an event. In this model the most likely next event would be a southern bend event that would be expected to occur 150 to 200 years after the 1725 event (1875 to 1925 A.D.) and would rupture from Cajon Pass to the Salton Sea.

All of these models suggest that the next event will be centered on the southern big bend. At least two of the models indicate that the

event is overdue, in the sense that more time than the average interval between events has passed since the last event. The one model that suggests that the next event is not overdue (Model A) has the advantage of the smallest number of events required to explain the data and symmetry in how the two big bends acquire slip. However, only more data will determine which of these models, if any, describes the activity on the southern San Andreas fault.

ACKNOWLEDGMENTS

This paper represents a portion of a Ph.D. project under way by Ray Weldon at Caltech. L. Mezger, J. Hopeck, C. Finch, R. Miller and C. Prentice (among many others) helped in the field or prepared radiocarbon samples. M. Hill, C. Allen and W. Bull provided criticism and suggestions during the work that led to useful insights and reinterpretations. J. Tinsley, M. Stout and R. P. Sharp provided detailed criticisms of the original manuscript that led to substantial improvements. Most radiocarbon samples were run by A. Fairhall and J. Erickson at the University of Washington and two early samples were analyzed at the University of Miami by R. Johnston and J. Stipp. J. Mayne, assisted by K. Kronenfeld, drafted many of the figures and A. Branch typed several early drafts of the manuscript. We thank the many private individuals who allowed access to their land and the U.S. Forest Service for permission to trench at Lost Swamp. Financial assistance was provided by the USGS, through its Earthquake Hazards Reduction Programs, Contract Numbers 14-08-0001-16774, 18285, 19756 and 21275. Caltech Contribution No. 3983.

APPENDIX - Worst-Case Evaluation

In Figure A, the same data from which Figure 10 (in the text) has been constructed are presented without all of the inferences that have gone into constructing a reasonable geologic history. In Case No. 1, the channel in which Qoa-c was deposited could have accumulated some offset before the sediment was deposited in it. Also, the edge of the channel is defined by outcrops that could have been modified by later erosion by Cajon Creek and may not define the original channel shape exactly. Either of these unlikely scenarios would lead to less offset than was actually measured, making the slip rate a maximum.

Neither of these possibilities is likely. Had offset occurred before the deposition of Qoa-c, an upstream-facing bedrock protrusion would have formed and Cajon Creek would have eroded or, at least, beveled it. On the southwest side of the fault there is no evidence that the smooth curve of the pre-Qoa-c channel was disrupted until Qoa-c buried and, thereby, protected it from erosion. Since the onset of deposition of Qoa-c, Cajon Creek only has been low enough to modify the Qoa-c bedrock contact immediately before Qoa-a was laid down. The edge of the bedrock has not been modified since before the small landslide east of Cajon Creek was emplaced (Fig. 9). Its offset of about 150 m indicates that the landslide occurred while the creek was near the Qt-5 level, long before the creek was low enough to modify the offset contact. Therefore, the bedrock edge must have been established immediately before Qoa-c as discussed in the text.

Case No. 2 has two possible problems: first, the rate of filling of Qoa-c, indicated by the radiocarbon dates, could change dramatically above the youngest date. The top of Qoa-c (Qt-1) is absolutely bracketed between 8350 - 500 B.P. and 13.2 ± 1 ka, the age of the base of the

Figure 2-A - "Worst Case" estimates of the slip rate at Cajon Creek.

Each line represents the absolute limits of the dates and measurements, coupled with unlikely scenarios to explain the data (see text). The combination of all of the cases requires a rate between 20 and 28 mm/yr.

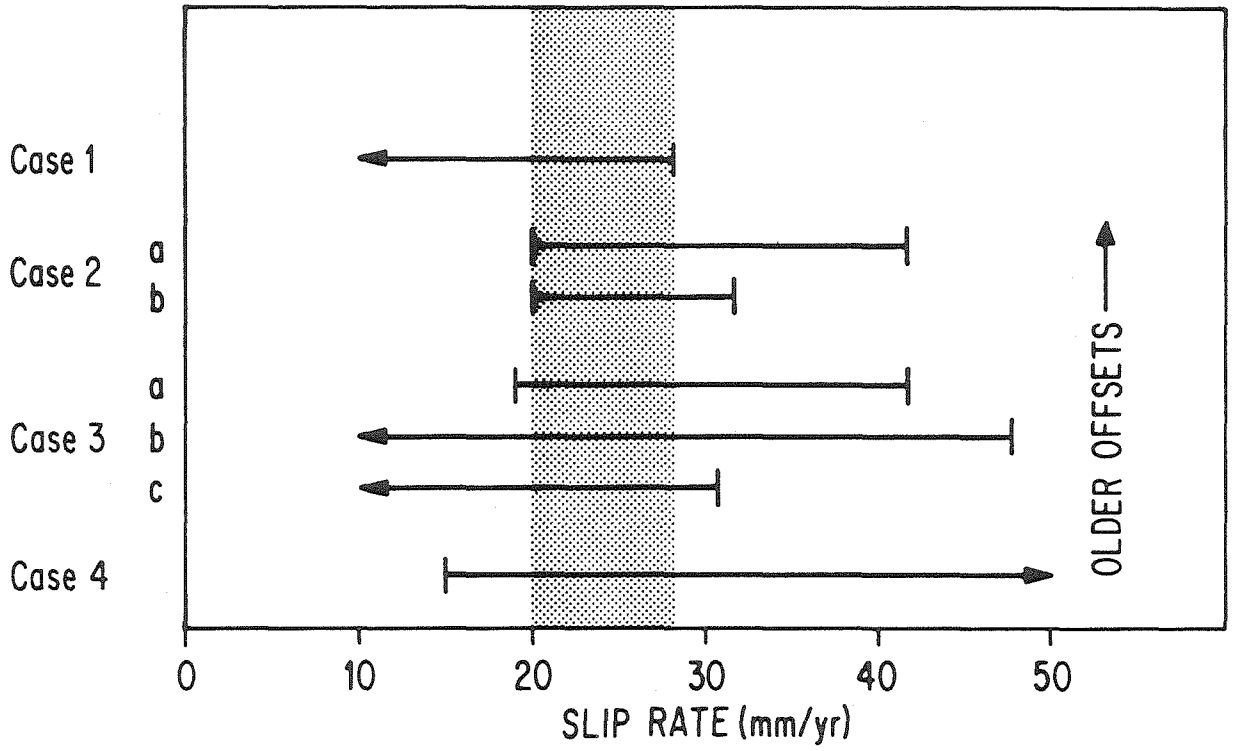


Figure 2-A

sediments on Qt-3 and the youngest date in Qoa-c. These limits yield a rate between 20 and 41 mm/yr (Fig. A, 2a). Another possibility is that Cajon Creek remained at the Qt-1 level long after it reached that level. The offsets measured on features incised into Qoa-c could therefore be minimums, yielding a minimum slip rate of 20 mm/yr (Fig. A, Case 2b). Neither of these cases is likely because of the lack of any geomorphic evidence that the creek remained at the Qt-1 level for any period of time and the necessity of having to incise and form two terraces (Qt-2 and Qt-3) between the deposition of Qoa-c and 8350 ⁺⁹⁵⁰ -500 B.P.

Case No. 3 has two possible problems that are considered here. First, the sediments in Lost Swamp lie on both Qt-2 and Qt-3. The history of the swamp and the continuity of the sediments suggest that the dated lake clays were deposited after Qt-3 was abandoned, but it is possible that the sediments on the Qt-2 terrace surface are older than Qt-3. If so, the 8350 ⁺⁹⁵⁰ -500 B.P. basal sediments are bracketed by the Qt-1 offsets of about 290 ⁺³⁰ -10 m and the Qt-3 offset of 200 ⁺³⁵ -20 m, limiting the rate to 19 ⁺³⁵ -41 mm/yr (Case 3a, Fig. A). Even if all of Lost Swamp rests on Qt-2, another constraint can be added because the formation of Pink River cut off the flow down Qt-3 into the swamp (Fig. 7). The flow of streams carrying pink sand ended by 5900 \pm 900 B.P. So Qt-3, across which these streams flowed, must be much older than 5900 \pm 900 B.P. This observation places a 47 mm/yr maximum limit on the rate since the abandonment of Qt-3 (Fig. A, 3b).

It is inferred that the sedimentation on Qt-3 at Lost Swamp began immediately after the Qt-3 level was abandoned by Lone Pine Creek. As Pink River had not yet captured the drainage from the north, streams flowing across Qt-2 and Qt-3 to the future site of Lost Swamp must have

continually provided water and sediment to fill the depression as soon as Lone Pine Creek abandoned the Qt-3 level. If some time passed before the lake clays began to accumulate, the 180-235 m offset of Qt-3 is a maximum. A maximum rate of 30 mm/yr can be calculated (Fig. A, Case 3c).

The only possible problem with Case No. 4 is the assumption that the sedimentation in the lake can be tied to the history of the streams that fed and drained it. Even if this causality is removed, the presence of pink sand in the fan on the edge of the swamp and mixed into the clay requires that some part of the lake predates the incision which isolated it from the flow from the north that delivered the pink sand. The incision is postdated by 145 ± 5 m, so a minimum of 15 mm/yr, based on the earliest age of the swamp, is calculated.

Because Figure A summarizes unlikely and extreme possibilities, the maximum additional error possible due to the discreteness of the slip events (estimated from the data in the excavation to be 300 years), has been added to all of the values. This assumes that all of the offset features formed immediately after earthquakes and that it has been 300 years since the last earthquake.

In summary, the "worst-case" analyses combine to suggest a slip rate of 20 to 28 mm/yr over the last 14,400 years because the combination of all of the "worst cases" require maximum or minimum rates that overlap in that range (Fig. A). This is not significantly different from the errors associated with the "best estimates". Only completely eliminating several of the cases or alternating changes in the rate can invalidate a slip rate of 20 to 28 mm/yr. However, if several of the "worst cases" are true, the inference of a constant slip rate is weakened.

REFERENCES

- Agnew, D. and Sieh, K., 1978, A documentary study of the felt effects of the great California earthquake of 1857, Seismo. Soc. Amer. Bull., v. 68, p. 1717-1729.
- Crowell, J.C., 1981, An outline of the tectonic history of southeastern California, in The geotectonic development of California, ed. Ernest, W.G., Ruby Volume #1, Prentice-Hall, New Jersey, p. 583-600.
- Davis, T., 1983, Late Cenozoic structure and tectonic history of the western "Big Bend" of the San Andreas fault and adjacent San Emigdio Mountains, Ph.D. Dissertation, Department of Geological Sciences, University of California, Santa Barbara.
- Dibblee, T.W. Jr., 1975a, Tectonics of the western Mojave Desert near the San Andreas fault, in San Andreas fault in Southern California: A guide to San Andreas Fault from Mexico to Carrizo Plain, ed. Crowell, J.C., Cal. Div. of Mines and Geology, Sp. Rep 118, p. 115-161.
- Dibblee, T.W. Jr., 1975b, Late Quaternary uplift of the San Bernardino mountains on the San Andreas and related faults, in San Andreas fault in southern California: A guide to San Andreas fault from Mexico to Carrizo Plain, ed. Crowell, J.C., Cal. Div. of Mines and Geology, Sp. Rep. 118, p. 127-135.
- Johnston, R.A. and Stipp, J.J., 1980, University of Miami Radiocarbon Dates XVIII, Radiocarbon, v. 22, p. 1116-1124.
- Keller, E.A., Bonkowski, M.S., Korsch, R.J. and Shlemon, R.J., 1982, Tectonic geomorphology of the San Andreas fault zone in the southern Indio Hills, Coachella Valley, California., Geol. Soc. Amer. Bull., v. 93, p. 46-56.

- Klein, J., Lerman, J.C., Damon, P.E. and Ralph, E.K., 1982, Calibration of radiocarbon dates: Tables based on the consensus data of the work shop on calibrating the radiocarbon time scale, Radiocarbon, v. 24, p. 103-150.
- Lisowski, M. and Prescott, W.H., 1981, Short-range distance measurements along the San Andreas fault system in central California, 1975 to 1979, Seismo. Soc. of Amer. Bull., v.71, p. 1607-1624.
- Meisling, K.E. and Sieh, K.E., 1980, Disturbance of trees by the 1857 Fort Tejon earthquake, California, Jour. Geophys. Res., v. 85, p. 3225-3228.
- Minster, J.B. and Jordan, T.H., 1978, Present-day plate motions, Jour. Geophys. Res., v. 83, p. 5331-5354.
- Minster, J.B. and Jordan, T.H., 1984, Vector constraints on Quaternary deformation of the western United States east and west of the San Andreas fault in Tectonics and sedimentation along the California Margin, eds. Crouch, J.K. and Bachman, S.B., Pac. Sect. S.E.P.M., in press.
- Morton, D.M. and Miller, F.K., 1975, Geology of the San Andreas fault zone north of San Bernardino between Cajon Creek and Santa Ana wash, in San Andreas fault in Southern California: A guide to San Andreas fault from Mexico to Carrizo Plain, ed. Crowell, T.C., Cal. Div. of Mines and Geology, Sp. Rep. 118, p.136-146.
- Rust, D.J., 1982, Radiocarbon dates for the most recent large pre-historic earthquake and for late Holocene slip rates: San Andreas fault in part of the Transverse Ranges north of Los Angeles, in Abstracts with Programs, Geol. Soc. Amer., v. 14, p. 229.
- Sharp, R.V., 1981, Variable rates of late Quaternary strike slip on the

- San Jacinto fault zone, So. Cal., Jour. Geophys. Res., v. 86, p. 1754-1762.
- Sieh, K.E., 1978, Prehistoric large earthquakes produced by slip on the San Andreas fault at Pallett Creek, California, Jour. Geophys. Res., v. 83, p. 3907-3939.
- Sieh, K.E., 1981, Seismic potential of the dormant southern 200 km of the San Andreas fault, EOS, Trans. Amer. Geophys. Union, v. 62, p. 1048.
- Sieh, K.E., 1984, Lateral offsets and revised dates of large prehistoric earthquakes at Pallett Creek, southern California, Jour. Geophys. Res., in press.
- Sieh, K.E. and Jahns, R., 1984, Holocene activity of the San Andreas fault at Wallace Creek, California, submitted to Geol. Soc. Amer. Bull.
- Stuiver, M., 1982, A high precision calibration of the AD radiocarbon timescale, Radiocarbon, v. 24, p. 1-26.
- Thompson, G.A. and Burke, D.B., 1973, Rate and direction of spreading in Dixie valley, Basin and Range Province, Nevada, Geol. Soc. Amer. Bull., v. 84, p. 627-632.
- Weber, G.E. and Lajoie, K.R., 1977, Late Pleistocene and Holocene tectonics of the San Gregorio fault zone between Moss Beach and Point Ano Nuevo, San Mateo County, California, in Abstracts with Programs, Geol. Soc. Amer., v. 9, p. 524.
- Weldon, R.J., Meisling, K.E., Allen, C.R. and Sieh, K.E., 1981, Neotectonics of the Silverwood Lake area, San Bernardino County: Report to the Calif. Dept. of Water Resources to accompany 50-sq. mile map of the NW San Bernardino Mountains around the Silverwood

Lake Reservoir, unpublished.

Weldon, R.J. and Meisling, K.E., 1982, Late Cenozoic tectonics in the western San Bernardino Mountains; Implications for the uplift and offset of the Central Transverse Ranges, in Abstracts with Programs, Geol. Soc. Amer., v. 14, p.243.

Weldon, R.J., 1983, Climatic control for the formation of terraces in Cajon Creek, Southern California, in Abstracts with Programs, Geol. Soc. Amer., v. 15, p. 429.

Yeats, R.S., 1983, Large-scale Quaternary detachments in Ventura Basin, southern California, Jour. Geophys. Res., v. 88, p. 569-583.

CHAPTER THREE

THE CAUSE AND TIMING OF TERRACE FORMATION
IN CAJON CREEK, SOUTHERN CALIFORNIA

by

Ray J. Weldon II¹
US Geological Survey
OEVE, MS 977
345 Middlefield Road
Menlo Park, California
94025

¹Also at Occidental College, Department of Geology, 1600 Campus Road,
Los Angeles, California, 90041.
Field work done while at Division of Geological and Planetary Sciences,
California Institute of Technology, Pasadena, California, 91125.

ABSTRACT

Cajon Creek in southern California has deposited a series of fill terraces in response to changes in climate. Cajon Creek has downcut at an average rate of 1 mm/yr for the last 700,000 years; this incision has been punctuated by at least 4 fill events that have been dated at about 500,000, 55,000, 17-6,000 and 2000-300 years BP. Channel aggradation during these periods occurred at rates as high as 20 mm/yr and was immediately followed by channel incision at rates as high as 5 mm/yr. Terrace deposits are thickest in the central part of the trunk stream and thin up and downstream. Deposits in the tributaries are thickest at their junction with the trunk stream and thin upstream. The shape, thickness and distribution of the fill deposits and terraces, coupled with a detailed understanding of the local tectonics, eliminate baselevel changes and tectonic deformation as primary causative agents in terrace formation.

Profiles of Cajon Creek, constructed for 1000 year intervals spanning the last 17,000 years, demonstrate that the locus of deposition during the 17-6,000 years BP event migrated upstream. Reincision began in the lower reach before filling started in the headwaters. The surface of the fill terrace represents only the local maximum heights of the migrating fill pulse and is not a surface everywhere occupied by Cajon Creek at any one time. Aggradational pulses left material up to 80 meters higher than the long-term level of the creek. The gradient in the central reach of Cajon Creek varied from 0.029 to 0.017 as the position of maximum deposition passed by. Net channel aggradation, calculated by subtracting contemporaneous erosion from the aggradation, occurred from about 16,000 to 10,000 years BP, and peaked sharply 13,500 years ago at a yearly rate 50% higher than the current total yearly sediment production. Actual peak sediment

production (net aggradation + material removed from the drainage) was an order of magnitude higher than it is today. Between 10,000 and 2,000 years BP the gravel was removed at a rate about 30% that of the maximum aggradational rate.

Fill terraces were formed by fluctuations in primary sediment supply that correlate with regional transitions from relatively wet and cold climate to dry and hot climate. These transitions created periods of hillslope instability that resulted in at least an order of magnitude increase in the sediment production. Similar series of fill terraces are found throughout the Transverse Ranges and are likely to be widely correlatable.

INTRODUCTION

This paper addresses the timing, distribution, and formation of the late Quaternary stratigraphy at Cajon Creek, southern California. Cajon Creek is a south-flowing stream that drains an area of 186 km² between the San Gabriel and San Bernardino Mountains in the Transverse Ranges. It descends from 2540 to 635 meters above sea level, flowing into the San Bernardino basin. About 100 km² of the drainage (Figure 1) was mapped by the author at a scale of 1:12,000 and a simplified map of the Quaternary deposits is presented in Figure 1. The rest of the drainage has been mapped by other workers (Foster, 1980; Woodburne and Golz, 1972; Dibblee, 1965; 1967) and contains the same deposits discussed here. Eighteen radiocarbon dates were obtained from sediments less than 15,000 years old, mainly to characterize the slip rate and recurrence interval for earthquakes on the San Andreas fault (Weldon and Sieh, 1985). The older sediments discussed here are dated by their offsets across faults and their relationship to underlying early Quaternary sediments (Weldon, 1984; Weldon et al., in preparation).

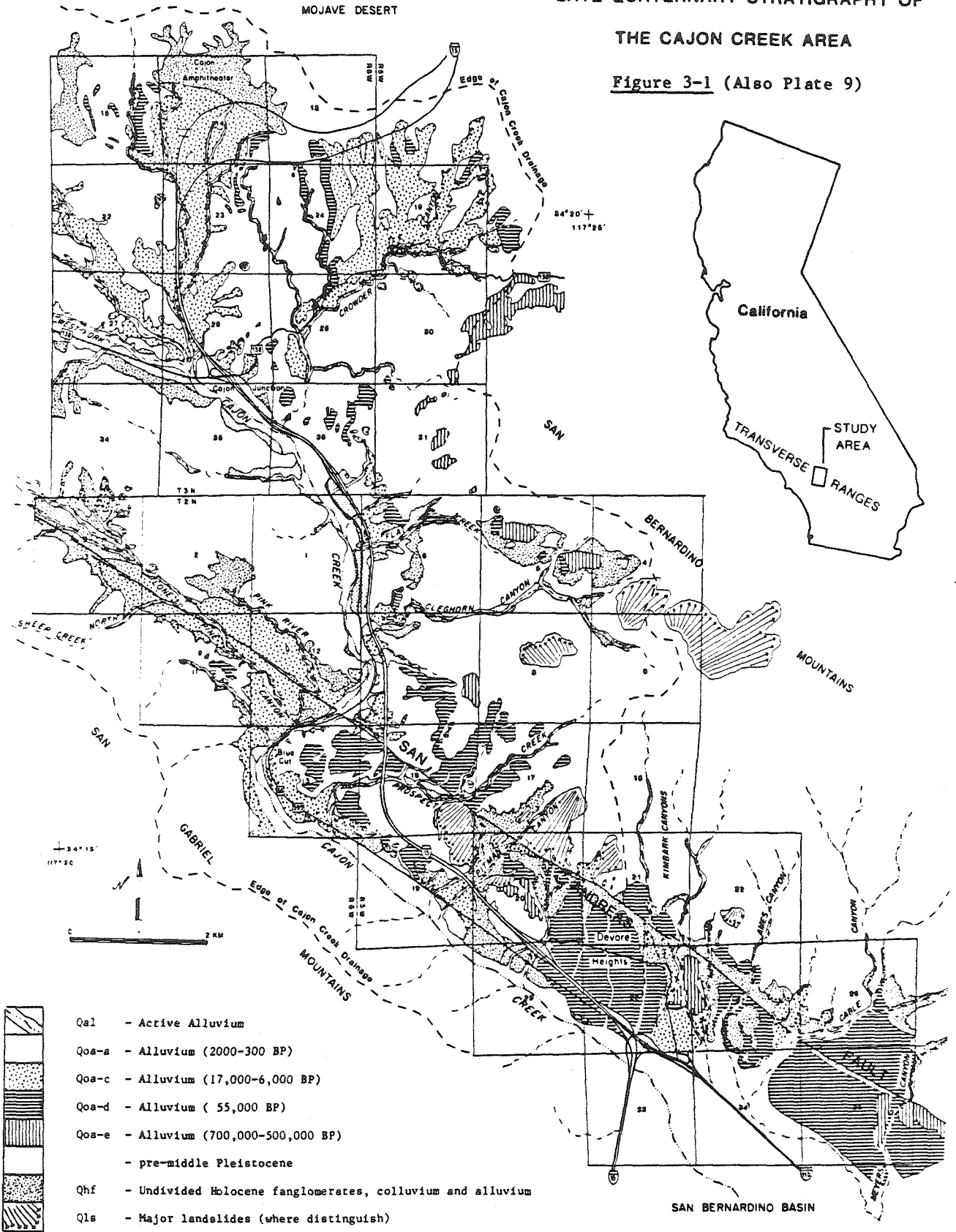
The study area includes essentially all of the transfer zone of the fluvial system (Zone 2 in the idealized system of Schumm, 1977), half of the production area (Zone 1) and the edge of the depositional basin (Zone 3). The focus of this paper is the formation and removal of deposits in the transfer zone of Cajon Creek.

The drainage basin of Cajon Creek is somewhat unusual in that the highest mountains and steepest slopes flank the middle part of the system. This is because capture has extended Cajon Creek through the Transverse Ranges into the relatively low Mojave Desert to the north (Fig. 1). The mountains create a rainshadow so that the greatest rainfall occurs on the

Figure 3-1 Distribution of the late Quaternary sediments in the Cajon Creek area. The study area includes most of Cajon Creek and several smaller canyons along the southern range front of the San Bernardino Mountains. Capture causes several deposits to cross the drainage divide.

LATE QUATERNARY STRATIGRAPHY OF
THE CAJON CREEK AREA

Figure 3-1 (Also Plate 9)



central part of the drainage, on the highest and steepest slopes. The average precipitation is 63 cm/yr but the "headwaters" (the farthest part of the creek from the mouth) receive only 25 cm/yr and the lower reach receives up to 81 cm/yr (rainfall map, Ahlborn, 1982, p. 19). Ninety percent of the precipitation falls between November and April, from Pacific winter storms. The unusual distribution of rainfall does not appear to have caused unusual deposits because adjacent creeks, with more "normal" rainfall distributions, contain the same units. The vegetation is mostly chaparral; the highest and wettest areas have pine forests and the driest, desert scrub. The upper half of the drainage basin is underlain by poorly indurated Cenozoic sediments and the lower part is underlain by bedrock.

STRATIGRAPHY

The late Quaternary sediments in Cajon Creek have been divided into two groups on the basis of the degree to which a deposit can be correlated throughout the drainage basin. The first group consists of the widely correlatable units; these are alluvial deposits found mainly along the trunk stream and major tributaries and formed during discrete periods of time. These deposits are named Qoa-a ("Quaternary old alluvium" -a), Qoa-c, Qoa-d, and Qoa-e. Their distribution is shown in Figure 1 and their relative heights in the middle of the drainage are shown in Figure 2. Qt-b ("Quaternary terrace" -b) is an erosional surface recognized throughout much of the drainage basin and is given a letter designation to indicate its importance in the sequence. Five other Holocene cut terraces are included on Figure 2 of this paper and are discussed in detail in Weldon and Sieh (1985). Other Pleistocene cut terraces have been mapped in Cajon Creek but are not discussed here (Weldon, unpublished maps). Qoa-N

Figure 3-2 Schematic cross-section through Cajon Creek showing the elevations and settings of the major alluvial units. The lower box is an enlarged cross-section of the inner gorge and shows some of the ^{14}C control. Qoa-N contains the Bruhnes-Matuyama magnetic polarity reversal, allowing the age of Qoa-e (which is slightly younger) to be inferred. The ages of both Qoa-d and e are also inferred from their offsets by the San Andreas and several other faults.

SCHEMATIC SECTION THROUGH CAJON CREEK

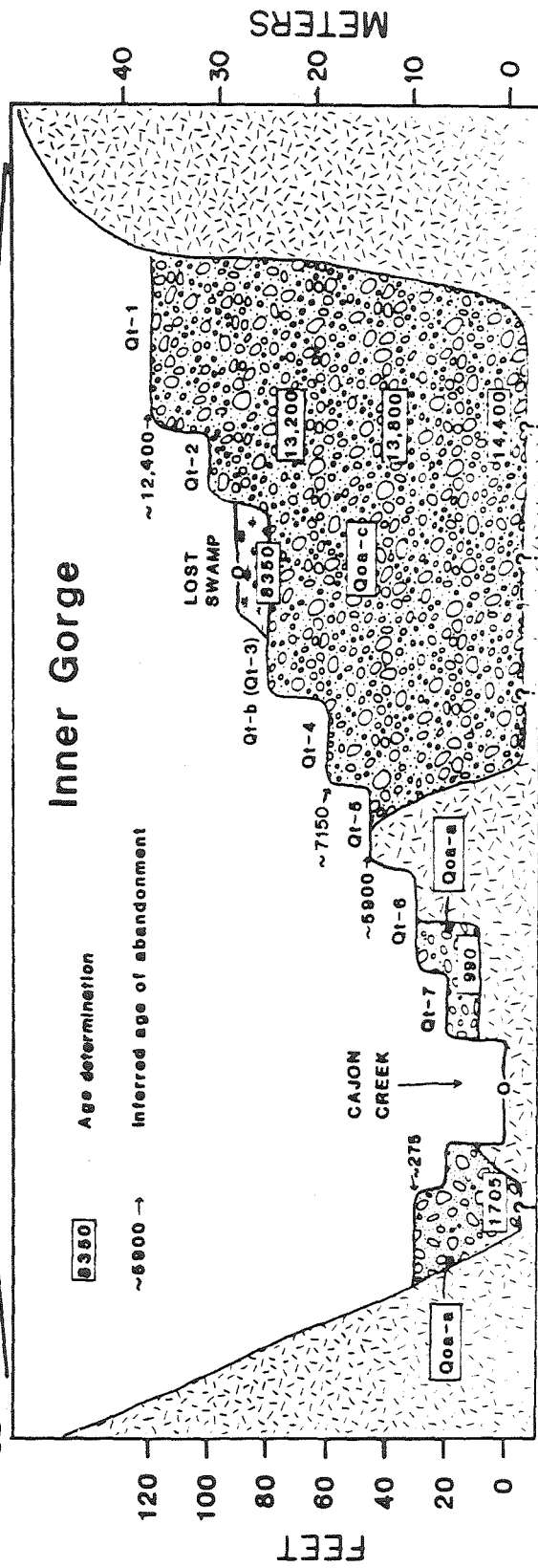
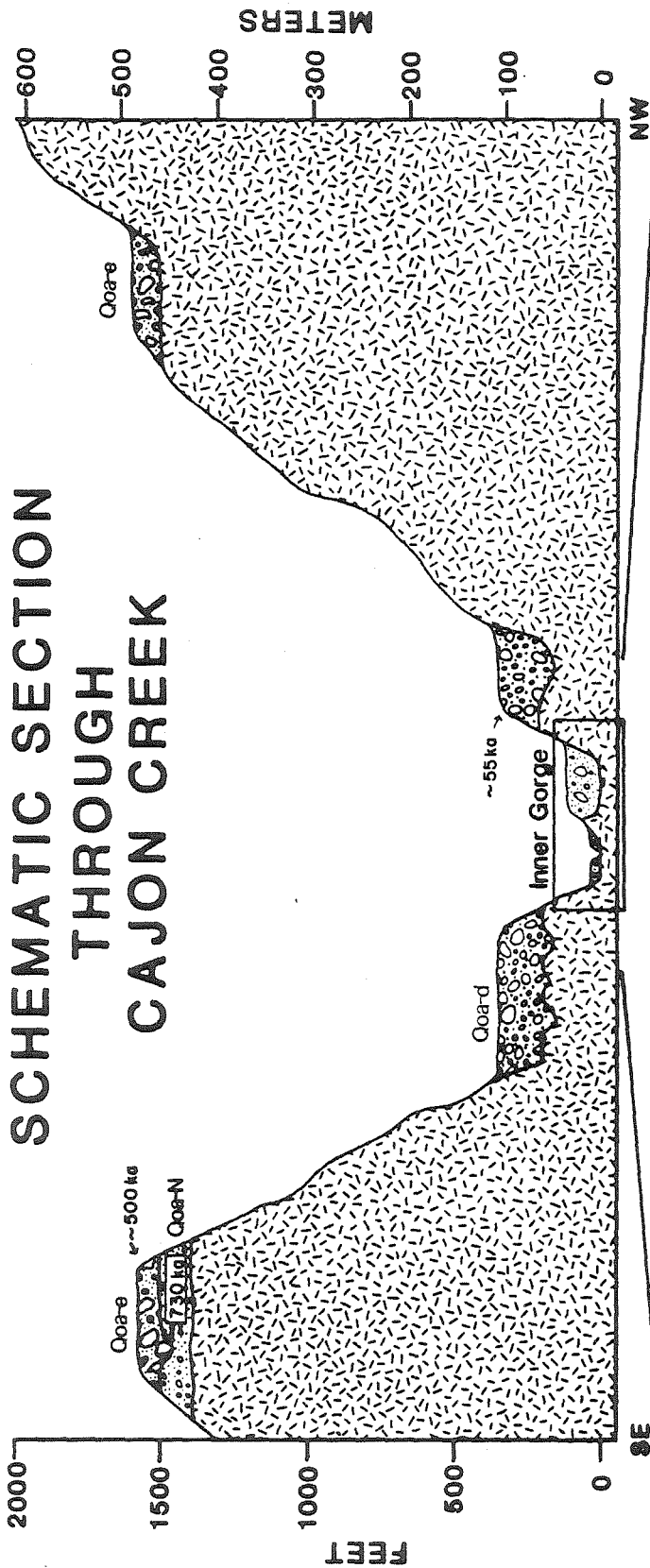


Figure 3-2

("Older Alluvium" of Noble, 1954) and older Quaternary deposits predate the incision of the current drainage and are discussed elsewhere (Foster, 1980; Weldon et al., 1981; Weldon, 1984; Weldon et al., in preparation). Qoa-e was deposited immediately after the onset of incision that continues today as Cajon Creek captures more and more of the Mojave River drainage.

The second group consists of units deposited during isolated events or in unique settings, like landslides, colluvium, scarp and sag pond deposits that are not generally correlative with similar deposits in the area. Fan deposits and fluvial gravels that were not formed during the discrete pulses of deposition common to the whole system are also included in the second group. Major landslides are distinguished in Figure 1 but the rest of the second group are combined as Qhf ("Quaternary, mainly Holocene, fan deposits") because Holocene fan deposits dominate this group.

It is argued below that the first group of deposits owe their existence to variations in the relative sediment supply caused by changes in the climate. The systems responsible for the deposition of sediments in the second group may also have responded to climate change but they were not forced back and forth across the depositional-erosional threshold by the climatic changes, so it is difficult to demonstrate any relationship. Because the first group of deposits formed during discrete periods of time separated by long hiatuses, they can be distinguished throughout most of the drainage basin. These units are correlated by their geomorphic position and the degree of soil development on undisturbed surfaces. Locally, thicknesses of deposits, heights above the active alluvium or position relative to some other unit were useful for correlation. Absolute heights or relative heights in different parts of the basin could not be used because of the steep and variable original dip of the deposits

and the dramatic variations in thickness and height of the units throughout the area.

Detailed field descriptions and laboratory analyses of the soils developed on all of the units discussed here are summarized in McFadden and Weldon (1984 and in review). The 5 major correlatable late Quaternary units (Qoa-a through e) are of such different ages that distinctive soils developed on their upper surfaces are easily recognized.

The Quaternary units are divided into correlatable and uncorrelatable units instead of standard lithologic divisions to highlight the units that are represented throughout the basin. These can be studied to understand how the total system acted through time. Also, determining which parts of the system act in unison and which do not yields insights into the responsible processes and permits rational interpretation of dates from different deposits. The distinction between fan deposits and gravels deposited by streams responding to a climate change and those formed continuously or out of phase with climatic fluctuations can be subtle. To illustrate this distinction and to gain insights into possible causes, several examples of the Qhf deposits are presented after the correlatable units are discussed in detail.

Qoa-e

Qoa-e consists of two groups of deposits formed in very different settings. In the northeast part, Qoa-e is a major fluvial deposit that closely postdates the onset of incision which followed the deposition of Qoa-N (Fig. 2). Qoa-N at Cajon Pass is about 0.7 my old and contains the Bruhnes-Matuyama magnetic polarity reversal near its base (Meisling, 1983; Weldon et al., in preparation). It is inferred that Qoa-e is about 0.5 my old based on its relationship to Qoa-N and its offset by several faults

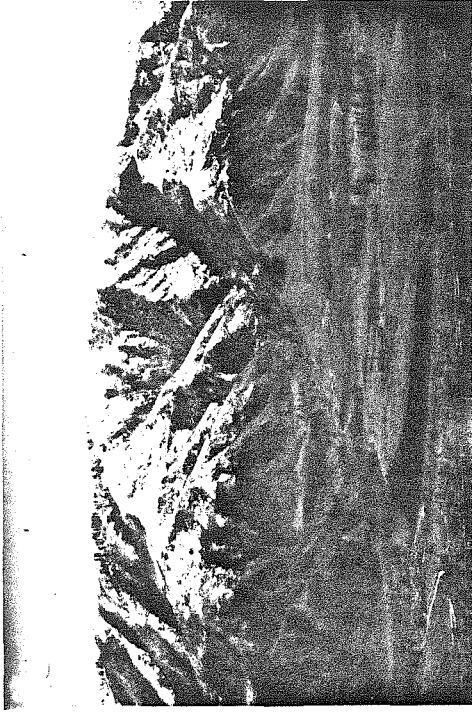
(Weldon et al., 1981). Qoa-e was formed by a discrete pulse of channel aggradation interrupting the downcutting that began after deposition of Qoa-N.

Qoa-e is also found on the northern edge of the San Bernardino basin in the southeast part of the area (Fig. 1). There, Qoa-e consists of fan deposits laid down during a major pulse of fan growth out onto the basin floor. The two sets of deposits are correlated by their extremely well-developed soils and the fact that each represents a major period of aggradation that occurred within long periods of downcutting or nondeposition. The excellent preservation of Qoa-e and the apparent lack of any major deposits preserved between Qoa-e and Qoa-d (deposited about 55,000 years ago) suggest that no deposits as large as these were formed during the interval between them.

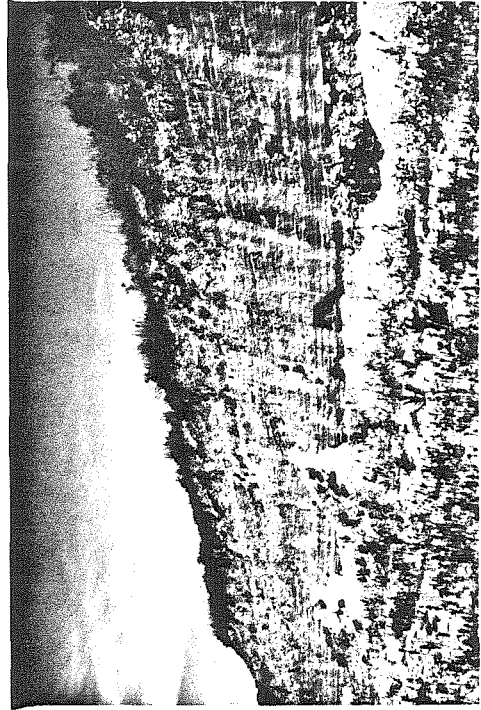
Qoa-d

The oldest, most widespread, and most voluminous late Quaternary unit deposited in Cajon Creek is Qoa-d. It can be recognized throughout the area on the basis of soil development, its unique geomorphic position, and, in many areas, by simple physical continuity between outcrops. For example, an almost continuous skirt of Qoa-d wraps around the northwest edge of the San Bernardino Mountains from Cleghorn Canyon to Cable Canyon (Figs. 1 and 3a). Qoa-d mantles an irregular topography to depths of as much as 85 meters. Many of the tributaries and the present topography close to the level of Cajon Creek are the result of the rapid reincision following the deposition of Qoa-d. The channels incised into Qoa-d are referred to as "inner gorges" and can be recognized in many of the major local streams. Figure 2, for example, shows Cajon Creek's "inner gorge". In Cajon Creek and other major drainages Qoa-d is a

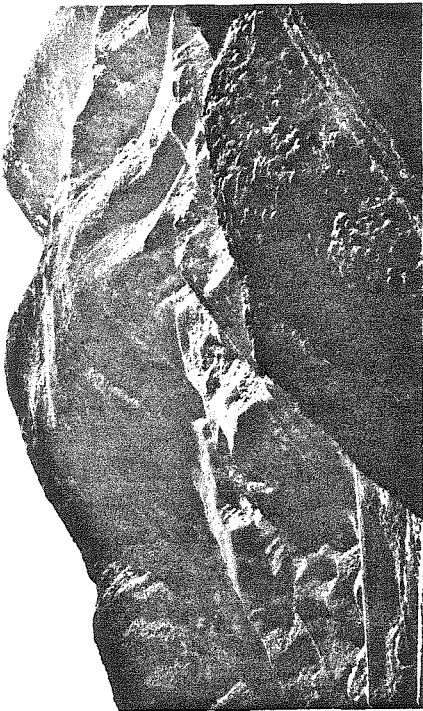
Figure 3-3 Photographs of the fill deposits: a) Qoa-d forms a continuous skirt around the mountain in the middle of the photo (sections 7, 17, 18, T2N R5W, Fig. 1). b) A Qoa-d fan built out onto the floor of the San Bernardino basin by Cable Canyon (sections 26, 27, 34, 35, T2N R5W, Fig. 1). c) Almost 40 m of Qoa-c exposed in a gravel pit at the mouth of Pitman Canyon (NW 1/4, section 7, T2N R5W, Fig. 1); 2 ^{14}C dates are from this deposit. The Qoa-a level is visible in the foreground. d) Qoa-a fill at Pitman Canyon (SE 1/4, section 19, T2N R5W, Fig. 1); a ^{14}C sample was found at the base of this deposit.



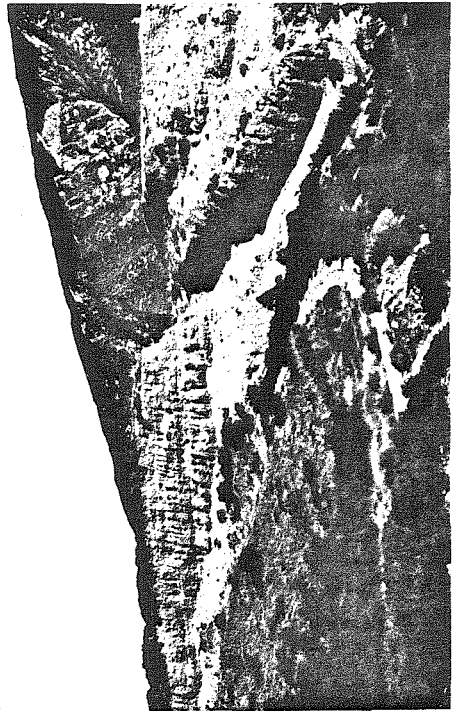
b



d



a



c

Figure 3

fluvial fill. Along the range front and at the mouths of smaller streams, Qoa-d is represented by thick fan deposits extending out onto the basin floor (Figs. 1 and 3b; generally Qoa₁ of Morton and Miller, 1975).

The Qoa-d fill in Cajon Creek has been almost completely removed by erosion. However, just east of Cajon Creek offset across the San Andreas fault forced Prospect Creek to incise a new channel, thereby preserving the Qoa-d deposited in the old channel (Fig. 1). The upper and lower surface of Qoa-d in the old Prospect Creek channel can be mapped on both sides of the San Andreas fault. In Figure 4, the 1.3 to 1.4 kilometers of right-lateral offset have been restored so that the thickness and gradient north and south of the San Andreas fault can be compared. The figure demonstrates that no measurable vertical offset or abrupt thickness change occurs at the fault. Apparently, the deposit formed so quickly that the San Andreas fault had little effect on its thickness or shape. The deposit thickens downhill to just below the fault and then maintains a relatively constant thickness to Cajon Creek.

Qoa-d is inferred to be about 55,000 years old, based on its horizontal offset and the slip rate of the San Andreas fault. Weldon and Sieh (1985) have shown that the slip rate has been 2.5 cm/yr for the past 15,000 years, and Weldon (1984; Weldon et al., in preparation) has demonstrated that the same rate holds for most of the Quaternary. The errors on these slip rates suggest that the fault can be used to date a unit it offsets with an accuracy of ± 15%. Also, the length of time spanned by the deposit can be estimated from the difference in offsets of the channel into which the unit was deposited and the channel postdating the fill. This difference is about 100 to 200 meters, yielding a deposition time of 4,000 to 8,000 years, comparable to the well-dated Qoa-c discussed below.

Figure 3-4 Longitudinal cross sections through Qoa-d at Prospect and Cable Creeks, showing the top and bottom of the deposit. Points indicate topographic control. 1.3 km of lateral motion has been restored across the San Andreas fault. Arrows indicate sense of dip-slip motion and A (away) and T (toward) indicate the sense of strike slip motion. Notice that the thickness and slopes of the deposits do not change appreciably at the fault zone.

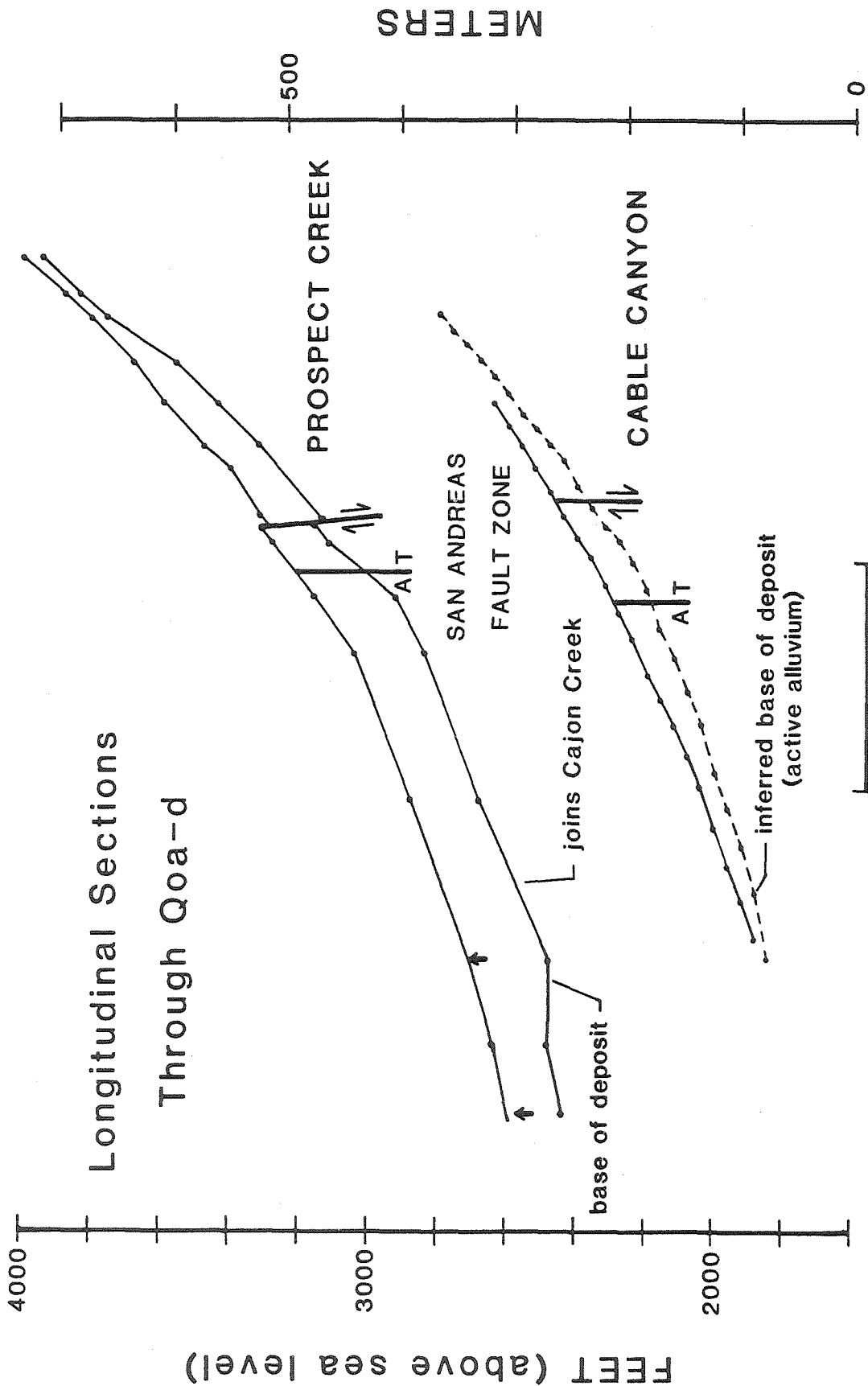


Figure 3-4

Restoring the 1.3 to 1.4 km offset measured at Prospect Creek removes the deflection of Cajon Creek, restores the offset of the thickest part of the Cable Canyon fan and aligns the fan deposits that underlie Devore Heights with the Qoa-d deposits at the mouth of Ames and the Kimbark Canyons north of the fault (Fig. 1). Therefore, most of what is mapped as Qoa-d must be contemporaneous with the deposit at Prospect Creek.

The Cable Canyon fan has been deeply incised so an estimate of the thickness and shape of this Qoa-d deposit can be made there as well (Fig. 4). The upper surface is well preserved and is fan-shaped. Exposures of bedrock and the older Qoa-e remnants under the fan indicate that the base of the deposit has about the same profile as the current stream. The thickest exposures of Qoa-d here (20 m) are at the range front (defined by the San Andreas fault in Fig. 1). The deposit certainly thins upstream and is inferred to thin downstream as well. If it does not thin downstream the base of Qoa-d would have to be at least 20 meters below the active alluvium at the south edge of the fan; this appears to be unlikely from the distribution of the bedrock and Qoa-e.

Qoa-d in Cajon Creek is also thickest in the middle and thins up and downstream (Fig. 5). While the preservation of Qoa-d is not as good as at Prospect or Cable Creeks, both the base and the upper geomorphic surface can be found in enough places to demonstrate its lenticular shape. The deposit appears to have been thickest in the same part of the creek where the younger deposits are thickest (discussed below). Unlike the Qoa-d at Cable and Prospect Creeks the thickest part is well within the mountain range. The significance of this difference is discussed below.

Qoa-c

The best preserved and most continuous unit in Cajon Creek is Qoa-c.

Figure 3-5 Longitudinal sections through Qoa-d and Qoa-c in Cajon Creek. The heights and positions of the data points are presented relative to the valley profile of the active alluvium. The base of Qoa-c is essentially at the same elevation as the active channel. Points without error bars are heights measured at the creek. Points with error bars are extrapolated to the trunk stream from deposits preserved in tributaries or on hillsides. Both Qoa-c and Qoa-d are thickest in the central portion of the drainage and thin to nothing up and downstream. The difference between the base of Qoa-d and the active wash represents long-term downcutting.

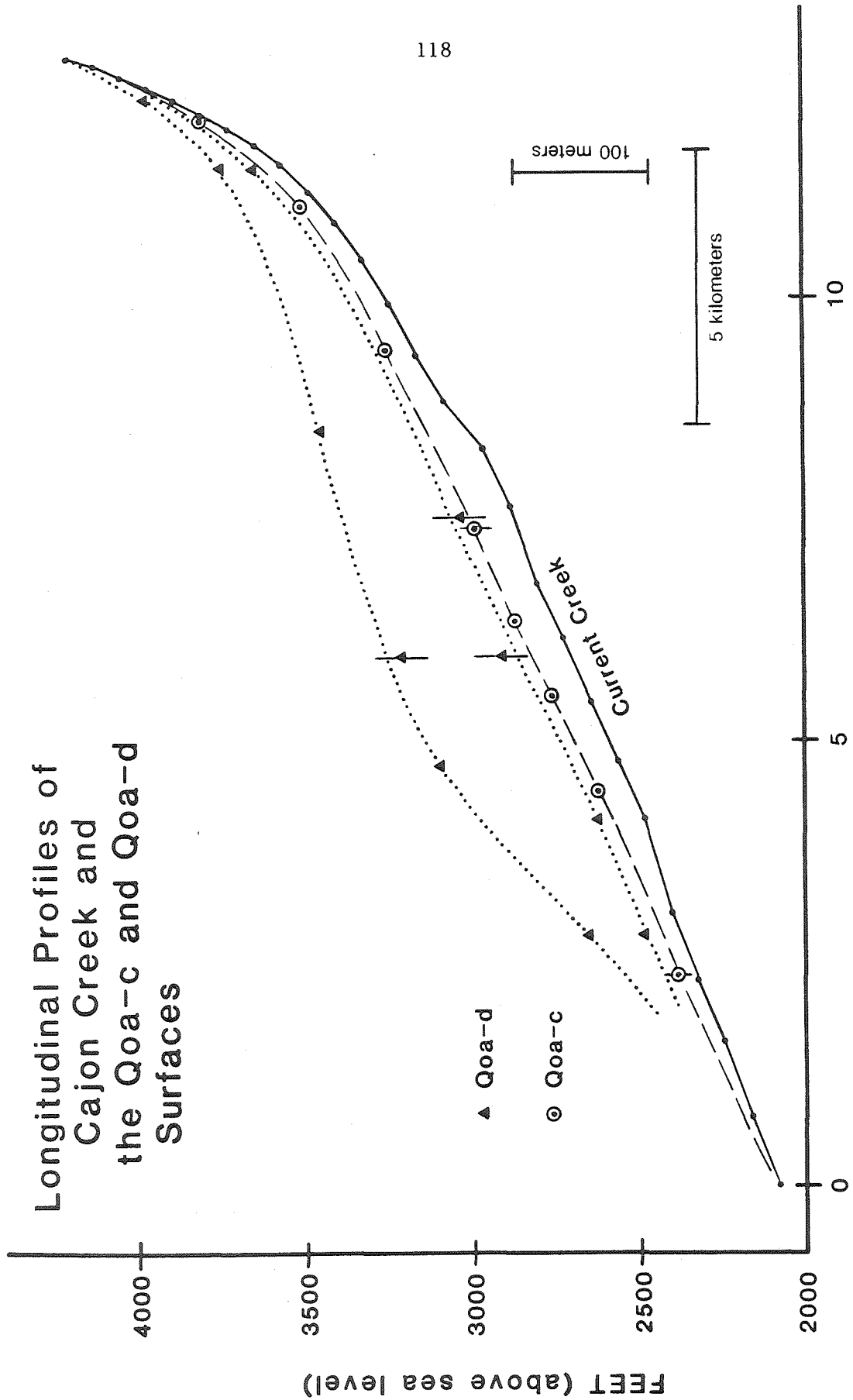


Figure 3-5

(vertical exaggerated 20X)

It can be recognized by its soil, its geomorphic position as the highest fill in the inner gorge (Fig. 2 and 3c), and its physical continuity along much of Cajon Creek (eg., Crowder and Lone Pine Canyons, Fig. 1). It is the most widespread unit that could be dated with radiocarbon and is offset in several places by the San Andreas fault, so considerable effort was expended to date it throughout the area. The height of the top of Qoa-c is determined in most places where the undisturbed geomorphic surface at the creek is preserved, but the heights at a few points are extrapolated from deposits preserved in tributaries (Fig. 5; extrapolated points have error bars). The base of Qoa-c in Cajon Creek can be found, locally, in the upper 1/3 of the drainage basin; elsewhere, the nature of the bedrock Qoa-c contact close to Cajon Creek suggests that the base is just below the active alluvium. In several tributaries the base of Qoa-c can be found above the active alluvium. Extrapolating these exposed lower surfaces of Qoa-c to the trunk stream also indicates that the base of Qoa-c is just below the active alluvium. Near the mouth of the drainage the base of Qoa-c is not exposed. The thickness of the deposit is believed to approach zero at the edge of the San Bernardino basin for two reasons. First, the presence of bedrock, Qoa-e, Qoa-d, Qoa-c, and the active alluvium at about the same height on the basin's edge indicates that little long-term degradation or aggradation has occurred there. Second, exposures of both the top and bottom of Qoa-d indicate that that fill does become very thin as it approaches the basin edge and the shape of Qoa-c, where both the top and bottom are exposed, mimics Qoa-d (Fig. 5). The difference in height between the upper Qoa-c surface and the active alluvium is therefore taken as the approximate thickness of the deposit where the base is not exposed.

Figure 3-6 Height of Qoa-c above Cajon Creek. In the upper part of the drainage the height is the same as the thickness of Qoa-c, and is inferred (see text) to approximate the thickness in the lower part as well. Major tributaries and the San Andreas fault are included for reference. Notice that the shape and thickness of Qoa-c does not change at the fault.

Figure 6

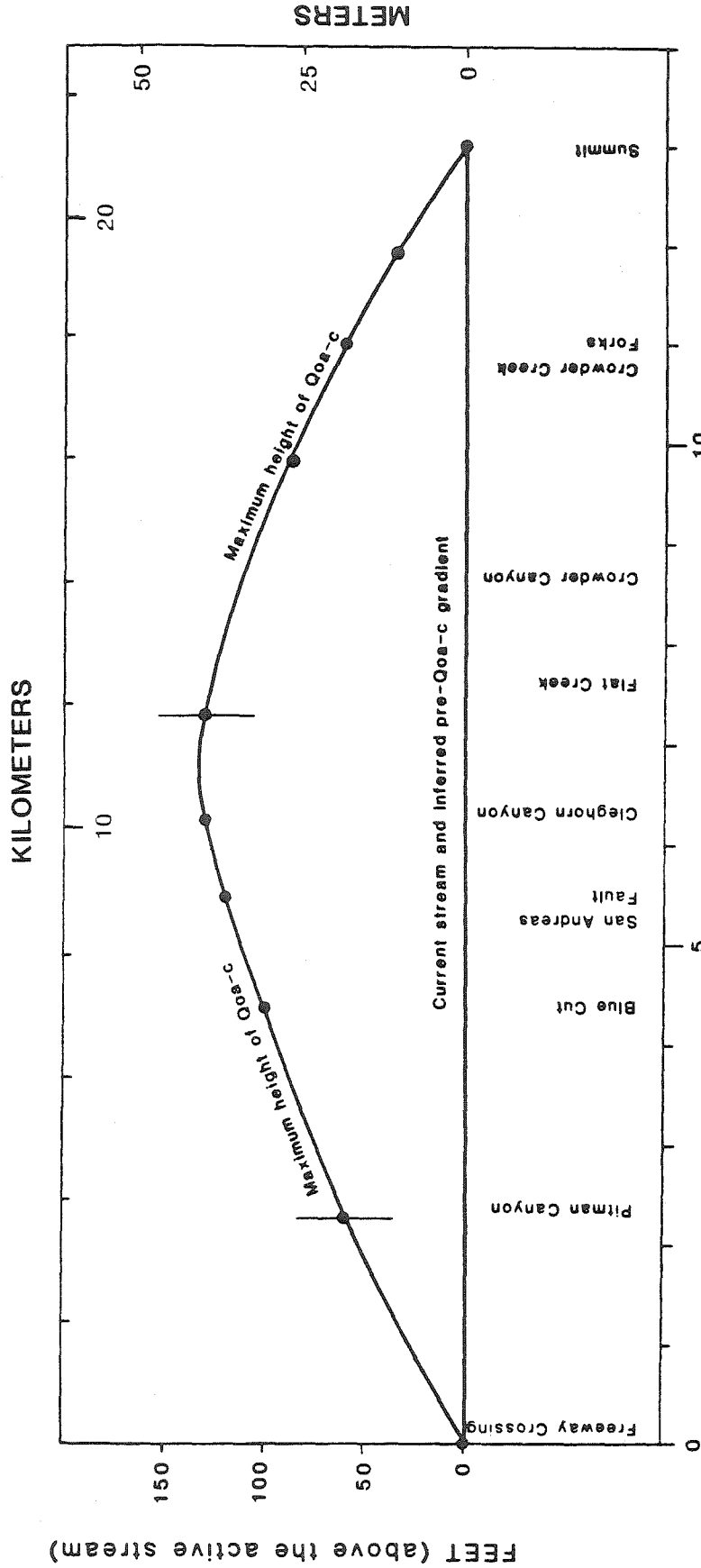


Figure 3-6

MILES (upstream from the basin edge)

vertical exaggerated 200X

The height of Qoa-c above the active alluvium is replotted in Figure 6 to emphasize the distribution of the thickness of Qoa-c along Cajon Creek. This is a simpler presentation of fill terrace data because stream profiles are commonly irregular, and fill terrace profiles closely parallel the irregularities in the active profiles (Bull, 1979; Leopold and Bull, 1979). This presentation focuses attention on the changes in the profiles throughout the system and not on the shape of the system itself.

The data for the thickness of Qoa-c forms a smooth lens-shaped curve that tapers at both ends of the drainage. The symmetry of the deposit's thickness is largely due to the choice of drawing the section up Crowder Canyon. If a longer or shorter branch of Cajon Creek were chosen, the lens would be correspondingly less symmetric. Many fill terraces in arid environments diverge from the active alluvium downstream from their headwaters (Leopold and Bull, 1979; Bull, 1979). The downstream convergence near the mouth has not been as widely recognized in the literature.

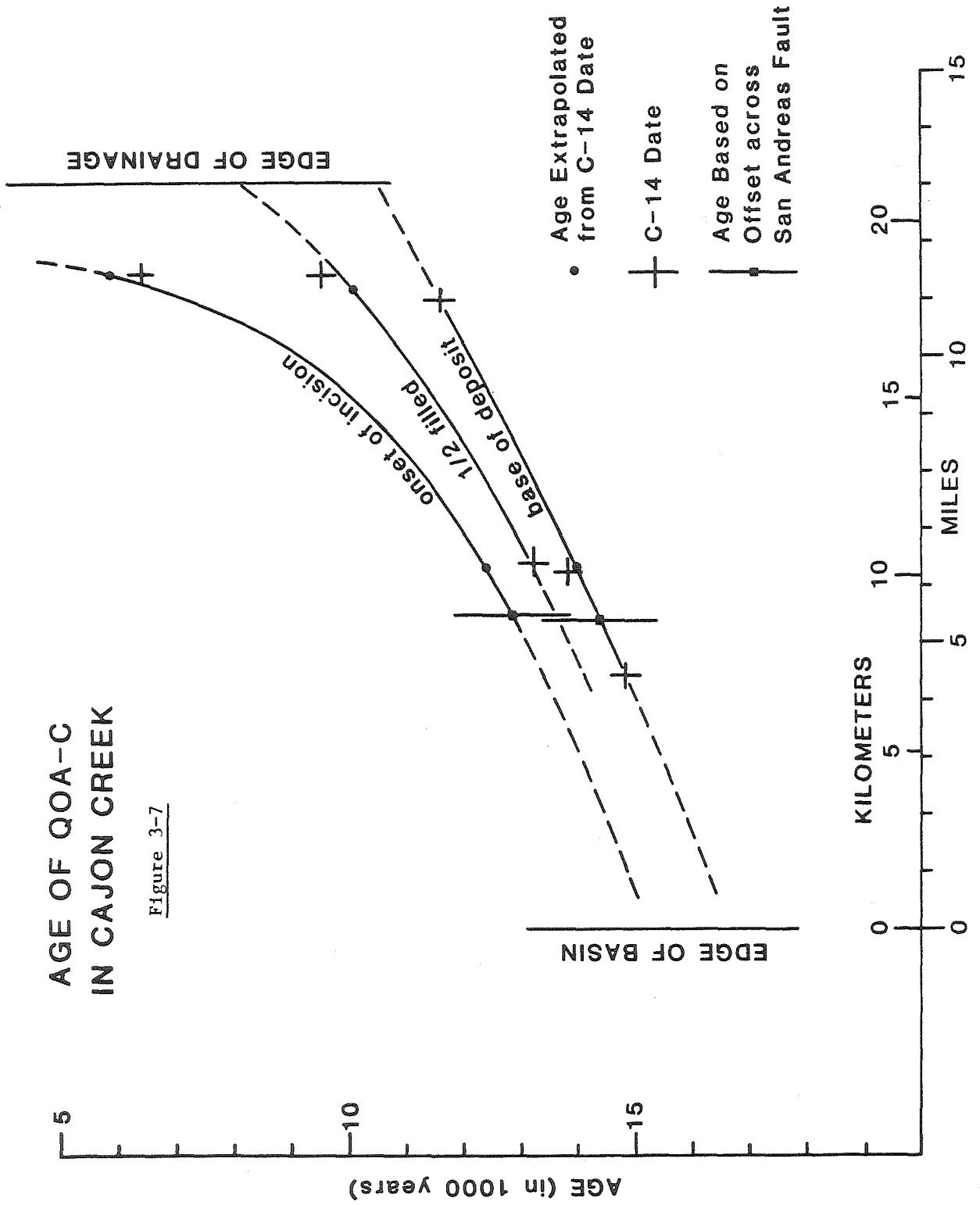
The lenticular shape of Qoa-c and Qoa-d in Cajon Creek demonstrates that the deposits were not formed in response to baselevel changes because fills formed by raising baselevel are wedge-shaped, not lens-shaped accumulations (Leopold and Bull, 1979). As will be discussed below, the the different shapes of deposits in adjacent drainages can be used to eliminate tectonic control for their formation as well.

To determine the timing of the accumulation of Qoa-c the dates in Qoa-c were plotted against their position upstream (Fig. 7). The three youngest dates in Qoa-c are within the range of dendrochronologic calibration and are so corrected. The older radiocarbon dates were recalculated with a half-life of 5730 years and assigned errors of ± 1000 years

Figure 3-7 The age of Qoa-c in Cajon Creek, plotted as a function of distance upstream. The ages have 95% confidence limits in calendar years (see text). The extrapolated ages are based on the sedimentation rates between samples. The ages at the San Andreas fault are based on the offsets of the base and top of the deposit, and the slip rate of the fault (see text). Lines are drawn through the dates at the base of the deposit, the 1/2-filled level, and the onset of incision. The age of the deposit clearly decreases upstream and spans a longer period of time near the headwaters. Extrapolation of the curves indicates that deposition began about 17,000 years BP at the mouth of the stream and continued well after 6,000 years BP near the headwaters.

AGE OF QOA-C IN CAJON CREEK

Figure 3-7



to assure 95% confidence in real age (Klein et al, 1982), despite having very narrow C-14 age limits. New C-14 calibration curves (Stuiver, written communication, 1985) indicates that these limits contain the actual ages for the past 13,000 years. However, the actual ages may be slightly older than the mean ages used here for the oldest dates in Qoa-c. The sedimentation rate between the two dates in Qoa-c at the mouth of Cleghorn Canyon was used to extrapolate the age to the top and the bottom of the deposit. The extrapolation appears to be justified because it yields ages for units that are consistent with their offsets by the San Andreas fault.

The base of Qoa-c at Blue Cut is about 14,800 years old and the extrapolated base at Cleghorn Canyon is 14,000 years old, so the onset of Qoa-c deposition is estimated to have occurred about 14,400 years ago at the San Andreas fault (Fig. 7). About 350 m of offset on the San Andreas fault have accumulated since the onset of Qoa-c deposition, which yields a slip rate of 25 mm/yr (Weldon and Sieh, 1985). Extrapolating the fill rate to the surface, and assuming that incision began as soon as aggradation ended (see Weldon and Sieh, 1985, for supporting evidence) indicates that incision began about 12,400 years ago. Offsets of streams and terrace risers, formed by the post-Qoa-c incision, are as great as 290 meters, again yielding a slip rate of 25 mm/yr (Weldon and Sieh, 1985). Two other radiocarbon dated terraces (Qt-3 and Qt-5, Fig. 2) and paleomagnetically dated middle Pleistocene deposits have offsets that also yield the same slip rate (Weldon and Sieh, 1985; Weldon, 1984; Weldon et al., in preparation). Because the extrapolated ages for the top and base of Qoa-c require consistent slip rates, the extrapolation is almost certainly valid and the surface of Qoa-c near the San Andreas fault is

late Pleistocene.

In Crowder Canyon there are dates from 3 stratigraphic positions: the base, 2/3 of the way to the top and just below the top of the section (Fig. 7). It is clear from the dates that the upper several meters formed much more slowly than the rest of the deposit. This change in sedimentation rate accompanies an obvious change in the character of the sediments. The bulk of the deposit is sandy gravel, mainly reworked from the early Quaternary deposits that ring the northern edge of the basin. The upper part of the deposit fines upward and the source of most of the sediments appears to be the underlying Crowder Formation, reflecting an increase of sheet wash off the surrounding low hills at the expense of channel flow from the headwaters. Also, the presence of sand dunes and other eolian deposits in upper Cajon Creek suggest an important eolian component in the fine-grained uppermost Qoa-c deposits.

Curves drawn through the basal dates, the 1/2 filled level and the top, which represents the onset of incision, demonstrate a marked decrease in the age of Qoa-c upstream (Fig. 7). The onset of Qoa-c deposition migrated upstream at an average rate of about 3.5 m/yr. Also, the deposit took longer to form upstream in Crowder Canyon than near the San Andreas fault. The onset of incision migrated upstream behind the aggradation but appears to have progressively lagged as it approached the headwaters. This is consistent with the observation that the edges of the drainage have only recently begun to incise. The dates and the geologic observations indicate that Qoa-c deposition actually spanned most of the last 17,000 years. However, at any given point in Cajon Creek the deposition lasted only a few thousand years. Also, it is clear from Figure 7 that the bulk of the deposit, even in Crowder Canyon, had been laid down by

10,000 years ago and the sedimentation rate during the Holocene was very slow. Perhaps the material younger than 10,000 years old in Crowder Canyon should not be included with Qoa-c, but there is no depositional break in the unit, only a progressive change in character toward the top.

Qoa-a

The youngest extensive prehistoric deposit in Cajon Creek is Qoa-a. It is thickest and most easily recognized in the central part of the drainage, between Pitman and Crowder Canyons (Fig. 1), where the older units are also thickest. Qoa-a deposits are about 2 orders of magnitude less voluminous than Qoa-c and at least 3 orders of magnitude less voluminous than Qoa-d (Fig. 2). Because of its low volume Qoa-a would probably not be recognizable if it were not the most recent fill in Cajon Creek.

The oldest radiocarbon date from Qoa-a is about 1705 years BP, from near the base of the deposit. Another date of about 990 BP was obtained from a sample collected from the middle of the deposit. It is inferred that the incision of Qoa-a began about 300 years ago (Weldon and Sieh, 1985). There is tenuous evidence that Qoa-a consists of two cut-and-fill episodes; however, it is clear that between about 2000 and 300 years ago Cajon Creek was generally aggrading in its central reaches. The fact that the uppermost part of Cajon Creek is only just beginning to incise suggests that post Qoa-a incision migrated upstream. However, with only 2 radiocarbon dates and the paucity of preserved deposits it is impossible to determine if the deposition of Qoa-a was time transgressive as was Qoa-c. For the purpose of discussion, the unit is assumed everywhere to span the period of time between about 2000 and 300 years ago. Qoa-a commonly merges upstream into active alluvium or Qhf deposits and cannot be confidently recognized at the basin edge downstream.

Cut Terraces and Tributaries

The fluvial deposits in Cajon Creek represent only a fraction of the time spanned by the record at Cajon Creek. Throughout most of the late Quaternary Cajon Creek was downcutting or laterally cutting to form cut or strath terraces. A cut is developed on fill and a strath is cut on bedrock. Remnants of these surfaces are found in Cajon Creek but the subsequent erosion and cultural modification have almost completely eliminated them. Mapping reveals that the most extensive and largest number of cut terraces were formed in the middle part of the drainage during the early Holocene.

At the junction of Lone Pine and Cajon Creeks seven terraces have been recognized that formed after the deposition of Qoa-c (Weldon and Sieh, 1985). Direct radiocarbon age control on several of these terraces and offsets across the San Andreas fault allows the construction of a detailed downcutting curve for Cajon Creek at this point (Fig. 8). The downcutting curve is only representative of the history at the San Andreas fault because the incision is time transgressive (Fig. 7) and the heights of the units (Fig. 5, 6) vary considerably up and downstream.

Most of the terraces mapped at the mouth of Lone Pine Canyon were also present upstream at the mouth of Cleghorn Canyon (Yerkes, 1951, photo p. 89, Fig. 17) but were destroyed by the construction of a freeway bridge. Farther up Lone Pine Canyon, at Pitman Canyon and in Crowder Canyon only Qoa-a, Qt-b, Qoa-c, Qoa-d, and Qoa-e can be found. Even farther up and downstream, Qoa-a and Qt-b cannot be found and, ultimately, no units or surfaces can be confidently distinguished near the edge of the drainage basin. The headwaters and the mouth of the drainage basin have not changed significantly in level since the deposition of Qoa-d,

Figure 3-8 The height of Cajon Creek at the San Andreas fault during the last 15,000 years. The curve is constructed from the heights of the terraces, the vertical positions of the ^{14}C dates within or on top of the deposits, and the dates of abandonment of some of the terraces. The points are age determinations (either radiocarbon dates or ages inferred from offsets along the fault). Terraces Qt-1 and Qt-6 represent the culmination of Qoa depositional episodes, whereas the other terraces are cut or strath terraces. The relative lengths of time represented by the Qt-2 and Qt-3 surfaces are based on their relative development and tenuous measurement of the offset of Qt-2. Qoa-a buries the record of cutting and filling below Qt-5.

so all of the surfaces and deposits would be expected to merge and become indistinguishable there.

Whereas the variations in cut and strath terrace heights are difficult to document in the trunk stream, several tributaries contain terraces that may lend insight into the variation. Two tributaries with well-preserved terraces are shown on Figure 9. In Lone Pine Canyon Qt-b merges with Qoa-c within 2 km of the junction with Cajon Creek. The other 5 minor Holocene cut terraces also merge with Qoa-c or Qoa-a (in the case of the cut younger than Qoa-a) within a few kilometers of Cajon Creek. Qoa-c, Qoa-a and the active alluvium merge within 10 kilometers, upstream of the study area. In Flat Creek, the fill surfaces merge with the active alluvium in less than a kilometer from Cajon Creek (Fig. 9), so the cut terraces, which are always between the two fills, also merge with the fill terraces in a very short distance.

The relative heights of both the cut-and-fill terraces where the various tributaries join Cajon Creek are consistent with the broad lens shape of Qoa-c (Fig. 6), but the distance over which the terraces merge up individual tributaries appears to be related to the size of the tributary. Flat Creek, for example, drains less than 1/10th of the area of Lone Pine Canyon and its terraces merge in about 1/10th the distance. The heights of the terraces in the tributaries do not converge significantly downstream towards the trunk stream in the way that the trunk stream does as it approaches the basin. The fill in the tributaries is wedge-shaped. This may indicate a baselevel response of the tributaries to the fluctuations of Cajon Creek that is not seen for Cajon Creek as a whole. It may also mean that overwhelming amounts of debris supplied by the tributaries caused the filling of the central reaches of Cajon

Figure 3-9 Longitudinal valley profiles up two tributaries of Cajon Creek. In medium-sized tributaries such as Flat Creek the terraces merge a short distance upstream and in the larger ones, such as Lone Pine Canyon, they merge much farther upstream.

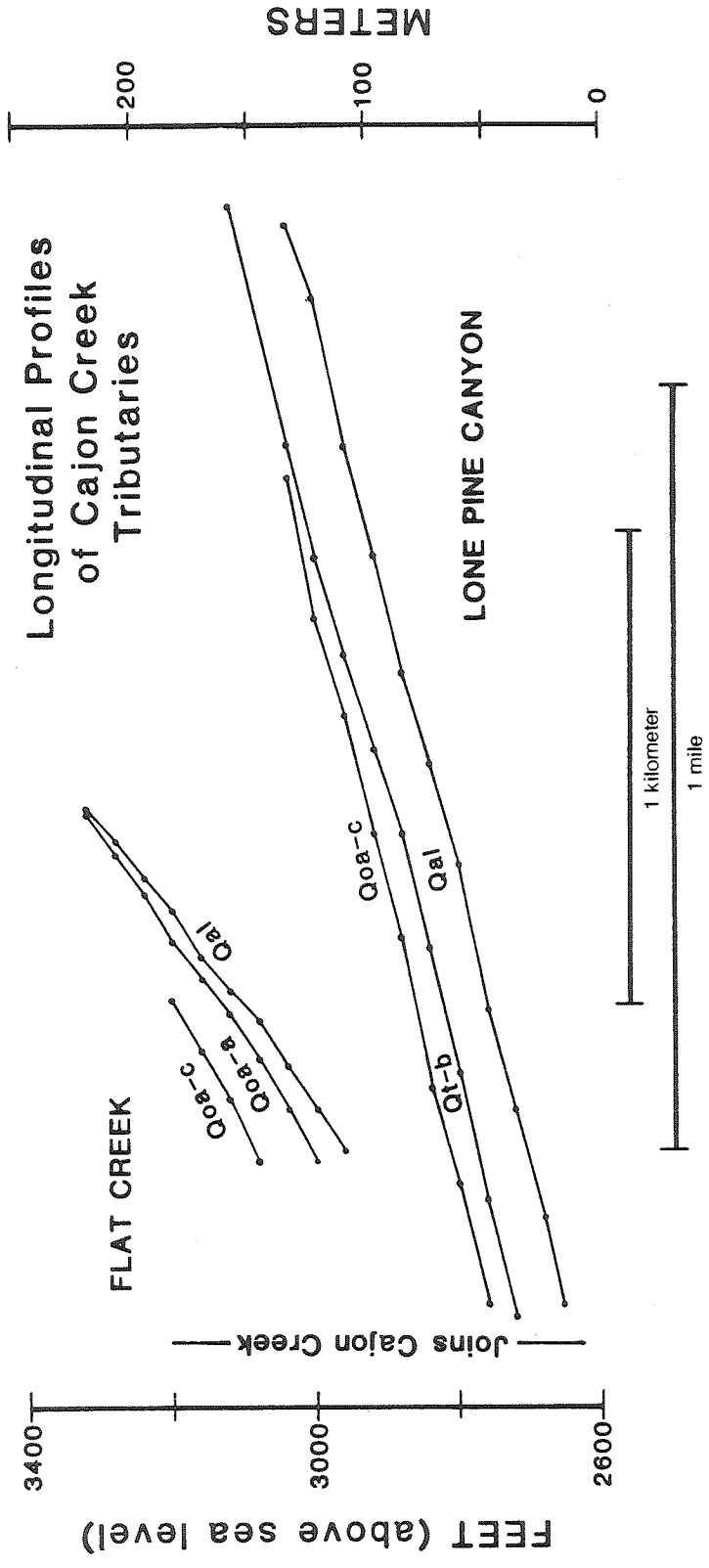


Figure 3-9

Creek.

The distinction between lens-shaped deposits found in Cajon Creek (Fig. 5) and Cable Canyon (Fig. 4), that reach the San Bernardino basin, and wedge-shaped deposits in all of the tributaries (Prospect Creek, Fig. 4; Lone Pine Canyon and Flat Creek, Fig. 9) suggests that the San Bernardino baselevel is not causing the highest order streams to aggrade but that the highest order streams may be exerting baselevel control on the lower order streams. This distinction can be used to eliminate tectonic control as the cause of terrace formation. Each stream, flowing across the San Andreas fault and associated minor faults and folds contains deposits that are lens-shaped or wedge-shaped depending on whether the stream reaches the basin or not. The size and shape of each stream's deposits are completely consistent with the size and order of the stream. If tectonic activity were called upon to deform the gradients and produce terraces, adjacent streams would be expected to respond to the tectonic impetus in the same way. This is clearly not the case for the study area.

Qhf

The Qhf deposits are very important because they are transitional between the channel deposits that can be mapped throughout the system and the hillslopes. Unfortunately, they are not widely correlatable such as the channel deposits and their formation and preservation are very site-dependent. For this reason, several examples are presented, instead of a general discussion, to characterize the unit.

A good example of the distinction between Qoa and Qhf deposits occurs at Pink River, a tributary of Lone Pine Creek just upstream of its junction with Cajon Creek (Fig. 1). The distinction is particularly

obvious because the Qoa-c deposited by Lone Pine Creek consists of blue and green Pelona Schist, whereas Pink River carries pink sand and gravel derived from the Cajon Punchbowl Formation. After the deposition of Qoa-c, Lone Pine Creek reincised south of its pre-Qoa-c course. The headwaters of Pink River were separated from the new Lone Pine Canyon by about a kilometer of Qoa-c whose surface gradient was too low for Pink River to transport its load. Even though Lone Pine Creek began to incise about 12,400 year ago (Fig. 7 and Weldon and Sieh, 1985), the upper part of Pink River continued to aggrade slowly, spreading pink sand out across the Qoa-c gravel deposited by Lone Pine Creek, and downcutting only where it entered Lone Pine Canyon. A radiocarbon sample from about 2 meters below the top of the pink sand yielded an age of 7,200 years BP, demonstrating that incision greatly postdated Lone Pine Canyon's incision. The sedimentary record in a swamp into which Pink River flowed indicates that incision actually reached its headwaters about 5,900 years ago (Weldon and Sieh, 1985), about 6,500 years after this portion of the Cajon Creek system had begun to downcut. The reason for this delayed response was a lack of power. Several thousand years were required for the small stream to erode a steep enough channel through Qoa-c to allow transport of the debris supplied by its catchment area. Clearly, the deposition was caused by local circumstance and occurred while this portion of the Cajon Creek drainage was incising.

Another example of Qhf is the sediment deposited across the San Andreas fault between Pitman and Cable Canyons (Fig. 1). Buried soils on fan deposits exposed in the canyons in this area indicate that the bulk of the broad plain underlying Devore Heights is made of Qoa-d derived from Ames and the Kimbark Canyons. Most of the surface, however, is

covered by Qhf that spans much of the late Holocene. The time span is demonstrated by 4 to 50 m offsets of stream channels cut into these deposits. A particularly illustrative case involves the Qhf deposit about 1 km southeast of Pitman Canyon. Between 1 to 10 meters of debris, reworked from the large landslide immediately uphill, overlie Qoa-d gravels. Incised into this Qhf deposit are four streams that are all offset about 50 m by the San Andreas fault. Based on the slip rate on the San Andreas fault in this area (2.5 cm/yr, Weldon and Sieh, 1985), incision of these small streams began about 2000 years ago. The deposits must have been laid down just before the incision because their source is immediately uphill, across the fault, and they contain no stratigraphic evidence of spanning a significant period of time. These sediments were certainly deposited just before 2000 years ago, while Cajon Creek was eroding. This Qhf deposit was then being eroded while Cajon Creek was aggrading to form Qoa-a between 2000 and 300 years ago. Clearly, Qhf was formed because the low, relatively flat Qoa-d surface had been juxtaposed across the fault from a very steep and easily eroded mountain front. Its deposition was not synchronous with aggradation in Cajon Creek. Material was deposited on Qoa-d until the Holocene incision of Cajon Creek reached the area, isolating the deposits by forming streams with gradients capable of removing the large amounts of debris reworked from the landslide.

In these two examples the distinction between the two groups of deposits is clear. Unfortunately, most Qhf deposits grade directly into Qoa deposits and the distinction is far more subtle. Pitman Canyon is a tributary of Cajon Creek that has a very steep catchment area and a relatively long and shallow transfer stretch from its catchment area to Cajon Creek. Throughout most of its length it flows across its own Quaternary deposits,

which have well-preserved geomorphic surfaces. Near Cajon Creek Qoa-c, Qt-b and Qoa-a can be easily distinguished. The surfaces associated with these units merge upstream and by halfway to the mountain front only one unit can be distinguished.

Two lines of evidence indicate that the deposits of Qoa-c and Qoa-a near Cajon Creek, that formed during brief pulses of alluviation, merge upstream into one continuously deposited unit and that a distinct Qoa-c deposit was not simply buried by a distinct Qoa-a deposit or the active alluvium. First, the surface of the Qhf deposit consists mainly of debris flow lobes and rills that are both older and younger than Qoa-a in Cajon Creek. Bob Matthews (of the Matthews Ranch in Pitman Canyon) reports that some of the Qhf was mobilized during the 1938 flood (pers. comm. 1982). However, the San Andreas fault, which has not broken here for more than 200 years (Weldon and Sieh, 1985), can be mapped across most of the Qhf deposit, offsetting channel rills and lobes distances ranging up to tens of meters. The fact that no consistent match can be made for these very distinctive offset geomorphic features suggests that they formed during a significant span of time and the 1938 flood record indicates that the Qhf deposit is still forming. In contrast, the surface of Qoa-a is offset only 4 meters (Weldon and Sieh, 1985). Second, ground water rises at the San Andreas fault, producing a narrow swampy area upstream of the fault. During dry years ranchers have excavated thick deposits of interbedded peat and gravels from the swamp for fuel (Bob Matthews, pers. comm. 1982). Although these peats are undated, they clearly indicate that the upper portion of Pitman Canyon has been slowly aggrading for a long time. Clearly, Pitman Canyon always supplies material to Cajon Creek. At the rangefront a small portion of the debris

appears to be deposited continuously across the San Andreas fault but where the stream joins Cajon Creek only pulses of deposition occur, in phase with Cajon Creek's cycle.

Southeast of Cajon Creek along the mountain front it becomes progressively more difficult to separate the major Qoa units. This is because the long-term rate of incision is not great enough to separate the units physically. The younger units bury the older units so soils and geomorphic position become less useful in distinguishing units. It also appears that the Qoa deposits merge in time where they merge in space. This is the case in Pitman and Crowder Canyons where Qoa deposits merge upstream. In Crowder Canyon this is seen in the increased age range of Qoa-c deposits, and in Pitman Canyon the continuously deposited Qhf at the range-front. These areas are transitional between the hillslopes and the major channels where no clear division between Qoa and Qhf deposits exists. Where the hillslopes and major channels are very close together, no gradational transition occurs and the distinction between the two groups is obvious.

PROFILES and VOLUMES

Cajon Creek's Profile since the onset of Qoa-c deposition

To understand the history of formation of the deposits and surfaces in Cajon Creek, profiles were constructed for 1000 year intervals through the time spanned by the deposition and erosion of Qoa-c and Qoa-a. This interval was chosen because of the excellent spacial and temporal control of the units. The profiles were constructed up Cajon Creek to its junction with Crowder Canyon and up Crowder Canyon to Summit Pass to utilize all of the radiocarbon dates in the Cajon Creek drainage. Constructing the profiles requires determining time lines through the migrating fill

and subsequent erosional episodes. This was accomplished by combining the age data for the filling of Qoa-c (Fig. 7) with the longitudinal shape of Qoa-c (Figs. 5 and 6) and the timing of the downcutting subsequent to Qoa-c at the San Andreas fault (Fig. 8).

To construct a profile, a time line was first drawn through Figure 7 to determine where in Cajon Creek Qoa-c was being deposited. For example, 11,000 years ago Cajon Creek was beginning to fill about 1 mile from the Summit, was 1/2 filled at about the 10 mile mark, in Crowder Canyon, and was beginning to incise just downstream of the mouth of Crowder Canyon at the 8.5 mark (Fig. 7). At the San Andreas fault Cajon Creek had incised about 35 feet below the top of Qoa-c (Fig. 8). The actual heights of the fill points can then be determined from the curve representing the height of Qoa-c above the active alluvium (Fig. 6). Eleven thousand years ago Qoa-c was just beginning to be deposited a mile from the summit, so a point is plotted 0 feet above the active alluvium there (Fig. 10, upright solid triangles are 11,000 year-old levels). Qoa-c was half filled at the 10 mile mark so the height of half the fill was measured on Figure 6, about 40 feet, and plotted on Figure 10. Incision was beginning just downstream of Crowder Canyon, placing the creek 100 feet above its current level at that point (Fig. 6). From Figure 8 the height of Cajon Creek was about 85 feet above the active alluvium at the San Andreas fault.

Due to the lenticular shape of the deposits, the profiles are required to merge with the active alluvium up and downstream. This requirement is certainly valid in the upper reaches where the base of Qoa-c is exposed. Near the San Bernardino basin the top of Qoa-c certainly merges with the active alluvium but the base cannot be found. However, as discussed above, the base is inferred to be at the level of the active alluvium.

Figure 3-10 Relative levels of Cajon Creek, constructed at 1000-year intervals for the last 17,000 years. The data points are calculated from Figures 6 - 8, as described in the text. Each set of points that defines a profile has a different symbol and each profile is labeled. There was no fill 17,000 years ago and the stream had a profile very similar to that of the modern creek. Stream levels after 6000 years BP are poorly constrained and, therefore, are not included here. The fill clearly migrated upstream and was being eroded in the lower part of the system even before it was deposited in the upper portions. The top of Qoa-c (the fill terrace surface mapped in the field) is not isochronous; it is an envelope formed by the migration of the locus of deposition upstream. Notice that, while the average gradient did not change (because the heights of the headwaters and the depositional basin are fixed in the short term), the local gradients change tremendously.

METERS

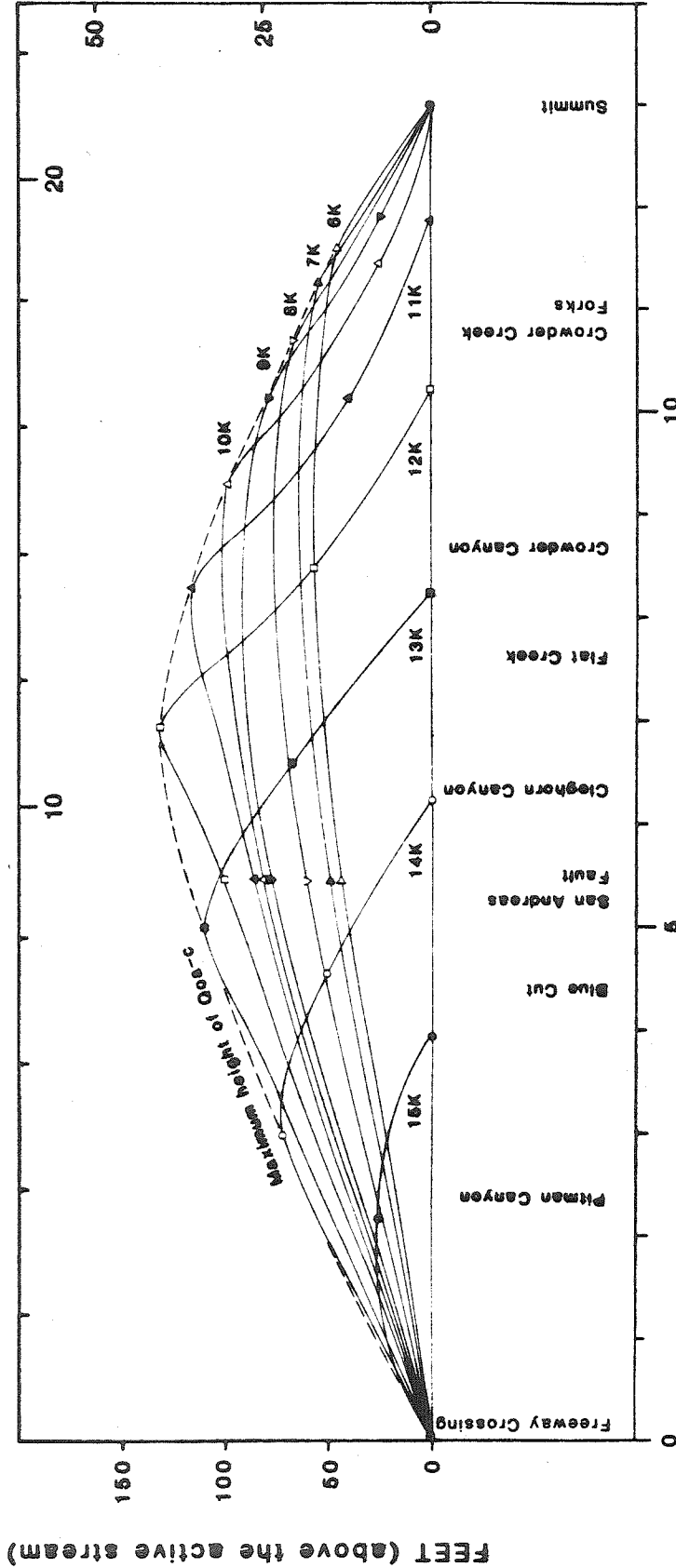


Figure 10

MILES (upstream from the basin edge)

vertical exaggerated 200X

A set of points like that described for 11,000 years ago was determined for each 1000 year time line. Each set is presented with a different symbol in Figure 10. The oldest sets have fewer points because old sediments exist only downstream of the San Andreas fault where there is little age control. Smooth curves were drawn through each set of points; however, it is likely that considerable variability existed in the actual profiles along their lengths (Fig. 10).

While each profile is only defined by 3 to 5 points, the similarity of successive profiles and consistent trends through the set suggest that some generalities can be drawn. The upstream migration of the deposition of Qoa-c is very marked. The average gradient cannot change significantly in the short term because it is fixed by the relative elevations of the basin and the headwaters; however, the local gradient fluctuates by large amounts. The portion of the stream that was aggrading maintained a relatively uniform gradient, 25 to 35% less than the modern gradient (Fig. 10). This constancy of gradient over such a wide range of deposit thicknesses and ages may reflect the minimum gradient down which Cajon Creek can transport its load.

Between 17 and 14,000 years ago, the gradient downstream of the aggrading reach was about 25% greater than the modern gradient and decreased to about 15% by 11 to 12,000 years ago. As the eroding stretch increased in length the gradient in the central part of the system approached the current (and pre-17,000) value. Between 9 and 6,000 years ago most of the system was eroding and the profiles between the San Andreas fault and the remaining aggrading reach are essentially parallel to the modern creek. The fact that all of these gradients are parallel to the modern creek, which is believed to be close to equilibrium (discussed below),

suggests that it is the optimal gradient that allows Cajon Creek to transport its load with out major aggradation or degradation. Most of the removal of material at this time was probably from the lowest, relatively steepest portion of the creek. The profiles are drawn with a slight upward relative concavity to make smooth profiles across the depositional-erosional threshold and to have smooth gradients to the basin edge. It is possible that there was a sharp break in slope where the creek switched from being depositional to erosional and most of the gradient was exactly parallel to the current one. Unfortunately, no evidence has been found to distinguish these two possibilities.

Volume Estimates

The volume of material stored as fill terraces or eroded from the channels per 1000 year interval was calculated from Figure 10. To do this the profiles were digitized and the area under each profile was calculated. Successive differences in these areas were multiplied by the cross-sectional width of the deposit (or channels, in the eroding areas) to determine the amount of material added or subtracted during each 1000 year interval.

Most of the material preserved in the drainage basin was stored in the main channel of Cajon Creek and its two largest tributaries, Lone Pine Canyon and Crowder Canyon. Even in medium-sized tributaries like Flat Creek (Fig. 1, 8) the volume of fill was insignificant and is ignored here. Seven cross sections through Qoa-c were constructed to determine the width of the deposit. These sections include Lone Pine and Crowder Canyons, upstream of their junctions. The width of the deposit, at the level that equally divides the cross-sectional area averaged about 920 m. For the area considered here there was little

systematic change; the channels are wider downstream but there are more channels upstream. Because each profile spans a large portion of the creek, and the width of the deposit does not change systematically, the areas between successive longitudinal profiles were multiplied by the average of 920 meters, resulting in the volumes presented in Figure 11.

It is difficult to estimate the errors associated with these calculations because several arbitrary, simplifying assumptions have necessarily been made. Fortunately, the best width and age control exists in the middle of the drainage where the deposits are thickest and the subsequent incision has been the greatest. The largest uncertainties exist at the edges of the system where the deposits are very thin and contribute little to the overall total. So, the general trends and relative magnitudes are likely to be meaningful.

A potential problem with the estimates is that the channels produced by downcutting are initially likely to be less wide than the channels into which Qoa-c was deposited. To test this problem the volume of material added per unit time was also calculated (Fig. 11), assuming no contemporaneous downstream erosion during the deposition of Qoa-c. Because this calculation assumes no channels and the first calculation assumes the widest possible channels, the actual value must be in between. It is clear from Figure 11 that the width of erosional channels does not become a serious problem until the Holocene, after most of Qoa-c was deposited. If this problem is significant for the latest Pleistocene, the peak in net aggradation may be as much as 500 years younger and the switch to net degradation may be a thousand years later. The major effect would be to increase the Holocene rate of erosion to widen the channels into their current configuration.

Figure 3-11 Channel aggradation and degradation in Cajon Creek during the last 17,000 years. The striped histogram represents the amount of material added to the channelized portion of the system per 1000 years. The solid histogram represents the net aggradation or degradation in the creek per 1000 year. The rate of channel filling peaked sharply about 13,000 years ago. The maximum rate of channel deposition was about 50% greater than the total amount of material carried by Cajon Creek today. The details of the curve after 6,000 years BP are uncertain due to the lack of complete profiles.

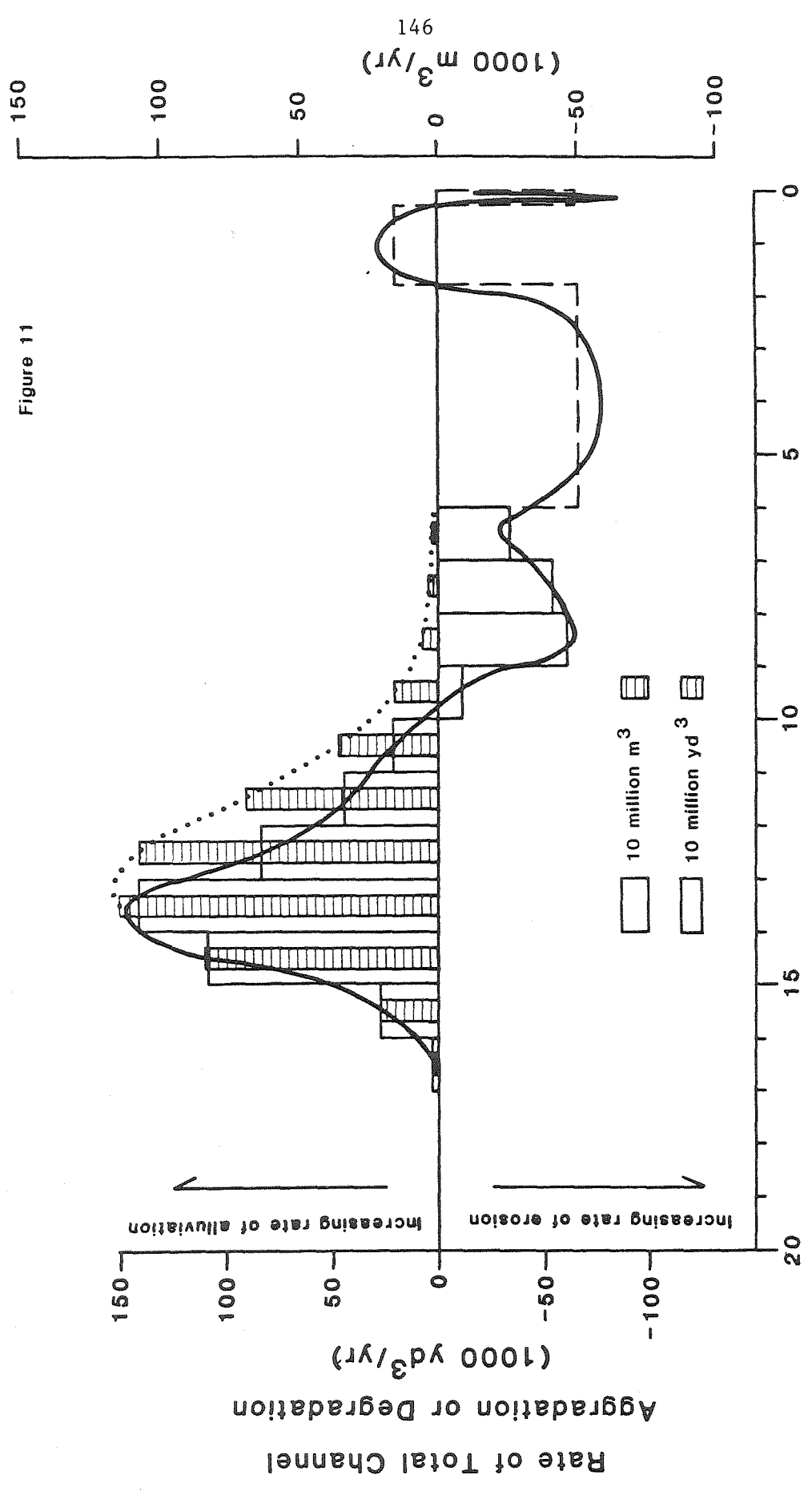


Figure 11

Figure 3-11

1000 Years Ago

The material under the 15 ka curve (Fig. 10) is inferred to have accumulated during the period of time between 17 and 15,000 years ago because the onset of Qoa-c deposition is extrapolated to have begun at the edge of the basin at about 17,000 years ago (Fig. 7). The existence of relatively thin deposits near the edge of the basin and the possibility of contemporaneous erosion upstream make it unlikely that significant net aggradation occurred until 16,000 years ago. The material below the 6,000 years-ago curve is assumed to have been removed by 2,000 years ago because Qoa-a deposition at the current level of the creek began at about that time. Also, the amount of material removed in the past 300 years is essentially unconstrained but has been estimated to complete the curve.

The problem of estimating volumes without complete profiles cannot be ignored. If the downcutting concurrent with the deposition of Qoa-c were not included, the total calculated amount of debris stored in the system would be overestimated by more than 25% and the amount added during a 1000 year interval in the Holocene would be completely meaningless. As noted, the problem of contemporaneous erosion and deposition may also be significant for the estimates of the early Qoa-c volumes because the upper reaches could still have been eroding while the lower parts were filling. However, the relative heights of the Qoa deposits, which are separated by 10s to 100s of thousands of years, suggest that the long-term erosion rate is only a fraction of the rates of addition or removal of material associated with the fill pulses. Certainly by 14,000 years ago deposition must have outweighed any contemporaneous erosion upstream..

A curve has been drawn through the histogram of Figure 11 to highlight the average yearly flux of debris through the part of the system

discussed here. The pulse of sedimentation represented by the Qoa-c deposits spanned more than 10,000 years (Fig. 7); however, net aggradation only spanned about 6000 years and peaked sharply 13,500 to 14,000 years ago. Net erosion began about 10,000 years ago and continued until about 1700 years ago. While the shape of the curve after 6,000 years ago is unknown, sediment removal appears to have taken place in two pulses, one at about 8000 years ago and the other about 4000 years ago. The period of lower erosion rates, between about 6 and 7000 years ago is real and may have extended farther into the poorly defined time period than shown on Figure 11.

The most sediment actually stored in the system at any time was about 1/2 billion cubic yards, the volume under the 10 ka curve (when the system switched from net aggradation to degradation). The maximum rate of aggradation occurred between 13,000 and 14,000 years ago and was about 150,000 cubic yards/yr (Fig. 11). The calculated rate of channel erosion does not exceed 75,000 cubic yards/yr, about 1/2 the maximum rate of aggradation; however, the erosional period during the last 6,000 years is poorly defined. The entrenchment and removal of Qoa-c took a much longer time to propagate up Cajon Creek than the deposition of the fill (Fig. 7). The greater range of aggradational values and the greater speed that aggradation migrated through the system may explain the observation that the best developed surfaces in the study area are aggradational.

Figure 11 shows net aggradation while Qoa-a was being deposited. However, Qoa-a has only been recognized as a significant deposit in the central part of the drainage and may have been associated with erosion elsewhere in the system. Thus, the magnitude and even the existence of net aggradation is not as clear as for Qoa-c. The erosional pulse that

has characterized the central part of the area for the last 300 years may indicate net erosion in the system but without complete coverage it is difficult to be certain. At present the total system is believed to be slightly erosional because along most of its length Cajon Creek flows across a floodplain, indicating stability (Bull, 1979), but incising gullies commonly characterize the uppermost reaches, indicating erosion. However, the complexity of the system and the extensive cultural modification make it difficult to determine the current status of the system with certainty.

Comparison of Modern and Holocene Sediment Supply Rates

The maximum rates of channel aggradation and degradation can be compared with what Cajon Creek currently delivers to the San Bernardino basin. No direct measurement of sediment transport exists for Cajon Creek but many other rivers and creeks in the Transverse Ranges have debris dams or reservoirs across them that capture the sediment that they produce. Several techniques have been developed to extrapolate the data from streams with catchment basins to other drainages in the Transverse Ranges. These techniques are not discussed here but several estimates for Cajon Creek are presented for comparison.

When one uses the technique of Rowe et al (1949, 1954) and assumes that the Cajon Creek area was completely burnt about every 150 to 200 years before the settlement of the area by Europeans (personal communication, 1984, Tim Passon, ecologist at the USDA Fire Research Station, Riverside, CA), one calculates that Cajon Creek would produce an average of about 140,000 cubic yards of sediment per year in the absence of cultural influences. When one uses the technique of Taylor (1981) the predicted yield for Cajon Creek would be 73,000 cubic yards per year.

Another approach is to compare Cajon Creek with the closest major drainage that has been measured. The Santa Ana river catchment area in the San Bernardino mountains is estimated to produce about 2.3 acre-feet of sediment per sq mi/year (Chuck Orvis, Army Corps of Engineers, personal communication, 1984). Orvis feels that Cajon Creek should be similar, which would imply a total production of 223,000 cubic yards/yr. However, Taylor (1981) estimated that the upper Santa Ana River produces about 2.25 times more/sq mile than Cajon Creek while Rowe et al. (1949) estimate that it should produce 30-40% less. The different estimates are due to the uncertainties in the effect of fire upon the average rate of sediment production and in scaling the geologic and geomorphic factors that control erosion rates. The long-term average for well studied drainages that are similar in size to Cajon Creek throughout the Transverse Ranges is about 100,000 cubic yards per year (Scott and Williams, 1974). Based on this range of estimates, Cajon Creek probably transports between 50,000 and 300,000 cubic yards of sediment per year, and is likely to be close to the 100,000 cubic yards average for similar drainages in the area.

During the period of maximum aggradation, about 13,500 years ago, Cajon Creek was annually storing between 1/2 and 3 times the amount it annually removes from the system today. The average rate of channel erosion between 9000 and 2000 years ago, when the system was removing the Qoa-c deposit, was between 1/5 and 1 times the total amount of sediment currently being transported by Cajon Creek. Because the prehistoric values include only the material added or removed from the channels and not material that simply passed through the system without any record, variations in the rate of total sediment removed from the drainage

fluctuated by much greater amounts.

An estimate of the actual amount of sediment transported by Cajon Creek during the periods of aggradation can be made by comparing the size distribution of the sediment in the terraces with the material transported today. Because the stream selectively deposited its coarse fraction relative to its finer fraction, a comparison of the size distribution of the sediment in the terraces with that which is currently being transported should yield some idea of what passed through the system while the terraces were being deposited. While detailed particle size analyses have not been made on the gravels from the Cajon Creek drainage, it is obvious that the mean size particle is a large pebble and that the gravels contain less than 10% sand and finer material. This estimate agrees well with particle size studies by Bull et al. (1978) on similar terrace gravels in the adjacent San Gabriel River; they found mean sizes of large pebbles to small cobbles and that the amount of material sand sized and smaller ranged from 2 to 15% (Bull et al., 1978, p. 38).

The size distribution of sediments carried by Cajon Creek today can be estimated by comparing it to similar drainages that flow into reservoirs or catchment basins. Small basins underlain by bedrock in the Transverse Ranges produce sediment of which 30% of the material is coarser than sand (Taylor, 1981, p. 64). Basins underlain by fine-grained sedimentary rocks produce less than 1% coarser than sand (Taylor, 1981, p. 64). For all substrates, larger drainages produce relatively less coarse material. The overall average for the upper Santa Ana River basin is 10% coarser than sand (Taylor, 1981, p. 69). Because Cajon Creek is underlain by both sedimentary and crystalline rocks and is a moderate-sized basin, a value of 10% coarser than sand is likely to be representa-

tive. This is close to Bull's estimate for Cajon Creek (written communication, 1985) of 15%. If, during the period of maximum aggradation, Cajon Creek was depositing everything coarser than sand, it was still transporting 10 times what it was depositing. Therefore, it must have been carrying 5 to 30 times the sediment it now carries because it was storing between .5 and 3 times what it carries today. This is a minimum requirement because some coarse material probably left the drainage. Regardless of what the actual value was, there can be no doubt that the sediment supply fluctuated by very large amounts during the deposition and erosion of the terraces.

DISCUSSION

Impact of tectonics on the alluvium

Many of the alluvial deposits discussed here were laid down by streams that cross the San Andreas and other active faults. Despite the high rate of activity on the faults (eg., 2.5 cm/yr for the San Andreas, Weldon and Sieh, 1985), the alluvial deposits have formed with little tectonic influence. Lateral reconstruction of offset units indicates that the thicknesses of the deposits do not change significantly at the faults (Fig. 4, 5). Warping of the area near the San Andreas fault might be called upon to produce the lens-shaped fill deposits in Cajon Creek but several lines of evidence discount this possibility. First, the similarity of the profiles of the streams between fill events would require alternating downwarping and bowing, returning the system to essentially the same gradient each time. Even if this were the case, the rates and extent of the bowing would have to be different at every stream that crosses the fault because of the different sizes and shapes of deposits in each drainage. In Cajon Creek a mechanism to cause the activity to

migrate upstream, as described above, would also have to be devised. Another problem with warping is that tributaries, such as Prospect Creek, also cross the San Andreas fault but produce deposits that only thicken downstream. Obviously, warping could not possibly affect individual streams in such different ways.

Tectonic deformation does have both long-term and short-term effects. Cajon Creek exists because the San Andreas fault laterally juxtaposed the low San Bernardino basin against the previously uplifted San Bernardino Mountains (Weldon and Meisling, 1982). Headward erosion of Cajon Creek into and through the mountains has caused net downcutting in the central part of the drainage of about 1 mm/yr during the past 0.5 my. This long-term rate is about 20 times slower than the maximum rate of Qoa-c accumulation and 5 times slower than Holocene incision rates (see Fig. 8).

Deposits and surfaces are offset so that different sized streams, different level terrace levels, and irregular topography are juxtaposed at the San Andreas fault. A confusing picture can result if the deposits and surfaces are not considered in the broader context of their depositional systems. This short-term effect of juxtaposition generally only extends a few hundred meters from the fault, where the drainage system is essentially unaffected by faulting. A good example is found near Lost Lake (Sec. 12, T2N, R6W, Fig. 1) where the relative heights between terraces vary across the fault. Offset that occurred between terrace-forming periods displaced the terraces up or downstream across the fault; so, when the next terrace was cut it had a different height relative to the older, offset terrace on each side of the fault.

In summary, tectonic control is the long-term impetus for downcutting in the area, but it has little influence on short-term aggradation or de-

gradation away from the faults. Near the faults, tectonic activity tends to produce more Qhf-type deposits and can obscure the relationships between units and geomorphological surfaces. However, the major alluvial deposits discussed here were laid down across the faults and are only recording subsequent offset.

Climatic control

The distribution and geometries of the alluvial deposits in Cajon Creek eliminate baselevel or tectonic control as driving mechanisms. This leaves climate as the most likely causative agent for the fill terrace formation. In order to demonstrate climatic control it is necessary to show that alluviation occurred only during periods of particular climatic conditions different from those characterized by erosion or at periods of climate change. Changes in climate through time are usually inferred from advances or retreats of glaciers, vegetation changes, sea level curves, oxygen isotope variations in marine sediment cores, and lake levels or salinities. While there are disagreements between these various records, there is little doubt that the latest period of extreme wet and cold climate occurred between about 16 and 25 thousand years ago and that the past 8 to 10 thousand years have been relatively hot and dry. The latest major alluvial deposit in Cajon Creek, Qoa-c (with net aggradation between 16 to 10,000 years ago), corresponds with neither of these climatic extremes, but with the transitional period in between.

Perhaps the most dramatic evidence of climate change is the advance and retreat of glaciers, recorded by moraines and other glacial deposits. Unfortunately, there are few direct dates available from glacial deposits in the Southwest and their ages are generally based on extrapolation from the few dates by relative dating techniques (e.g., Sharp, 1972; Gillespie,

1982), correlation with dated lacustrine sections from lakes fed by glaciers (e.g., Smith, 1979; Lajoie and Robinson, 1982), or global sea level (Shackleton and Matthews, 1977; Aharan, 1983) and oceanic oxygen isotope fluctuations (e.g., Shackleton and Opdyke, 1973) that are inferred to record changes in global ice volume. Based on these extrapolations there is a consensus that the latest Pleistocene glaciation in the Sierra (Tioga) occurred between about 25 and 10 thousand years ago (Sharp, 1972; Smith, 1979; Gillespie, 1982).

Global sea level and oxygen isotope curves show good agreement where data are available, and indicate that the latest worldwide glacial maximum was between 18 and 25 thousand years ago and that major deglaciation began between 13,000 and 16,000 years ago (Duplessy et al., 1981; Ruddiman and Duplessy, 1985). It appears that early deglaciation was characterized by thinning of the ice sheets that catastrophically retreated immediately before the Holocene. While there remains considerable debate about the nature and rates of deglaciation between 16 and 10 thousand years ago (Ruddiman and Duplessy, 1985), globally this period is best characterized as a transitional time between climatic extremes.

Vegetation changes, recorded by detritus in packrat middens (Wells and Berger, 1967; Wells, 1979) or by pollen recovered from lake cores (Adam et al., 1981; Wright et al., 1973; Martin and Mehringer, 1965) have been used to determine paleoclimates in the Southwest. Vegetation collected by packrats in the arid Southwest records the local presence of particular plants from which the climate can be inferred. Vegetation preserved in packrat middens indicate that much of the now arid Southwest was covered by a juniper or pinyon-juniper woodland between 8,000 and 20,000 years ago (Wells and Berger, 1967; Wells, 1979). This major climate

difference is inferred to have been due to greater abundance of monsoonal, summer rain relative to today (Wells, 1979). The relatively late change from semi-arid woodlands to desert in the arid Southwest was due to the relatively slow response of summer monsoons to the climate change (Wells, 1979). Wells (1979) notes that the effect of summer precipitation drops dramatically to the northwest and probably did not significantly affect the northwestern Mojave or the coastal ranges of California. Cajon Creek, in the Transverse Ranges, currently receives more than 90% of its precipitation from winter storms off the Pacific (Ahlborn, 1982), and probably did during the Pleistocene as well (Wells, 1979). So it is unlikely that the packrat middens in the arid Southwest record exactly the same changes that influenced Cajon Creek.

Most of the pollen records come from areas strongly affected by winter precipitation (Adam et al., 1981; Wright et al., 1973; Martin and Mehringer, 1965), and all of these records show a significant climate change before the end of the Pleistocene. Perhaps the best dated pollen record comes from Clear Lake in northern California (Adam et al., 1981). Several well-dated cores from Clear Lake record changes in pollen representative of change from full "glacial" conditions towards "Holocene-like" conditions between 16 and 17 thousand years ago (Adam et al., 1981; J. Sims, personal communication, 1985; new dates confirm the 16 to 17,000 transition that appeared to have occurred somewhat later in some of the earlier cores). Sims (personal communication, 1985) suggests that this more rapid response to the onset of global climate change, relative to the interior continental record in the Southwest, was due to the singular influence of Pacific winter storms on the coastal climate.

If the precipitation at Cajon Creek is always dominated by winter rain

off the Pacific, as it is today, the onset of vegetation change recorded at Clear Lake may be correlated with the onset of deposition of Qoa-c at Cajon Creek. However, regardless of whether Cajon Creek was influenced by summer, winter, or a mixture of precipitation throughout the year, all of the vegetation data indicate "full glacial" conditions (whatever they were) as early as 20 to 25 thousand years ago. If alluviation at Cajon Creek was simply due to the abundance of precipitation or differences in the ratio of summer to winter precipitation, fill terraces would have formed well before they did at Cajon Creek.

Some of the best records of local climate change in the Southwest are from lake levels and sediments in closed basins. Lake Bonneville was the largest lake in the West and it preserves a record of relatively wet climate between about 26 and 11 thousand years ago (Scott et al., 1983; Passey, 1982; Scott, 1980; Currey, 1980). The level of the lake was almost certainly controlled by overflow between 15 and 13 thousand years ago so it is not possible to determine exactly when during this period the wettest conditions prevailed. While the wettest condition may correlate with the early deposition of Qoa-c in Cajon Creek, one-half of Qoa-c was deposited while the lake was below its sill and diminishing to its current size (between 13 and 11,000 years ago, Scott et al., 1983; Passey, 1982). If alluviation at Cajon Creek was caused by the same climatic factors that filled Lake Bonneville, alluviation would have begun around 26,000 years ago and ended between 13 and 11,000 years ago, not 16,000 and 10,000, respectively, recorded at Cajon Creek.

Sediments deposited in Lake Searles indicate a deep, permanent lake between about 23 and 16 thousand years ago (Smith, 1979; 1984). While there was a relatively wet period between 13 and 11 thousand years ago,

the period between 16 and 10 thousand years ago was generally characterized by increasingly saline conditions, associated with the transition to Holocene climate.

Several other western lakes had a relatively late persistence of high water levels or a pulse of wet conditions during the latest Pleistocene. For example, there were 3 high stands of Mono Lake between 36-34, 28-24, and 14-12 thousand years ago (Lajoie and Robinson, 1982). The latest high stand correlates with the last pulse of relatively wet conditions at Lake Searles (Smith, 1979; 1984) and the peak in alluviation seen at Cajon Creek. While it may be tempting to correlate Qoa-c deposition with a pulse of precipitation centered about 13,000 years ago, earlier equally wet periods did not produce aggradation at Cajon Creek so the correlation would be fortuitous. There is no record of significant alluviation between Qoa-d and Qoa-c (about 55 to 16 thousand years ago), a period that includes two of the peaks at Mono Lake and most of the latest high stand at Lake Searles. While it is possible that minor fill deposits like Qoa-a could have been removed during this interval, there is some evidence that Cajon Creek was lower than it is today by 25,000 years ago and stayed at about its current level until the onset of Qoa-c deposition (Weldon and Sieh, 1985). This probably eliminates any possible correlation with the 28-24,000 high stand at Mono Lake or the 23-16,000 high stand at Lake Searles, and suggests that the correlation with the 13-11,000 high is coincidence.

In summary, the deposition of the latest major fill terrace in Cajon Creek correlates in time with most indicators of climate change from "glacial", "pluvial", or "vegetative" maxima to Holocene climate. While several indicators of climate change suggest a late persistence of

relatively wet and cold conditions that may overlap with Qoa-c deposition, all climatic records indicate equally wet and cold periods when Cajon Creek was not aggrading. The correlation with the period of climate change supports the hypothesis that climate is responsible for the fill terraces but suggests that some process acting during the transitional period caused alluviation.

If Qoa-c was formed by some process acting during the transition from relatively wet and cold climate to hot and dry conditions, the other Qoa deposits should have occurred during similar periods of climatic transitions. Unfortunately, there are few well-dated climate records that span the period of downcutting at Cajon Creek to test this hypothesis. Perhaps the most widely-cited long-term indicators of climate change are deep sea oxygen isotope records (Shackleton and Opdyke, 1973; van Donk, 1976). The only record from the Southwest that spans the total history at Cajon Creek is the lacustrine record at Lake Searles, California (Smith, 1979; 1984). As discussed by Smith (1984), there are major differences in these 2 long-term records so both are compared with that at Cajon Creek (Fig. 12).

The deposition of Qoa-c corresponds with the transition from Stage II to I at Searles Lake and the transition from Stage 2 to 1 in the O-18 record. Qoa-d corresponds with the previous similar change recorded at Searles Lake at about 55,000 years ago but is somewhat later than the transition from O-18 Stage 4 to 3 (about 65,000 years ago). Because the age of Qoa-d is based on the slip rate on the San Andreas fault, which may not be uniform, it is not known whether this difference is significant.

The next youngest major transition from wet to dry climate at Searles Lake is about 105,000 years ago. No deposit of this age has been recog-

Figure 3-12 Comparisons of the record at Cajon Creek with two records of long-term climate change. A is the fluctuation in salinity recorded at Searles Lake, California (Smith, 1984) and B is the fluctuation in global ice volume, as inferred from ^{18}O variations in sediments and fossils from ocean cores (also reproduced from Smith, 1984; originally from Shackleton and Opdyke, 1973 and van Donk, 1976). Qoa-c and Qoa-d are contemporaneous with transitions from nonsaline (wet) to very saline (dry) conditions at Searles Lake. Qoa-c is also contemporaneous with the boundary between oxygen isotope stages 1 and 2. The deposition of Qoa-d, however, occurred during the middle of oxygen isotope stage 3. Qoa-e is too poorly dated to correlate exactly but may have formed at the boundary between hydrologic regimes IV and V at Searles Lake. Both Searles Lake and Cajon Creek record a lack of transitions from periods of very wet to very dry climate between about 500,000 and 100,000 years BP.

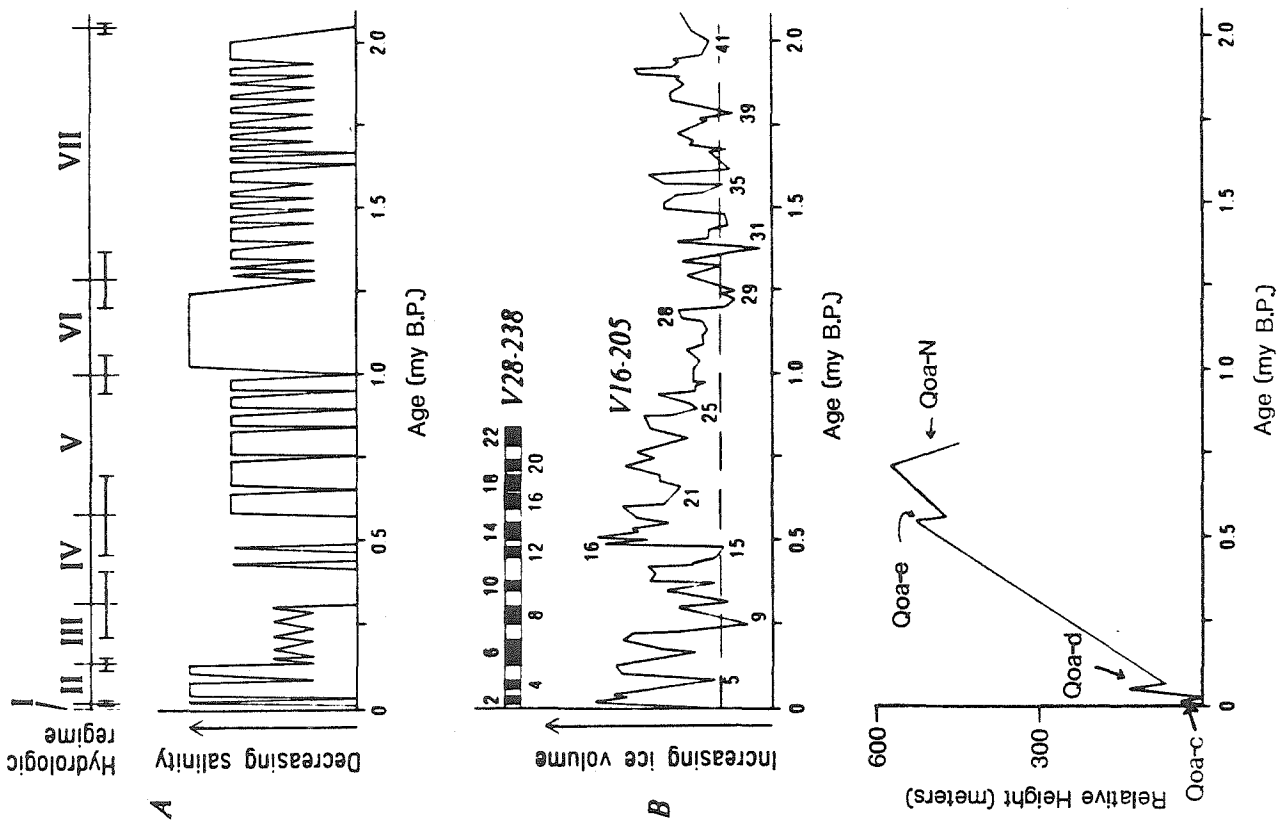
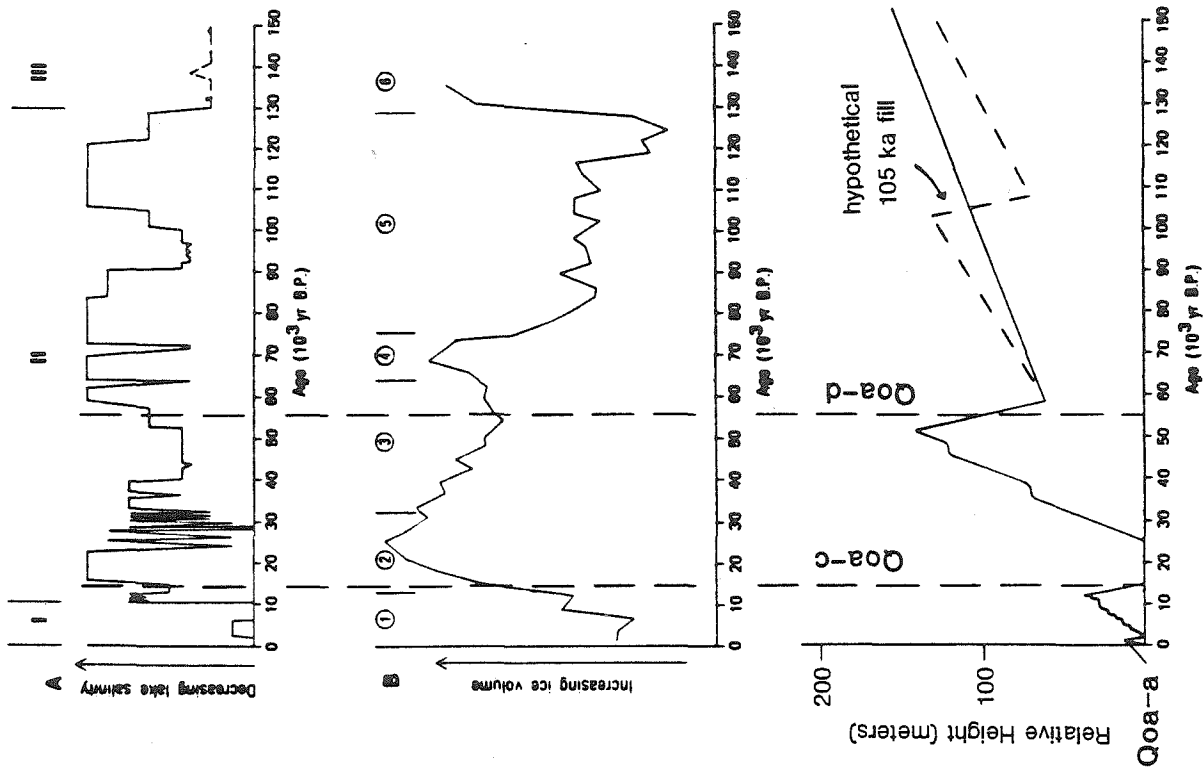


Figure 3-12



nized at Cajon Creek. However, it must be remembered the Qoa-d is only really dated at Prospect Creek, where unquestionable offsets exist. The other Qoa-d deposits near Cajon Creek are correlated by their soils, geomorphic position and the fact that their offsets are consistent with those at Prospect Creek. In several places there is suggestive evidence that Qoa-d may be a composite unit. Near Blue Cut (Fig. 1) there are 2 geomorphic surfaces on the Qoa-d deposit, with the higher one having a much better developed soil. In the Devore area (Fig. 1) soils with development comparable with Qoa-d deposits near Prospect Creek are commonly buried by deposits of unknown age. If a hypothetical 105,000 year old unit existed at about the same geomorphic level as Qoa-d and was buried in most places by the tremendous 55,000 year old deposits, it may not have been recognized because of the poor exposure and limited number of soil descriptions in the area.

Several other workers have noted a double deposit formed during this period. Bull (written communication, 1985) notes that his T3 fill terrace in the adjacent San Gabriel River drainage consists of two periods of deposition and the second just buries the first. McFadden (in Bull, et al., 1978; personal communication, 1985) notes that the two soils have comparable development and each is similar to that on Qoa-d (McFadden and Weldon, in review). So there could be two deposits, one around 55,000 and one around 100,000 years ago. Direct evidence for a 100,000 year old deposit may exist across the San Bernardino basin in the Grand Terrace unit of Haner (1982). Haner reports a uranium series date on a buried soil in this unit of 97 ± 5 thousand years. While uranium series dates on paleosols are difficult to interpret, and the site may have some problems (T. Rockwell, personal communication, 1984), the

approximate correlation with the 105,000 year old transition at Lake Searles and the possibility that Qoa-d is a composite unit suggests that more work should be done to determine if Qoa-d is indeed 2 units.

While it is possible that Qoa-d buried a hypothetical 105,000 year old deposit, the long-term downcutting of Cajon Creek makes it unlikely that Qoa-d buried a deposit much older than 150,000 years because the river was probably at a higher level before then (Fig. 12). The lack of significant aggradation in the Cajon Creek area between Qoa-d and Qoa-e (about 55,000, or perhaps 105,000, to 500,000 years ago) is matched by a lack of transitions from wet to dry conditions at Searles Lake (Fig. 12). The oxygen-18 records, however, contain numerous transitions during this time that appear to be similar to that at the Holocene boundary that are not found at Lake Searles or Cajon Creek (Fig 12). Smith (1984) suggests that whatever causes the 100,000 year cycle in ice volume does not always affect middle latitude climate. If this is the case, the long gap in alluviation seen at Cajon Creek may reflect a long period without major wet-to-dry transitions like those during the latest Pleistocene.

Qoa-e may correlate with the next youngest major transition from non-saline to saline conditions at Searles Lake about 550,000 years ago (Stage V to IV) (Fig. 12). Searles Lake records 6 transitions from wet-to-dry conditions between 550,000 years and 1 my. This may explain the possible range in Qoa-e-like deposits in the Transverse Ranges that at least one worker (Crook, 1985) suggests spans the Bruhnes-Matuyama polarity boundary 730,000 years ago. Most of these earlier events would not be recorded at Cajon Creek because downcutting began after the polarity reversal.

The 0.4 to 0.5 my gap in major fluvial deposition is believed to be characteristic of the Transverse Ranges. This belief is based on the

geomorphic position and soils described on fill terraces throughout the ranges (McFadden, 1982; McFadden and Weldon, in review). The correlation with the long period of aridity experienced at Lake Searles strongly suggests a regional climatic influence quite different than that experienced during the latest Pleistocene.

Finally, the beginning of Qoa-a, about 2000 years BP, corresponds to a minor transition from wet to dry at Searles Lake. While this was a very minor transition, it may have occurred at the same time as a major decrease in lake level at Mono Lake between 3400 and 1200 years BP (Stine, 1984) and many streams in the Southwest are known to have aggraded during the time of the deposition of Qoa-a (examples can be found in Leopold and Bull, 1979, Bull et al, 1978, Crook et al, 1978, and Sieh, 1984). While debate continues about the exact contemporaneity of these latest prehistoric fill episodes and subsequent incision (for an alternative view see Schumm, 1977; Kottlowski, et al., 1965), many streams in the Southwest did aggrade within a few 100 years of this time, indicating that a regional climatic cause is possible.

Qoa-a is a very minor unit that probably would not be recognized if it were not so young. Many such deposits were probably laid down and subsequently eroded or buried by larger, younger units. This may also be the fate of Qoa-c sized events that predate Qoa-d. However, it is unlikely that anything as large as Qoa-d or Qoa-e could have been missed unless it was deposited immediately before one of these deposits, before significant downcutting had occurred, and was buried.

In summary, there is excellent agreement between the records at Cajon Creek and Searles Lake. Within the errors of the dating techniques, every alluvial event at Cajon Creek formed when Lake Searles was drying and the

only wet-to-dry transition at Searles Lake not found at Cajon Creek may have been buried. Also, the correlation of the remarkable 0.4 my gap in wet-to-dry transitions recorded at both places makes fortuitous correlation due to poor age control unlikely. While there is agreement with the O-18 record for the latest climatic transition at Cajon Creek, the record at Cajon Creek supports the hypothesis of Smith (1984) that the global O-18 record may not always be appropriate for correlating climatic change in the Southwest.

Correlation with other drainages

The existence of relatively few, climatically controlled major alluvial deposits in Cajon Creek raises the possibility of constructing a regional alluvial stratigraphy. While fill terraces are widespread in the Transverse Ranges, there is little age control, so a regional correlation is premature at this time. It does appear that many drainages experienced a latest Pleistocene to early Holocene aggradational event (for example, Bull et al., 1978; Crook et al., 1978), and as discussed above, many streams contain significant deposits of latest Holocene alluvium. Most drainages in the Transverse Ranges contain middle-to-late Pleistocene fill deposits (for examples, see: Weldon et al., 1981; Eckis, 1928; Morton and Miller, 1975; Haner, 1982; Mezger, 1982; Bull et al., 1978; Crook et al., 1978) but to date the only way to correlate them is geomorphic position, weathering characteristics, and soil development. While these techniques can indicate approximate contemporaneity, more absolute dates and refinement in soils and other relative techniques will be needed before a "grand synthesis" can be made.

The record at Cajon Creek illustrates that correlations may be difficult even when age control exists. Qoa-c contains radiocarbon dates

that span 9000 years, some of which postdate the onset of subsequent incision in most of the drainage. So in comparing dates, the setting and potential age range of a unit must be considered. Also, dates taken from Qhf deposits cannot be used for correlation, so careful consideration must be given to the relationship between the deposit containing the datable material and the system as a whole. Perhaps these problems will limit the usefulness of correlations involving the very young units; however, the periods of time between the older units are likely to be much greater than the range in time within a unit, so correlations involving the older units will be very useful.

Response to the Climate change

It is generally inferred that the late Quaternary climatic change involved changes in temperature and precipitation that were manifested by changes in hydrology and sediment supply. These changes could be called upon to explain the formation of fill terraces in Cajon Creek. For example, the Langbein-Schumm relationship could be used to estimate how sediment supply varied as a function of likely precipitation and temperature differences associated with climate change at Cajon Creek (Langbein and Schumm, 1958; Schumm, 1977).

There are two problems with applying this approach to Cajon Creek. First, the Cajon Creek drainage currently receives an average of about 63 cm of rain per year, which corresponds to the maximum sediment yield in the Langbein-Schumm curve (adjusted for the average temperature of 60° F at Cajon Creek; see Schumm, 1977), so it is not clear whether more or less effective precipitation will increase the sediment supply in the area. Second, the large increases in sediment supply are associated with the transitional period and not the climatic regimes themselves.

The sediment supplied during the wettest times may have been different from the driest times, such as the middle Holocene, but during both extremes the creek could transport all of its load and no fill terraces were formed. The problem appears to be that the system is complex and the process of change produces a far more dramatic effect than the absolute difference between the states separated by the change. To understand the fill terraces in Cajon Creek, one must focus on what happened at the transition in climate as much as the actual conditions on each side of the transition.

Three end-member possibilities for the pulses of sedimentation at climate boundaries are considered here. The first is that the amount of sediment supplied by the hillslopes somehow increased by much more than any accompanying increase in the creek's ability to transport it, forcing the deposition of the fill terraces. The second is that the Pleistocene hillslopes held an excess of debris that was released by some change associated with the climate boundary. The third possibility is that the sediment supply has been relatively constant but the creek's ability to transport it has varied through time due to changes in the average runoff, size or timing of storms.

The sheer magnitude of the deposit and the rates of sedimentation calculated above make the third and probably the second possibilities impossible. The amount of sediment supplied by the hillslopes at the peak of the Qoa-c event was about an order of magnitude greater than the total sediment production by Cajon Creek today. So, simply varying the discharge could not produce the required amount of channel aggradation even if no sediment at all reached the basin (which was clearly not the case anyway because the terraces do not contain the fine material that

makes up the bulk of Cajon Creek's sediment load). Variations in discharge are certainly involved because Cajon Creek could not have moved all of the sediment required without much greater discharge than it has today. However, it is clear that the variations in the sediment production rates, whether from stored or primary sediment sources, exceeded the fluctuations in the stream's ability to carry it.

The second possibility, forming the fill deposits from material previously stored on the hillslopes, has gained recent acceptance. Bull et al. (1978) proposed a complex response to the Pleistocene - Holocene climatic transition that could have caused a pulse of alluviation in the early Holocene. They proposed that the vegetation on Pleistocene slopes could hold much more debris than the Holocene slopes and that the excess was released when the vegetation changed. The most common change appealed to in the Transverse Ranges was from pine forest to a more fire-prone chaparral (Bull et al., 1978). Fires periodically removed the chaparral, which released the excess debris, which overwhelmed the system, which responded by depositing fill terraces. Once the system was "cleaned off", incision occurred because the system was really in a regime in which it should have been actively incising. This was a classic complex response (Schumm, 1977), because the system actually filled when a steady state consideration of the variables indicates that it should have been incising.

The differences in the timing of vegetation changes, recorded by pollen from lake cores and packrat middens, discussed above, make it difficult to determine if aggradation occurred exactly when the vegetation changed. Because the vegetative make-up of the area is complex and changes probably varied even within the Transverse Ranges, a clear test

of this hypothesis may be difficult. The hypothesis may be tested by comparing the volume of material deposited during the fill event with the amount that can be stored on the hillslopes today. The maximum volume of material stored in the channels at any one time during the aggradational pulse was about 1/2 billion cubic yards. This is about 5000 times the amount that is removed in a year under the current climatic regime and represents, as discussed above, less than 10% of the actual amount of material eroded from the hillslopes during Qoa-c deposition.

A comparison can be made with the amount of material stored on the hillslopes today from the amount of sediment being carried by Cajon Creek. If the current yearly production is divided evenly across the drainage area, about 0.5 mm/yr is eroded. Major storms following fires can cause the sediment yield to increase 20 to 50 times in the Transverse Ranges (Rowe et al, 1949, 1954; Taylor, 1981), suggesting that the hillslopes store much more than is actually transported each year. However, because later storms in a sequence of storms typically do not remove much additional material (unpublished study, Wade Wells, personal communication, 1984, USDA Fire Research Station, Riverside, CA), the total available sediment on the hillslopes is believed to be about the amount that is moved during a single large storm after a fire. So, there is at most an average of 25 mm (50 X 0.5 mm) of transportable material stored on the hillslopes above Cajon Creek. To store the 1/2 billion cubic yards represented by Qoa-c on the hillslopes would require that the Pleistocene slopes held at least 100 times the current amount or about 2.5 meters averaged over the entire catchment area. Because debris is really only derived from just under 1/3 of the total drainage area, an average of about 6 meters would have to be derived from producing hillslopes. To

store the amount of material that actually passed through the system during the deposition of Qoa-c would require about 10 times this amount. Clearly, no reasonable hillslope system could hold so much loose material.

There are several other reasons why the prior storage of material is unlikely. Qoa-d, the previous fill deposit, was far more voluminous than Qoa-c. Outcrops of Qoa-d are typically twice as thick as adjacent deposits of Qoa-c and Qoa-d was more widespread because it was not confined to as narrow a channel as were the Qoa-c deposits. While Qoa-d may be a composite deposit, the final aggradational pulse was probably almost an order of magnitude greater than Qoa-c and would therefore require even greater amounts of prior storage.

The final problem with the storage model is the presence of well-developed fill terraces in areas that probably do not store material in the way that a crystalline bedrock slope does. In the Bull et al. (1978) model the difference in the erodability of the bedrock and the colluvium stored on the bedrock caused first a pulse of sedimentation and then incision when the slopes were laid bare. If no difference in erodability exists between the substrate and the colluvium the pulse should not occur. In Crowder Canyon a particularly compelling case can be made because the underlying Crowder Formation and early to middle Quaternary deposits are virtually unconsolidated. It is probably as easy to erode the material that makes up the hills as it is to erode any material stored on the slopes derived from them. Therefore, any stored material would act essentially like the parent and there should be no pulse of sediment due to the release of stored material when the climate changed.

In Crowder Canyon there is also little difference in the resistance to erosion between the material in the fill terraces and the material in-

to which the channels are cut. In fact, the distribution of the current channels suggests that the "bedrock" is slightly easier to erode than the fill deposits, which contain coarser debris from farther upstream. So the variation in the rate of downcutting may not be due to bedrock control either. Periods of rapid downcutting or aggradation in Crowder Canyon must simply be due to the variations in sediment supply and hydrologic parameters because there is no difference in moving primary or stored material in this area. The fact that Crowder Canyon experienced pulses of aggradation and degradation with the rest of Cajon Creek suggests that stored material, either on the hillslopes or in the channels, is not a significant factor in the fluctuation between deposition and erosion.

It is concluded that the period of time represented by the deposition of Qoa-c was characterized by relatively high primary sediment production and not simply the processing of previously stored material from the hills or the failure of the system to carry its normal sediment supply. While the latter factors almost certainly played a role, large changes in the rate of sediment production must have been the dominant factor. Changes in vegetation may be responsible for the large amount of hillslope erosion but the changes could not have simply released stored material. The development of a chaparral fire ecology certainly could produce more sediment but the fire ecology exists today and the drainage is quite capable of processing all of the sediment it receives.

Weldon (1983) proposed that the magnitude of the fill reflected the length or relative intensity of the previous wetter or colder climate. If the magnitude of the change in climate were reflected in the magnitude of the fill, Qoa-c would be larger than Qoa-d, according to both the 0-18 record and the Lake Searles record (Fig. 12). The length hypothesis,

however, is supported by the climate changes inferred from the record at Searles Lake. The 55,000 and .55 my transitions follow long periods of wet and/or cool climate. While the latest transition appears to be more significant in magnitude, it followed a relatively short period of wet and/or cold climate and produced less fill.

A mechanism must therefore be proposed that allows the prior wet and cold climate to impress itself on the magnitude of the fill. It is proposed that the degree to which the hillslope system adjusted to the relatively wet climate determines the magnitude of the fill at the subsequent transition to Holocene-like conditions. The system may return to a Holocene equilibrium faster than it can completely adjust to being a Pleistocene system, because the fill event lasts less time than the prior wet and cool period. However, if a Holocene "equilibrium" is not attained until the fill is also removed, then the timing of the two adjustments may be similar. This may be why the creek profiles after fill events do not return to their prefill shapes until the stored material is also removed, returning the system to the long term "equilibrium" controlled by downcutting and tectonics.

Two mechanisms are proposed by which the previous climate controls the magnitude of the subsequent fill. The first is a variation of the prior storage model of Bull et al. (1978). Rather than storing eroded material on the hillslopes, wetter climate may produce a more deeply weathered regolith. This regolith is more susceptible to latter erosion as the climate and vegetation change. While this hypothesis helps solve the problem of storage of tremendous amounts of debris and would perhaps yield more sediment following longer periods of regolith development, it does not solve the problem in Crowder Canyon where the material is

already about as susceptible to erosion as it can be.

Another mechanism is based on comparisons of humid and arid hillslopes and the nature of small remnants of old hillslopes preserved above Cajon Creek. Small, generally triangular wedges of relatively smooth slopes are locally isolated from the active slopes that have a much greater density of first- and second-order streams. These small remnants of smoother slopes are thought to have been active before and during the deposition of the Qoa deposits because sediments on these slopes locally interfinger with the Qoa deposits. Comparisons of drainage densities on arid, semi-arid and humid hillslopes (Schumm, p. 83, 1977) support the inference that during more humid conditions slopes would have a lower drainage density than do today's. Both the currently active slopes and the hillslopes that existed during wetter or colder periods supplied debris that the drainage network could accommodate. However, when slopes that had adjusted to relatively humid conditions were suddenly subjected to semi-arid conditions, as they would have been during a climate change, the drainage density would have to increase to accommodate the new hydrologic conditions. Incising the additional first- and second-order streams necessary to make the hillslope texture consistent with the new climate may produce a large enough increase in sediment supply to cause the formation of the fill terraces. When the proper drainage density was achieved, the hillslope system was again compatible with the climate and downcutting began to occur in the transfer part of the system, where the excess debris had accumulated, reestablishing the fluvial gradient consistent with the drainage system as a whole. Once the prefill gradient was achieved, the downcutting would continue at a lower rate, consistent with the long-term expansion and maturation of the Cajon Creek system.

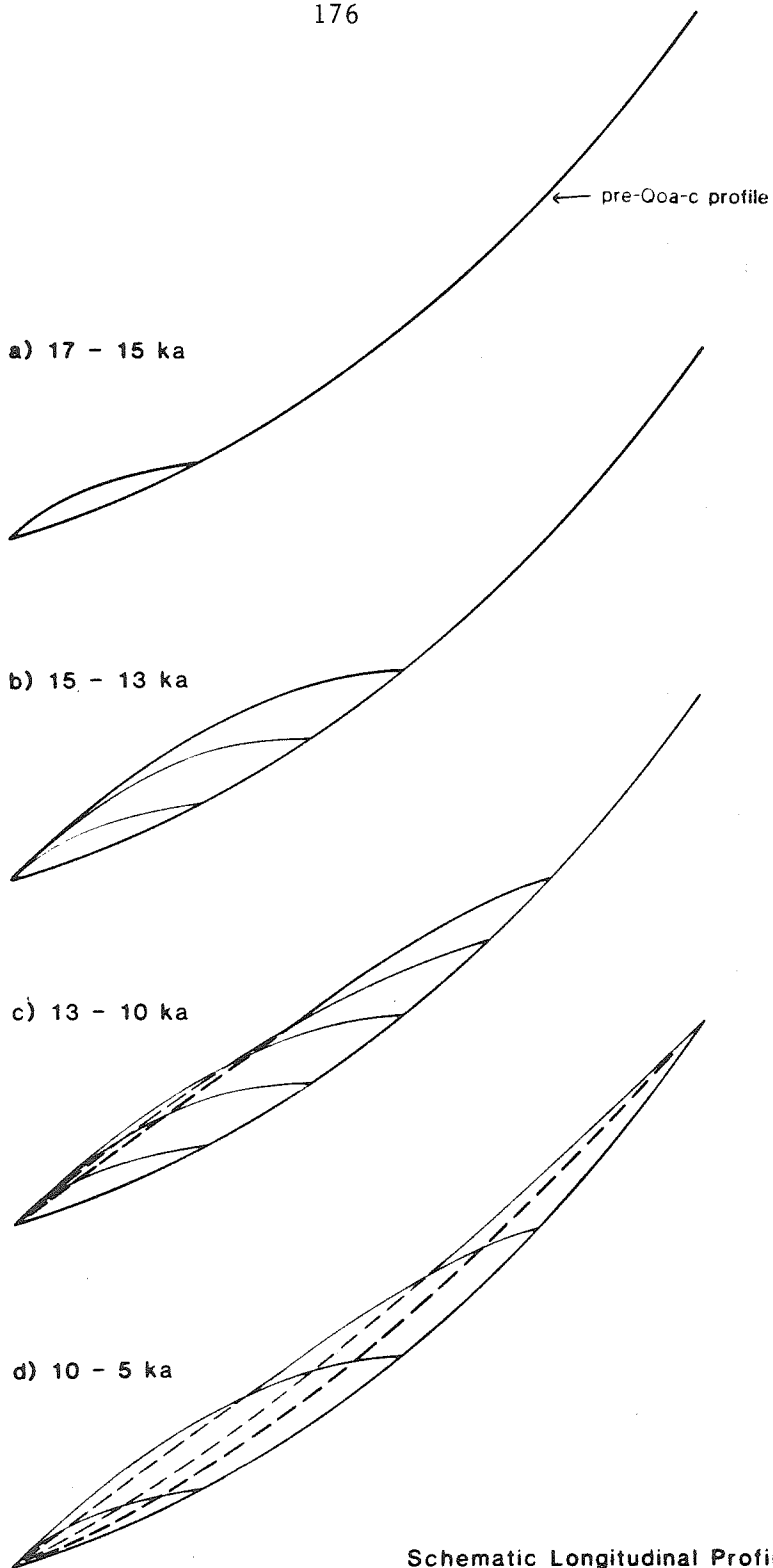
If it takes a long time to establish a hillslope system consistent with relatively humid conditions, by filling or erosional smoothing of the excess first- and second-order drainages, the degree to which the humid hillslope differs from the relatively arid slopes depends on the length of the relatively humid conditions. The time would then be reflected in the magnitude of the subsequent change required to return the system to the more arid condition, and the size of the fill event.

It is not clear that this hypothesis is really different from a vegetative change because the vegetation and hillslope texture are certainly related. Perhaps a number of interrelated processes, including vegetation, weathered regolith, stored loose material, hillslope textural changes, and precipitation differences all interact to produce the aggradation, and no single process should be singled out.

Upstream migration of the fill

It is not understood why the Qoa-c fill pulse migrated upstream. Possibly, hypothetical vegetation or drainage density changes migrated up the system. However, the fill event may have started at the basin edge and migrated upstream because that part of the drainage was most sensitive to an excess of sediment supply experienced by the whole system. An excess of debris may have required the system to steepen its gradient to move the excess material. However, because the relative level of the hillslopes and the basin are fixed (in the short term), the average gradient of the system cannot be changed; so Cajon Creek can increase its gradient only locally, decreasing it immediately upstream. If the creek began to deposit material near the basin, it increased its gradient downstream of the locus of deposition and decreased it upstream (Fig. 13a). Material would rapidly accumulate in the flatter, upstream reach until

Figure 3-13 The deposition of Qoa-c in Cajon Creek, represented by successive profiles. The filling, associated with a steepening of the local gradient below the locus of deposition and a lowering above, migrates upstream. Degradation also migrates upstream as the rate of aggradation began to decrease. However, deposition continued to migrate upstream after the system switched from net aggradation to degradation.



Schematic Longitudinal Profiles of
Cajon Creek during the Deposition of Ooa-c

Figure 3-13

downcutting profile

aggrading profile

it reached a thickness such that the downstream reach could transport all of its load. Because the sediment supply continued to increase, the reach upstream of the steepened reach also steepened by aggradation. The locus of filling therefore migrated farther upstream and the steeper reach to the basin lengthened (Fig. 13b).

The aggrading reach maintained a constant gradient (Fig. 10) as it migrated upstream. It is likely that little coarse debris could cross the relatively flat aggrading reach so it was laid down to form the fill terraces. In this way, essentially all of the coarse sediment produced upstream of that point was stored. All of the sediment produced downstream of the aggrading reach could leave the system because of the steeper gradient. Ultimately, the sediment supply began to decrease and the gradient from the aggrading reach to the basin began to decrease. This probably happened about 13,500 years ago when the rate of total aggradation began to decrease (Fig. 11), and was manifested by the progressive flattening of the downstream reach after that time (Fig. 10).

Material continued to build up in the relatively flat portion and minor erosion occurred in the steep portion to achieve a gradient consistent with the decreasing sediment supply (Fig. 13c). The relatively steep reach continued to lengthen, and the fill continued to thicken upstream. At about 10 ka the amount of erosion downstream surpassed the amount of filling upstream. However, the fill continued in the upper reaches at least until 6,000 years ago. The material deposited between 10,000 and 6,000 years ago may have been a baselevel response to the thick fill in the center of the drainage. Most of the system was eroding after about 6,000 years ago when incision reached the upper part of the drainage (Fig. 13d). From that time on the creek slowly approached its

current (and prefill) configuration by downcutting everywhere. The gradient in the central part of the system was essentially parallel to the prefill profile but at a higher level until all of the stored material was removed.

Long-term storage and preservation of the fill

While it appears that the controlling factor in fill terrace accumulation was sediment supply, the gradient of the trunk stream and the relative size of the tributaries determined where the sediment was stored. The streams form gradients consistent with the overall drainage regardless of the width of the channel. The Qoa units form very narrow terraces where the drainage was deeply channelized or very wide deposits where the gradient required it to overtop the pre-existent channel. In Flat Creek, for example, the width of Qoa-a varies by a factor of 3 (Fig. 1) but it maintains a smooth gradient throughout (Fig. 9). The same relationship is seen in Lone Pine Canyon (Fig. 1), where the width of Qoa-a varies by an order of magnitude while maintaining a smooth gradient.

To a large degree the local preservation of a fill deposit depends on the degree of channelization in the area before the fill was laid down. If the fill did not overtop and exceed the main channel it was quickly removed by subsequent erosion. If it did exceed the channel height, the fill became a broad deposit, apparently limited only by the relationship between the gradient of the overall system and the local topography. When the fill overtops the channels the deposit is likely to be preserved because subsequent incision will be localized to new channels, leaving widespread isolated remnants of the unit. This happened in the case of Qoa-d and Qoa-e and, locally, for Qoa-c. Many less voluminous deposits that did not exceed the channels were probably eroded,

leaving no trace of their existence. Also, because this process caused many drainages to begin incising at about the same time it provides a useful marker for tectonic studies. Many of the streams that cross an active fault were "reset" at the same time so offsets of channels incised into the major correlatable deposits are comparable over wide areas.

Distinguishing Qoa from Qhf deposits

Qoa deposits occur in the transfer portion of the fluvial system where sedimentation occurs only occasionally. Because Qoa units form during brief pulses separated by long periods of nondeposition, it is possible to recognize and correlate the deposits. Qhf deposits can also occur in these areas but a local cause can usually be found. Therefore, Qhf deposits, like landslides, scarp and sag pond sediments, and even alluvial deposits like those at Pink River and along the San Andreas near Devore (discussed above) have distinct contacts with the local Qoa units. In areas of transition from the transfer part of the system to the hillslopes, as in Crowder and Pitman Canyons, Qhf deposits form continuously through time. Qoa-c (Fig 7), and probably the other Qoa units, increase in age range towards the hillslopes so there is no real distinction between the Qoa and Qhf at the hillslope-channel interface. In these areas the deposits are long-term storage repositories where the system cannot accommodate all of its sediment supply and are only removed during exceptional periods of erosion.

The fact that the Qoa and Qhf deposits merge at the edge of the system lends insight into their distinction. In the ideal fluvial system only the transfer portion is close to the threshold of critical power (Bull, 1979). In the depositional basin the stream (available) power is far less than the resisting power (that required to move sediment) and

in the production area the stream power generally exceeds the resisting power. For this reason, the transfer portion of the system where resisting power is close to stream power switches from deposition to erosion in response to small changes in the system such as a climate change. Near the edges, where the stream and resisting power diverge, the system is less sensitive and only large changes can cause the system to cross the threshold between deposition and erosion. This difference in the sensitivity of the system results in the difference between Qoa and Qhf deposits.

CONCLUSION

The widespread fill terraces in Cajon Creek were formed during the late Quaternary, during periods of climatic change from relatively wet and/or cold regimes to dry and/or hot periods. The fill terraces were deposited in pulses between about 2000 and 300 BP, 17,000 and 6,000 BP, about 55,000, and about 500,000 years ago. All of the fill events were followed by periods of relatively high incision rates that returned the system to its prefill level. The correlation of the stratigraphy in Cajon Creek with climatic change, and the existence of similar sequences of units in other drainages in the central Transverse Ranges may allow the correlation of undated deposits throughout the area with those dated at Cajon Creek.

The exact age of individual deposits varies laterally within the drainage. The age of the Qoa-c fill terrace in Cajon Creek varies laterally by at least 9000 years. Dates from outcrops of fill terraces must be understood to represent only the age of the deposit near where the sample was taken. However, the periods of time separating the older major units appears to be much less than the variation in age within

individual units, so correlations can be useful.

Care must be used in deciding which deposits can be correlated between and within drainages. Often the uncorrelatable deposits can be easily distinguished on the basis of their lithology. However, in principle there is no lithologic distinction between units formed in concert with others in the system and those that do not, so accurate discrimination may require studying individual deposits in the broader context of their depositing systems.

The rapidly fluctuating fluvial gradients associated with the fill deposits in Cajon Creek indicate that a greater degree of caution is required in using terrace profiles as reference levels than is commonly practiced. Many workers have compared terrace profiles through time and have appealed to tectonics, baselevel changes or long-term drainage basin evolution to explain differences in the heights or shapes of terraces. It is clear from the record at Cajon Creek that the surface of a fill terrace is not necessarily parallel to another fill terrace, cut terrace, or any other arbitrary fluvial profile (like today's). The surface of a fill terrace probably rarely even represents a profile in the sense that water actually flowed down the whole surface at any one time. If most fill terraces are like Qoa-c in Cajon Creek, the surface mapped in the field is only an envelope of the actual gradients occupied by the creek during the migrating depositional event. As the creek never actually had a profile shaped like the fill surface, comparing it to other surfaces to determine tectonic deformation or fluvial development of the system will obviously lead to misinterpretations.

Cut terraces are a little better for comparison but even they are not completely parallel. Also, the fact that cut terraces merge with

the migrating fill surfaces suggests that they may also transgress time. Cut and strath terraces are generally produced when a large part of the system is at equilibrium (Bull, 1979). Cajon Creek produced its most extensive cut terraces during the early-to-middle Holocene while the upper portion of the system was still alluviating and the lower portion was slowly downcutting, so the overall system was near equilibrium. The cut-and-strath terraces represent transport surfaces between the alluviating and downcutting sections so their gradients were quite similar and their slopes could be reasonably compared. However, their heights vary considerably, depending on when, during the post-fill erosional period, they formed. Inferring uplift or subsidence from these surfaces will give erroneous results. The requirement that the system be at equilibrium is a necessary but not a sufficient condition for comparing profiles.

It does appear that the gradient before a fill event and the gradient after the fill have subsequently been removed are virtually identical. Therefore, to accurately compare fluvial gradients the system must be near the threshold of critical power throughout most of its length and must not have large amounts of material stored in the transport part of the system. In this case the only difference in gradients should be the long-term downcutting rate, which is relatively low. Unfortunately, such profiles are difficult to determine in the field unless they are preserved as the base of a particular channel fill that can be correlated throughout the area. Comparisons of the gradients formed by the base of fill deposits with one another or the present profile, which is generally near the base of the late Holocene fill, may allow tectonic inferences to be accurately drawn. However, because the really major fills (eg. Qoa-d

and Qoa-e in Cajon Creek) are separated by long periods of time it will remain a difficult problem to separate tectonic effects from long-term fluvial effects such as the capture and maturation of the depositing system.

ACKNOWLEDGMENTS

The field work presented in this paper was part of a Ph.D. thesis carried out under the supervision of K. Sieh at Caltech, supported by the U.S.G.S. Earthquake Hazards Reduction Programs, contract numbers 14-08-0001-16774, 18285, 19756, and 21275. Subsequently, part-time support by the U.S.G.S. made the writing of this paper possible and their contribution is gratefully acknowledged. Particularly insightful suggestions by Bill Bull, University of Arizona, during the course of the work led to many of the results presented here. Criticism of a first draft by Bill Bull, Dick Crook and Kerry Sieh led to substantial improvements in the paper.

BIBLIOGRAPHY

- Adam, D. P., Sims, J. D., Throckmorton, C. K., 1981, 130,000-year continuous pollen record from Clear Lake, California, Geology, v. 9, p. 373-377.
- Aharon, P., 1983, 140,000-year isotopic climatic record from raised coral reefs in New Guinea, Nature, v. 304, p. 720-723.
- Ahlborn, A. O., 1982, Santa Ana River basin flood hazard, San Bernardino County Museum Association Quarterly, v. 29, #2, 95 p.
- Bull, W. B., 1979, Threshold of critical power in streams, Geol. Soc. Amer. Bull., v. 90, p. 453-464.
- Bull, W. B., Menges, C. M., McFadden, L. D., 1978, Stream terraces of the San Gabriel Mountains, southern California, Final Technical Report, south front of the San Gabriel Mountains, southern California, unpublished, US Geol. Survey Report, 139 p.
- Crook, R. C. Jr., 1985, Relative dating of Quaternary deposits based on P wave velocities in weathered granitic clasts, submitted to Quaternary Research 1984, 18 p.
- Crook, R. C. Jr., Allen, C. R., Kamb, B., Payne, C. M., and Proctor, R. L., 1978, Quaternary geology and seismic hazard of the Sierra Madre and associated faults, western San Gabriel Mountains, California, Final Technical Report, unpublished US Geol. Survey Report, 117 p.
- Currey, D. R., 1980, Coastal geomorphology of Great Salt Lake and vicinity, Bull. Utah Geol. Miner. Survey, v. 116, p. 69-82.
- Dibblee, T. W., Jr., 1967, Areal geology of the western Mojave Desert, US Geol. Survey Prof. Paper 522, 153 p.
- Dibblee, T. W., Jr., 1965, Geologic map of the Cajon 7-1/2 - minute Quadrangle, San Bernardino County, California, U.S.G.S Open File Map.

- Duplessy, J.-C., Delibrias, G., Turon, J. L., Pujol, C., and Dupret, J., 1981, Deglacial warming of the northeastern Atlantic Ocean: Correlation with the paleoclimatic evolution of the European continent, *Palaeogeog., Palaeoclimo., and Palaeoeco.*, v. 35, p. 121-144.
- Eckis, R. P., 1928, Alluvial fans of the Cucamonga district, southern California, *Jour. Geol.*, v. 36, p. 224-247.
- Foster, J. H., 1980, Late Cenozoic tectonic evolution of Cajon Valley, southern California, *Ph.D. Dissertation*, University of California, Riverside, 242 p.
- Gillespie, A. R., 1982, Quaternary glaciation and tectonism in the southeastern Sierra Nevada, Inyo County, California, *Ph.D. Dissertation*, California Institute of Technology, Pasadena, California, 695 p.
- Haner, B. E., 1982, Quaternary geomorphic surfaces on the northern Perris block, Riverside County, California; Interrelationship of soils, vegetation, climate and tectonics, *Ph.D. Dissertation*, University of Southern California, Los Angeles, California, 227 p.
- Klein, J., Lerman, J. C., Damon, P. E., and Ralph, E. K., 1982, Calibration of radiocarbon dates: Tables based on the consensus data of the work shop on calibrating the radiocarbon time scale, *Radiocarbon*, v. 24, p. 103-150.
- Kottlowski, F. E., Cooley, M. E., Puhe, R. V., 1965, Quaternary geology of the Southwest, in Wright, H. E. Jr. and Morrison, R. B., eds., *Quaternary of the United States*, Princeton University Press, p. 287-293.
- Lajoie, K. R. and Robinson, S. W., 1982, Late Quaternary glacio-lacustrine chronology Mono Basin, California, G.S.A. Cordilleran Section Meeting (78th), Abstracts with Programs, v. 14, p. 179.

- Langbein, W. B. and Schumm, S. A., 1958, Yield of sediment in relation to mean annual precipitation, Am. Geophys. Union Trans., v. 39, p. 1076-1084.
- Leopold, L. B. and Bull, W. B., 1979, Baselevel, aggradation, and grade, Proc. Amer. Phil. Soc., v. 123, #3, p. 168-202.
- Martin, P. S. and Mehringer P. J. Jr., 1965, Pleistocene pollen analyses and biogeography of the Southwest, in Wright, H. E. and Frey, D. G., eds., The Quaternary of the United States, Princeton University Press, Princeton, N. J., p. 433-452.
- McFadden, L. D., 1982, The impact of temporal and spacial climate change on alluvial soils genesis in southern California, Ph.D. Dissertation, University of Arizona, Tucson.
- McFadden, L. D. and Weldon, R. J., 1984, The recognition of a new threshold of soil formation in soils at Cajon Creek, southern California, in Abstracts with Programs, 97th Annual Meeting, Geol. Soc. Amer., v. 16, p. 588.
- McFadden, L. D. and Weldon, R. J., Rates and process of soil development in Cajon Pass, southern California, in review, submitted Geol. Soc. Amer. Bull. March, 1986.
- Meisling, K. E., 1983, Neotectonics of the north frontal fault system of the San Bernardino Mountains, southern California: Cajon Pass to Lucerne Valley, Ph.D. Dissertation, Caltech, Pasadena, 394 p.
- Mezger, L., 1982, Tectonic implications of the Quaternary history of lower Lytle Creek, southeastern San Gabriel Mountains, Senior Thesis, Pomona College, Claremont, 21 p.
- Morton, D. M. and Miller, F. K., 1975, Geology of the San Andreas fault zone north of San Bernardino between Cajon Creek and Santa Ana Wash,

- in San Andreas fault in southern California: A guide to San Andreas fault from Mexico to Carrizo Plain, ed. Crowell, T.C., Cal. Div. of Mines and Geol., Sp. Rep. 118, p. 136-146.
- Noble, L. F., 1954, Geology of the Valyermo Quadrangle and vicinity, California, U.S.G.S. Quadrangle Map GQ-50.
- Passey, Q. R., 1981, Upper mantle viscosity derived from the difference in rebound of the Provo and Bonneville shorelines: Lake Bonneville Basin, Utah, Jour. Geophys. Res., v. 86, p. 11,701-11,708.
- Rowe, P. B., Countryman, C. M., and Storey, H. C., 1954, Hydrologic analysis used to determine effects of fire on peak discharge and erosion rates in southern California watersheds, USDA Forest Service, California Forest and Range Experiment Station Report (February, 1954).
- Rowe, P. B., Countryman, C. M., and Storey, H. C., 1949, Probable peak discharges and erosion rates from southern California watersheds as influenced by fire, USDA Forest Service, California Forest and Range Experiment Station Report (February, 1949).
- Ruddiman, W. F., and Duplessy, J.-C., 1985, Conference on the last deglaciation: Timing and mechanism, Quaternary Research, v. 23, p. 1-17.
- Schumm, S. A., 1977, The fluvial system, John Wiley & Sons, New York, 338 p.
- Scott, W. E., 1980, Quaternary stratigraphy of the Wasatch Front, U. S. Geol Surv. Open File Rept., 80-842 (X), p. 121-124.
- Scott, W. E., McCoy, W. D., Shroba, R. R., Rubin, M., 1983, Reinterpretation of the exposed record of the last two cycles of Lake Bonneville, Western United States, Quaternary Research, v. 20, p. 261-285.
- Scott, K. M., and Williams, R. P., 1974, Erosion and sediment yields in mountain watersheds of the Transverse Ranges, Ventura and Los Angeles

- Counties, California - Analysis of rates and processes, US Geol. Sur. Water Resources Investigations, # 47-73.
- Shackleton, N. J. and Matthews, R. K., 1977, Oxygen isotope stratigraphy of late Pleistocene coral terraces in Barbados, Nature, v. 268, p. 618-620.
- Shackleton, N. J. and Opdyke, N. D., 1973, Oxygen isotope and palaeomagnetic stratigraphy of equatorial Pacific core V28-238: Oxygen isotope temperatures and ice volumes on a 10^5 year and 10^6 year scale, Quat. Res., v. 3, p. 39-55.
- Sharp, R. P., 1972, Pleistocene glaciation, Bridgeport basin, California, Geol. Soc. Amer. Bull., v. 83, p. 2233-2260.
- Sieh, K. E., 1984, Lateral offsets and revised dates of large prehistoric earthquakes at Pallett Creek, southern California, Jour. Geophys. Res., v. 89, p. 7641-7670.
- Smith, G. I., 1984, Paleohydrologic regimes in the southwestern Great Basin, 0-3.2 my ago, compared with other long records of "global" climate, Quat. Res., v. 22, p. 1-17.
- Smith, G. I., 1979, Subsurface stratigraphy and geochemistry of late Quaternary evaporites, Searles Lake, California, US Geol. Survey, Prof. Paper, 1043.
- Stine, S., 1984, Late Holocene lake level fluctuations and island volcanism at Mono Lake, California, in, Holocene paleoclimatology and tephrochronology east and west of the central Sierran crest, Field Trip Guidebook for the Friends of the Pleistocene, Pacific cell, 1984.
- Taylor, B. D., 1981, Sediment management for southern California mountains, coastal plains and shorelines; part b, Inland sediment movements by natural processes, Environmental Quality Lab Report, # 17-B,

California Institute of Technology.

- van Donk, J., 1976, O¹⁸ record of the Atlantic Ocean for the entire Pleistocene epoch, in Investigations of late Quaternary paleoceanography and paleoclimatology, eds., Cline, R.M. and Hays, J.D., Geol. Soc. Amer. Memoir # 145, p. 147-163.
- Weldon, R. J., 1984, Implications of the age and distribution of late Cenozoic stratigraphy in Cajon Pass, southern California, in San Andreas fault - Cajon Pass to Wrightwood, eds., Hester, R. I. and Hallinger, D. L., A.A.P.G. Pacific Section Guidebook # 55, p. 9-16.
- Weldon, R. J., 1983, Climatic control for the formation of terraces in Cajon Creek, southern California, in Abstracts with Programs, Cord. Sec., Geol. Soc. Amer., v. 15, p. 429.
- Weldon, R. J. and Meisling, K. E., 1982, Late Cenozoic tectonics of the western San Bernardino Mts; Implications for the uplift and offset of the central Transverse Ranges, in Abstracts with Programs, Cord. Sec. (78th), Geol. Soc. Amer., v. 14, p. 243-244.
- Weldon, R. J., Meisling, K. E., Allen, C. R., and Sieh, K. E., 1981, Neotectonics of the Silverwood Lake area, San Bernardino County, unpublished report to Cal. Dept. of Water Resources to accompany 50-sq. mile map of the NW San Bernardino Mountains around the Silverwood Lake Reservoir.
- Weldon, R. J. and Sieh, K. E., 1985, Holocene rate of slip and tentative recurrence interval for large earthquakes on the San Andreas fault in Cajon Pass, southern California, Geol. Soc. Amer. Bull.
- Weldon, R. J., Meisling, K. E., Kirschvink, J. L., and Graymer, R. W., in preparation, Paleomagnetic constraints on the uplift and rate of offset of the central Transverse Ranges across the San Andreas fault

system, southern California.

Wells, P. V., 1979, An equable glaciopluvial in the West: pleniglacial evidence of increased precipitation on a gradient from the Great Basin to the Sonoran and Chihuahuan Deserts, Quaternary Research, v. 12, 311-325.

Wells, P. V. and Berger, R., 1967, Late Pleistocene history of coniferous woodlands in the Mojave Desert, Science, v. 155, p. 1640-1647.

Woodburne, M. O. and Golz, D. J., 1972, Stratigraphy of the Punchbowl Formation, Cajon Valley, southern California, Univ. Cal. Pub. Geol. Sci., v. 92, 73 p.

Wright, H. E., Bent, A. M., Hansen, B. S., and Maher, L. J., 1973, Present and past vegetation of the Chuska Mountains, northwestern New Mexico, Geol. Soc. Amer. Bull., v. 84, p. 1155-1179.

Yerkes, R. F., 1951, The geology of a portion of the Cajon Pass area, California, MA Thesis, Claremont Graduate School, 97 p.

CHAPTER FOUR

PALEOMAGNETIC CONSTRAINTS ON THE
UPLIFT AND RATE OF OFFSET OF THE CENTRAL TRANSVERSE RANGES
ACROSS THE SAN ANDREAS FAULT SYSTEM, SOUTHERN CALIFORNIA

By

Weldon, Ray J.¹
USGS, OEVE, M/S 977
345 Middlefield Road
Menlo Park, California 94025

Meisling, Kristian E.
ARCO Oil and Gas Company,
Dallas, Texas 75221

Kirschvink, Joseph L. and Graymer, Russell W.
Division of Geological and Planetary Sciences
California Institute of Technology
Pasadena, California 91125

¹Field work done at Caltech, Pasadena, CA 91125

ABSTRACT

Sediments shed northward from the central Transverse Ranges into the Mojave Desert record the uplift of the central Transverse Ranges and dextral slip on the San Andreas fault throughout the Quaternary Period. New paleomagnetic age data for the Harold Formation, Shoemaker Gravels, and Noble's Older Alluvium, derived from distinctive source areas in the San Gabriel Mountains southwest of the San Andreas fault, allow determination of a Quaternary slip rate of 37.5 ± 2 mm/yr for the San Andreas fault northwest of its junction with the San Jacinto fault and 21 ± 7 mm/yr for the San Andreas fault southeast of this junction. The change in rate at the junction approximates the 8-12 mm/yr of Quaternary dextral slip attributed to the San Jacinto fault by Sharp (1981), and supports the hypothesis that the slip rate of the San Andreas northwest of their junction is simply the sum of the San Andreas and San Jacinto faults to the southeast. The similarity between these data and the Holocene rate of slip on the San Andreas fault (Weldon and Sieh, 1985; Sieh and Jahns, 1984) supports the hypothesis that the San Andreas and San Jacinto faults have maintained relatively constant slip rates throughout the Quaternary Period.

The eastern San Gabriel Mountains were a major topographic high as early as 1.5 my ago, as evidenced by sedimentary rocks in Cajon Pass which record the lateral translation of distinctive source terranes in the mountains to a position opposite the relatively low Mojave Desert across the San Andreas fault. The western San Bernardino Mountains were uplifted as the high San Gabriel Mountains passed by across the San Andreas fault. This uplift occurred about 1 my ago in Cajon Pass and migrated northwest; the same style of activity is currently uplifting the area between Wrightwood and Valyermo.

INTRODUCTION

The central Transverse Ranges are being both laterally offset by the San Andreas fault and uplifted across it. The San Andreas and other major faults in the area generally juxtapose rocks that are much older than the ongoing Quaternary deformation, so the rocks are of little use in deciphering the timing and rates of deformation associated with Quaternary movement on these structures. Very young alluvium, on the other hand, commonly overlies or is only slightly deformed by the major faults. Even where deformed alluvial deposits can be radiocarbon dated one is generally left extrapolating rates several orders of magnitude beyond the age control to characterize gross features such as the uplift and offset of the Transverse Ranges. Minor faults, folds, and regional tilting simply do not deform young alluvium enough to allow geologists to characterize their rates and styles of offset, and are therefore commonly ignored.

This lack of crucial data on long-term rates of deformation in the central Transverse Ranges is characteristic of the San Andreas system throughout southern California. There are many documented offsets of rocks and structures that are older than the San Andreas fault (e.g., Crowell, 1962, 1981; Silver, 1968; Ehlig et al., 1975; Powell, 1981). There are also a growing number of Holocene deformational rates, determined by dating alluvial deposits with radiocarbon, or, in the areas that are creeping or contain geodetic networks, measured in real time (e.g., Sieh and Jahns, 1984; Weldon and Sieh, 1985; Lisowski and Prescott, 1981; Savage, 1983; Christodoulidis et al., in review). There remains a critical Plio-Pleistocene gap in offset data which must be bridged before we can really understand the San Andreas system and its relationship to contemporaneous vertical tectonics, like that occurring in the Trans-

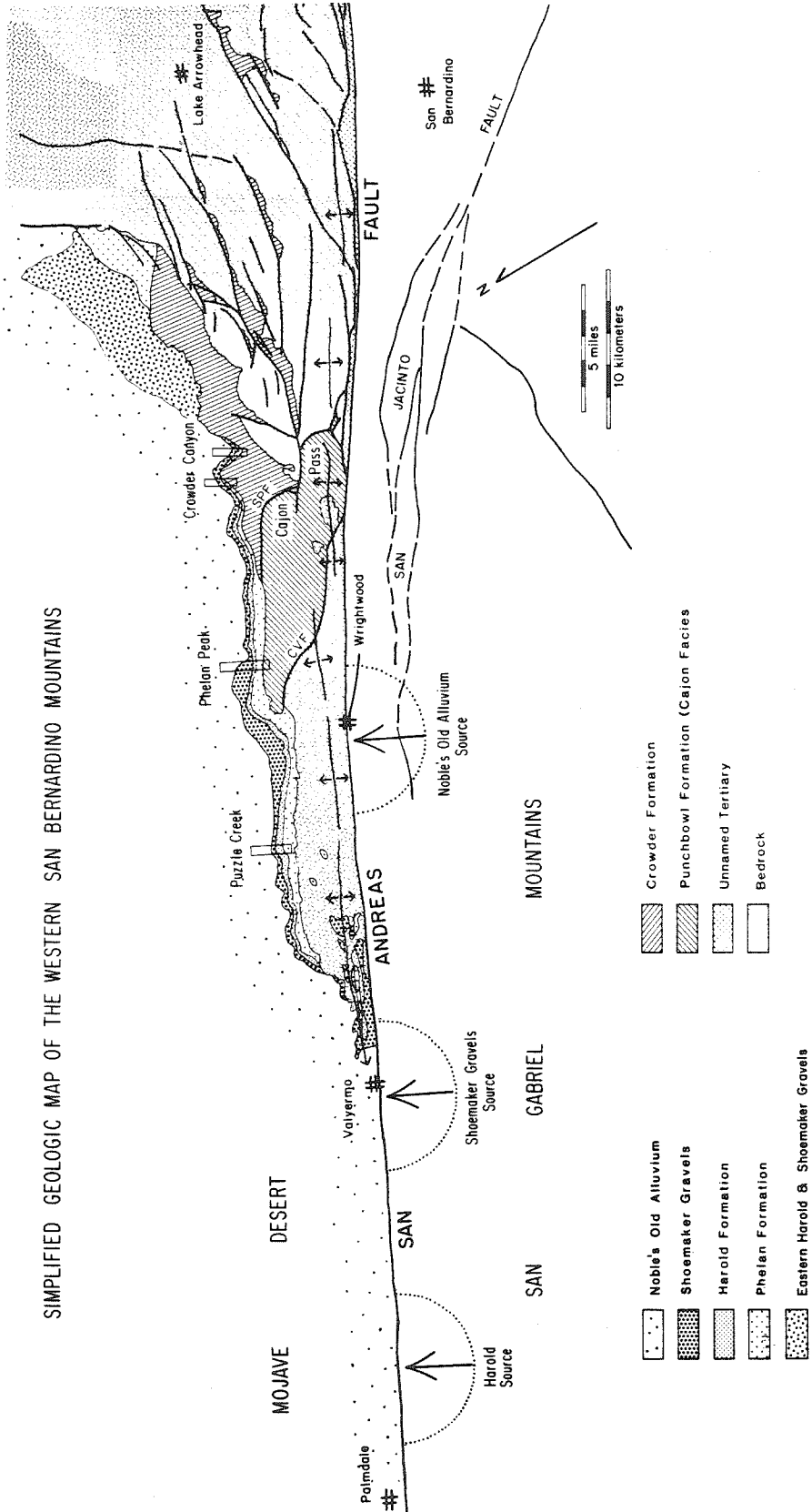
verse Ranges.

Through the use of magnetostratigraphic techniques, we have been able to date deposits that preserve the record of the Plio-Pleistocene tectonics in the Cajon Pass area. Our magnetostratigraphic data, coupled with fossil age determinations (Reynolds, 1983, 1984, 1985; Woodburne and Golz, 1972), two fission track dates on volcanic ashes (C.F. Naeser, written communication, 1981; 1982) and detailed mapping (Weldon, 1984a, 1985; Meisling, 1984; Weldon et al., 1981; Foster, 1980), provide the basis for a major reassessment of the late Cenozoic stratigraphy and tectonics of Cajon Pass. This paper briefly outlines the new age constraints in the Cajon Pass area (Fig. 1), and discusses implications for the Quaternary motion on the San Andreas fault and the local history of uplift. Related papers by Weldon (1984a) and Meisling and Weldon (in preparation) address the overall evolution of the late Cenozoic tectonics of the western San Bernardino Mountains, and Weldon et al. (1984 and in preparation) document the age and stratigraphy of the Tertiary units that generally predate the activity on the modern San Andreas fault.

The Quaternary sediments of the Harold Formation, Shoemaker Gravels, and Noble's Older Alluvium (together called the Victorville Fan) contain the first evidence of the current episode of uplift of the central Transverse Ranges near Cajon Pass and are the focus of this paper. These sediments were shed across the San Andreas fault from the San Gabriel Mountains and formed huge fans in the Mojave Desert. Through time these fans coalesced to form a continuous band of fanglomerates across the area that was to become Cajon Pass. Distinctive facies in the Victorville Fan can be traced to local source areas in the San Gabriel Mountains. The long outcrop belts of distinctive facies from the San Gabriel Mountains (Fig.

Figure 4-1 - The geology of the western San Bernardino Mountains, southern California. The Miocene basins (line patterns) have been truncated by Mio-Pliocene faults. The Plio-Pleistocene Phelan formation overlies these early faults and, with the early-to-middle Quaternary deposits, outcrops in a narrow belt along the northern edge of the western "wing" of the San Bernardino Mountains. The Harold Formation, Shoemaker Gravels, and Noble's Older Alluvium in Cajon Pass were deposited from discrete source regions in the San Gabriel Mountains, as indicated on the map. The sections where the Quaternary units have been dated are shown as rectangles. SPV is the Squaw Peak fault and CVF is the Cajon Valley fault.

SIMPLIFIED GEOLOGIC MAP OF THE WESTERN SAN BERNARDINO MOUNTAINS



- Noble's Old Alluvium
- Shoemaker Gravels
- Harold Formation
- Phelan Formation
- Eastern Harold & Shoemaker Gravels

- Crowder Formation
- Punchbowl Formation (Cajon Facies)
- Unnamed Tertiary
- Bedrock

1) are reminiscent of "hopper car" sedimentation proposed for the Violin Breccia of the Ridge Basin by Crowell (1952, 1982b).

The lower members of the Victorville Fan were deposited at fairly low elevations northwest of the uplifting San Bernardino Mountains. They were then warped into the broad northwest-trending folds that form the western San Bernardino Mountains, locally eroded, and overlain unconformably by the upper members of the Victorville Fan. By studying the character of these sediments and dating them precisely, we can determine the timing and style of uplift in the area and the slip rate on the San Andreas fault.

For the purposes of this paper, the San Andreas fault is taken to be the division between the San Bernardino and San Gabriel Mountains rather than Cajon Pass, which is the physiographic boundary (Fig. 1). This division emphasizes geologic differences across the San Andreas fault and includes what is generally taken to be the northeastern San Gabriel Mountains, near Wrightwood, with the San Bernardino Mountains.

LATE CENOZOIC STRATIGRAPHY

Late Cenozoic stratigraphy in Cajon Pass can be subdivided into 3 packages of sedimentary rocks, formed during three different tectonic regimes. In late Early to early Late Miocene time basins formed in an extensional environment characterized by relatively low relief and a south-southwest regional slope. The shape and extent of these basins are unknown, as the basins are obscured by a Mio-Pliocene deformational event (Weldon, 1984a; Meisling and Weldon, in preparation). Pliocene to early Pleistocene rocks were deposited in narrow east-west trending basins reflecting the Mio-Pliocene structural grain. They include a

wide variety of lithologies from lacustrine clays with volcanic ashes to conglomerates. Middle-to-late Pleistocene deposits are composed of coarse conglomerates and fluvial gravels shed off the rapidly uplifting central Transverse Ranges.

Late Tertiary Sediments

The Crowder Formation was thought to unconformably overlie the middle Miocene Cajon facies of the Punchbowl Formation (Woodburne and Golz, 1972; Foster, 1980) until fossils of middle Miocene age were discovered at its base (Reynolds, 1983). Additional fossils (Reynolds, 1984; 1985) and magnetostratigraphic data (Weldon et al., 1984 and in preparation; Winston, 1985) demonstrated that the type section of the Crowder Formation spans a period of time from about 17 my to 9.5 my ago and is therefore at least partly contemporaneous with the Cajon facies of the Punchbowl Formation.

The sedimentary rocks overlying the Miocene basins, the "western Crowder" of Foster (1980), were, upon reexamination, found to range in age from 4.1 to between 1.5 and 1.2 my ago (Fig. 2). The match with the absolute time scale, based on fission track-dated volcanic ashes (C.F. Naeser, written communication, 1981, 1982), is discussed by Weldon (1984a) and Weldon et al. (in preparation). These Plio-Pleistocene rocks have been informally renamed the Phelan formation (Weldon, 1984a). The lithologic similarity of the Phelan formation over a distance of 50 km suggests that it formed in a narrow west-northwest-trending basin subparallel to the San Andreas fault, the axis of which may be defined by the gravity low of Cajon basin (p. 159, Dibblee, 1975b). If the Juniper Hills Formation of Barrows (1980) is contemporaneous with the Phelan formation (suggested by Foster (1980) for his "western Crowder") the basin may have once ex-

Figure 4-2 - Magnetic stratigraphy of the Phelan formation at Phelan Peak (Fig. 1). White indicates reversed polarity and black normal. Vertical stripes indicate uncertain polarity zones that contain too few samples or contradictory results. Samples with stable demagnetization paths (discussed in text) are presented as points and samples with demagnetization paths that form planes are plotted with tails to show the final orientation and the amount that the sample changed during demagnetization. The match is based on two fission track dated ashes and sparse fossil control, and is consistent with the unit's position between the middle Miocene and Quaternary sediments. The fine grained facies of unit A (Foster, 1980) was deposited much more slowly than the conglomeratic unit B, and yields more stable magnetic results.

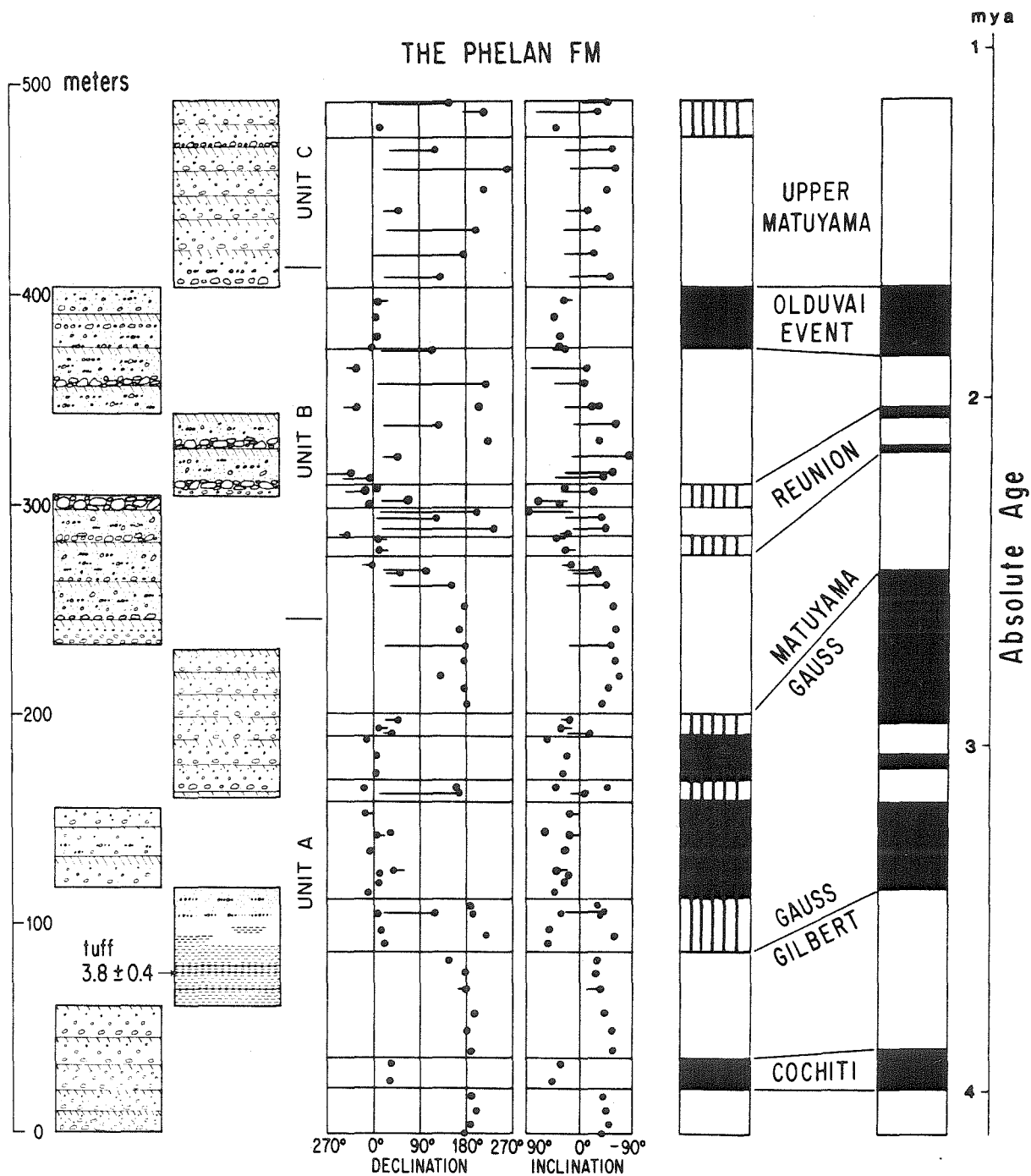


Figure 4-3

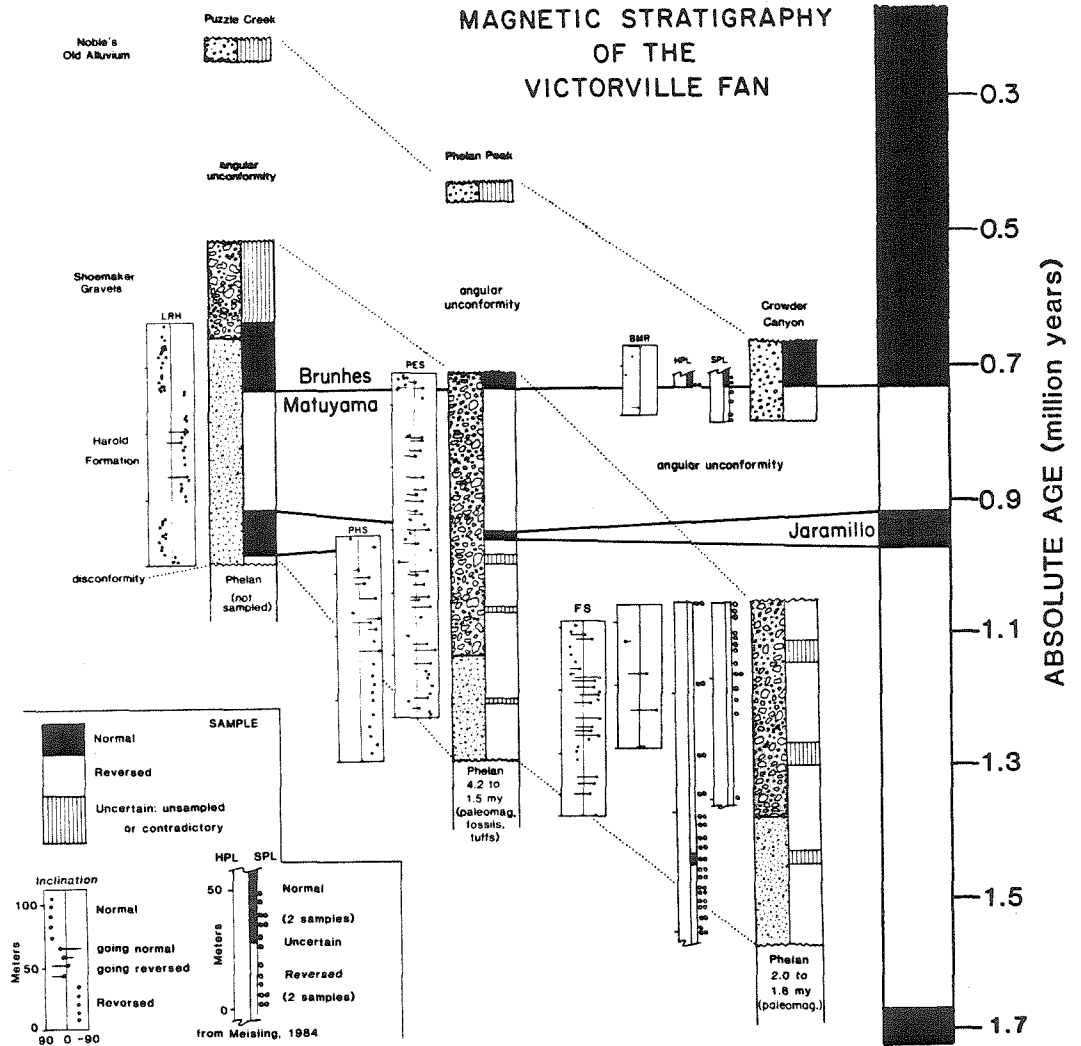
tended across the San Andreas fault between Palmdale and Valyermo (Fig. 1). The Phelan formation is overlain by the Victorville Fan and young alluvium.

Quaternary stratigraphy

The Victorville Fan is a sequence of distal to medial fan sediments shed northeast across the San Andreas fault from the San Gabriel Mountains and north from the western San Bernardino Mountains into the Mojave Desert as a broad, continuous bajada. This style of deposition continues today northwest and southeast of Cajon Pass, where the streams have not yet been captured from the south. The units contain sparse Pleistocene faunas, including the "early Pleistocene" Barrel Springs assemblage in the Harold Formation (C.A. Repenning, written communication, 1981) and several "Pleistocene" faunal assemblages from either the Shoemaker Gravels or Noble's Older Alluvium near Victorville (R. E. Reynolds, unpublished San Bernardino Museum Reports). The fact that the Victorville Fan overlies the Plio-Pleistocene Phelan formation, contains Pleistocene fossils, and is overlain by deposits with middle-to-late Pleistocene soils (McFadden and Weldon, in preparation) and geomorphologic surfaces (Weldon, 1985) leaves no doubt that all of the Victorville Fan units are early-to-middle Pleistocene in age. Magnetostratigraphic sections through the Harold Formation, Shoemaker Gravels, and Noble's Older Alluvium, constructed at three localities (Figs. 1 and 3), firmly support this conclusion.

The Harold Formation in Cajon Pass marks the onset of deposition from the central San Gabriel Mountains source terrane to the Mojave Desert. The base of the Harold Formation is inferred from the magnetic stratigraphy (discussed below) to range in age from about 1.6 my at Crowder Canyon to about 1.3 my near Phelan Peak and 1.0 my at Puzzle Creek. The Harold Formation consists of distal fan material, dominated by pebbly

Figure 4-3 - Magnetic stratigraphy of the Quaternary sediments in the western San Bernardino Mountains region. The match is based on the recognition of the Olduvai event in the upper Phelan formation (Fig. 2) and the presence of Quaternary fossils in the units. Only inclination is shown but the declination results are consistent. Most of the data has been processed like that presented on Figure 2. The HPL and SPL sections are taken directly from Meisling (1984) because they were processed in a different manner. All of the units and the unconformities become younger to the northwest. This is consistent with the northwest migration of the sources through time.



sands, conglomerates and local playa deposits. Clast lithologies in the conglomerates are dominantly leucocratic Cretaceous(?) granitics, with locally common volcanic and Pelona Schist clasts referred to sources southwest of the San Andreas fault near Palmdale (Fig. 1). The Harold Formation in the Cajon Pass area is therefore interpreted to have been derived from the northeastern San Gabriel Mountains now opposite Palmdale (Fig. 1), deposited across the San Andreas fault near the type area of the formation (Noble, 1954a).

The Shoemaker Gravels gradationally overlie the Harold Formation in the Victorville Fan sequence (Noble, 1954a). They consist of coarse conglomerates with a distinctive assemblage of clasts, including Mt. Lowe granodiorite, San Francisquito sandstone, and reworked clasts from the Devil's Punchbowl Formation. This makes it an obvious marker unit in the Victorville Fan. Several workers, including Sharp and Silver (1971), Barrows (1979), and Foster (1980), have speculated on the activity of the San Andreas fault as recorded by the offset of these gravels. The lack of age control, however, has made quantitative conclusions impossible. In this study the Shoemaker Gravel is shown to be about 1.3 to 1.0 my old in Cajon Pass, 1.0 to 0.7 my old at Phelan Peak and 0.7 to 0.4 my old at Puzzle Creek (Fig. 3).

Noble's Older Alluvium is the uppermost unit in the Victorville Fan sequence, overlying the Shoemaker Gravels with an angular unconformity throughout the area. To avoid confusion we call this unit Noble's Older Alluvium, to distinguish it from other Older Alluviums mapped in the area. From Cajon Pass to Phelan Peak it consists predominantly of Pelona Schist debris similar to that currently being shed across the San Andreas fault near Wrightwood (Fig. 1). Farther northwest, Noble's Older Alluvium

includes a variety of alluvial deposits that lie unconformably on the Shoemaker Gravels and contain locally derived clasts from the rising western San Bernardino Mountains, and as such cannot be used to constrain slip across the San Andreas fault. At Cajon Pass Noble's Older Alluvium is about 0.7 my old (Fig. 3), and is inferred to young to the northwest based on its soils, geomorphic position and the age of the underlying units. Most of it is too young to be dated with magnetostratigraphic techniques.

East of Cajon Pass the Victorville Fan thins, becomes progressively richer in clasts derived from the San Bernardino Mountains, and distinguishing between the Harold and Shoemaker Gravels becomes progressively more difficult. The angular unconformity between the Shoemaker Gravels and Noble's Older Alluvium can be traced to the east as far as Deep Creek (Meisling, 1984), where it separates two deposits derived from the western San Bernardino Mountains to the south. Clast compositions clearly show that streams carrying clasts from the San Gabriel Mountains never flowed north across the western San Bernardino Mountains southeast of Cajon Pass. These observations suggest that the San Bernardino Mountains east of Cajon Pass had already developed some relief prior to the deposition of the Harold Formation. Alternatively, the San Gabriel Mountains might not have been a high source of sediments until they faced the Cajon Pass area. This alternative requires that the San Gabriel Mountains developed their high relief when they passed Cajon Pass because the Harold Formation and Shoemaker Gravels in Cajon Pass contain coarse fanglomerates similar to those being shed from their present-day sources. It would be extremely fortuitous if the San Gabriel Mountains first uplifted just in time to shed sediments into Cajon Pass and were not a high source as they passed

the area immediately to the southeast. It is far more likely that the area to the east had sufficient relief to block flow to the north.

MAGNETIC STRATIGRAPHY

Technique

A new impact-coring technique made efficient magnetostratigraphic studies in poorly consolidated sediments possible. A nonmagnetic stainless steel tube with a beveled edge was gently pounded into an exposure that had been cleaned with brass tools. The orientation of the tube was measured using standard techniques prior to removal from the outcrop. The end of the sample (sticking out of the tube) was smoothed and scribed with an orientation mark. The sample was then extruded into quartz glass sample holders of the same diameter as the steel tube and sealed with Parafilm®, to prevent loss of moisture which maintains the sample's integrity. The samples were cemented into their quartz tubes in a magnetically shielded environment with a solution of sodium silicate and processed like rock cores. In an accompanying study (Weldon et al., in preparation) 30 samples were collected both by the impact-coring technique and by hand carving of oriented samples. Comparison of these two sets of samples demonstrated that the impact-coring technique did not cause any measurable realignment of the magnetic remanence.

We conducted a variety of alternating field (AF), thermal, and chemical demagnetization experiments. The best results were obtained by several low AF steps, followed by stepwise thermal demagnetization until the samples became nonmagnetic; most of our samples were processed this way. Characteristic components of the natural remanent magnetization were visually identified using orthogonal projections, and directions

Figure 4-4 - Typical demagnetization paths of samples that preserve stable primary directions shown on stereonet and Zijderveld diagrams. The divisions on the Zijderveld diagrams are 10^{-5} emu. The demagnetization steps (here and Figure 5) are 1)AF50, 2)AF100, 3)T150, 4)T300, 5)T400, 6)T500, 7)T600, where AF is alternating field and T is thermal demagnetization. LRH-89 is a normal sample, with a weak present field overprint that was removed by the first demagnetization step. The present field overprint has a north-northeast declination and a shallow inclination because that component was acquired after the beds were deformed, and the deformation has been removed here. LRH-40 is a reversed sample with a moderately strong present field overprint that was removed by 150° C.

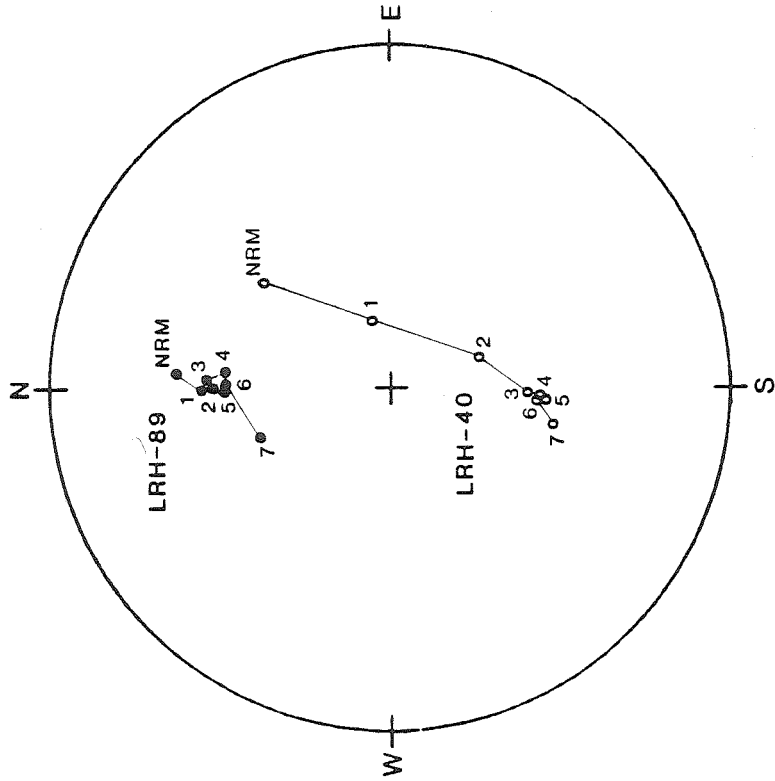
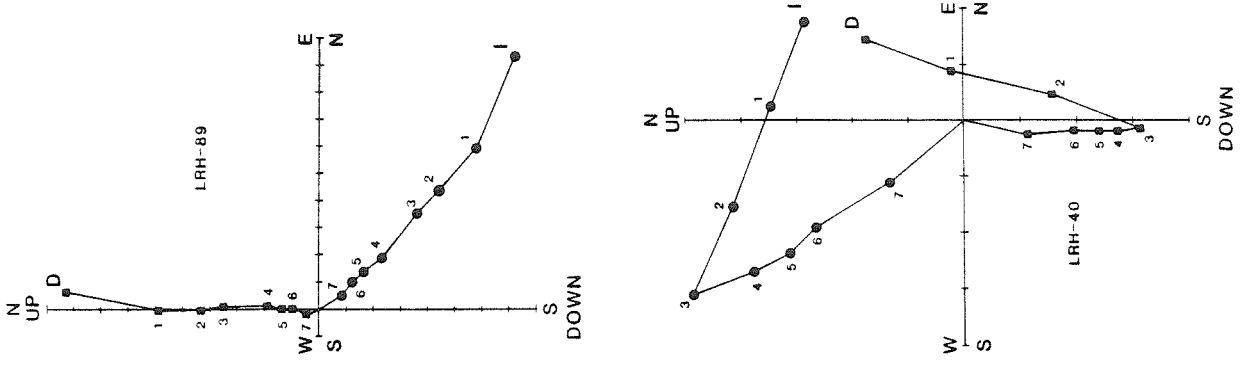
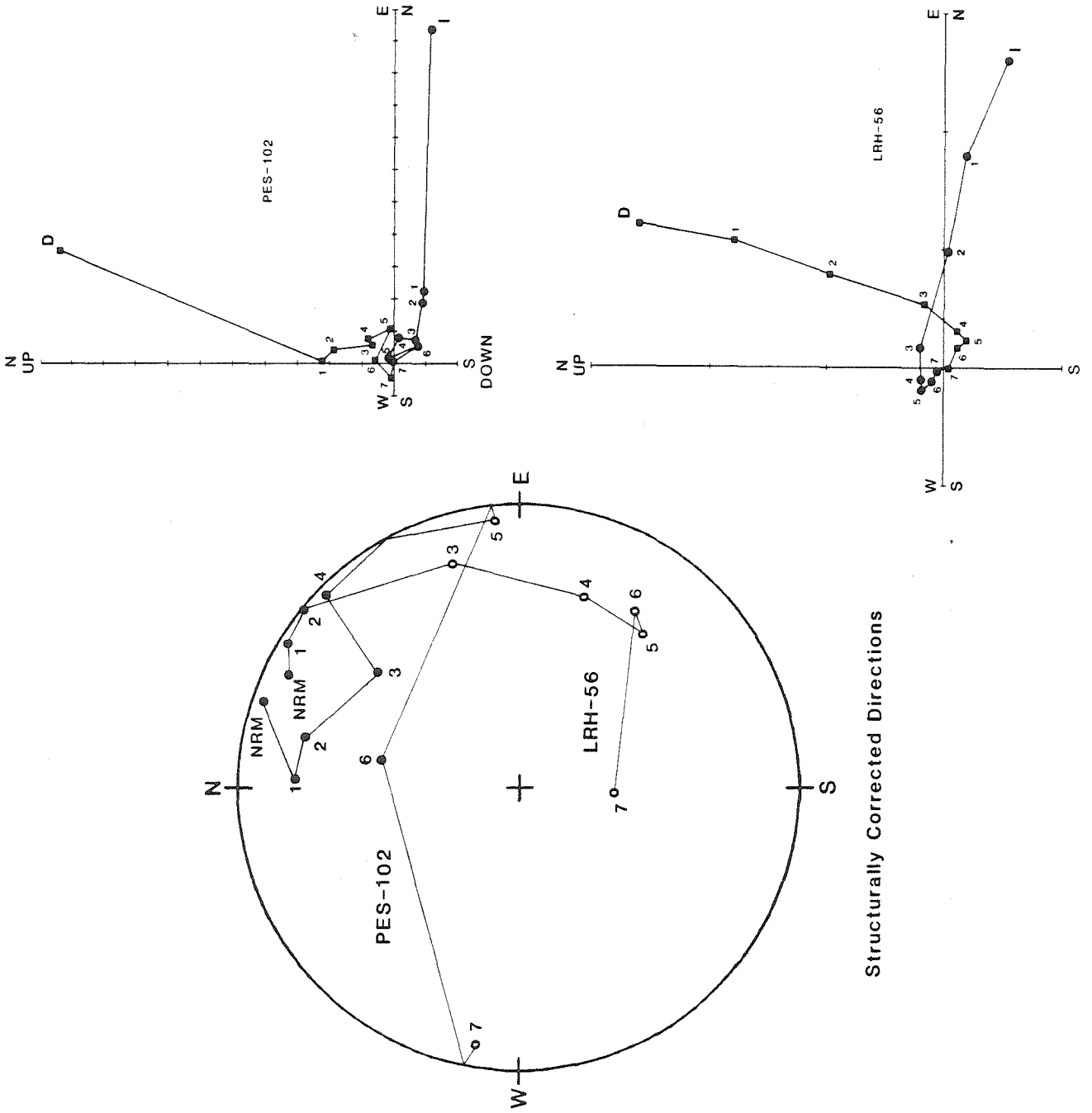


Figure 4-5 - Demagnetization paths of samples without stable primary remanence. LRH-56 probably began reversed and has a very strong overprint that was not completely removed by the time the sample was demagnetized. With the exception of the 600° C step all demagnetization vectors fall on a plane, indicating that the remanence is the sum of two magnetic directions. Because demagnetization removes a component in the direction of the present local field, successive steps result in directions closer to what was probably the primary direction, in this case reversed. On Figures 2 and 3, this sample would be plotted with a point, in the direction of step 5, with a tail extending to its NRM direction. PES-102 is an unstable sample. It has a present field overprint that was easily removed, and shows random behavior during demagnetization. No primary polarity can be determined. Notice that PES-102 demagnetized to 500°C (step 6) or LRH-56 directly demagnetized to 600°C (step 7) would be misinterpreted as good normal and reversed samples, respectively.



Structurally Corrected Directions

for the lines and planes of best fit were found using principal component analysis (Kirschvink, 1980). Only directions for which the maximum angular deviations were less than 10° were accepted. Almost all samples had an overprint of the present axial field, or, rarely, a reversed field direction that was generally removed at low demagnetization steps (Fig. 4). Samples in which this component could not be completely removed before the remanence became unmeasurable produced great circle paths across a stereonet, which could be fit only with a plane (LRH-56, Fig. 5). The trajectory of the path towards either a normal or reversed polarity usually allowed the primary polarity to be inferred.

We collected single samples from many sites, stepwise demagnetized each sample and analyzed each sample's demagnetization history, rather than the standard approach of collecting multiple samples per site and blanket-demagnetizing the samples to determine their primary directions. Our approach has several advantages in these sediments. First, many samples do not record primary directions, so the examination of each demagnetization path was considered necessary to weed out the bad samples. For example, PES-102 (Fig. 5), directly demagnetized to 500° C (which would be appropriate with the standard approach), would appear to be a normal sample, but it is clearly bad when the demagnetization path is considered. Second, many samples do not reach stable terminal directions, and a lot of valuable data could be rejected. However, if the demagnetization directions form a plane, the primary remanence can generally be correctly inferred. For example, samples like LRH-56 (Fig. 5), demagnetized to 500° C would probably be rejected (depending on the error used). However, from its demagnetization behavior it can be inferred to be reversed. Also, it was found that a particular bed generally yielded either good or bad re-

sults, so multiple samples per site gave little additional information, for a lot of extra work. It was decided that taking extra sites, not extra samples, would help assure finding all of the reversals in the discontinuously deposited sediments.

On Figures 3 and 4 samples with linear, terminal demagnetization paths (like samples LRH-89 and LRH-40, Fig. 4) are plotted as points, representing the least-squares direction of the primary direction (Kirschvink, 1980). Samples with demagnetization paths fit with planes are plotted with points at their final direction and with tails to show how far they traveled before becoming nonmagnetic. We have also included two earlier sections in their original form, as they were collected and processed in a slightly different way (Fig. 3; from Meisling, 1984). In all of our sections each magnetozone is defined by consistent stable results from at least 3 samples. Also, where we have collected closely adjacent sections, results must be consistent between sections (Phelan Peak and Crowder Canyon, Fig. 3). This approach yields a large number of minor uncertain zones, particularly in the coarse Shoemaker Gravel; these uncertain zones are interpreted as strongly overprinted samples because of the sediment coarseness and the position of the samples relative to the certain samples. The ages of the polarity boundaries are from Harland et al. (1982).

Quaternary Magnetostratigraphic Correlation

The key to the proposed correlation in the Quaternary sequence is the presence of the Olduvai event in the Phelan formation at Phelan Peak (Fig. 2). If the magnetic stratigraphy in the Phelan formation is correct only one match is possible for the Victorville Fan at this locality because there are only three polarity boundaries to match (Fig. 3). The

Pleistocene fossils, soils, and geomorphic setting of the uppermost units as discussed above, are consistent with the match. The normal zone near the base of the Shoemaker Gravels is considered tenuous because of the poor magnetic properties of this unit. Due to the coarseness of the Shoemaker Gravels at the lower normal zone it would be impossible to absolutely rule out a secondary remanence for these samples. However, stable normal samples were found at the same level in two adjacent sections, so we tentatively assign a normal polarity zone. We are certain about the normal zone at the top of the Shoemaker Gravels despite its narrow width because there are 6 stable samples, sampled from about 100 meters of strike, from a variety of fine-grained lithologies. It is possible that the upper normal zone is the Jaramillo event if the lower event is not real; however, the proposed match is preferred because of its consistency with the other sections, as discussed below.

At Crowder Canyon both the Harold Formation and the Shoemaker Gravels fall in one polarity zone, interpreted to be the portion of the upper Matuyama chron between the Jaramillo and Olduvai events (Fig. 3). Here again the match is based on the age of the underlying Phelan formation. There is an incomplete, 30-meter section of the Phelan formation exposed beneath the Victorville Fan that we believe contains the Olduvai event. On the basis of 8 samples, the lower half is reversed and the upper is normal. The dense red paleosols characteristic of this thin section occur only in the lowest 60 m or uppermost 130 m in the type section (Fig. 3). We correlate the Phelan section in Crowder Canyon to the uppermost red unit because it contains volcanic clasts like the uppermost Phelan in the type area and is essentially conformable with the overlying Victorville Fan. The incomplete section of the Phelan formation in Crowder Canyon is

therefore inferred to be about 2.0 to 1.8 my old. Several fossils have been found in this section, but none is diagnostic enough to resolve the two possibilities (R. E. Reynolds, pers. comm., 1984). The relationship of the Harold Formation to the Phelan formation and the sparse fossil control in the Harold Formation suggest that the base of the Harold Formation is close to the base of the Olduvai event here (Fig. 3). The fossils and the polarity certainly demonstrate that it was deposited during the upper part of the Matuyama chron.

The Shoemaker Gravels were also deposited during the upper Matuyama chron. However, the coarseness and poor preservation of the primary remanence in the Shoemaker Gravels make it difficult to eliminate the possibility of minor normal zones. Polarity in this unit is dominantly reversed, and we believe that it was completely reversed before weathering of the coarse gravels. Each section contains normal samples but they all overlap with reversed samples in adjacent sections, suggesting that they were probably overprinted by the present field (Fig. 3). It is impossible to rule out the presence of the Jaramillo event in this unit, but it most likely fell in the unconformity, as discussed below.

The lowest part of Noble's Older Alluvium at the top of the Crowder Canyon sections is certainly reversed (Fig. 3). The uppermost part of the unit is normal and is inferred to have formed during the Bruhnes chron. It is possible that this uppermost normal zone is the Jaramillo event, but this alternative would require that the Harold Formation, Shoemaker Gravels, and the angular unconformity formed in the same period of time as the Harold Formation alone at Phelan Peak. We feel that this possibility is unlikely enough to be rejected, placing the Jaramillo event in the unconformity below Noble's Older Alluvium. The unconformity

represents a significant period of time, ending just before the Bruhnes-Matuyama boundary; so, it is very reasonable that the unconformity began before the Jaramillo event.

At Puzzle Creek the upper normal polarity zone must be the Bruhnes, because of its length and position at the top of a section that is known to be Pleistocene (Fig. 3). We infer that the normal zone in the lower Harold Formation is the Jaramillo event. The excellent preservation of the primary remanence and the dense sampling of these rapidly deposited sediments make it unlikely that we could have missed this event. If the Jaramillo event did not exist in this section, this magnetozone would have to be the Olduvai event. This alternative, however, would require that the Harold Formation at Puzzle Creek span the same length of time as the upper Phelan Formation, the Harold Formation and the Shoemaker Gravels combined at Phelan Peak. It would also require the lower Harold Formation and upper Phelan formation to be older than the same units to the southeast, violating the gross age trends in all of the units, as well as the northwest movement of their sources. This alternative is therefore highly unlikely.

Taken alone, each of these paleomagnetic sections would be difficult to match uniquely to the absolute time scale due to the unconformities and the poor preservation of magnetic remanence in the coarser facies. However, the sections are from a continuous outcrop belt (Fig. 1), derived from source areas moving past across the San Andreas fault. So, each match must be made with a view to satisfying the stratigraphic relationships with neighboring sections. Taken together, and in context with the geology and the other time control, no alternative match can satisfy the paleomagnetic results and produce consistent results between sections.

DISCUSSION

Slip Rate across the San Andreas fault system

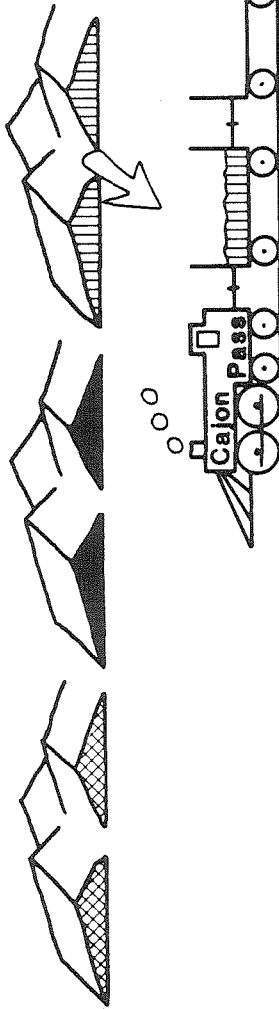
The offset of the sediments in the Victorville Fan from their sources in the San Gabriel Mountains can be used to determine the Quaternary slip rate on the San Andreas system. The long outcrop belts of the units derived from the San Gabriel Mountains were formed by lateral motion on the San Andreas fault that left "trails" of distinctive debris on the Mojave Desert as the San Gabriel Mountains passed by. This depositional style is analogous to "hopper car" sedimentation documented along the San Gabriel fault by Crowell (1952, 1982b), and is represented on Figure 6.

It has been argued that the motion on the San Andreas fault northwest of its junction with the San Jacinto fault is essentially the vector sum of its motion southeast of the junction and the motion of the San Jacinto fault (Weldon, 1984b; Weldon and Sieh, 1985; Weldon and Humphreys, in press). The geology near the junction is complex, however, and it is not possible to find a simple junction on the surface (Morton, 1975). The geometry of the junction requires that compression occur northwest of the point where the motion is transferred from the San Jacinto fault to the San Andreas fault. Thus, the general location of the junction can be inferred to lie just southeast of the position where significant compression is now occurring across the San Andreas fault zone (Weldon, 1984b). This compressional zone occurs between Wrightwood and Valyermo (Fig. 1). Therefore, the offset of the Shoemaker Gravels and the Harold Formation should record the slip rate on the San Andreas fault northwest of the San Jacinto fault, and Noble's Older Alluvium in Cajon Pass should record the slip rate southeast of the junction. Noble's Older Alluvium is therefore considered separately below.

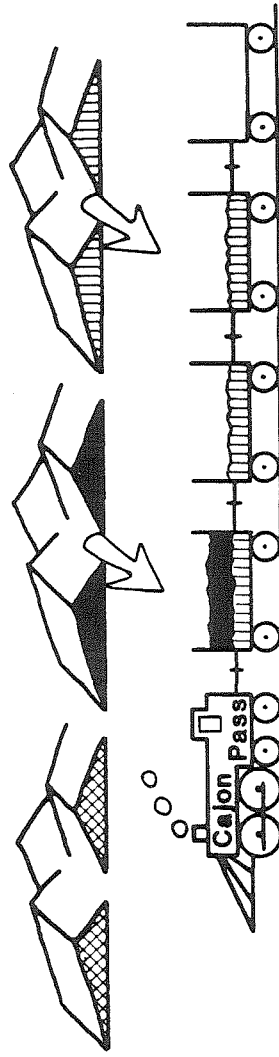
Figure 4-6 - Hopper car analogy (after Crowell's Violin Breccia Coal Train, Crowell, 1982b) of sedimentation in the Cajon Pass area. The sources of distinctive clasts are in the San Gabriel Mountains and the depocenters, represented by hopper cars are in the Mojave Desert. As a car moves along the mountain front it is first filled with Harold Formation, then by Shoemaker Gravels, and finally by Noble's Older Alluvium; hence a vertical stack of sediments represents the lateral distribution of sources. Notice in part three that all three formations are being deposited at the same time in different places, and the outcrops of individual units all must become younger to the northwest.

Noble's Older Alluvium Source Shoemaker Gravels Source Harold Formation Source

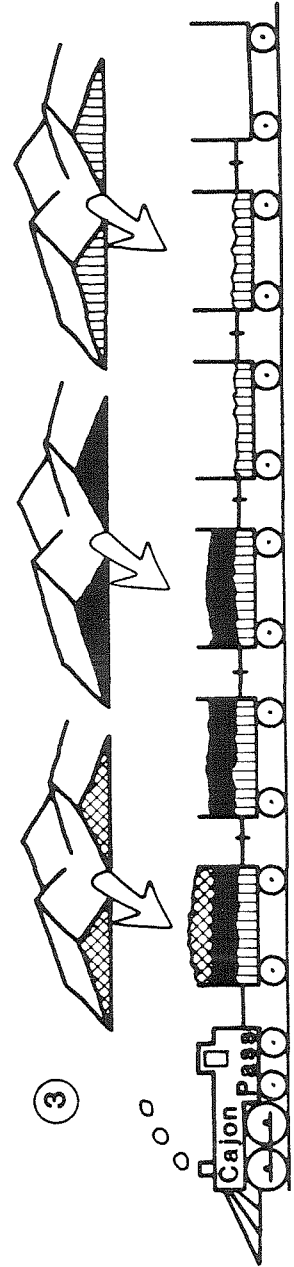
①



②



③



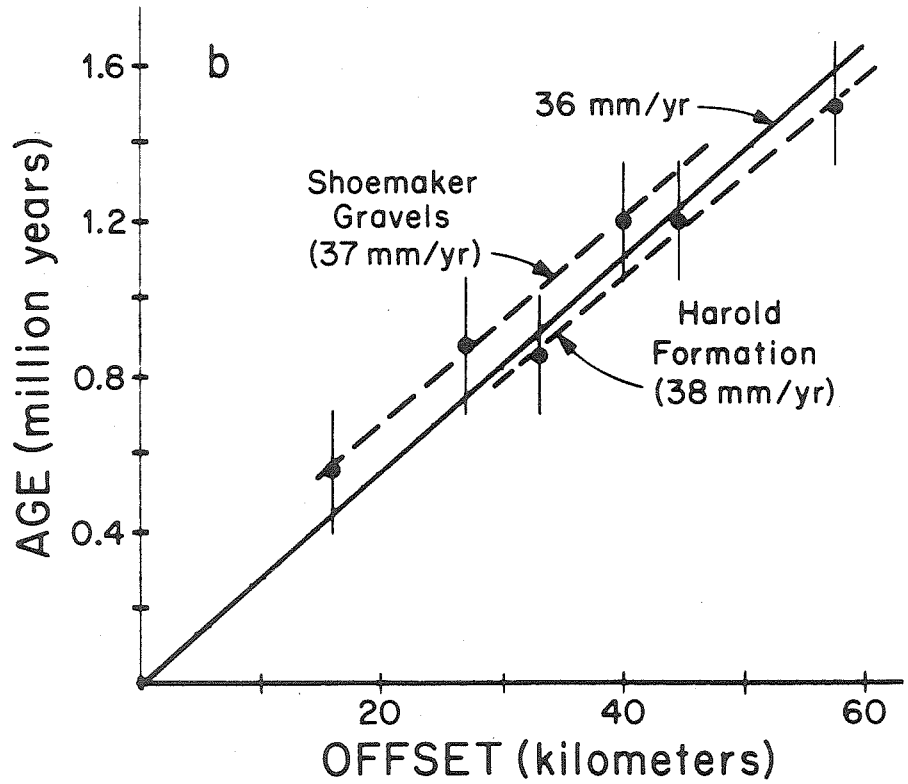
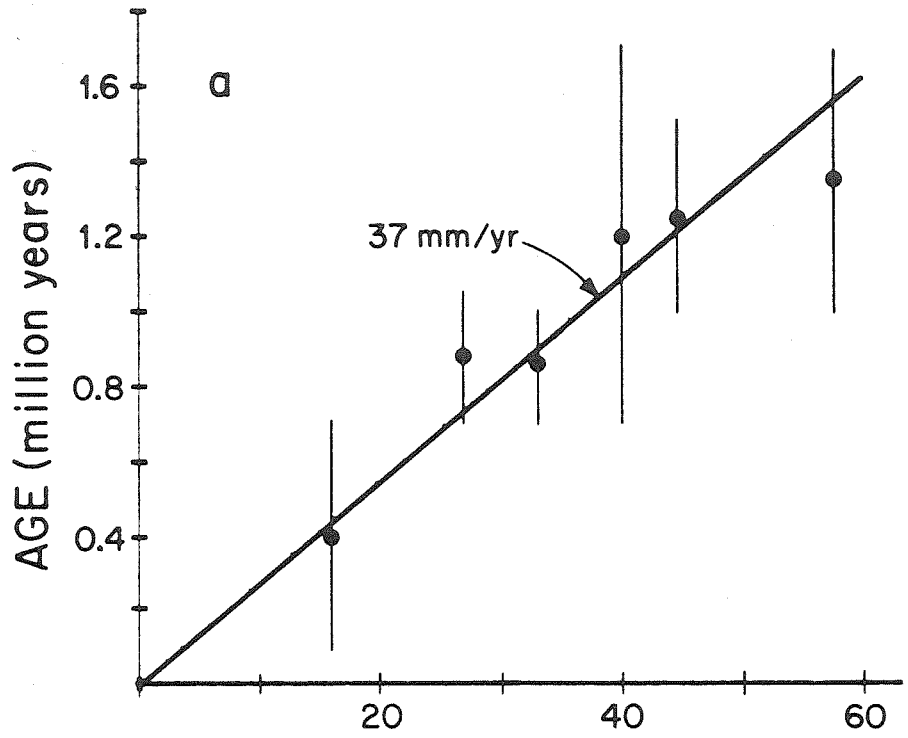
To calculate the slip rate we assume that some part of each dated deposit formed facing the center of its potential source in the San Gabriel Mountains (Fig. 1). This assumption allows us to handle the statistics in a straightforward fashion. Our assumption implies that at some time during the approximately 300,000 year long period (see below) that a "hopper car" takes to pass its source area and be "loaded" with sediments (Fig. 6), the streams carrying the sediments flowed perpendicular to the San Andreas fault. Obviously, the "best estimate" would be that the center of a distinctive deposit in a section in the Mojave Desert formed directly opposite the center of its source area in the San Gabriel Mountains. Stating the problem in this manner places all of the uncertainty in the time domain, because the distance between the center of the possible source area and the dated section can be measured with essentially no error. This assumption is tested below by calculating the slip rate independent of the source locations and comparing the actual source locations with the predicted locations.

Slip rate north of the San Jacinto fault

The Harold Formation at Puzzle Creek and the Shoemaker Gravels at Phelan Peak record 3 magnetic reversals, which permits the age at the top, bottom and middle of these units to be estimated quite precisely (Fig. 3). Their offsets are measured from Figure 1 and plotted in Figure 7. Elsewhere, the Harold Formation and Shoemaker Gravels were deposited during one polarity zone so only limits can be placed on their ages without additional assumptions about sedimentation rates.

The Shoemaker Gravels at Puzzle Creek is certainly younger than the Bruhnes-Matuyama boundary at 0.73 my (Fig. 3). The overlying Noble's Older Alluvium there is estimated to be at least 0.1 my old based on

Figure 4-7 - Quaternary slip rate across the San Andreas system northwest of the junction with the San Jacinto fault. a) Regression of offset and time, using conservative limits on the dates of the units (see text). b) Regressions of the same data, with the ages refined to allow time for the unconformities and the same length of time for the deposition of similar units. Data from the Shoemaker Gravels are consistently above the average and the Harold Formation data are consistently below. Because each data set falls on a line, and the Harold Formation line passes through the origin, we assume that the discrepancy is due to an error in our assumption that streams depositing the Shoemaker Gravels flowed perpendicular to the San Andreas fault (see text). We recalculate the slip rate independent of the sources by assuming only that the average source does not change. This allows us to calculate the slip rate from the distances and age differences between dated sections. This yields our best estimate of 37.5 ± 2 mm/yr (2 sigma) for the slip rate on the San Andreas fault during the Quaternary.



soils and geomorphic criteria, so an age range of 0.1 to 0.7 my is used for the Shoemaker Gravel at Puzzle Creek. This estimate does not allow any time for the angular unconformity between the two units to form and is therefore overly conservative.

The Harold Formation at Phelan Peak is only constrained to be older than the Jaramillo event and younger than the Phelan formation. We estimate that the top of the Phelan formation is younger than 1.5 my, because the fastest sedimentation rate observed in the deposit would require about 0.15 my to form the portion above the Olduvai event (Fig. 2). We therefore use a maximum age range of 1.5 to 1.0 my for the Harold Formation at Phelan Peak (Fig. 7a).

Both the Harold Formation and Shoemaker Gravels at Crowder Canyon are inferred to have been deposited between the Olduvai event and the Bruhnes-Matuyama boundary because of the presence of the Olduvai event in the Phelan formation and the Bruhnes-Matuyama reversal in Noble's Older Alluvium, as discussed above. So both units are only required to have been deposited between about 1.7 and 0.7 my ago (Fig. 7a). However, because of the thick section of Shoemaker Gravels and the unconformity below the Bruhnes-Matuyama boundary, we are confident that the Harold Formation predates the Jaramillo event. The Shoemaker Gravels, however, may contain the Jaramillo event so we only constrain it to have been deposited at some time between the Olduvai event and the Bruhnes chron. Individually, this produces very conservative limits because it allows no time for the angular unconformity to form and requires the units to overlap in time; clearly the Shoemaker Gravels were deposited during the latter part, and the Harold Formation during the early part, of this interval.

An average slip rate of 37 ± 3.5 mm/yr (2 sigma) is calculated from

this data set (Fig. 7a). There appears to be no systematic variation from the average so we suggest that the average is representative of the actual slip rate throughout this time period.

A refined average slip rate can be estimated by adding an assumption about the deposition of the units that frees us from the excessively conservative age constraints used in the estimate presented in Figure 7a. The assumption is that the average period of time represented by either the Harold Formation or Shoemaker Gravels is about 300,000 years. This assumption is based on the observation that the Harold Formation at Puzzle Creek and the Shoemaker Gravels at Phelan Peak were deposited in about 300,000 years (Fig. 3). Also, the time represented by the Harold and Shoemaker Gravels together at Crowder Canyon appears to be about 600,000 years. The deposition of these units on the Mojave block from fixed sources in the San Gabriel Mountains in a "hopper car" fashion favors this hypothesis because any point on the Mojave block should take a fixed length of time to pass by any source area in the San Gabriel Mountains across the San Andreas fault. This time period should be relatively constant if the slip rate does not change significantly through time. The data presented in Figure 7a, which does not involve any assumption about the constancy of slip, certainly support a uniform accumulation of slip through time.

The Shoemaker Gravels at Puzzle Creek are therefore inferred to have been deposited between about 0.7 and 0.4 my (the 0.3 my period after deposition of the Harold Formation there), the Harold Formation at Phelan Peak was deposited between about 1.05 and 1.35 my (the 0.3 my preceding the Shoemaker Gravels there), the Shoemaker Gravels at Crowder Canyon were deposited between about 1.05 to 1.35 my (the latter half of the time span

between the Jaramillo and Olduvai events), and the Harold Formation at Crowder Canyon was deposited between 1.35 and 1.65 my (the first half of the interval between the Jaramillo and Olduvai events). These inferred ages are consistent with all of the data available and also allow an average of 300,000 years for the unconformity between the Shoemaker Gravels and Noble's Older Alluvium.

Combining these more restricted age estimates with the offset distances produces the data shown on Fig. 7b. The average slip rate would now be calculated to be 36 mm/yr. However, all of the Harold Formation estimates fall on a line and all of the Shoemaker Gravel estimates fall on another line, both with higher slip rates than the average (Fig. 7b), suggesting a systematic error. The line through the Harold Formation estimates passes through the origin, but the line through the Shoemaker values does not. In fact, the Shoemaker data appear to indicate that the deposits were formed an average of about 4.7 km northwest of the center of their source.

Two possibilities could explain the discrepancy between the Harold and Shoemaker lines. There could have been a rate change on the San Andreas fault after the deposition of the Shoemaker Gravels or the streams depositing the Shoemaker Gravels may not have flowed perpendicular to the fault. We prefer the latter possibility because the Harold data do not suggest a rate change and the age range overlaps with that of the Shoemaker Gravels. The streams draining the Shoemaker Gravels source area today indeed flow north after crossing the San Andreas fault and not northeast perpendicular to the fault as our initial assumption requires. This nonperpendicular flow direction is due to the uplift occurring between Wrightwood and Valyermo (Fig. 1). As discussed below, the uplift

migrates with the San Gabriel Mountains and has probably always forced the streams coming out of the Shoemaker Gravels source area to flow more to the north. We believe that the offset of the Shoemaker Gravels are consistently underestimated for this reason.

The whole problem can be avoided by changing our assumption. We can instead assume only that the average source locations and stream flow directions do not change, regardless of what they might have been. The slip rate can be determined simply from the slope of the lines through the data, reflecting only the ages of the units and the distances between the dated sections. The actual position of the source (the intercept) is not necessary. In this way we can combine the Harold Formation and Shoemaker Gravels data, eliminating all uncertainties in the source characteristics, and can assume only that they do not change. This yields our best estimate slip rate of 37.5 ± 2 mm/yr (2 sigma) for the San Andreas fault northwest of its junction with the San Jacinto fault. If we are correct in our interpretation of the problem with the Shoemaker Gravels source, the slip rate on the San Andreas fault has remained remarkably constant during the Quaternary Period, because the assumption a constant rate yields such consistent results.

Slip rate south of the San Jacinto fault

The offset of Noble's Older Alluvium in the Cajon Pass area should yield the slip rate on the San Andreas fault southeast of its junction with the San Jacinto fault. The Older Alluvium contains a polarity reversal that allows it to be dated accurately only at Crowder Canyon. The middle of the deposit is about 700,000 years old there (Fig. 3) and has been offset about 15 km (Fig. 1). This yields a slip rate of 21 ± 7 mm/yr. This estimate must be considered tenuous because it is based only

on one offset and because the topography after the uplift of the westernmost San Bernardino Mountains may have affected the direction of flow from the San Gabriel Mountains to the dated section at Crowder Canyon. Streams that carried Noble's Older Alluvium could have flowed parallel to the San Andreas fault a significant distance before they crossed the westernmost San Bernardino Mountains and deposited the material at the Crowder Canyon section. As discussed in detail below, this is only a problem for Noble's Older Alluvium because the uplift north of the San Andreas fault postdates the Harold Formation and Shoemaker Gravels.

Integration of the slip rates with the San Jacinto fault's history

If the slip rate on the San Andreas fault southeast of the junction with the San Jacinto fault, 21 ± 7 mm/yr, is added to the slip rate of the San Jacinto fault measured for the same period of time, 10 ± 2 mm/yr (Sharp, 1981), the result, 31 ± 7 mm/yr, is indistinguishable from the slip rate on the San Andreas fault northwest of the junction, 37.5 ± 2 mm/yr. The 24.5 ± 3.5 mm/yr Holocene slip rate on the San Andreas southeast of the junction (Weldon and Sieh, 1985) and the 34 ± 3 mm/yr rate northwest of the junction (Sieh and Jahns, 1984) are indistinguishable from the Quaternary rates determined here and suggest that the rates of motion on these faults have not changed during the Quaternary.

As discussed in Weldon and Sieh (1985), models involving alternating periods of activity on the San Jacinto and San Andreas faults (Sharp, 1981) or a long-term increase in the slip rate on the San Jacinto fault at the expense of the San Andreas fault (e.g., Crowell, 1981) are not supported by the data from the Cajon Pass area.

In fact, it has been suggested by Matti (unpublished manuscript, 1984) and Weldon (1985) that the approximately 35 to 37 mm/yr rate on the

San Andreas system has held for the last 4-5 my. While this is in conflict with plate tectonic models that require the entire Pacific-North American motion to be taken up on the San Andreas fault system, new models (e.g., Minster and Jordan, 1984; Weldon and Humphreys, in press) may explain the relatively low rate on the San Andreas system in the broader context of the plate margin.

The low rate for the last 1.5 my, and the tenuous evidence of this rate for the last 4-5 my, suggests that the approximately 300 km of off-set documented for the San Andreas system in southern California (e.g., Crowell, 1981) must have taken longer than the 5 my duration of the opening of the Gulf of California (Larson et al. 1968; Moore and Currey, 1982). This inconsistency has long been recognized in central California (e.g., Huffman, 1972) and has been implicitly recognized in southern California by documented activity on faults within the San Andreas system long before the opening of the Gulf of California (see Crowell, 1982a; Powell, 1981, for specific examples). The San Andreas fault is certainly now the most important fault in the Pacific - North American plate boundary. However, a significant fraction of the relative plate motion of 56 mm/yr (Minster and Jordan, 1978) must occur on other faults and probably always has.

The uplift of the Central Transverse Ranges

The revised stratigraphy in the Cajon Pass area motivates a new model for the uplift of the western San Bernardino Mountains. The Cajon Valley (Woodburne and Golz, 1972) and Squaw Peak (Foster, 1980; Weldon, 1984a) faults bound the Cajon-Punchbowl and Crowder basins and are overlain by the newly recognized Phelan formation (Fig. 1). They must therefore be late Miocene to early Pliocene in age. East-west trending faults, which

commonly bound the the Crowder Formation in the western San Bernardino Mountains, are not found in the Cajon-Punchbowl basin. These faults predate the deposition of the Phelan formation, and subsequently either predate (Weldon, 1984a) or are contemporaneous with (Meisling and Weldon, in preparation) juxtaposition of the two basins along the Squaw Peak fault. These structures were previously believed to have been active during the uplift of the western San Bernardino Mountains (Dibblee, 1975a; Weldon and Meisling, 1982). It is now clear that all of these structures predate the uplift of the current mountains and must have been associated with an earlier Mio-Pliocene uplift event. The previously uplifted area was eroded to low or moderate relief by late Pliocene time, prior to the development of the current high relief (Meisling and Weldon, in preparation).

Little evidence of major vertical relief is found in the Phelan formation, which was deposited between the Mio-Pliocene and Quaternary uplift events in the western San Bernardino Mountains. A narrow region near the San Andreas fault and an area east of the Phelan basin occasionally shed coarse debris into the generally fine-grained sediments (Foster, 1980; Meisling, 1984; Meisling and Weldon, in preparation). Mid to late Pliocene relief was moderate compared to today's or that likely to have accompanied the Mio-Pliocene event. Not until early Pleistocene did the main mass of the San Bernardino Mountains begin uplifting to the east (Meisling and Weldon, in preparation), foreshadowing the uplift of the western San Bernardino Mountains.

The Victorville Fan sequence contains the first evidence of the relief seen in the western San Bernardino Mountains today. The uplift of the western San Bernardino Mountains was not associated with activity on any of the major faults in the mountains because they all predate the

Phelan formation. The uplift of the Cajon Pass area of the San Bernardino Mountains appears to have occurred across broad asymmetric anticlines and monoclines with axes parallel to the San Andreas fault, which have been recognized in the pre-Quaternary rocks from Lake Arrowhead to Valyermo (Fig. 1). This warping uplifted and exposed the pre-Quaternary rocks and structures near the San Andreas fault and tilted the older members of the Victorville Fan to the northeast, creating the unconformity in the Victorville Fan between the Shoemaker Gravels and Noble's Older Alluvium. Locally, the Shoemaker Gravels are more deformed than the Harold Formation and young alluvium is less deformed than Noble's Old Alluvium, indicating that some of the uplift occurred during the deposition of these units as well. However, the deformation was certainly centered on and was commonly completely within the period of time represented by the angular unconformity between the Shoemaker Gravels and Noble's Older Alluvium.

The timing of uplift can be determined for any point between Lake Arrowhead and Valyermo from the age of Victorville Fan deposits bracketing the unconformity. The area between Cajon Pass and Lake Arrowhead (Fig. 1) was uplifted between about 1.5 and 1.0 my ago, Cajon Pass was uplifted between about 1.0 and 0.7 my ago, the Wrightwood area was uplifted during the last 500,000 years and the area between Puzzle Creek and Valyermo is being uplifted today.

This progressive migration of uplift to the northwest is coincident with the passage of the highest San Gabriel Mountains across the San Andreas fault. The deformation on the northeast side of the San Andreas fault moves with, and is therefore probably related to, the uplift of the high San Gabriel Mountains, now located across the San Andreas fault between Valyermo and Cajon Pass (Weldon, 1984b). Early workers in the area

(e.g. Noble, 1954b) called this rapidly uplifting area across the San Andreas fault "the San Gabriel Arch". More recent work (Ehlig, 1975, 1981; Morton, 1975) supports the broad arch concept, but as the sum of the detailed complexity where the San Jacinto fault approaches the San Andreas fault.

The Arch is where the San Andreas and San Jacinto fault zones merge and compression due to the junction appears to be uplifting both the high eastern San Gabriel Mountains, moving with the junction, and the western San Bernardino Mountains, moving past the junction. On a regional scale, the high eastern San Gabriel Mountain area can be thought of as being uplifted along a northeast trending axis that crosses the San Andreas fault at its junction with the San Jacinto fault. This appears to be a consequence of the fact that the San Jacinto fault adds its motion to the San Andreas fault but trends 15° more northwesterly than the San Andreas fault (Weldon and Humphreys, in press). A possible mechanism for transferring the compression and uplift across the San Andreas fault at depth is discussed by Meisling and Weldon (in preparation).

The Harold and Shoemaker Gravels were deposited from a steep scarp onto the relatively low Mojave Desert in a setting like that existing between Palmdale and Valyermo today (Fig. 1). As the junction with the San Jacinto fault approached across the San Andreas fault these deposits were upwarped and removed in a belt along the San Andreas fault, resulting in the excellent exposures at the edge of the uplifted area (Fig. 1). The paleomagnetic data clearly show that this uplift, centered on the angular unconformity between the Shoemaker Gravels and Noble's Older Alluvium, migrated with the high San Gabriel Mountains and the junction with the San Jacinto fault.

Although major relief between Lake Arrowhead and Valyermo is due to uplift across broad northwest trending folds, faults in the area certainly bound areas of different relief. As warping uplifted different rocks that had been juxtaposed during the Mio-Pliocene deformational event, erosion occurred much faster in the sedimentary rocks than in the bedrock. The old Mio-Pliocene reverse faults between Cajon Pass and Lake Arrowhead were exhumed as the sediments were stripped away, creating the prominent east-west fabric. The current relief associated with the margins of the Cajon facies of the Punchbowl Formation and that defines the central part of Cajon Pass, is also erosional and does not indicate young activity on the bounding faults.

Lateral juxtaposition of the broadly uplifted western San Bernardino Mountains against the lower San Bernardino Valley has produced the steep southern boundary of the western San Bernardino Mountains. Similarly, the relief on the north side of the San Gabriel Mountains is mainly due to the lateral movement of the high San Gabriel Mountains into their present position adjacent to the Mojave block.

About 1.5 my from now, assuming the current style of deformation continues, the high eastern San Gabriel Mountains will face Palmdale, which will have been uplifted to the height of Wrightwood. The part of Wrightwood northwest of the San Andreas fault will be across from the town of San Bernardino, on top of a mile-high escarpment much like that between Lake Arrowhead and San Bernardino today. Ongoing erosion into the sediments in Cajon Pass will completely separate the San Bernardino Mountains proper from a narrow ridge running from Wrightwood to Palmdale (Fig. 1). All of this relief will have been produced without any vertical motion on the San Andreas fault itself. The deformation documented here demon-

strates that the uplift of the central Transverse Ranges is locally taking place across broadly upwarped areas and not dip-slip faults. Erosion and lateral faulting of broad uplifts create escarpments as impressive as those formed by dip-slip faulting elsewhere in the Transverse Ranges.

CONCLUSIONS

The establishment of temporal control in the early-to-middle Quaternary sedimentary rocks north of the central Transverse Ranges permits a detailed understanding of the interaction between the San Andreas fault and the uplifting Transverse Ranges. Distinctive facies in the sediments northeast of the San Andreas fault have been traced to their sources in the San Gabriel and San Bernardino Mountains, allowing us to determine the slip rate on the San Andreas fault, and to tie together the uplift on both sides of the fault zone.

The San Andreas fault, northwest of its junction with the San Jacinto fault, has been slipping at an average rate of 37.5 ± 2 mm/yr throughout the Quaternary. Southeast of the San Jacinto fault junction, the San Andreas fault has slipped at an average of 21 ± 7 mm/yr since the middle Quaternary. The difference is accounted for by the San Jacinto fault.

The eastern San Gabriel Mountains were a high source of sediments by the early Quaternary and the San Bernardino Mountains east of Cajon Pass probably had low to moderate relief. The eastern San Gabriel Mountains are being uplifted by contemporaneous lateral activity on the nonparallel San Andreas and San Jacinto faults. This deformation also uplifted the western San Bernardino Mountains as the structural knot created by their junction passed by. As the deformation migrated northwest, relative to the San Bernardino Mountains, erosion and lateral

faulting modified the broadly uplifted mass, creating Cajon Pass and the distinctive physiography of the central Transverse Ranges.

ACKNOWLEDGMENTS

We would like to thank J. Boley, L. Mezger, A. Kirschvink, J. Freymuller, and S. R. Chang for assistance in the lab or field. J. Mayne assisted in the preparation of the figures. K. Sieh acted as thesis adviser to the first author and read the first draft. Portions of this work were funded by the USGS Earthquake Hazard Reduction Programs, contract numbers 14-08-0001-16774, 18285, 19756, and 21275, the California Department of Water Resources, agreement number B-53653, and NSF Grant PYI-8351370.

BIBLIOGRAPHY

- Barrows, A. G., 1980, Geologic map of the San Andreas fault zone and adjoining terrane, Juniper Hills and vicinity, Los Angeles County, California, Cal. Div. Mines and Geology, OFR - 80-2 LA.
- Barrows, A. G., 1979, Geology and fault activity of the Valyermo segment of the San Andreas fault zone, Los Angeles County, California, Cal. Div. Mines and Geology, OFR - 79-1 LA, 49 p.
- Christodoulidis, D. C., Smith, D. E., Minster, J. B., Jordan, T. H., in review, Relative movement of tectonic plates in California observed by satellite laser ranging, sub Science 1984.
- Crowell, J. C., 1982a, The tectonics of Ridge basin, southern California, in Geologic history of Ridge basin, southern California, eds., Crowell, J. C. and Link, M. H., Geol. Soc. Amer., Cordilleran section (78th) guidebook #1, p. 25-42.
- Crowell, J. C., 1982b, The Violin breccia, Ridge basin, southern California, in Geologic history of Ridge basin, southern California, eds., Crowell, J. C. and Link, M. H., Geol. Soc. Amer., Cordilleran section (78th) guidebook #1, p. 89-97.
- Crowell, J. C., 1981, An outline of the tectonic history of southeastern California, in The geotectonic development of California, ed. Ernst, W. G., Kuby Volume #1, Prentice-Hall, New Jersey, p. 583-600.
- Crowell, J. C., 1962, Displacement along the San Andreas fault, California, Geol. Soc. Amer. Spec. Paper 71, 61 p.
- Crowell, J. C., 1952, Probable large lateral displacement on the San Gabriel fault, southern California, Amer. Assoc. Petro. Geol. Bull., v. 36, p. 2026-2035.
- Dibblee, T. W. Jr., 1975a, Late Quaternary uplift of the San Bernardino

Mountains on the San Andreas and related faults, in San Andreas fault in southern California: A guide to San Andreas fault from Mexico to Carrizo Plain, ed. Crowell, J.C., Cal. Div. of Mines and Geology, Spec. Report 118, p. 127-135.

Dibblee, T. W., Jr., 1975b, Tectonics of the western Mojave Desert near the San Andreas fault, in San Andreas fault in southern California: A guide to San Andreas fault from Mexico to Carrizo Plain, ed. Crowell, J. C., Cal. Div. Mines and Geology, Spec. Report 118, p. 155-161.

Ehlig, P. L., 1981, Origin and tectonic history of the basement terrane of the San Gabriel Mountains, central Transverse Ranges, in The geotectonic development of California, ed. Ernst, W. G., Rubey Volume #1, Prentice-Hall, New Jersey, p. 253-283.

Ehlig, P. L., 1975, Basement rocks of the San Gabriel Mountains, south of the San Andreas fault in southern California, in San Andreas fault in southern California: A guide to San Andreas fault from Mexico to Carrizo Plain, ed. Crowell, J. C., Cal. Div. Mines and Geology, Spec. Report 118, p. 177-186.

Ehlig, P. L., Ehlert, K. W., and Crowe, B. M., 1975, Offset of the upper Miocene Caliente and Mint Canyon Formations along the San Gabriel and San Andreas faults, in San Andreas fault in southern California: A guide to San Andreas fault from Mexico to Carrizo Plain, ed. Crowell, J. C., Spec. Report 118, p. 83-92.

Foster, J.H., 1980, Late Cenozoic tectonic evolution of Cajon Valley, southern California. Ph.D. thesis, University of California, Riverside, 242 pp.

Harland, W. B., Cox, A.V., Llewellyn, P. G., Pickton, C. A. G., Smith, A. G., and Walters, R., 1982, A geologic time scale, Cambridge University

Press, 131 p.

Hill, M. L., 1971, A test of new global tectonics: Comparisons of north-east Pacific and California structures, A. A. P. G., Bull., v. 55, p. 3-9.

Huffman, O. F., 1972, Lateral displacement of upper Miocene rocks and the Neogene history of offset along the San Andreas fault in central California, Geol. Soc. Amer. Bull., v. 83, p. 2913-2946.

Kirschvink, J. L., 1980, The least-squares line and plane and the analysis of paleomagnetic data, Geophys. Jour. Roy. Astro. Soc., v. 62, p. 699-718.

Larson, R. L., Menard, H. W., and Smith, S. M., 1968, Gulf of California: A result of ocean-floor spreading and transform faulting, Science, v. 261, p. 781-784.

Lisowski, M., and Prescott, W. H., 1981, Short-range distance measurements along the San Andreas fault system in central California, 1975 to 1979, Bull. Seis. Soc. Amer., v. 71, p. 1607-1624.

Matti, J. C., unpublished manuscript, Distinctive megaporphyritic monzogranite offset 160 km by the San Andreas fault, southern California: a new constraint for palinspastic reconstructions, 18 p.

McFadden, L. D. and Weldon, R. J., in preparation, Rates and process of soil development in Cajon Pass, southern California.

Meisling, K. E., 1984, Neotectonics of the north frontal fault system of the San Bernardino Mountains: Cajon Pass to Lucerne Valley, California, Ph.D. Dissertation, Calif. Inst. of Tech., Pasadena, Calif., 394 p.

Meisling, K. E. and Weldon, R. J., in preparation, The late Cenozoic tectonics of the western San Bernardino Mountains, southern California.

Minster, J. B. and Jordan, T. H., 1984, Vector constraints on Quaternary

deformation of the western United States east and west of the San Andreas fault in Tectonics and sedimentation along the California margin, eds. Crough, J. K. and Bachman, S. B., Pac. Sect. SEPM, v. 38, p. 1-16.

Minster, J. B. and Jordan, T. H., 1978, Present-day plate motions, Jour. Geophys. Res., v. 83, p. 5331-5354.

Moore, D. G. and Curray, J. R., 1982, Geological and tectonic history of the Gulf of California, Initial Reports of the Deep Sea Drilling Project, v. 64, p. 1279-1296.

Morton, D.M., 1975, Synopsis of the geology of the eastern San Gabriel Mountains, southern California, in San Andreas fault in southern California: A guide to San Andreas fault from Mexico to Carrizo Plain, ed. Crowell, J.C., Cal. Div. of Mines and Geology, Sp. Report 118, p. 170-176.

Noble, L. F., 1954a, Geology of the Valyermo Quadrangle and vicinity, California, U. S. Geol. Survey Quad. Map #GQ-50.

Noble, L. F., 1954b, The San Andreas fault zone from Soledad Pass to Cajon Pass, Calif. Div. Mines Geol. Bull., v. 170, Ch. 4, p. 32-48.

Powell, R. E., 1981, Geology of the crystalline basement complex, eastern Transverse Ranges, southern California: Constraints on regional tectonic interpretations, Ph.D. Dissertation, Cal. Inst. of Tech., 441 p.

Reynolds, R. E., 1985, Tertiary small mammals in the Cajon Valley, San Bernardino County, California, in Geologic investigations along Interstate 15 - Cajon Pass to Manix Lake, California, ed. Reynolds, R. E., Field Trip Guide for the 60th meeting, western Assoc. Verte. Paleon. p. 49-58.

Reynolds, R. E., 1984, Miocene faunas in the lower Crowder Formation,

- Cajon Pass, California: A preliminary discussion, in San Andreas fault - Cajon Pass to Wrightwood, eds. Hester, R. L. and Hallinger, D. E., Pac. Sect., AAPG Guidebook #55, p. 17-21.
- Reynolds, R. E., 1983, Paleontologic salvage, Highway 138 Borrow Cut, Cajon Pass, San Bernardino County, California. San Bernardino County Museum Association, Redlands, for State of California Dept. of Transportation District VIII, San Bernardino, 205 pp.
- Savage, J. C., 1983, Strain accumulation in western United States, Ann. Rev. Planet. Sci., v. 11, p. 11-43.
- Sharp, R. V., 1981, Variable rates of late Quaternary strike slip on the San Jacinto fault zone, southern California, Jour. Geophys. Res., v. 86, p. 1754-1762.
- Sharp, R. V. and Silver, L. T., 1971, Quaternary displacement on the San Andreas and Punchbowl faults at the San Gabriel Mountains, southern California, Geol. Soc. Amer. Abstr. with Programs, v. 3, p. 191.
- Sieh, K. E. and Jahns, R., 1984, Holocene activity of the San Andreas fault at Wallace Creek, California, Geol. Soc. Amer. Bull., v. 95, p. 883-896.
- Silver, L. T., 1968, Pre-Cretaceous basement rocks and their bearing on large-scale displacements in the San Andreas fault system, Stanford Univ. Pubs. Geol. Sci., v. 11, p. 279-280.
- Weldon, R. J., 1985, The late Cenozoic geology of Cajon Pass; Implications for tectonics and sedimentation along the San Andreas fault, Ph. D. Dissertation, Calif. Inst. of Tech., Pasadena, Calif., 382 p.
- Weldon, R. J., 1984a, Implications of the age and distribution of late Cenozoic stratigraphy in Cajon Pass, southern California, in San Andreas fault - Cajon Pass to Wrightwood, eds. Hester, R. L. and

- Hallinger, D. E., Pac. Sect. A.A.P.G., Guidebook, 55, p. 9-16.
- Weldon, R. J., 1984b, Quaternary deformation due to the junction of the San Andreas and San Jacinto faults, southern California, in Abstracts with Programs, 97th Annual Meeting, Geol. Soc. Amer., v. 16, p. 689.
- Weldon, R. J., Reynolds, R. E., Winston, D. S., Meisling, K. E., Kirshvink, J., and Burbank, D. W., in preparation, Age, distribution, and significance of the Crowder and Phelan formations, central Transverse Ranges, southern California.
- Weldon, R. J. and Humphreys, in press, A kinematic model of southern California, submitted to Tectonics 1984.
- Weldon, R. J. and Sieh, K. E., 1985, Holocene rate of slip and tentative recurrence interval for large earthquakes on the San Andreas fault in Cajon Pass, southern California, Geol. Soc. Amer. Bull. v. 96, p. 793-812.
- Weldon, R.J., Winston, D.S., Kirshvink, J.L. and Burbank, D.W., 1984, Magnetic stratigraphy of the Crowder Formation, Cajon Pass, southern California, in Abstracts with Programs, 97th Annual Meeting, Geol. Soc. Amer., v. 16, p. 689.
- Weldon, R. and Meisling, K., 1982, Late Cenozoic tectonics in the western San Bernardino Mts; Implications for the uplift and offset of the central Transverse Ranges, in Abstracts with Programs, Cordilleran Section (78th), Geol. Soc. Amer., v. 14, p. 243-244.
- Weldon, R. J., Meisling, K. E., Sieh, K. E., and Allen, C. R., 1981, Neotectonics of the Silverwood Lake area, San Bernardino County: Report to the Calif. Dept. of Water Resources, 22p., 11 Figs., 1 map.
- Winston, D. S., 1985, Magnetic stratigraphy of the Crowder Formation, southern California, M.S. Dissertation, USC, Los Angeles, CA, 100 p.

Woodburne, M.O. and Golz, D.J., 1972. Stratigraphy of the Punchbowl Formation, Cajon Valley, Southern California, Univ. Cal. Pub. in Geol. Sci., v. 92, 73 pp.

CHAPTER FIVE

A KINEMATIC MODEL OF SOUTHERN CALIFORNIA

by

Ray J. Weldon II¹ and Eugene D. Humphreys²

Division of Earth and Planetary Sciences

California Institute of Technology

Pasadena, California 91125

¹Now at USGS-OEVE, M/S 977, 345 Middlefield Road, Menlo Park, CA 94025 and Dept. of Geology, Occidental College, 1600 Campus Road, Los Angeles, CA 90041

²Now at Dept of Geological Sciences, University of California, Riverside

ABSTRACT

We propose a kinematic model for southern California based on late Quaternary slip rates and orientations of major faults in the region. Internally consistent motions are determined assuming that these faults bound rigid blocks. Relative to North America, most of California west of the San Andreas fault is moving parallel to the San Andreas fault through the Transverse Ranges and not parallel to the motion of the Pacific plate. This is accomplished by counterclockwise rotation of California south of the San Andreas fault and by the westward movement of central California north of the Garlock fault. The velocities of the blocks are calculated along several paths in southern California that begin in the Mojave Desert and end off the California coast. A path that crosses the western Transverse Ranges accumulates the accepted relative North America-Pacific plate velocity, whereas paths to the north and south result in a significant missing component of motion. This implies the existence of a zone of active deformation in southern California that is interpreted to include the western Transverse Ranges and northwest trending, predominately strike-slip faults close to the coast both north and south of the Transverse Ranges. Strain on this system accounts for about a third of the total North America-Pacific plate motion.

INTRODUCTION

Southern California is a tectonically active region, experiencing continental rifting, transform faulting, and small-scale collision. The forces that drive this activity are only partially understood, and despite a great deal of work, even the fundamental aspects of the kinematics are being debated. In this paper the "instantaneous" kinematics are modeled using late Quaternary slip rates and orientations of the major faults in southern California. The assumption is made that these faults bound rigid blocks. The two primary observations which motivate this model are that little convergence occurs across the San Andreas fault (including the portion in the vicinity of the Transverse Ranges)

and that the San Andreas system onshore does not account for the total plate motion. The following two conclusions are reached: (1) Relative to North America, most of California west of the San Andreas fault is moving parallel to the San Andreas fault in the Transverse Ranges (The Transverse Ranges portion of the San Andreas fault trends about $N65^{\circ}W$ and lies between the two abrupt changes in the San Andreas fault's trend: the big bend [Hill and Dibblee, 1953] in the San Andreas fault near the Garlock fault and the southern bend [Hill, 1982b] near the Banning fault (Figure 1).) and not parallel to the Pacific plate motion or the San Andreas fault north and south of the Transverse Ranges; (2) Major nearshore right-lateral faulting with a significant component of convergence is necessary on the northwest trending faults north and south of the Transverse Ranges.

The kinematic model developed here is a block model of the upper crust and assumes that no deformation occurs within the interior of the blocks. The consistency of the block motions, which have been derived from several independent data sets, supports the assumption of undeforming blocks. There has been, however, considerable discussion recently on the manner in which the lower crust is moving with respect to the upper crust [e.g., Hadley and Kanamori, 1977; Yeats, 1981; Webb and Kanamori, 1985]. Seismicity suggests that approximately the upper 10 km is acting coherently, and the model developed here is meant to apply to this region.

PROBLEMS WITH PREVIOUS KINEMATIC MODELS

The present tectonic regime is usually modeled with western California attached to the Pacific plate and moving about $N35^{\circ}W$ relative to North America [e.g., Atwater, 1970; Anderson, 1971; Hill, 1982a; Bird and Rosenstock, 1984]. This relative motion is roughly parallel to the sections of the San Andreas fault north and south of the Transverse Ranges. The Transverse Ranges are commonly attributed to compression in a zone of collision between the Pacific and North American plates. Several problems

Figure 5-1. The principal faults of southern California and the subdivisions of the Transverse Ranges referred to in the text. These faults are assumed to bound rigid blocks which have been modeled as moving in directions consistent with the faults that bound them. The broad deformation within the western Transverse Ranges has been modeled as a simple boundary parallel to the trend of the major structures in the area. This and the other figures are Mercator projections about the RM2 pole of Minster and Jordan [1978].

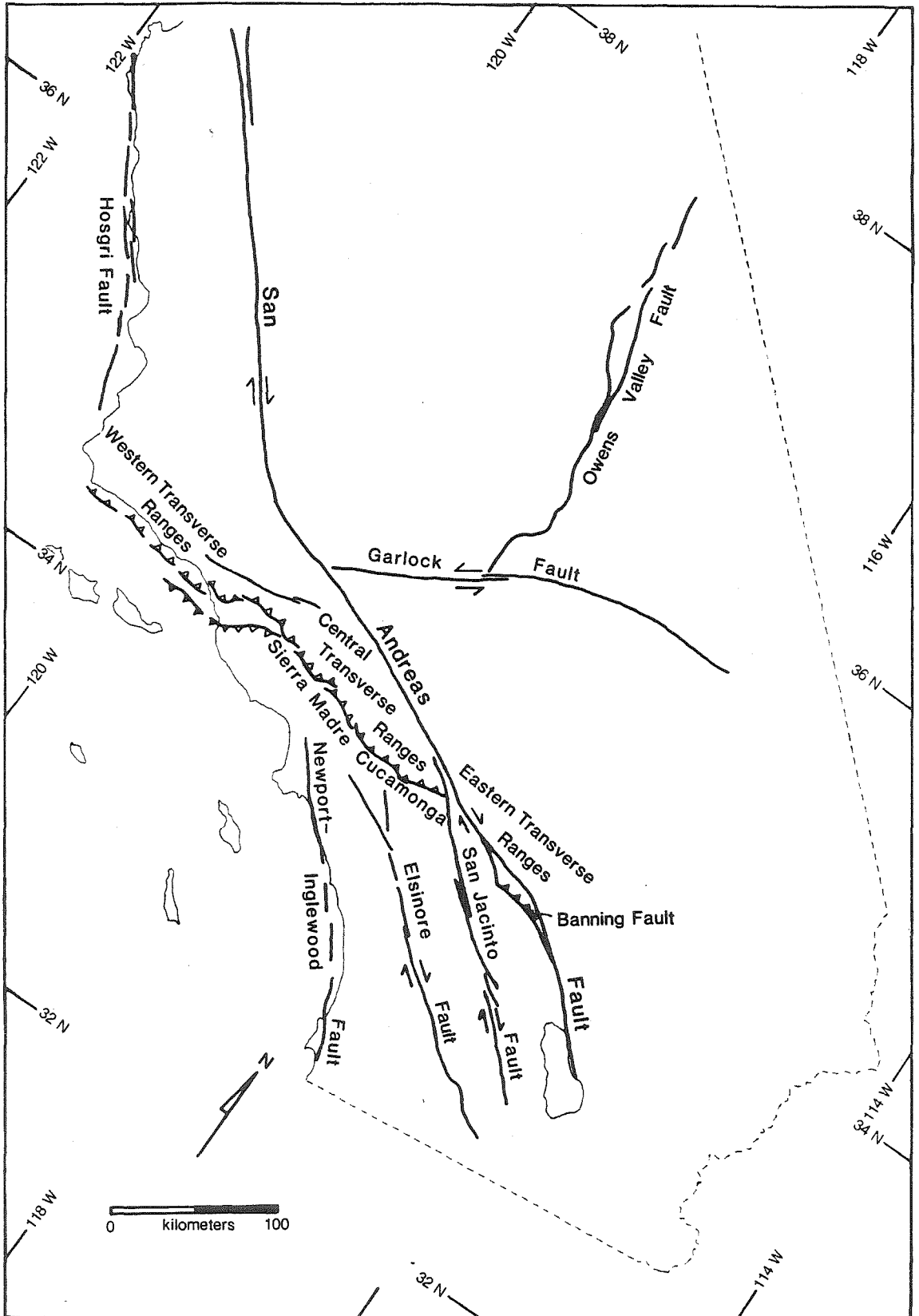


Figure 5-1

with this interpretation are discussed below.

1. The net shear strain rate across southern California, determined from recent geologic studies of active faults, does not add up to the relative Pacific-North American plate velocity [Weldon and Sieh, 1985; Sieh and Jahns, 1984]. Apparently, one third of the total plate velocity of 56 mm/yr [Minster and Jordan, 1978, 1984] is presently not accounted for by major onshore faults in southern California. Other workers [e.g., Bird and Rosenstock, 1984; Christodoulidis et al., 1985] have addressed the problem of the total slip rate across southern California and account for the total relative Pacific-North American plate motion onshore. Reliable Quaternary geologic information on the slip rates of the southern San Andreas fault [Weldon and Sieh, 1985] and the San Jacinto fault [Sharp, 1981], however, constrains the rates of each of these faults to be about 10 mm/yr less than assumed by Bird and Rosenstock [1984] and implied, in sum, by Christodoulidis et al. [1985]. The slip rates used in our model are shown in Figure 2.

2. A mass balance problem exists if southern California is moving with the Pacific plate because a great deal of crustal convergence in the Transverse Ranges would be required. The width of the left-stepping collision zone (normal to the relative plate motion) is about 150 km, and if we assume that the amount of convergence is equal to the slip on the San Andreas system (about 300 km) [e.g., Hill and Dibblee, 1953; Huffman, 1972; Crowell, 1981] and that the average crustal thickness of southern California is 28 km [Hearn, 1984a, b], a volume of crust greater than one million km³ must be accounted for. This calculation assumes that the left step in the San Andreas fault has always existed; a progressively widening step would reduce the volume of crust to be accounted for. Weldon [1985] argues that at least half of the left step in the San Andreas fault existed when the fault began its modern activity, and it has grown to its present size. If, for the sake of argument, the San Andreas fault initially had no step and the left step grew as the slip on the San Andreas fault accumulated, the total volume of crust that encountered the left step would be one-half million cubic

Figure 5-2. The major blocks in southern California and the data used to calculate their relative velocities. The two arcs have been fit to the trend of the San Andreas fault to determine the direction of motion of southern California southwest of the fault. Only the blocks southwest of the San Andreas fault and east of the Pacific coast are rotating along the arcs. The principal strain rates from three trilateration networks in southern California and the average velocity field within the Salton network [Savage, 1983] are included to demonstrate the consistency of these data with the curvature of the San Andreas fault. Slip rates (millimeters per year) used in the model are located where the integration paths in Figure 3 cross the faults. The letters associated with the rates give the sources of the information from which the rates were chosen: (a) Sieh and Jahns [1984]; (b) Carter [1980, 1982]; (c) Weldon [1984a, 1985]; (d) Weldon and Sieh [1985]; (e) Sharp [1981]; (f) Matti et al. [1982]; (g) see text; (h) average of Yeats [1983] and Rockwell [1983].

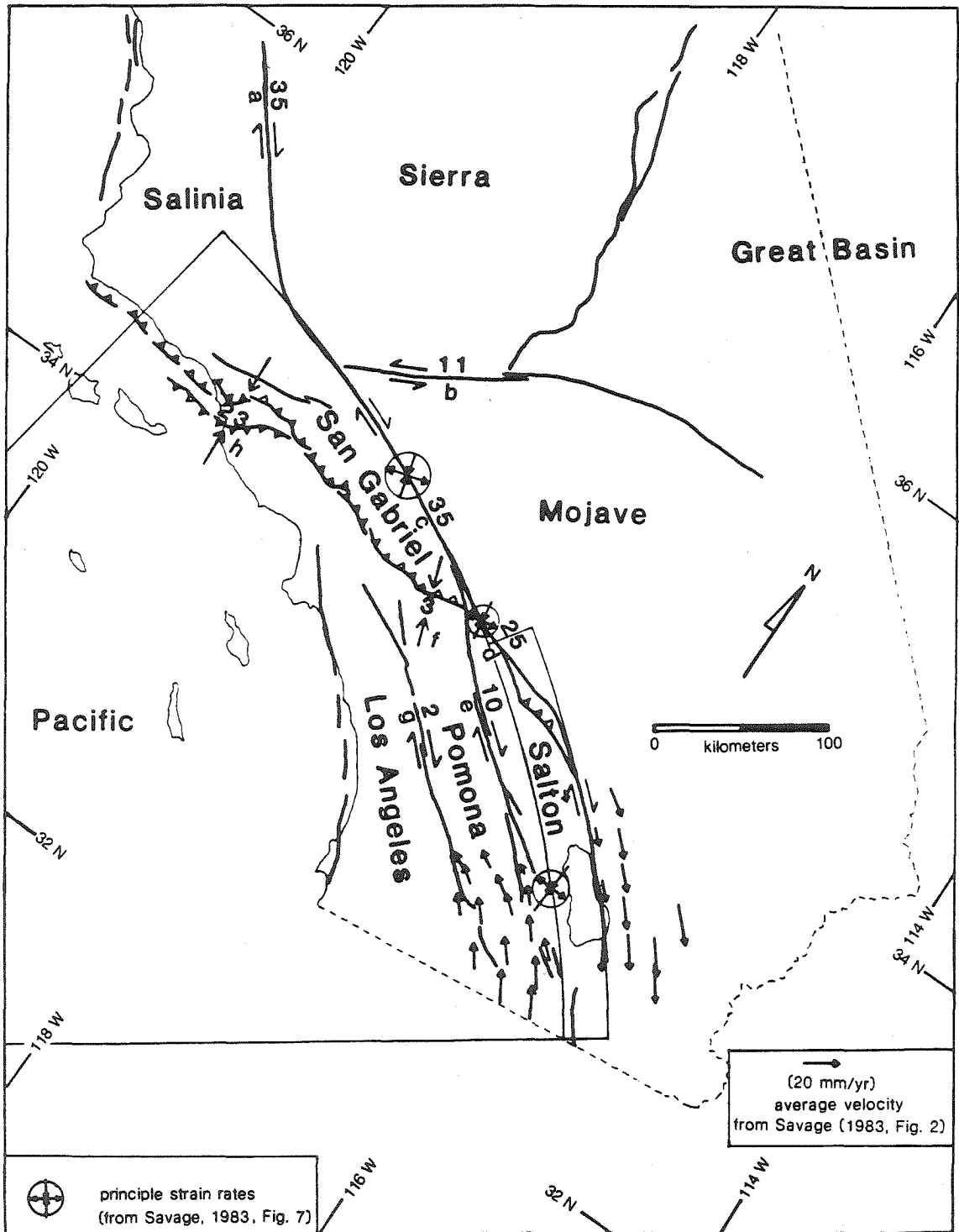


Figure 5-2

kilometers.

In accounting for the observed excess volume of crust, the dominant contribution is due to crustal thickening in the Transverse Range area (32 versus 28 km [Hearn, 1984b; Humphreys, 1985]). The volume of excess crust due to crustal thickening is only 140,000 km³. The volume due to the elevated topography of the mountains themselves is very small; using average dimensions of 200 km long, 40 km wide, and 1.5 km in height, the volume calculated is only 12,000 km². If the rest of the volume is attributed to uplift and erosion over the area of the present mountains, 45 km of uplift and subsequent erosion would be needed just to account for the conservative volume estimate of one-half million cubic kilometers.

3. There is little geologic support for large-scale Quaternary convergence in the central Transverse Ranges, and the convergence that has been found can be attributed to the local geometry of the fault system [Weldon, 1984b, 1985]. By using the orientation of the San Andreas and Sierra Madre-Cucamonga faults and the minimum possible rate of slip on the San Andreas fault (30 millimeters per year [Weldon, 1984a]), the assumption that the Los Angeles block is part of the Pacific plate results in at least 21 mm/yr of right-oblique convergence across the Sierra Madre-Cucamonga fault. This is certainly not happening. (This assumes that the Mojave block is part of North America; Bird and Rosenstock [1984], for example, calculate 14 mm/yr across the central Transverse Ranges by allowing the Mojave to move relative to North America.) Essentially all the convergence across the central Transverse Ranges occurs on the Sierra Madre-Cucamonga fault system (Figure 1), which is estimated to be slipping at a rate of only 1 to 6 mm/yr [Ziony and Yerkes, 1984].

In the eastern Transverse Ranges considerable convergence has been assigned to the Banning strand of the San Andreas fault [Allen, 1957; J. C. Matti et al., unpublished manuscript, 1985]. Furthermore, Morton and Herd [1980] document an uplift rate of 18-36 mm/yr immediately north of the Banning fault (Figure 1), indicating very high

local rates of convergence. But between these two regions of active thrusting lies a section of the San Andreas fault 50 km in length along which little convergence has been documented (Figure 1). Despite local northeast dips of the San Andreas fault in the area, features offset by the fault can be restored by pure strike slip motion [Weldon, 1985]. In fact, extension locally takes place on secondary faults north [Weldon, 1984b; 1985] and south (J. C. Matti et al., unpublished manuscript, 1985) of the San Andreas fault in this area, and earthquake focal mechanisms with normal components have been recognized here (L. M. Jones, personal communication, 1985). It is impossible to appeal to simple northwest-directed collision between the North American and Pacific plates to explain the Banning and Sierra Madre-Cucamonga thrusts without also having major convergence between them.

Other longer-term geologic observations limit the amount of convergence that has occurred across the Sierra Madre-Cucamonga and San Andreas fault systems. The recognition of proximal, early Pleistocene and Pliocene sediments derived from the San Gabriel Mountains, both to the north [Barrows, 1979; Foster, 1980; Weldon, 1984a, 1985] and south [Matti and Morton, 1975; Morton and Matti, 1979] of these range-bounding faults rules out large amounts of convergence. Also, the detailed match of bedrock terranes, Tertiary deposits, and early Cenozoic structures across the San Andreas fault zone in the Transverse Ranges [e.g., Ehlig et al., 1975; Ehlig, 1981; Crowell, 1981; Powell, 1981; Silver, 1982] argues strongly against "consumption" of significant volumes of crust across the San Andreas fault in the central and eastern Transverse Ranges since at least Miocene time.

4. If California south of the Transverse Ranges were moving in the Pacific plate direction of Minster and Jordan [1978], the Transverse Range segment of the San Andreas fault forms an obstacle to the northwestward movement of southern California and results in other crustal fractures being more favorably aligned to accommodate the shearing motion (e.g., the San Jacinto and Elsinore faults). Using a finite element

method, Kosloff [1978] modeled the southern California crust as elastic blocks separated by relatively weak viscous faults. When driven by a far-field shear oriented so as to drive northwest directed right-lateral shear, an active southern San Andreas fault could not be produced because the other more favorably situated faults relieved the stress. This result led Kosloff [1978] and Humphreys and Hager [1984] to postulate that the mantle is contributing forces that tend to drive the southern California crust toward the Transverse Ranges. However, calculations of the mantle derived forces [Humphreys, 1985] result in too little net force to drive convergence along the entire Transverse Ranges front. With the kinematic model suggested here, however, the magnitude of these forces is reduced to a level that can be supplied by locally concentrating stresses in only the active areas and relying on prior uplift and the strength of the crust to account for the remaining elevated topography [Humphreys, 1985].

5. Trilateration strain measurements [Savage, 1983] indicate that nearly pure strike-slip motion occurs along the length of the San Andreas fault in southern California. These data demonstrate that the strain field remains nonconvergent and changes in orientation with the local trend of the San Andreas fault. While the geodetic data represent a much shorter interval of time than do the geologic slip rate data used here, the compatibility is remarkable. The principal strain axes across the three southern Californian networks are shown in Figure 2. The lack of convergence is particularly striking in the central Transverse Ranges where the greatest amount of north-south shortening would be predicted by existing models.

Overall, the evidence does not support the magnitude of Quaternary convergence in the central and eastern Transverse Ranges that is required by models with northwest directed motion of the crust south of the San Andreas fault. Local convergence does occur, but it can be attributed to either abrupt changes in fault trends or junctions between major faults. In fact, if major regional convergence across the San Andreas fault is assumed during the Quaternary (and perhaps throughout its modern history),

serious problems with the geology arise. The same problems exist in reconciling northwest directed motion of southern California with the geodetic strain data [Savage, 1983].

PROPOSED MODEL

The proposed model has three major new features. First, we suggest that southern California between the San Andreas fault and the Pacific coast is rotating in a counter-clockwise direction about a pole located approximately 650 km southwest of the Transverse Ranges portion of the San Andreas fault. This rotation is a consequence of strike-slip movement along the San Andreas fault both in the Salton Trough and through the Transverse Ranges (Figure 2), in agreement with the geologic slip data for the major faults and the strain data of Savage [1983]. Note that except for a 30-km step in the trend of the San Andreas fault at the Banning fault, the San Andreas fault can be fit remarkably well with a circular arc centered at the proposed pole position (Figure 2). From the Salton Trough to the northern end of the Transverse Ranges, a distance of 400 km, where we believe this rotation occurs, there are no deviations from the arc greater than three km other than the step at the Banning fault. Also note that the velocity field presented by Savage [1983] for the trilateration network across the Salton Trough is itself suggestive of rotation about a pole located in the vicinity of the predicted position (Figure 2).

The second feature of our model is that a significant amount of fault activity must take place in southern California west of the Elsinore fault. If the slip is occurring on northwest trending offshore faults, about 20 mm/yr of right lateral slip and 5 mm/yr of convergence are required. A few authors have proposed relatively large amounts of slip offshore (e.g., Anderson [1979]: ≥ 10 mm/yr), but most authors have inferred that it is onshore. In particular, Bird and Rosenstock [1984, p. 952] begin by assuming that a total of 56 mm/yr is occurring on the San Andreas and San Jacinto faults. The space-

based geodetic work of Christodoulidis et al. [1985] addresses the motion of Monument Peak, at the southern end of the Los Angeles block, relative to Quincy, at the northern end of the Sierran block. They conclude that if Monument Peak is attached to the Pacific plate and Quincy is attached to stable North America (i.e., they exclude Great Basin extension), the measured rate of shortening between the two monuments yields a Pacific plate velocity of 61 ± 25 mm/yr relative to North America, using the relative direction of Minster and Jordan [1978]. This is compatible with the expected North America-Pacific rate of plate motion (56 ± 3 mm/yr [Minster and Jordan, 1978, 1984]), and T. H. Jordan et al. (unpublished manuscript, 1985) calculate that no more than 7 mm/yr of offshore slip can be occurring.

Our concern with the results of Christodoulidis et al. [1985] stems primarily from their need to put large amounts of convergence across the Transverse Ranges and slip rates on the San Andreas system much greater than supported by the geologic and land-based geodetic rates mentioned here. The net velocity acquired across the Salton Trough is 35-40 mm/yr [Savage, 1983]. While it is possible that the geodetic network does not cover the entire breadth of the zone being strained, the rate documented agrees with our kinematic model. We also have reservations about the velocity they determine for the Pacific plate, 61 mm/yr (as compared to 56 mm/yr from Minster and Jordan [1978] as being representative of the long term average rate. While these rates may be compatible, the value of Christodoulidis et al. [1985] is a minimum because it does not include either the relative motion of the northern Sierra site with respect to North America or any motion in the southern California Borderland. Both of these factors would add to the velocity of the Pacific plate, making the difference between the two estimates of plate rate even larger.

The difference between the geologic and the space-based geodetic estimates of the relative North American-Pacific plate velocity may be due to variations in plate velocities through time or to near-fault strain rate variations associated with the earthquake cycle.

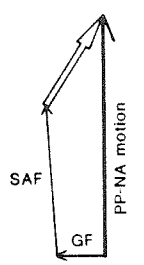
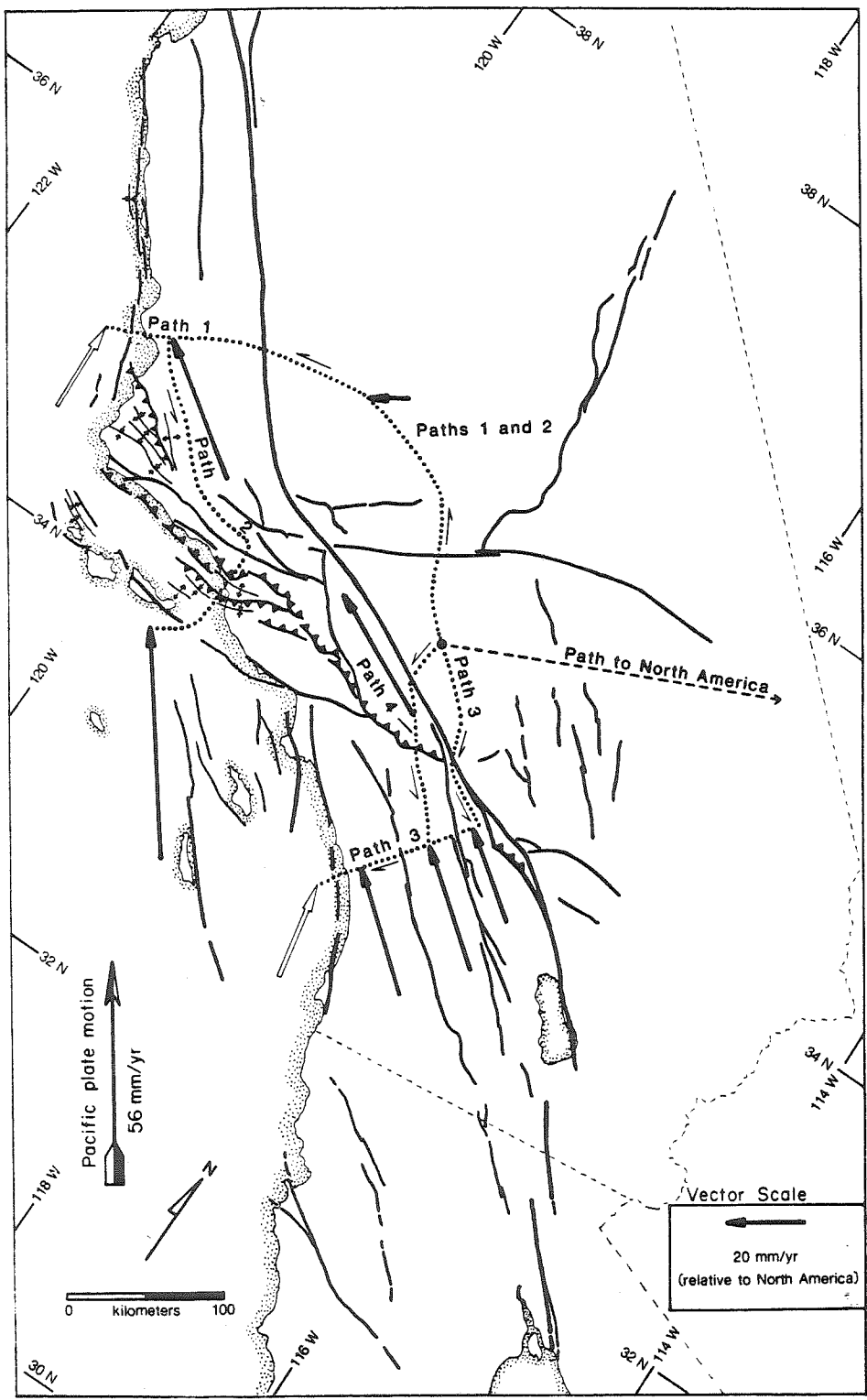
The difference in rate could then be attributed to the very different durations in time over which the two methods average. If this is true, however, it remains difficult to explain the similarity between the inferred slip rate along the San Andreas fault derived from the land-based geodetic experiments and the Quaternary slip rate values.

The third feature of our model is that the tectonics of southern California can be largely explained by three fault systems bounding rigid blocks. Since the San Andreas fault was first placed in its plate tectonic setting, there has been considerable debate about whether the San Andreas fault itself is the plate boundary or whether there is a "broad soft zone" [Atwater, 1970]. In our model the plate boundary is neither. The San Andreas system (including the San Andreas and San Jacinto faults in southern California) accounts for just under $2/3$ of the plate motion, and the coastal system about $1/3$; there are really two fault systems bounding a relatively coherent block in between. Because the total plate motion is obtained by adding only the motion on the Garlock fault, the San Andreas fault, and the coastal system, the activity of smaller faults and possible distributed shear across the blocks are almost insignificant in the total deformation across the plate boundary.

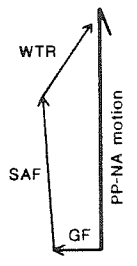
The internal consistency of our model is tested by performing line integrals of the strain rate between points of interest. If all of the motion along any chosen path is considered, the results are independent of the path, and different paths connecting the same end points will yield the same values. In particular, if this integral is evaluated between a point on the North American plate and one on the Pacific plate, the total relative plate motion will be accumulated. This method has been described by Minster and Jordan [1984] and applied by them to a path across the Great Basin and central California.

We have considered the four paths shown on Figure 3. When the path over which the integration is carried out does not encounter rotation or distributed deformation of the blocks, the integral reduces to a simple sum of the relative slip rate vectors across each velocity discontinuity, generally a fault. Paths 1 and 2 have been integrated in this

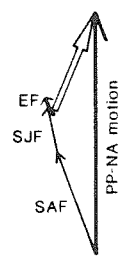
Figure 5-3. Integration paths and slip rate vectors for the major blocks in southern California. Solid arrows are velocity vectors relative to North America for points along the path. The corresponding vector diagrams show the construction of these vectors. Because the southern California blocks are rotating about relatively close poles, the velocity vectors vary across these blocks by small but significant amounts (see text). These corrections are shown in the vector diagrams as vectors with dots instead of arrowheads. The open arrows at the ends of paths 1, 3, and 4 on the map and the vector diagrams are the discrepancy vectors (the motion needed to bring the velocity up to the relative velocity of the Pacific Plate, determined for path 2 and given by Minster and Jordan [1978]). Abbreviations used in the vector diagrams are SAF (San Andreas fault), GF (Garlock fault), WTR (western Transverse Ranges), SJF (San Jacinto fault), CF (Cucamonga fault), EF (Elsinore fault), PP (Pacific Plate), and NA (North American Plate).



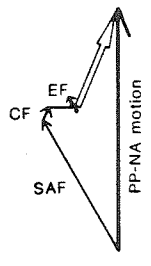
Path 1



Path 2



Path 3



Path 4

Vector Diagrams

manner. Paths 3 and 4, which cross blocks rotating on a relatively small arc, require accounting for the continuous variation in velocity. For simplicity the overall deformation in the western Transverse Ranges is treated as though it were a single thrust fault parallel to the trend of the major faults and folds in the area. The effects of errors in the slip rates are discussed separately in the next section.

The paths begin in the Mojave Desert, which we infer is part of the North American plate; a fiducial point is shown on Figure 3. There are several reasons that lead us to believe that the Mojave block is part of North America. A path from cratonic North America to the Mojave Desert can be constructed south of the Great Basin that crosses very little significant Quaternary deformation. Such a path would cross the Rio Grande Rift, which is extending at a rate of less than 1 mm/yr [e.g., Golombek, 1981], and the southern Basin and Range Province, which does not presently have significant activity south of the Great Basin [Zoback et al., 1981]. Alternatively, a path across the Colorado Plateau to the Mojave Desert would encounter less than 1 mm/yr across the Rio Grand Rift [Golombek, 1981] and less than 1 mm/yr at the southwest margin of the Colorado Plateau [Hamblin et al., 1981]. Within the Mojave block there is geologic and paleomagnetic evidence [Dibblee, 1967; Dokka, 1983; Weldon et al., 1984] that the region has not experienced the significant late Cenozoic rotations or deformations that most previous models require. Garfunkel [1974] and Calderone and Butler [1984] have proposed large-scale counterclockwise rotations, and Luyendyk et al. [1980] and Bird and Rosenstock [1984] have proposed large-scale clockwise rotations within the Mojave Block, accompanied by major shear on the many northwest trending faults that exist in the region. However, Dibblee [1967] and Dokka [1983] have demonstrated that these faults have not experienced enough total displacement to deform the Mojave significantly. Furthermore, Weldon et al. [1984] and Weldon [1985] have recently provided paleomagnetic evidence indicating that the southwestern Mojave has rotated less than 4° since middle Miocene time. Also, there is no active tectonic boundary recognized between the Mojave block

and North America, which any rotation model would require.

Geodetic studies in the Mojave region give contradictory results. Sauber and Thacher [1984] have argued for about 5 mm/yr of net strain rate across the northwest trending faults in the Mojave region, while King [1985] observes rates of strain over the same area which are not significantly different from zero. We conclude that the data are consistent with the Mojave region being a part of North America and use the Mojave block as the starting point for our paths of integration. The possibility of a few millimeters per year of deformation between the Mojave block and North America does not significantly alter our conclusions.

Path 1 begins on the Mojave block and crosses the Garlock fault to the Sierran block (Figure 3). We assume that the trend of the Garlock fault west of the Owens Valley fault (i.e., west of the Great Basin) indicates the direction of motion of the Sierran block (S55°W) and that the slip rate is 11 mm/yr (the best estimate of Carter [1980, 1982]). There is considerable variability in the trend and uncertainty in the slip rate of the Garlock fault, which will be addressed below. The path continues across the Sierran block to the west and crosses the San Andreas fault. Slip on the San Andreas fault contributes a velocity vector parallel to the trend of the San Andreas fault (N40°W) with a magnitude of 35 mm/yr [Sieh and Jahns, 1984]. The resulting velocity vector of the Salinian block (relative to North America) is 38 mm/yr directed N58°W. If this is compared to the velocity of the Pacific plate (56 mm/yr, [Minster and Jordan, 1978]), a discrepancy of 23 mm/yr oriented N5°W exists. The discrepancy vector is shown in Figure 3 as an open arrow located at the end of path 1. The discrepancy vector is similar to the preferred discrepancy vector of Minster and Jordan [1984], though we find slightly more convergence west of the Great Basin as a result of the more southerly drift of the Sierran block in our model. As noted by Minster and Jordan [1984], much of the discrepancy vector may be taken up on the San Gregorio-Hosgri fault system. Weber and Lajoie [1977] report a rate of 6-13 mm/yr of right-lateral slip for the fault, and

Crouch et al. [1984] present evidence for considerable convergence across this and other faults west of the San Andreas fault.

Path 2 follows path 1 across the Garlock and San Andreas faults and then heads south through the western Transverse Ranges to the Continental Borderland. Yeats [1983] calculated a rate of convergence across the Ventura Basin of 23 mm/yr for the last 200,000 years. More recent results from this area also give a high, though somewhat lesser rate of convergence (17 ± 4 mm/yr) [Rockwell, 1983; Rockwell et al., 1984, also personal communication, 1985]. It is not yet known how the rate varies across the province or whether the numbers represent the total convergence across the western Transverse Ranges. We have chosen to average these two values, and we infer a direction of $N5^{\circ}W$, perpendicular to the trend of the major faults and folds in the area (Figure 2). Path 2 results in a relative motion (53 mm/yr, $N37^{\circ}W$) that is indistinguishable from the relative Pacific plate velocity of 56 ± 3 mm/yr directed $N35^{\circ}W$ [Minster and Jordan, 1978]. This suggests that the borderland south of the western Transverse Ranges (the end of path 2, Figure 3) is moving with the Pacific plate.

Path 3 (Figure 3) crosses the San Andreas fault east of the junction with the San Jacinto fault and continues onto the Salton block, picking up a velocity of 25 mm/yr [Weldon and Sieh, 1985] directed $N55^{\circ}W$, which is parallel to the tangent of the arc fit to the San Andreas fault where path 3 crosses it. From there the path turns southwest and heads directly toward the pole of rotation. By heading in this direction the only effect due to block rotation is to decrease the magnitude of the velocity vector. The faults encountered along the path contribute velocities that are summed to determine the relative velocity for any point along the path. Path 3 crosses the San Jacinto fault, picking up 10 mm/yr (the long-term Quaternary slip rate of Sharp [1981] directed parallel to the fault ($N47^{\circ}W$), and the San Andreas component of velocity decreases by 1.5 mm/yr due to the approach toward the pole of rotation. This results in a velocity vector for the Perris block of 33 mm/yr oriented $N52^{\circ}W$. Continuing to the southwest, the

Elsinore fault is crossed next, adding about 2 mm/yr (this value is discussed in the next section) of right-lateral motion oriented $N49^{\circ}W$, and passes onto the Los Angeles block. Subtracting an additional 1.5 mm/yr from the San Andreas component of motion for the continued approach toward the pole yields a velocity vector of 33 mm/yr directed $N53^{\circ}W$. The path is finally brought offshore and another 2 mm/yr is removed from the San Andreas component, yielding a net relative velocity vector of 32 mm/yr pointing $N50^{\circ}W$. The discrepancy vector at the terminus of path 3 is indicated in Figure 3 with an open arrow that is 25 mm/yr pointing $N11^{\circ}W$.

Another route similar to path 3 is one that begins on the Mojave block and crosses the San Andreas fault to the San Gabriel block, and then continues across the Sierra Madre-Cucamonga fault to the Perris block. This route is shown on Figure 3 as path 4. Crossing the San Andreas fault picks up 35 ± 5 mm/yr (Weldon [1984a]; unpublished work has refined this to 37.5 ± 2 mm/yr, [Weldon, 1985; R. J. Weldon et al., unpublished manuscript, 1985]. We use the published value here.) parallel to the San Andreas fault, $N65^{\circ}W$. This yields a velocity vector for the San Gabriel block that is similar to that found for the Salinian block with path 1. This similarity is expected because there are no structures with more than a few millimeters per year recognized between the two blocks. If counterclockwise rotation of the Sierran block along the curved Garlock fault (as discussed below) is occurring, the velocity vectors describing the motion of the Salinian and San Gabriel blocks would be even more similar.

Crossing the Cucamonga fault to the Perris block adds about 3 mm/yr [Matti et al., 1982, also personal communication, 1984] oriented $N18^{\circ}W$ to the relative velocity vector, which rotates it clockwise about 15° . The resultant Perris block vector at the junction of paths 3 and 4 (corrected for the rotation of the San Gabriel and Perris blocks) is virtually identical to that calculated with path 3. Again, the consistency of the results determined from different data sets along different paths supports the accuracy of the rates and the kinematic model. Also, because the Los Angeles block is moving parallel

to the Perris block, about the same angular discordance remains between the velocity vectors of the San Gabriel and the Los Angeles blocks as exists between the San Gabriel and Perris blocks. The change in orientation of the Sierra Madre-Cucamonga fault zone to the west and the relative rates of the Perris and Los Angeles blocks will affect the relative amounts of convergence and the sense and magnitude of lateral faulting along this boundary. The left-lateral component of activity across the Sierra Madre-Cucamonga fault zone is explained by the more westerly motion of the San Gabriel block relative to those to the south.

If paths 3 and 4 were continued to the terminus of path 2, a velocity vector would need to be included that nulls the discrepancy vector, implying the existence of a zone of significant dextral shear strain across northwest trending faults between the Los Angeles block and the end of path 2. Because the north-south rate of convergence decreases from the western Transverse Ranges to the central Transverse Ranges (Figure 1), nearshore faults are thought to accommodate most of discrepancy vector 3.

It is impossible, based on current mapping, to connect the activity in the western Transverse Ranges directly to northwest trending structures to the north and south of the Transverse Ranges, as proposed by our model. This is probably in part due to the difficulty in characterizing structures under the ocean, but it may also indicate something different about the coastal system. The western Transverse Ranges are characterized by a zone of convergent deformation that is unlike the relatively simple fault zones that characterize the rest of southern California. This lack of simplicity may be due to the youth of deformation or to the existence of major low angle detachment faults (both possibilities suggested by Yeats [1981]). Another possibility is that the coastal system is developed on crust of more oceanic character, whereas the San Andreas fault system onshore is developed on continental crust. Whatever the reason, the apparent lack of a simple, throughgoing structure connecting the western Transverse Ranges with faults to the north and south could be viewed as consistent with the lack of a simple,

throughgoing structure within the western Transverse Ranges themselves. For this reason and because of the lack of information about offshore faults we have not attempted to identify particular structures in the coastal system that accommodate the predicted strain.

UNCERTAINTIES IN THE MODEL

The kinematic description of southern California presented above is based on the best estimates of the Quaternary slip rate data available today. No errors have been included. Ideally, uncertainties could be accumulated along the route of integration as the strain rate is calculated, so that an uncertainty could be given at any point, relative to the beginning of the path. However, the data are poor in several critical areas, and smaller structures have been completely ignored. Furthermore, the nature of the uncertainties makes them poorly suited to statistical treatment; the slip rates are the best estimates of the workers from their field areas, and the probability distributions of the estimates are asymmetric and highly non-Gaussian. In lieu of a formal treatment of the error we discuss probable sources and magnitudes of error and their effects on the block motions and on the overall kinematic model.

There is considerable uncertainty in both the magnitude and direction of motion of the Sierran block that affects the velocities determined along paths 1 and 2. Carter's slip rate of 11 mm/yr, which we use in deducing the motion of this block, is only absolutely bracketed between 5 and 30 or more mm/yr [Carter, 1980; 1982]. However, his best estimate of 11 mm/yr is based on several lines of geologic inference that we find convincing, and it is the best slip rate study on the Garlock fault that we are aware of. Unfortunately, Carter's rate estimate is for the portion of the Garlock fault east of the Owens Valley fault, whereas paths 1 and 2 cross the Garlock fault just to the west of the Owens Valley fault. The Owens Valley fault cannot contribute more than a few millimeters per year even in its more active northern segment [Gillespie, 1982], so no

significant error is introduced by extending Carter's estimate for the Garlock westward past its junction with the Owens Valley fault. Furthermore, because of the small amount of activity on the Owens Valley fault and the relative lack of recent deformation within the Mojave and Sierran blocks, kinematic necessity requires that Carter's slip rate estimate also applies to the motion of the southern portion of the Sierran block relative to the Mojave. An interesting observation is that the Garlock fault west of the Owens Valley fault appears to be geologically less active than the fault to the east [L. T. Silver, personal communication, 1985]. This is probably due to the westward-increasing activity on other, subparallel faults north of the Garlock fault such as the White Wolf fault (Figure 3). For simplicity in our model, we have included such kinematically associated deformation with the Garlock fault and have avoided it with our choice of integration path.

A related problem is that the Garlock fault is quite curved. We have chosen the trend of $S55^{\circ}W$ because it is the trend of the fault in the region where it separates the Mojave block from the Sierran block and should therefore best describe the Sierran block's local relative motion. Choosing this segment of the Garlock fault yields a slip vector orientation that is more southerly than would be determined from any other part of the Garlock fault. If the motion of the Sierran block relative to North America were in a more westerly or northwesterly direction, our results would be more compatible with those of Minster and Jordan [1984], which are based on the average recent extension direction of the Great Basin [Zoback et al., 1981]. However, a west or northwest motion for the Sierran block would require either major extension across the western Garlock fault or motion of the Mojave block with respect to North America, neither of which has been documented.

The effect of a greater slip rate on the Garlock fault would be an increase in the amount of convergence offshore north of the Transverse Ranges and more left-lateral shear on east trending faults in the western Transverse Ranges.

In our model the Sierran block translates S55° W relative to the Mojave block (and by inference to North America). The curvature of the bounding Garlock fault and the presence of westward increasing contractile faulting parallel to the Garlock fault suggest that the motion of the Sierran block may be more complex. If the northern part of the block is moving faster than the southern part, the motion of the block relative to our reference in the Mojave block must be described with a rotation. The curvature of the Garlock fault is consistent with a rotational pole of the Sierran block located about 200 km southeast of the Garlock fault, geographically near the Banning fault (Figure 1). Rotation of the Sierran block about this pole, relative to the Mojave block (and therefore North America), provides pure strike slip motion along the Garlock fault east of the Owens Valley fault, increasingly contractile deformation across the less curved portion west of the Owens Valley fault, and more rapid extension in the northern Great Basin. Rotation may also explain the discrepancy between the apparent west-southwest motion of the southern Sierran block and the west-northwest direction of average extension in the Great Basin [Zoback et al., 1981]. If the Sierran block is rotating, our relative velocity vector for paths 1 and 2 should be rotated counterclockwise 20°-25° at the point where the integration path encounters the San Andreas fault. This would increase the predicted offshore strike-slip motion north of the western Transverse Ranges by about 4 mm/yr and increase the convergence through the western Transverse Ranges by about 3 mm/yr.

In our model the movement of the Sierran block is determined from the Garlock fault. An alternative approach, chosen by Minster and Jordan [1984] and T. H. Jordan et al. (unpublished manuscript, 1985), is to consider a path that begins on stable North America and arrives at central California by crossing the Great Basin. The route we have chosen involves uncertainty mainly in the slip rate of the Garlock fault, whereas determining extension across the Great Basin involves uncertainties in the rate and sense of movement of the many faults within the Great Basin. It is reassuring that these two

independent approaches determine similar velocities for the Sierran block.

An additional uncertainty in the velocity along path 2 is the poorly constrained left-lateral activity in the western Transverse Ranges. In our model strain in the western Transverse Ranges is assumed to be purely convergent perpendicular to the trend of the major faults and folds and ignores the left-lateral faults that, combined, are believed to accommodate less than 2 mm/yr [Clark et al., 1984].

Path 3 has the least uncertainty associated with its relative velocity vectors because the slip rates and orientations of all three onshore strike-slip faults crossed have small errors. For the San Andreas fault we use Weldon and Sieh's [1985] rate of 24.5 ± 3.5 mm/yr and the orientation tangent to the circular arc shown in Figure 2 that produces pure strike-slip motion along the San Andreas fault. Sharp's [1981] rate of 10 ± 2 mm/yr on the San Jacinto fault is supported by more recent work [Weldon, 1985; R. J. Weldon et al., unpublished manuscript, 1985], and we have chosen an orientation that on average best describes this fault. Estimates of the slip rate across the Elsinore fault vary from 1 [Ziony and Yerkes, 1984] to 7 mm/yr [Kennedy, 1977]. New work on the southern Elsinore fault (Pinault and Rockwell [1984], about 4 mm/yr) may help narrow the range, but at the moment, none of the estimates for the Elsinore fault are based on absolute dates and well-defined piercing points. In our model we arbitrarily chose 2 mm/yr to reflect the consensus that the northern Elsinore fault accommodates very little slip. If the lower estimate of 1 mm/yr is correct, it increases the discrepancy vector by a negligible amount. The maximum rate of 7 mm/yr reduces the discrepancy vector offshore from 25 to about 20 mm/yr. No reasonable slip rate on the Elsinore fault can change the conclusion that a large fraction of the plate motion must be west of the Los Angeles block. In fact, even in the unlikely situation that the maximum rates for all of these faults are correct ($28 + 12 + 7$ mm/yr), more than 10 mm/yr still must be accounted for offshore.

Another possible source of error in the velocities along paths 3 and 4 is the

uncertainty of the pole position about which the blocks in southern California are rotating. If the Salton Trough is opening with a component normal to the San Andreas fault, the pole may be farther away from the Transverse Ranges. A normal component in the Salton Trough, however, is not supported by Savage's [1983] strain data or by the arcuate fit of the San Andreas fault shown in Figure 2. This source of error is small because the paths span less than 20% of the distance to the pole and were chosen so that no change occurs in orientation. The uncertainty in the pole position can contribute at most a few millimeters per year of error to the total.

IMPLICATIONS

An important feature of our kinematic model is the requirement of a zone of very active deformation offshore. This is illustrated by the discrepancy vectors for paths 1, 3 and 4 and the convergence in the western Transverse Ranges all being nearly the same (vector diagrams, Figure 3). We propose that the discrepancy vectors for paths 1, 3 and 4 are accommodated on northwest trending, predominantly strike-slip faults in the Continental Borderland near the coast, while the same activity is manifested by convergence on east trending thrusts and folds in the western Transverse Ranges. The style of activity varies because the structures differ in orientation, even though the strain is the same. In this coastal system the western Transverse Ranges form a left step between the northwest trending offshore elements. Seismicity studies support the switch from predominantly strike-slip motion on northwest trending faults in the borderland to essentially pure convergence in the western Transverse Ranges [e.g., Corbett, 1984]. Unfortunately, the length of the seismic record is inadequate to estimate rates of deformation. The diminishing of convergent deformation to the east and west of the western Transverse Ranges places the site of the offshore faulting near the coastline both north and south of the Transverse Ranges. The coastal system separates the Pacific plate to the west from a slice of relatively intact continental crust to the east, just as the San

Andreas fault system separates the slice from North America.

In southern California the coastal system is partially exposed onshore in the western Transverse Ranges. Measurements of the rate and direction of convergence across the western Transverse Ranges at various longitudes may provide a direct means of quantifying the location, rate, and style of motion on the northwest trending elements of the system which are not exposed onshore. We have calculated that the end of path 2 is moving with the Pacific plate, but the spatial distribution of activity on the faults within the borderland between the end of path 2 and the Los Angeles block cannot be determined until the distribution of the convergent activity in the Transverse Ranges east of path 2 has been worked out in detail or until the slip rates of the offshore faults are determined. Another area where the rate of activity across the coastal system may be measured is in Baja California. Allen et al. [1960] report Quaternary deformation on the Agua Blanca fault that may indicate up to centimeters per year of activity joining the Gulf of California with the California Borderland. Yeats and Haq [1981] also describe active faults along the western length of Baja, suggesting that some of the Pacific-North American plate motion is occurring west of the Gulf of California.

Another important consideration is the relation between the offshore activity and the generally accepted value for the Pacific-North American plate relative motion. We accept the plate motion value of 56 ± 3 mm/yr N35⁰W, determined by Minster and Jordan [1978, 1984], and compare our integrated velocity to theirs. The motion on the northwest trending faults of the coastal system is determined by assigning the difference between the integrated strain and the Pacific-North American plate motion to these features. We are justified in doing this because it is equivalent to calculating the slip rate by extending paths 1, 3 and 4 to the end of path 2, which is an internal kinematic requirement. The acquisition of the Pacific plate velocity by the end of path 2 supports the Pacific-North American plate rate of Minster and Jordan [1978, 1984]. However, this should not be taken as strong evidence for the accuracy of their value, because we have

accumulated an uncertain amount of error along path 2 and because Minster and Jordan's [1978] rates are based on a 3-m.y. average, whereas ours are late Quaternary. Weldon [1985], however, presents evidence that the slip rate on at least the San Andreas fault has remained constant for the last 4-5 million years, suggesting that our kinematic model may be valid back into the Tertiary.

We agree with the conclusion of Minster and Jordan [1984] that the convergence across the Pacific-North American plate boundary north of the Transverse Ranges is due to the westward motion of central California in response to the opening of the Great Basin and not due to the geometry of the San Andreas system. In our model the Garlock fault plays the kinematic role of the southern boundary of the Great Basin [Davis and Burchfiel, 1973; Wernicke et al., 1982]. Further, if the Sierran block is rotating as it moves west, as suggested by the curvature of the Garlock fault, the convergence in the Transverse Ranges near the junction of the Garlock and the San Andreas faults can be explained by the impingement of the southwestern corner of the Sierran block into the Salinian-San Gabriel block. This hypothesis satisfies the north-south convergence in the area [e.g., Davis, 1982; Davis and Lagoe, 1984] without appealing to the changes in trend of the San Andreas fault near its junction with the Garlock fault.

Finally, our model suggests that the tectonic activity in the Transverse Ranges is quite different than generally thought. These ranges have long been taken as evidence that southern California, as part of the Pacific plate, is colliding with North America across the San Andreas fault. However, our model produces uplift in the eastern Transverse Ranges with convergence across a step in the otherwise arcuate and strike-slip southern San Andreas fault (Figure 4). The convergence across this 30-km step is therefore 25 mm/yr oriented N50°W (parallel to the local trend of the San Andreas fault). The central Transverse Ranges are being uplifted by the Sierra Madre-Cucamonga fault system. Convergence across this boundary is due to the slightly different directions of motion of the San Gabriel block and the blocks to the south. As shown in Figure 4, this geometry

Figure 5-4. Schematic representation of the active compressive deformation in the Transverse Ranges. The eastern Transverse Ranges are being uplifted by convergence across a left step in the San Andreas fault in the Banning fault area, indicating a rate of convergence of 25 mm/yr oriented N50°W. The western Transverse Ranges are being shortened by a similar left step in the postulated coastal system at a rate of 20 mm/yr in the direction N5°W. The central Transverse Ranges are experiencing low rates of convergence due to the direction of motion of the San Gabriel block relative to the rest of southern California. The direction and magnitude of this convergence are very sensitive to the slip rates on the San Andreas and other faults and are therefore difficult to deduce accurately from the model. Simply determining the difference in motion between the San Gabriel block and the Perris block results in 3 mm/yr directed N25°W, as shown in the vector construction. If the Sierran block is moving to the west by rotating along the curved portion of the Garlock fault, 3-5 mm/yr of north-south convergence is necessary in the region of the southwest corner of the Sierran block. North of the Garlock fault there is about 11 mm/yr of convergence between the Sierran block and the Pacific plate, in a direction that is normal to the trend of the San Andreas fault in central California. This convergence appears to be occurring mainly on faults west of the San Andreas fault.

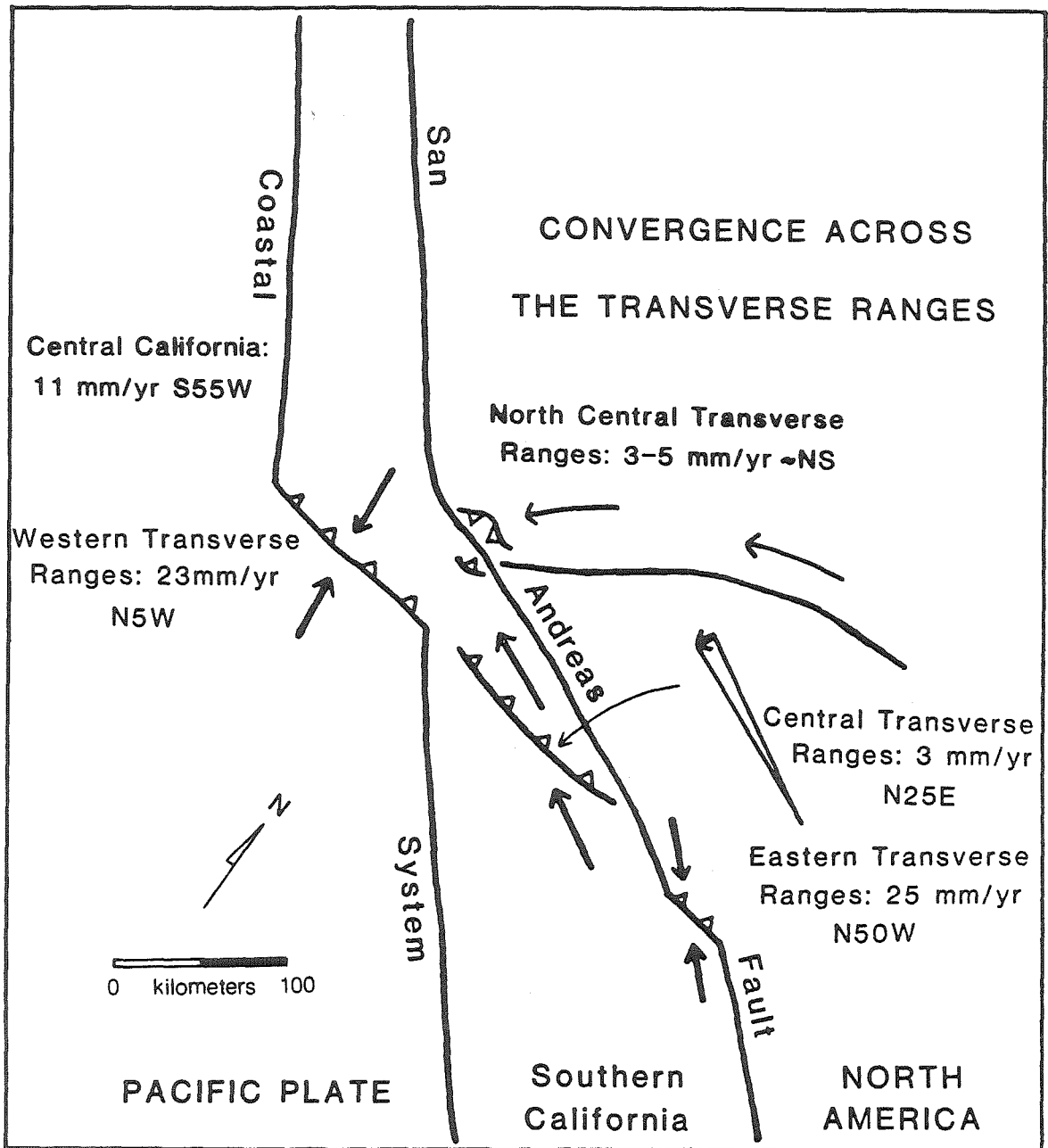


Figure 5-4

requires about 3 mm/yr of convergence across this zone, consistent with measured values [Matti et al., 1982]. Convergence in the western Transverse Ranges is due to a left step in the coastal system, and is unrelated to the San Andreas fault.

In our model the convergence usually inferred to exist across the central Transverse Ranges is shifted to the coastal system. Much of the North America-Pacific plate collision is occurring in the western Transverse Ranges, with lesser amounts occurring all along the southern and central California coast.

Our kinematic model has exceptional rates of convergence in two regions, the Banning fault area and in the western Transverse Ranges. Corbett [1984] noted that all well-located earthquakes (from 1971-1981) that occurred deeper than 20 km and most that occurred deeper than 15 km were in these same areas. We explain this by the presence of cold, brittle material at an unusually great depth due to the exceptional rates of convergence in these areas. This is supported by the anomalously high seismic velocity of the deep crust in the same locations [Humphreys et al., 1984] as well as the regionally depressed Moho in the Transverse Range region [Hearn, 1984a,b].

In our model the major uncertainties in the tectonics of southern California are due to motions external to the region modeled. The opening of the Great Basin appears to control the motion of the Sierran block, which in turn controls the amount of convergence along the central California coast. The similar velocity of the Salinian and San Gabriel blocks may indicate that the extension in the Great Basin (which controls the motion of the Salinian block) is related to the rotation of southern California (which controls the motion of the San Gabriel block). Furthermore, the amount of motion between the Mojave block and North America directly affects the amount of strain required offshore if the relative plate motion of Minster and Jordan [1978] is to be satisfied. In spite of these external uncertainties it is the internal consistency of the model within southern California itself that most strongly supports the major aspects of the model. The single tie across the western Transverse Ranges to the Continental Borderland leaves the

coastal system as the least certain part of the model; however, the agreement of the velocity at the end of path 2 (which crosses the western Transverse Ranges) with the externally derived value for the velocity of the Pacific plate [Minster and Jordan, 1978, 1984] lends credence to the existence and nature of tectonic deformation of the coastal system postulated here. The magnitude of the offshore activity implies that the region between the San Andreas fault and the coastal system is neither part of the North American plate nor the Pacific plate and may be considered a miniplate.

ACKNOWLEDGEMENTS

This paper is based on the field work and thoughts of innumerable people who have worked in southern California. We would like to acknowledge all of those workers referenced in the bibliography and to especially thank those who have freely shared their unpublished data and ideas upon which our model is based. We are particularly grateful to Leon Silver, Clarence Allen, Brad Hager, Kerry Sieh, Kris Meisling and Steve Wesnousky, who lent critical discussion or detailed reviews of the first draft of this manuscript. Reviews by Tom Jordan and Art Sylvester led to substantial improvements in the paper and we appreciate their efforts. We thank Jan Mayne for assistance in the preparation of the figures. This work was funded by grants from NASA (NAS5-27226) and the U.S. Geological Survey (Earthquake Hazards Reduction Programs, contracts: 14-08-0001-16774, 18285, 19756, and 21275).

REFERENCES

- Allen, C. R., San Andreas fault zone in San Geronimo Pass, southern California, *Geol. Soc. Am. Bull.*, 68, 315-350, 1957.
- Allen, C. R., L. T. Silver, and F. G. Stehli, Agua Blanca fault: A major transverse structure of northern Baja California, Mexico, *Geol. Soc. Am. Bull.*, 71, 457-482, 1960.
- Anderson, D. L., The San Andreas fault, *Sci. Am.*, 225, 5, 52-68, 1971.
- Anderson, J. G., Estimating the seismicity from geological structure for seismic-risk studies, *Bull. Seismol. Soc. Am.*, 69, 135-158, 1979.
- Atwater, T., Implications of plate tectonics for the Cenozoic tectonic evolution of western North America, *Geol. Soc. Am. Bull.*, 81, 3513-3536, 1970.
- Barrows, A. G., Geology and fault activity of the Valyermo segment of the San Andreas fault zone, *Open File Rep. 79-1 LA*, 49 pp., Cal. Div. of Mines and Geol., Sacramento, Calif., 1979.
- Bird, P., and R. W. Rosenstock, Kinematics of present crust and mantle flow in southern California, *Geol. Soc. Am. Bull.*, 95, 946-957, 1984.
- Calderone, G., and R. F. Butler, Paleomagnetism of Miocene volcanic rocks from southwestern Arizona: Tectonic implications, *Geology*, 12, 627-630, 1984.
- Carter, B. A., Quaternary displacement on the Garlock fault, California, in *Geology and Mineral Wealth of the California Desert, Dibblee volume*, edited by D. L. Fife and A. R. Brown, pp. 457-465, South Coast Geological Society, Santa Ana, Calif., 1980.
- Carter, B. A., Neogene displacement on the Garlock fault, California (abstract), *Eos, Trans. AGU*, 63, 1124, 1982.
- Christodoulidis, D. C., Smith, D. E., Kolenkiewicz, R., Klosko, S. M., Torrence, M. H., and Dunn, P. J., Observing tectonic plate motions and deformations from satellite laser ranging, *J. Geoph. Res.*, v. 90, p. 9249-9263, 1985.
- Clark, M. M., K. K. Harms, J. J. Lienkaemper, D. S. Harwood, K. R. Lajoie, J. C. Matti,

- J. A. Perkins, M. J. Rymer, A. M. Sarna-Wojcicki, R. V. Sharp, J. D. Sims, J. C. Tinsley, and J. I. Ziony, Preliminary slip-rate table for late Quaternary faults of California, *U.S. Geol. Surv. Open File Rep.* 84-106, 1984.
- Corbett, E. J., Seismicity and crustal structure studies of southern California: Tectonic implications from improved earthquake locations, Ph.D. dissertation, 231 pp., Calif. Inst. of Technol., Pasadena, 1984.
- Crouch, J. K., S. B. Bachman, and J. T. Shay, Post Miocene compressional tectonics along the central California margin, in *Tectonics and Sedimentation Along the California Margin*, vol. 38, edited by J. K. Crouch and S. B. Bachman, pp. 37-54, Society of Economic Paleontologists and Mineralogists, Pacific Section, Los Angeles, Calif., 1984.
- Crowell, J. C., An outline of the tectonic history of southeastern California, in *The Geotectonic development of California: Rubey vol. 1*, edited by W. G. Ernst, pp. 583-600, Prentice-Hall, Englewood Cliffs, N. J., 1981.
- Davis, G. A., and B. C. Burchfiel, Garlock Fault: An intracontinental transform structure, southern California, *Geol. Soc. Am. Bull.*, 84, 1407-1422, 1973.
- Davis, T. L., Late Cenozoic structure and tectonic history of the "Big Bend" of the San Andreas fault and adjacent San Amigdio Mountains, Ph.D. dissertation, 580 pp., Univ. of Calif., Santa Barbara, 1982.
- Davis, T., and M. Lagoe, Cenozoic structural development on the north-central Transverse Ranges and southern margin of the San Joaquin Valley, *Geol. Soc. Am., Abstr. Programs*, 16, 484, 1984.
- Dibblee, T. W., Jr., A real geology of the western Mojave Desert, California: *U.S. Geol. Surv. Prof. Pap.*, 522, 1-153, 1967.
- Dokka, R. K., Displacements on late Cenozoic strike slip faults of the central Mojave Desert, California, *Geology*, 11, 305-308, 1983.
- Ehlig, P. L., Origin and tectonic history of the basement terrane of the San Gabriel

- Mountains, central Transverse Ranges, in *The geotectonic development of California: Rubey vol. 1*, edited by W. G. Ernst, pp. 253-283, Prentice-Hall, Englewood Cliffs, N. J., 1981.
- Ehlig, P. L., K. W. Ehlert, and B. M. Crowe, Offset of the upper Miocene Caliente and Mint Canyon Formations along the San Gabriel and San Andreas faults, in *San Andreas Fault in Southern California: A Guide to the San Andreas Fault From Mexico to Carrizo Plain*, edited by J. C. Crowell, *Calif. Div. Mines Geol., Spec. Rep.*, 118, 83-92, 1975.
- Foster, J. H., Late Cenozoic tectonic evolution of Cajon Valley, southern California, Ph.D. dissertation, 242 pp., Univ. of Calif., Riverside, 1980.
- Garfunkel, Z., Model for the late Cenozoic tectonic history of the Mojave Desert, California, *Geol. Soc. Am. Bull.*, 85, 1931-1944, 1974.
- Gillespie, A. R., Quaternary glaciation and tectonism in the southeastern Sierra Nevada, Inyo County, California, Ph.D. dissertation, 695 pp., Calif. Inst. of Technol., Pasadena, 1982.
- Golombek, M. P., Geometry and rate of extension across the Pajarito fault zone, Espanole basin, Rio Grande rift, northern New Mexico, *Geology*, 9, 21-24, 1981.
- Hadley, D. M., and H. Kanamori, Seismic structure of the Transverse Ranges, California, *Geol. Soc. Am. Bull.*, 88, 1461-1478, 1977.
- Hamblin, W. K., P. E. Damon, and W. B. Bull, Estimates of vertical crustal strain rates along the western margins of the Colorado Plateau, *Geology*, 9, 293-298, 1981.
- Hearn, T. M., Crustal structure in southern California from array data, Ph.D. dissertation, 130 pp., Calif. Inst. of Technol., Pasadena, 1984a.
- Hearn, T. M., P_n travel times in southern California, *J. Geophys. Res.*, 89, 1843-1855, 1984b.
- Hill, D. P., Contemporary block tectonics: California and Nevada, *J. Geophys. Res.*, 87, 5433-5450, 1982a.

- Hill, M. L., Anomalous trends of the San Andreas Fault in the Transverse Ranges, California, in *Geology and Mineral Wealth of the California Transverse Ranges: Hill volume*, edited by D. L. Fife and J. A. Minch, *South Coast Geol. Soc., Annu. Symp. Guideb. 10*, 367-369, 1982b.
- Hill, M. L., and T. W. Dibblee, Jr., San Andreas, Garlock and Big Pine faults, California - A study of the character, history, and tectonic significance of their displacement, *Geol. Soc. Am. Bull.*, *64*, 443-458, 1953.
- Huffman, O. F., Lateral displacement of upper Miocene rocks and Neogene history of offset along the San Andreas fault in central California, *Geol. Soc. Am. Bull.*, *83*, 2913-2946, 1972.
- Humphreys, E. D., Studies of the crust-mantle system beneath southern California, Ph.D. dissertation, 189 pp., Calif. Inst. of Technol., Pasadena, 1985.
- Humphreys, E., and B. H. Hager, Small-scale convection beneath southern California (abstract), *Eos, Trans. AGU*, *65*, 195, 1984.
- Humphreys, E., R. W. Clayton, and B. H. Hager, A tomographic image of mantle structure beneath southern California, *Geophys. Res. Lett.*, *11*, 625-627, 1984.
- Kennedy, M. P., Recency and character of faulting along the Elsinore fault zone in southern Riverside County, California, *Calif. Div. Mines Geol. Spec. Rep. 131*, 1-12, 1977.
- King N. E., Horizontal deformation in the Mojave Desert near Barstow, California, 1979-1983, *J. Geophys. Res.*, *90*, 4491-4494, 1985.
- Kosloff, D. D., Numerical models of crustal deformation, Ph.D. dissertation, 187 pp., Calif. Inst. of Technol., Pasadena, 1978.
- Luyendyk, B. P., M. J. Kamerling, and R. Terres, Geometric model for Neogene crustal rotations in southern California, *Geol. Soc. Am. Bull.*, *91*, 211-217, 1980.
- Matti, J. C., and D. M. Morton, Geologic history of the San Timoteo badlands, southern California, *Geol. Soc. Am. Abstr. Programs*, *7*, 344, 1975.

- Matti, J. C., J. C. Tinsley, D. M. Morton, and L. D. McFadden, Holocene faulting history as recorded by alluvial stratigraphy within the Cucamonga fault zone: A preliminary view, in *Late Quaternary Pedogenesis and Alluvial Stratigraphy Within the Cucamonga Fault Zone, Field Trip Guide #12*, edited by J. C. Tinsley et al., pp. 21-44, Cordilleran Section, Geological Society of America, Boulder, Colo., 1982.
- Minster, J. B., and T. H. Jordan, Present-day plate motions, *J. Geophys. Res.*, *83*, 5331-5354, 1978.
- Minster, J. B., and T. H. Jordan, Vector constraints on Quaternary deformation of the western United States east and west of the San Andreas Fault, in *Tectonics and Sedimentation Along the California Margin, vol. 38*, edited by J. K. Crouch and S. B. Bachman, pp. 1-16, Society of Economic Paleontologists and Mineralogists, Pacific Section, Los Angeles, Calif., 1984.
- Morton, D. M., and D. G. Herd, Earthquake hazards studies, Upper Santa Ana valley and adjacent areas, southern California, in *Summaries of Technical Reports, vol. IX, NEHRP, U. S. Geol. Surv. Open File Rep., 80-6*, 1-15, 1980.
- Morton, D. M., and J. C. Matti, Evidence for a vanished post-middle Miocene pre-late Pleistocene alluvial-fan complex in the northern Perris block, southern California, *Geol. Soc. Am. Abstr. Programs*, *11*, 118, 1979.
- Pinault, C. T., and T. K. Rockwell, Rates and sense of Holocene faulting on the Elsinore fault: Further constraints on the distribution of dextral shear between the Pacific and North American plates, *Geol. Soc. Am. Abstr. Programs*, *16*, 624, 1984.
- Powell, R. E., Geology of the crystalline basement complex, eastern Transverse Ranges, southern California: Constraints on regional tectonic interpretation, Ph.D. dissertation, 441 pp., Calif. Inst. of Technol., Pasadena, 1981.
- Rockwell, T. K., Soil chronology, geology and neotectonics of the north-central Ventura basin, California, Ph.D. dissertation, 424 pp., Univ. of Calif., Santa Barbara, 1983.
- Rockwell, T. K., E. A. Keller, M. N. Clark, and D. L. Johnston, Chronology and rates of

- faulting of Ventura River terraces, California, *Geol. Soc. Am. Bull.*, 95, 1406-1474, 1984.
- Sauber, J., and W. Thacher, Geodetic measurements of deformation in the central Mojave Desert, California (abstract), *Eos, Trans. AGU*, 65, 993, 1984.
- Savage, J. C., Strain accumulation in western United States, *Annu. Rev. Planet. Sci.*, 11, 11-43, 1983.
- Sharp, R. V., Variable rates of late Quaternary strike slip on the San Jacinto fault zone, southern California, *J. Geophys. Res.*, 86, 1754-1762, 1981.
- Sieh, K. E., and R. Jahns, Holocene activity of the San Andreas fault at Wallace Creek, California, *Geol. Soc. Am. Bull.*, 95, 883-896, 1984.
- Silver, L. T., Evidence and a model for west-directed early to mid-Cenozoic basement overthrusting in southern California, *Geol. Soc. Am. Abstr. Programs*, 14, 617, 1982.
- Webb, T. H., and H. Kanamori, Earthquake focal mechanisms in the eastern Transverse Ranges and San Emigdio Mountains, southern California and evidence for a regional decollement, *Bull. Seismol. Soc. Am.*, 75, 737-757, 1985.
- Weber, G. E., and K. R. Lajoie, Late Pleistocene and Holocene tectonics of the San Gregorio fault zone between Moss Beach and Point Ano Nuevo, San Mateo County, California, *Geol. Soc. Am. Abstr. Programs*, 9, 524, 1977.
- Weldon, R. J., Implications of the age and distribution of the late Cenozoic stratigraphy in Cajon Pass, southern California, in *San Andreas Fault - Cajon Pass to Wrightwood, Guideb. #55*, edited by R. L. Hester and D. E. Hallinger, pp. 9-16, American Association of Petroleum Geologists, Pacific Section, Los Angeles, Calif., 1984a.
- Weldon, R. J., Quaternary deformation due to the junction of the San Andreas and San Jacinto faults, southern California, *Geol. Soc. Am. Abstr. Programs* 16, 689, 1984b.
- Weldon, R. J., The late Cenozoic geology of Cajon Pass; Implications for tectonics and sedimentation along the San Andreas fault, Ph.D. dissertation, 382 pp., Calif. Inst. of Technol., Pasadena, 1985.

- Weldon, R. J., and K. E. Sieh, Holocene rate of slip and tentative recurrence interval for large earthquakes on the San Andreas fault in Cajon Pass, southern California, *Geol. Soc. Am. Bull.* 96, 793-812, 1985.
- Weldon, R. J., D. S. Winston, J. L. Kirschvink, and D. W. Burbank, Magnetic stratigraphy of the Crowder Formation, Cajon Pass, southern California, *Geol. Soc. Am. Abstr. Programs*, 16, 689, 1984.
- Wernicke, B., J. E. Spencer, B. C. Burchfiel, and P. L. Guth, Magnitude of crustal extension in the southern Great Basin, *Geology*, 10, 499-502, 1982.
- Yeats, R. S., Quaternary tectonics of the California Transverse Ranges, *Geology*, 9, 16-20, 1981.
- Yeats, R. S., Large scale Quaternary detachments in Ventura Basin, southern California, *J. Geophys. Res.*, 88, 569-583, 1983.
- Yeats, R. S., and B. U. Haq, Deep-sea drilling off the Californias: Implications of leg 63, *Initial Rep. Deep Sea Drill. Proj.*, 63, 949-961, 1981.
- Ziony, J. I., and R. F. Yerkes, Fault slip-rate estimation for the Los Angeles region: Challenges and opportunities (abstract), *Earthquake Notes, Eastern Section, Seismol. Soc. Am.*, 55, 8, 1984.
- Zoback, M. L., R. E. Anderson, and G. A. Thompson, Cenozoic evolution of the state of stress and style of tectonism of the Basin and Range province of western United States, *Philos. Trans. R. Soc. London, Ser. A* 300, 407-434, 1981.

CHAPTER SIX

**The Late-Cenozoic Tectonics of the
Northwestern San Bernardino Mountains,
Southern California¹**

Kristian E. Meisling

ARCO Resources Technology,
P. O. Box 2819, Dallas, Texas 75221

and

Ray J. Weldon²

U. S. Geological Survey, OEVE, MS 977,
345 Middlefield Rd., Menlo Park,
California, 94025

¹Work done at Division of Geological and Planetary Sciences, California Institute of Technology
Pasadena, California, 91125

²Also at Department of Geology, Occidental College, 1600 Campus Rd., Los Angeles,
California, 90041

ABSTRACT

Synthesis of structural and stratigraphic field data for the western San Bernardino Mountains documents a three-phase history of deformation and uplift on low-angle structures beneath the range. The distribution and nature of late Cenozoic sedimentary rocks and their relationship to key structural elements provide the basis for five interpretive paleotectonic reconstructions for the following selected time intervals: 17 to 9.5, 9.5 to 4.5, 4.5 to 2.0, 2.0 to 1.5, and 1.5 to 0.7 Ma. The resulting tectonic evolution suggests an intimate association of low-angle thrusting and strike slip deformation along the San Andreas fault, in which thrusts both deform and are cut and offset by the San Andreas fault.

Late Miocene to Early Pliocene thrusting disrupted southward drainage to the broad, homogeneous Miocene basins of the Crowder and Punchbowl Formations, uplifting their northern margin to form the ancestral San Bernardino Mountains. The Mio-Pliocene thrust system crossed the inactive San Andreas fault, emplacing the Liebre Mountain thrust at the northern margin of the Ridge basin while transform activity was concentrated on the San Gabriel fault to the southwest. The Phelan formation (informal) and Old Woman Sandstone, deposited in an east-west trending hinterland trough following Mio-Pliocene thrusting, are unconformably overlain by early Pleistocene conglomerates that record the rapid development of relief at the margins of the range. We propose that the flat north-central plateau of the San Bernardino Mountains was uplifted by north-directed movement

up a deep ramp, resulting in development of the north frontal thrust system, range front warps, and lateral tears and imbricates. In late Pleistocene time uplift shifted to a narrow zone adjacent to the San Andreas fault in the extreme western end of the range near Cajon Pass and the San Gorgonio Pass areas. This final phase of uplift is occurring on steep, north-dipping ramps, locally coincident with the deformed trace of the San Andreas fault itself.

INTRODUCTION

The San Bernardino Mountains are the principal topographic expression of the central Transverse Ranges east of the San Andreas fault (Figure 1). The northern San Bernardino Mountains are capped by a broad plateau that rises in elevation from the level of the Mojave Desert at its eastern and western ends to over 6000 feet in the center of the range. Along the northern range front, the plateau abruptly descends over 3000 feet to the floor of the Mojave Desert at Fifteenmile, Lucerne, and Johnson Valleys. South of the Santa Ana River, some of the highest peaks in southern California climb to 11,000 feet before dropping off precipitously into San Gorgonio Pass to the south. The San Bernardino Mountains abut the San Gabriel Mountains at Cajon Pass, together forming the divide between drainage internal to the Mojave Desert, and basins draining to the Pacific Ocean. The steep, youthful canyons of the range margins contrast sharply with the reduced, mature landforms of the central plateau, underscoring both the recency and rapidity of uplift in the San Bernardino Mountains.

The history of the San Bernardino Mountains has direct bearing on many of the key problems in relating the histories of the Transverse

Figure 6-1. Index map of southern California. Study area is shown in dashed line (Figure 2). Locations of major physiographic features and gross distribution of late Cenozoic sedimentary rocks are shown, in addition to locations discussed in text. Line of seismicity cross section (Figure 6-10) is shown at longitude of 117°W. (WCF) Wilson Creek Fault of Matti et al., (1985).

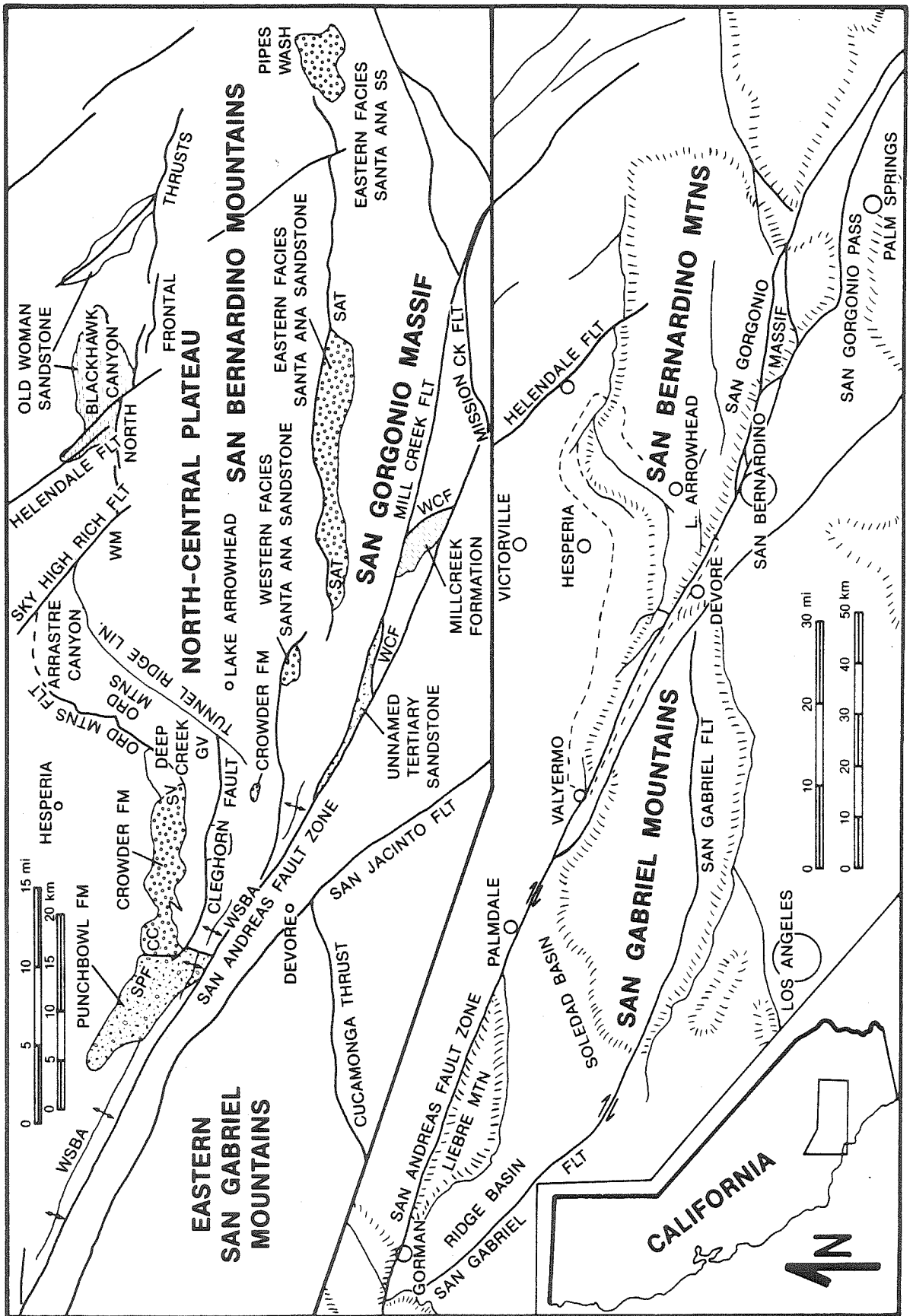


Figure 6-1

Ranges, San Andreas fault, and Mojave Desert. The origin and evolution of the Transverse Ranges Province and their relation to the history of the San Andreas fault have long been a subject of debate among those attempting to develop a coherent tectonic model for southern California. The youthful, physiographic expression of the Transverse Ranges trends obliquely to the prevailing northwest tectonic grain for several hundred kilometers, from the California coast to the Arizona border. A wide variety of models have been advanced for the structural evolution of the Transverse Ranges Province and its relation to the history of the San Andreas fault.

Large components of upward relief and thrusting have been invoked to alleviate inferred strain accumulation resulting from either different movement histories for the San Andreas fault north and south of the Transverse Ranges (Chinnery, 1965; Baird et al., 1974) or the change in trend of the San Andreas fault through the Transverse Ranges region (Bird and Rosenstock, 1984; Allen, 1968; Hill, 1982; Crowell, 1982, 1981). If this is the case, timing of uplift in the central Transverse Ranges should be closely tied to the timing of activity on the San Andreas fault.

Antipodal symmetry displayed by the frontal fault systems of the San Bernardino and San Gabriel Mountains led to the hypothesis that the entire Transverse Ranges province has been rotated up to 55 degrees about a central vertical axis (Garfunkel, 1974; Baird et al., 1974; Luyendyk et al., 1980, 1985). This model predicts large displacements on range front thrusts (Baird, et al., 1974). Based on paleomagnetic data, Kamerling and Luyendyk (1979, 1985) propose rotation of smaller blocks in a regional right-lateral shear couple. However, recent data

suggest little or no rotation in the area western San Bernardino Mountains (Weldon et al., 1984; Weldon, 1984; Winston, 1985) or in the Ridge Basin (Ensley and Verosub, 1982).

Sadler and Reeder (1983; also Sadler, 1982b) interpret the structure of the San Bernardino Mountains as a transpressional welt rooted beneath the long axis of the range. Antipodal symmetry of thrusting in the central Transverse Ranges has also been used to argue for a transpressional welt rooted in the San Andreas fault zone, which has subsequently been offset to form the San Gabriel and San Bernardino Ranges (Sadler, 1981). Transpressional welt models predict early fold development, rough contemporaneity of thrust development on both sides of the uplift, and extensional deformation along the axis of the uplift (Lowell, 1972; Sylvester and Smith, 1976; Bartlett et al., 1981).

Hadley and Kanamori (1977) advance a hypothesis in which the plate boundary in the upper mantle lies east of the crustal trace San Andreas fault in the region of the central Transverse Ranges. In this model, enhanced coupling across a low-angle discontinuity beneath the San Bernardino Mountains results in buckling of the crust to produce the Transverse Ranges. Yeats (1980, 1981) argues for a similar geometry in his proposal for "flake tectonics" in which the entire Mojave Desert is underlain by Pelona Schist or ductile granitic rocks beneath a regional detachment zone. Powell (1981) suggests that deformation in the southeastern Mojave could be occurring within a thin plate above a detachment.

Weldon and Humphreys (1985) propose a kinematic model, based on Quaternary slip rates and orientations of major faults in southern California, in which the region west of the southern San Andreas fault

is rotating counterclockwise relative to the North American plate. Their model may explain the presence of paleomagnetic rotations and thrusting the the western Transverse Ranges, as well as their absence in the central Transverse Ranges. A step in the curved trace of the San Andreas fault near San Geronio Pass is invoked to uplift the San Bernardino Mountains, not regional convergence through the central Transverse Ranges.

Clearly the above models have widely differing implications for the nature and history of deformation in the western San Bernardino Mountains. In this paper we will present field data on the spatial distribution and timing of deposition and deformation in the western San Bernardino Mountains in an effort to test and constrain model predictions.

TECTONIC EVOLUTION

The following tectonic synthesis is based on our detailed mapping of over 200 square miles in the western San Bernardino Mountains (Figure 2), as well as the fieldwork and thoughts of numerous others as referenced below. Structural and stratigraphic field evidence serve as the basis for a series of generalized paleotectonic reconstructions (Figures 4, 5, 6, 7, and 8) spanning selected periods of geologic time. Our reconstructions represent an interpretive history, subject to future refinement, that we hope will provide a basis for discussion and future study.

The late-Cenozoic stratigraphy is the primary key to the history, nature, and modes of deformation and uplift of the western San Bernardino Mountains (Figure 3). A regional early(?) Miocene

Figure 6-2. Simplified geologic map of the study area. (Tp) Punchbowl Formation, (Tc) Crowder Formation (Tph) Phelan formation, (Qhs) Harold Formation and Shoemaker Gravel, (Qoa) Older Alluvium, (Qya) Younger Alluvium, (Trs) Rock Springs Road deposits, (b) crystalline basement (1) San Andreas fault, (2) Squaw Peak thrust, (3) Cleghorn fault, (4) Cajon Valley fault, (5) Waterman Canyon Fault, (6) Tunnel Ridge lineament, (7) Ord Mountain frontal fault zone, (8) Sky High Ranch fault, (9) North frontal thrust system, (10) Western San Bernardino Arch, (V) Valyermo, (W) Wrightwood, (CP) Cajon Pass.



Geology by K. E. Meising and
R. J. Welton, 1981-1984

Figure 6-2

unconformity marks the base of the Cenozoic stratigraphic column in all but a few localities. Middle Miocene time is represented by the development of relatively large, homogeneous basins of the Punchbowl Formation in Cajon Valley and Crowder Formation in the westernmost San Bernardino Mountains. The Santa Ana Sandstone in the central and eastern part of the range may record the transition from the large, homogeneous Miocene basins to structurally controlled Plio-Pleistocene basins contemporaneous with the first phase of deformation and uplift in the San Bernardino Mountains. Widespread uplift of the ancestral San Bernardino Mountains in Pliocene time resulted in drainage disruption which led to the deposition of the Phelan formation (informal), and Old Woman Sandstone in a narrow east-west trending structural trough. Pleistocene deposits of the Victorville Fan record rapid uplift of the central and western San Bernardino Mountains, and the appearance of the San Gabriel Mountains as an important source of sediment across the San Andreas fault to the southwest.

A three-phase history of deformation in the San Bernardino Mountains block can be deduced from observed structural geometries and timing constraints imposed by the stratigraphic record. A late-Miocene to early-Pliocene south-directed thrust belt collapsed and uplifted the mid-Miocene basins, creating the ancestral San Bernardino Mountains and confining Pliocene deposition to the axes of structural troughs in its hinterland. Thrusting on the northern range front in early Pleistocene time led to a second phase of deformation, creating the northern escarpment and uplifting the northern plateau. In the third and final phase, southwest-directed thrusting produced arching and high-angle faulting along the San Andreas fault. These events are interpreted as

Figure 6-3. Stratigraphy, age and correlation chart for the late Cenozoic sedimentary rocks of the western San Bernardino Mountains. An Early Miocene unconformity occurs at the base of the Cenozoic section. Thick, homogeneous, continental basins of the Punchbowl and Crowder Formations, exposed in the western part of the study area, are unconformably overlain by the more restricted Plio-Pleistocene basins of the Phelan Formation and Old Woman Sandstone, which were deposited in the hinterland of the Squaw Peak thrust system. The Rock Springs Road deposits suggest that the Phelan and Old Woman depositional troughs may have once been continuous. The Plio-Pleistocene basins are unconformably overlain by the alluvial fanglomerates of the Harold Formation, Shoemaker Gravel, Older Alluvium, Ord River Gravel, Arrastre Canyon fan and Cushenbury Springs Formation which record the appearance of the San Gabriel Mountains crystalline source terrane along the San Andreas fault, and the uplift of the San Bernardino Mountains plateau. These alluvial units display local clast provenance, but form a continuous depositional package around the northern margin of the central Transverse Ranges. They share a common origin as the products of vigorous Quaternary uplift and tectonism. Sources of age data include: (m) magnetostratigraphy, (f) vertebrate fossils, and (r) fission-track data on tuff (see text for references). Thicknesses shown are local maximum values as all units are highly variable in thickness.

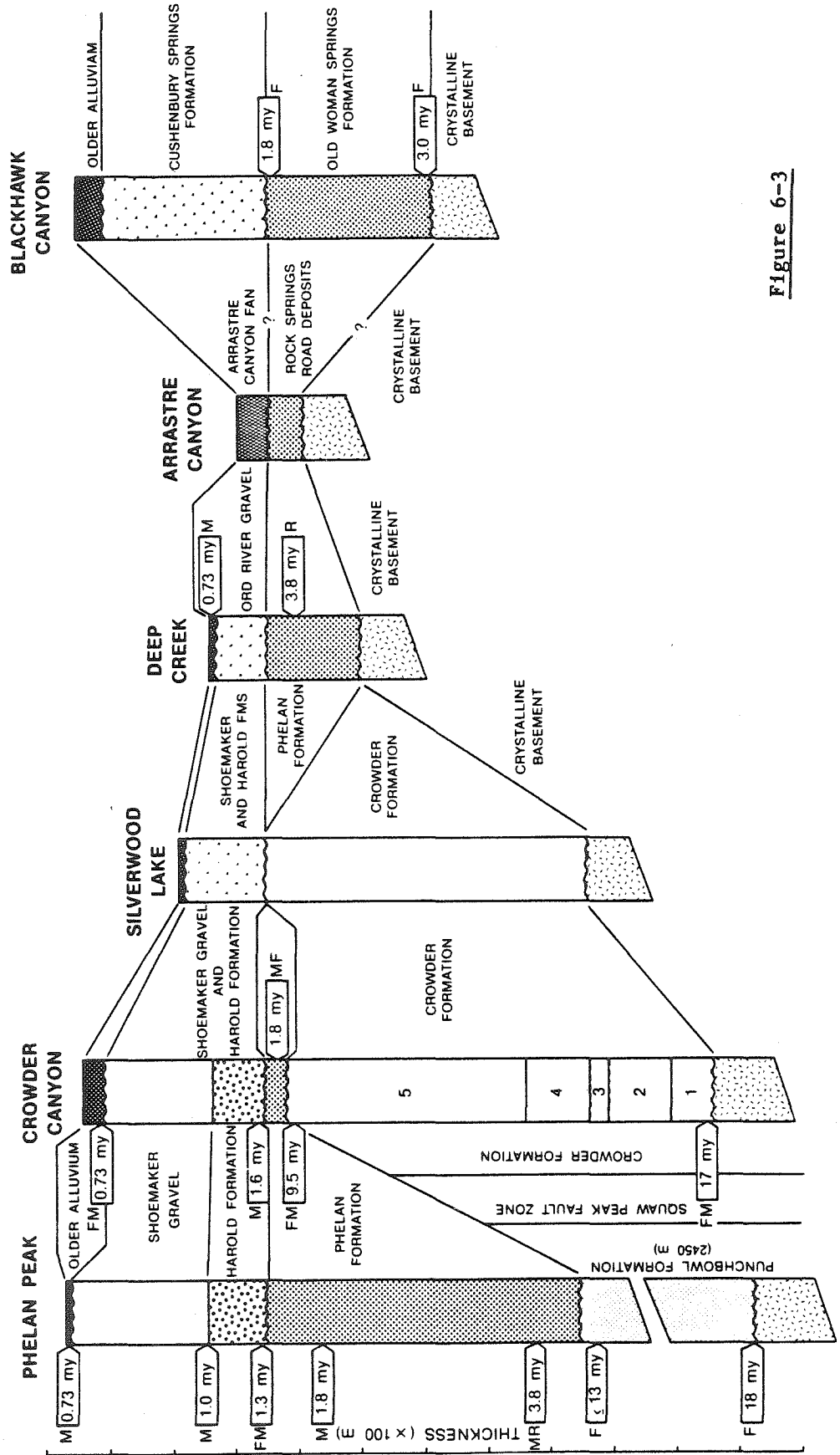


Figure 6-3

the surface expression of repeated reactivation of low-angle structures formed during the early Cenozoic.

The Pre-Middle-Miocene Weathering Surface

In early(?) Miocene time the western San Bernardino Mountains area was the site of a mature landscape of rolling hills underlain by subaerially weathered crystalline basement rocks (Noble, 1954b; Woodburne and Golz, 1972; Weldon et al., 1981). The exhumed bedrock-soil interface of this low-relief surface can be traced to laterally extensive Miocene weathering horizons developed throughout the central and eastern San Bernardino Mountains and southern Mojave Desert (Mendenhall, 1905; Vaughan, 1922; Blackwelder, 1925; Oberlander, 1972; Sadler and Reeder, 1983). Although the low-relief surface is a composite feature representing several cycles of erosion and weathering (Vaughan, 1922), it is essentially flat over much of the central part of the range (Sadler, 1982a) and has been deformed along the edges. The surface serves as a crude structural surface for delineating structural deformation of basement rocks on the margins of the range where sedimentary cover is absent (Meisling, 1984; Sadler and Reeder, 1983). Any uplift mechanism for the San Bernardino Mountains must explain the remarkable lack of deformation of this elevated surface, particularly in the west-central San Bernardino Mountains. This same surface is probably represented by the unconformity between the Punchbowl Formation and underlying Vaqueros Formation in Cajon Pass (Woodburne and Golz, 1972).

Miocene Basins

The oldest sedimentary rocks deposited on the weathering surface are middle-Miocene continental arkoses and conglomerates of the Punchbowl and Crowder Formations in the western San Bernardino Mountains, and the middle to late Miocene Santa Ana Sandstone in the central and eastern San Bernardino Mountains (Figure 4). Distribution and thickness of the Miocene units suggest that the San Bernardino Mountains block was the site of an extensive middle Miocene system of basins. Clast studies in Miocene units establish southward transport paths from nearby crystalline and volcanic terranes in the Mojave block, placing an effective northern limit on the basin margin. Although the original geographic relationship between the extensive and long-lived Miocene basins has been obscured by later deformation, obvious differences in character and provenance between the Miocene basins suggest that they were probably physically separate systems.

The Crowder Formation

Fluvial sandstone and conglomerate of the Crowder Formation (Figure 3) were deposited on the early-Miocene(?) surface by southward-flowing braided streams crossing a broad alluvial plain (Foster, 1979, 1980, 1982) that covered much of the westernmost San Bernardino Mountains (Dibblee, 1965a, 1965b, 1967; Meisling and Weldon, 1982b). Distinctive clast lithologies and paleocurrent indicators in the Crowder Formation reflect southerly drainage from volcanic, metamorphic, and plutonic source areas near Victorville (Foster, 1980). Mammalian fauna (Reynolds, 1984) and magnetostratigraphic data (Weldon et al., 1984; Winston, 1985) show that the Crowder Formation was deposited in late-Early to early-Late Miocene time, between 17 and 9.5

Figure 6-4. Interpretive paleotectonic reconstruction of the western San Bernardino Mountains: 17 to 9.5 Ma (Late Early Miocene to Early Late Miocene). The Crowder Formation was deposited on an early Miocene weathered erosion surface of low relief by southward-flowing drainages carrying clasts derived from exposed volcanic and granitic terranes to the northeast. The weathered surface was widely exposed throughout the San Bernardino Mountains and Mojave blocks. The western facies of the Santa Ana Sandstone may represent a similar, yet separate basin to the east. Motion on the San Andreas fault began during this time period. Towns of Hesperia (H) , Lake Arrowhead (A), and Devore (D) are shown for reference. Block margins trend north-south and east-west, and vertical scale equals horizontal scale. Features are shown in their present geographic location since data are inadequate to allow palinspastic restoration of most structural offsets. Events occurring within each time slice are grouped for illustrative purposes, and are therefore not perfectly contemporaneous.

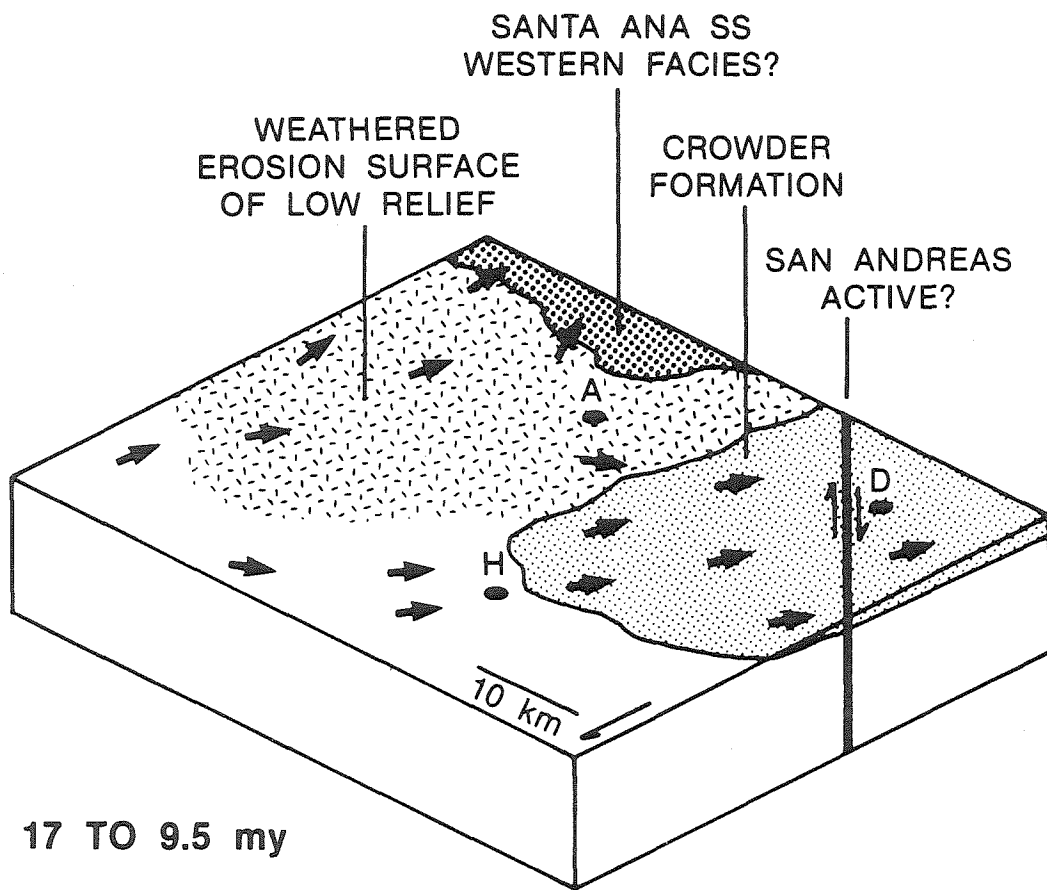


Figure 6-4

Ma.

The original geometry and extent of the Crowder Formation are not known, but lithologic similarity of remnants preserved throughout the western San Bernardino Mountains (Figure 2) argues for a large, continuous, homogeneous basin (Figure 4). The Crowder Formation is not found east of Lake Arrowhead. There, Sadler and Reeder (1983) report a discontinuous mantle of quartzite cobbles which they propose are contemporaneous with the Crowder Formation, indicating an area of low relief and little sedimentation. The edge of the San Bernardino plateau and the Tunnel Ridge lineament coincide with the limit of Crowder deposition.

The upper Crowder Formation was divided into a western and eastern facies by Foster (1980). Magnetostratigraphic studies, however, reveal that Foster's western facies is Pliocene in age (Weldon, 1984), and it has since been informally renamed the "Phelan formation". Middle Pliocene volcanogenic sediments in east Summit Valley are now correlated with the Phelan formation rather than with the upper Crowder Formation (cf. Foster, 1980, 1982; Meisling and Weldon, 1982; Meisling, 1984).

The Cajon Beds of the Punchbowl Formation

Non-marine sandstone and conglomerate of the Cajon beds of the Punchbowl Formation (Figure 3; Noble, 1954b; Dibblee, 1967), extensively exposed in Cajon Valley (Figure 2), were deposited by southwest-flowing streams (Woodburne and Golz, 1972), with sources in granitic and volcanic terranes to the northeast, characteristic of the Mojave block (Robinson and Woodburne, 1971). The uniformity of

lithologic character and long depositional history of the Cajon beds implies deposition in a basin of considerable size. The informal term "Cajon beds" is used to emphasize important differences in lithology, fossil age, and geologic history between the Cajon Valley exposures and the type locality of the Punchbowl Formation south of the San Andreas fault near Pearblossom (Noble, 1954b; Woodburne and Golz, 1972).

The Cajon beds are assigned an age of middle-to-late Miocene (18 to 13 Ma) based on mammalian fauna (Woodburne and Golz, 1972). They overlie an Early Miocene unconformity and overlap in age with the Crowder Formation. Because the upper part of the Cajon beds (part of unit 5 and all of 6, Woodburne and Golz, 1972) has not been dated, the upper age limit of the Cajon beds is simply pre-early-Pliocene based on the unconformable contact with the overlying basal Phelan formation. The Crowder and Punchbowl Formations may be entirely contemporaneous.

The variations in the Cajon beds of the Punchbowl Formation, represented by its subdivision into six members, appear to encompass the entire basin. Distinctive members, such as the hogsback-forming member 2, red-bed member 3, variegated member 5, and the unusual volcanic and red sandstone clast suite of member 6, are laterally extensive and probably represent basin-wide variations in sediment source and depositional environment. Only member 5a (as defined by Woodburne and Golz, 1972) and member 4 occur only locally, and may be lateral facies of the more widespread member 5. This is in contrast to the type Punchbowl Formation where differences represent lateral variations along a long narrow trough. This trough was almost certainly a strike-slip rift, probably in the early San Andreas fault. In contrast, the Punchbowl Formation in Cajon Pass was deposited in a broad, homogeneous basin.

The Santa Ana Sandstone

The conglomerate, sandstone, and shale of the Santa Ana Sandstone are exposed discontinuously from south of Lake Arrowhead (Figure 1) to Pipes Wash (Sadler, 1982; Sadler and Reeder, 1983; Vaughan, 1922; Dibblee, 1964b). Rounded volcanic clasts in the conglomerate facies of the eastern Santa Ana Sandstone were derived from the Mojave block to the north, implying southward drainage across the north central San Bernardino Mountains block in Miocene time (Figure 4; Sadler and Reeder, 1983). Rounded quartzite clasts, derived from the Delamar Mountain area, suggest the existence of local relief to the north (Sadler and Reeder, 1983). Rapid facies changes and wide lithologic variation suggest that exposed rocks may have been deposited near the basin margin or in an active tectonic setting. This impression is strengthened by the extensive preservation of thin gravel veneers and soil profiles in the central and eastern San Bernardino Mountains. The southern extent of the Santa Ana basin is not known.

The Santa Ana Sandstone is, in part, late Miocene age, based on K-Ar ages on basalts correlated with those overlying the eastern facies (8.2 ± 0.5 and 8.9 ± 0.9 Ma, Oberlander, 1972; Sadler, 1981; Neville and Chambers, 1982) and basalts interbedded with the central facies (6.2 Ma, Woodburne, 1975). The western facies is postulated to be younger by Strathouse (1983), but preliminary fossil data suggest that it may, in fact, be older (Reynolds, pers. comm., 1984). We postulate that the western facies of the Santa Ana Sandstone is contemporaneous with the Crowder Formation (Figure 4), based on the similarity of structural and stratigraphic setting near Lake Arrowhead.

Our paleotectonic reconstruction suggests that the Santa Ana

Sandstone may record the transition in depositional regime between the relatively broad late-Miocene basins, and narrower, structurally controlled Pliocene basins. The lacustrine and volcanogenic parts of the formation might have been confined to an intra-montane or foreland trough by an early phase of Mio-Pliocene thrusting and uplift of the ancestral San Bernardino Mountains, which greatly modified the Miocene basin geometry.

Late Miocene to Early Pliocene Thrusting

On the basis of structural relationships in the western San Bernardino Mountains, we propose a regional Mio-Pliocene thrusting event, perhaps localized along the margins of the Miocene basins (Figure 5). This thrusting event created the relief that led to the structural troughs, local clast provenance, and drainage disruption that characterize the Pliocene basins. We believe that this thrusting placed San Bernardino Mountains basement across an early branch of the San Andreas system, and was contemporaneous with movement on the San Gabriel fault (Crowell, 1982). Matti et al. (1985a, b) propose that the Liebre Mountains are offset from the San Bernardino Mountains. We propose that the Liebre Mountain thrust is the toe of the Mio-Pliocene thrusting in the San Bernardino Mountains that has since been displaced 160 kilometers by the modern San Andreas fault.

The Squaw Peak Fault

The lower parts of the Cajon beds and Crowder Formation are essentially the same age (Figure 3; Weldon, 1984; Reynolds, 1984; Weldon et al., 1984; Winston, 1985), yet they differ markedly in

Figure 6-5. Interpretive paleotectonic reconstruction of the western San Bernardino Mountains: 9.5 to 4.5 Ma (Early Late Miocene to Early Pliocene). The early Miocene weathered erosion surface and overlying basins were uplifted to form the ancestral San Bernardino Mountains by motion on the Squaw Peak thrust and related structures. The upper plate of the Squaw Peak thrust system, which rooted in the Mojave block to the north, developed moderate relief due to offsets on numerous north-dipping reverse faults. The Squaw Peak thrust system overrode the inactive trace of the San Andreas fault, transferring about a 60-km-long flap of San Bernardino Mountains lithologies to the southwest side of the fault zone.

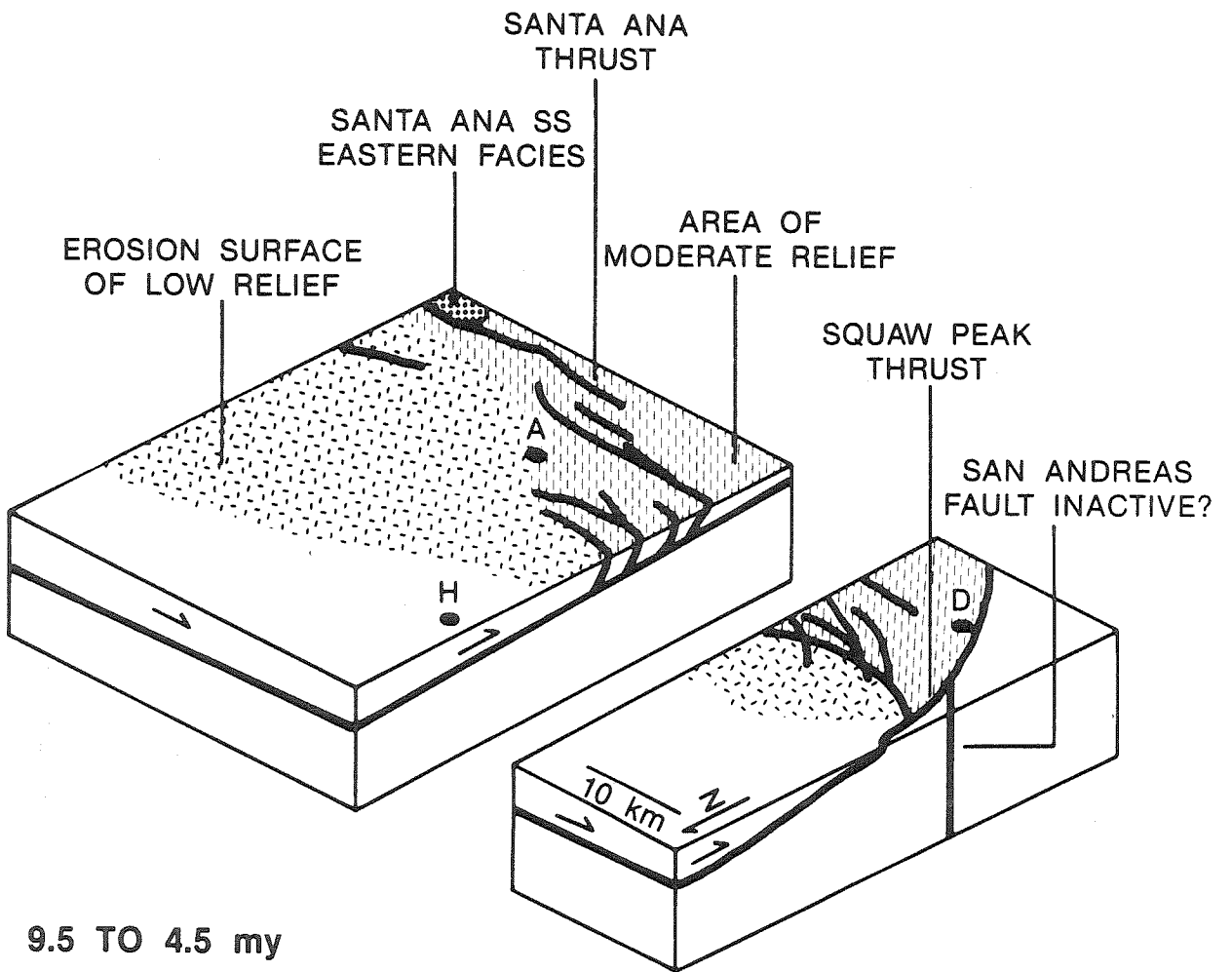


Figure 6-5

provenance and character (Woodburne and Golz, 1972; Foster, 1980, 1982). Although they could represent different parts of the same basin, the juxtaposition of these two distinctly different Miocene depositional packages argues for significant displacement on the Squaw Peak fault (Figure 3; Weldon, 1984; Meisling, 1984). Furthermore, facies relationships in the Crowder Formation indicate that the center of the basin lay to the west of the Squaw Peak fault (Foster, 1980; Weldon, 1984), suggesting that a large part of the basin is missing.

Weldon (1984) initially proposed that the Squaw Peak fault might be an abandoned strand of the San Andreas system, with abrupt changes in trend producing the intense deformation along its trace. Paleomagnetic fold tests on folded Crowder sediments within the Squaw Peak fault zone, however, showed no evidence of the rotation about a vertical axis expected for major strike-slip deformation. In fact, none of the paleomagnetic samples collected in the Crowder Formation display appreciable tectonic rotation (Weldon et al., 1984). We observe that the bedding-parallel attitude and low-angle secondary structures along the Squaw Peak fault (Weldon, 1984) are much more consistent with thrust-style deformation, and propose that the Squaw Peak fault is a late-Miocene or early-Pliocene thrust fault. The variation in styles of deformation can be understood in terms of changes in trend along the fault with the high angle portions being tears in the low angle fault. Our interpretation of the Squaw Peak fault as a thrust has major implications for late Miocene deformation in the western San Bernardino Mountains, and southern California.

The Cedar Springs Reverse Fault System

The regional importance of the Squaw Peak fault is underscored by the structural features in the westernmost San Bernardino Mountains, which appear to be related to the Squaw Peak fault in both structural style and timing. A set of north-plunging, east-block-down monoclines and a crosscutting system of curved, south-block-down reverse faults that are developed throughout the westernmost San Bernardino Mountains (Figure 2; Cedar Springs system of Meisling and Weldon, 1982) are not found west of the Squaw Peak fault. Forced folds contemporaneous with the reverse faults are deformed by a large syncline within the Crowder Formation along the Squaw Peak fault (Weldon, 1984; cf. Foster, 1980).

These relations suggest that widespread reverse faulting occurred during or before motion on the Squaw Peak fault. The large syncline strongly resembles the asymmetric, north-plunging monoclines near Silverwood Lake to the east, but these monoclines are clearly cut by the same set of reverse faults (Meisling and Weldon, 1982), in disagreement with the cross-cutting relationships observed in Cajon Pass. The apparent conflict in timing of these structures can be explained if the north-plunging monoclines, reverse faults, and Squaw Peak fault were all part of the same deformational event, related to movement on the Squaw Peak fault.

The Proposed Squaw Peak Thrust System

The late Miocene to earliest Pliocene structures in the western San Bernardino Mountains can now be understood in the context of a thrust model (Figures 2 and 5). The reverse fault system is interpreted as a set of minor thrust imbricates in the upper plate of the Squaw Peak system. The curvature and southward vergence of these imbricates is

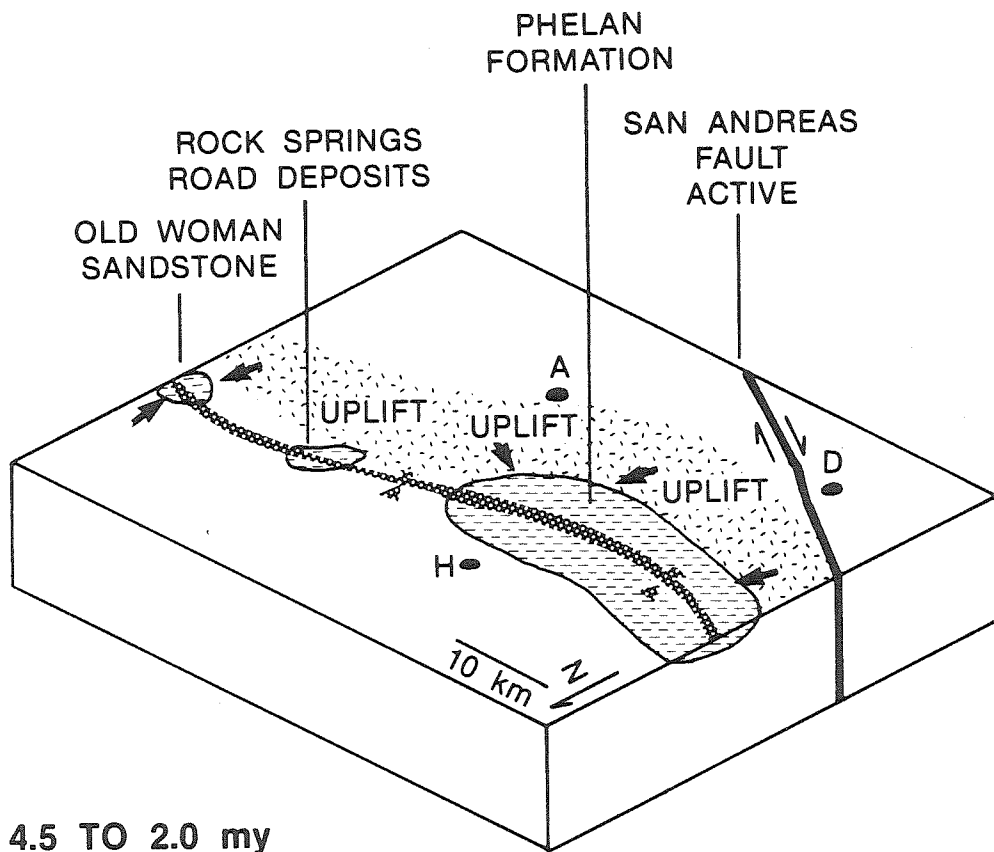
consistent with deformation within the upper plate of a south/southwest-directed thrust. We interpret the Santa Ana thrust (Sadler, 1981, 1982) and Bear Creek thrust (Stout, 1979) as the eastern extension of this zone of upperplate imbricates. This system is herein named the Squaw Peak thrust system. Thrust faults south of San Gorgonio Peak, such as the Mill Creek fault, Mission Creek fault, and Banning fault, show evidence of significant Pliocene motion (Allen, 1957), and juxtapose rocks of exotic and San Bernardino Mountains affinities (Matti et al., 1985). We believe that they could be all part of the Squaw Peak system.

The proposed Squaw Peak thrust system postdates the deposition of the upper Crowder Formation (9.5 Ma), which it deforms, and predates deposition of the basal Phelan formation (4 Ma), which appears to be undisturbed. Motion on the proposed thrust should have been contemporaneous with motion in the Santa Ana thrust (Sadler and Reeder, 1983) and the Waterman Canyon fault. The Santa Ana thrust is younger than 6 Ma old (Strathouse, 1982). Motion on the Squaw Peak fault is therefore tentatively constrained to be between 6 and 4 Ma.

Early Pliocene to Early Pleistocene Basins

A marked change in depositional patterns throughout the western San Bernardino Mountains is reflected in the Pliocene and early Pleistocene rocks of the Old Woman Sandstone, Phelan formation, and possibly the eastern Santa Ana Sandstone (Figures 3 and 6). Deposition appears to have been confined a narrow east-west to northwest-southeast trending, structurally controlled troughs (Weldon, 1984; Sadler and Reeder, 1983; Sadler, 1981, 1982b). Strata deposited in these troughs

Figure 6-6. Interpretive paleotectonic reconstruction of the western San Bernardino Mountains: 4.5 to 2.0 Ma (Early Pliocene to Late Pliocene). Relief attributed to the Squaw Peak thrust system disrupted Miocene drainage patterns, leading to deposition of the Phelan formation, and Old Woman Sandstone in a trough behind the thrust system. This east-west trending trough may have been continuous across the northern study area, based on the proposed correlation of the Rock Springs Road deposits. Uplift south of the trough is evidenced by local clast affinities in the Phelan formation and Old Woman Sandstone. This uplift may have been an early expression of northward motion on a deep crustal ramp, or residual relief related to the Squaw Peak thrust system.



4.5 TO 2.0 my

Figure 6-6

are characterized by distinctive fine-grained facies, volcanogenic components, and rapid facies and thickness variations (Shreve, 1968; Sadler and Reeder, 1983; Weldon, 1984; Meisling and Weldon, 1982; Meisling, 1984; Sadler, 1982). These characteristics are believed to be the result of tectonic disruption of Miocene drainage patterns during the Mio-Pliocene uplift of the ancestral San Bernardino Mountains (Figure 6; Sadler, 1981, 1982b; Meisling, 1984).

The Phelan Formation (Informal)

The informal name "Phelan formation" is proposed for distinctive Pliocene sedimentary rocks exposed between Summit Valley and Valyermo (Figure 2; Weldon, 1984; Meisling and Weldon, 1982; Meisling, 1984). These rocks, which overlie the major structural unconformity associated with deformation on the Squaw Peak fault system (Figure 3), are generally medium-grained pebbly sands, with locally significant volcanogenic and lacustrine components. Coarse conglomerates testify to the existence of substantial local relief. Distribution and lithologic characteristics of the Phelan formation are most consistent with deposition in a narrow north-west-southeast structurally controlled trough (Figure 6; Weldon, 1984; Foster, 1980). Deposition of the Phelan formation spans the period of time during which drainage in the western San Bernardino Mountains underwent a complete reversal in direction from southerly flow in the Crowder Formation to northerly flow in the Victorville Fan Complex. Thus the Phelan formation is interpreted as the product of drainage diversion and ponding reflecting the topographic expression of thrusting on the Squaw Peak system.

Rocks assigned to the Phelan formation were first correlated with

the upper Crowder Formation (Foster, 1980; Meisling and Weldon, 1982; Meisling, 1984) until magnetostratigraphic data established a clear difference in age (Weldon et al., 1984; Weldon, 1984)). The eastern facies of the Phelan formation contains interbedded tuffs dated at 3.8 ± 0.4 Ma (C. F. Naeser, written comm., 1981, 1982). Western exposures of the Phelan formation were deposited between ~ 4.1 and ~ 1.5 Ma, based on magnetostratigraphic polarity zonation (Weldon, 1984). We note the striking similarity in age and origin between the Phelan formation and the Old Woman Sandstone to the east (Figure 3).

The Old Woman Sandstone

The first evidence of pronounced relief along the northern range front is found in the Old Woman Sandstone (Dibblee, 1964a, 1967; Shreve, 1968; Sadler, 1981, 1982). The sudden appearance of clasts derived from San Bernardino Mountains in the Cushenbury Formation (Figure 3; Shreve, 1968; o2 of Sadler, 1981) signals the development of frontal thrusts. The Old Woman Sandstone is thought to have been deposited in a narrow, downwarped "moat" peripheral to the ancestral San Bernardino Mountains (Figure 6; Sadler, 1982b). Incipient uplift of the San Bernardino Mountains may also have obstructed southward-flowing Miocene drainage systems, leading to sediment ponding. Distinctive clasts in the upper Old Woman Sandstone record an abrupt change from Mojave to San Bernardino Mountains source area (Sadler, 1982b), indicating the rapid emergence of range front relief. Mammalian fossil assemblages extracted from the Old Woman Sandstone indicate an age of about 3.0 to 2.0 Ma (May and Repenning, 1982). We take the onset of thrusting, as indicated by appearance of the

Cushenbury Formation above the Old Woman Sandstone, to be about 2.0 Ma.

Sadler (1982b) suggests that the trough occupied by the Old Woman Sandstone may have been connected with the Phelan basin. A small exposure of fine-grained sediment in Arrastre Canyon (Figure 3; Rock Springs Road deposit of Meisling, 1984) may support Sadler's hypothesis (Figure 6). These sediments, which are tilted and faulted along the Tunnel Ridge lineament (Meisling, 1984), are paleomagnetically reversed (>0.73 Ma old) and therefore could have been contemporaneous with the Phelan Formation and Old Woman Sandstone (Meisling, 1984).

The Santa Ana Sandstone

Sadler and Reeder (1983) conclude that the Santa Ana Sandstone was deposited in an elongate intramontane depression that preceded south-directed thrusting on the Santa Ana thrust, noting similarities with the Old Woman Sandstone on the northern range front. The eastern facies of the Santa Ana Sandstone may have occupied an east-west trending, structurally controlled depression prior to thrusting (Figure 6); however, this depression is at least 3 Ma older than the Old Woman trough, and therefore is more likely due to the Mio-Pliocene thrusting event.

Pleistocene Thrusting

The prominent north frontal escarpment of the San Bernardino Mountains developed by thrusting in early-to-middle Pleistocene time, as recorded by the influx of coarse, angular clastic debris onto the Pliocene basins. North frontal thrusting extended from Summit Valley

to Old Woman Springs (Figure 7). Motion on the thrust system decreased dramatically in late Pleistocene time, giving way to high-angle range-front faulting.

Geometry of the Thrust System

A number of major thrust faults collectively contributed to the development of pronounced relief along the north range front, including the Santa Fe and Voorheis thrusts of Woodford and Harris (1928); Grapevine thrust of Shreve (1968), White Mountain system of Meisling (1984; see also Sadler, 1981), and Apple Valley Highlands-Deep Creek fault zone of Meisling (1984). Total shortening on the range front thrust system is probably not more than a few kilometers (2-3 km, Baird et al., 1974; 4000+ feet, Shreve, 1968, pl. 1), and thrust displacement decreases westward and eastward from the central range front as evidenced by a systematic decrease in range-front relief. The exhumed Miocene(?) weathering surface descends northward from Lake Arrowhead to Fifteenmile Valley and westward from White Mountain to Arrastre Canyon, defining a gentle western ramp similar to the eastern ramp between Old Woman Springs and Pipes Wash (Figure 2).

The frontal thrust system takes an abrupt 90° bend at the Ord Mountains, and trends roughly north-south between the Apple Valley Highlands and Deep Creek (Figure 2). We infer that displacement on the frontal thrusts was being transferred to a lateral ramp or tear fault (Meisling, 1984) localized along the trend of the Tunnel Ridge lineament and Ord Mountains frontal system. A similar southward bend is reported by Sadler (1981, 1982b) at the east end of the range. By analogy, a similar ramp structure may exist beneath the eastern end of

Figure 6-7. Interpretive paleotectonic reconstruction of the western San Bernardino Mountains: 2.0 to 1.5 Ma (Early Pleistocene). A sudden pulse of uplift is recorded in alluvial fan conglomerates bordering the San Bernardino Mountains. The uplift of the flat north central plateau is ascribed to northward motion on a deep detachment ramp which is inferred to have merged with a detachment within the Mojave block. Range front relief was created on north frontal thrusts, lateral ramp structures, and major warps marginal to the range. The role of lateral motion on the Cleghorn fault is not well understood. Deposition continued in the Phelan basin, receding to the west.

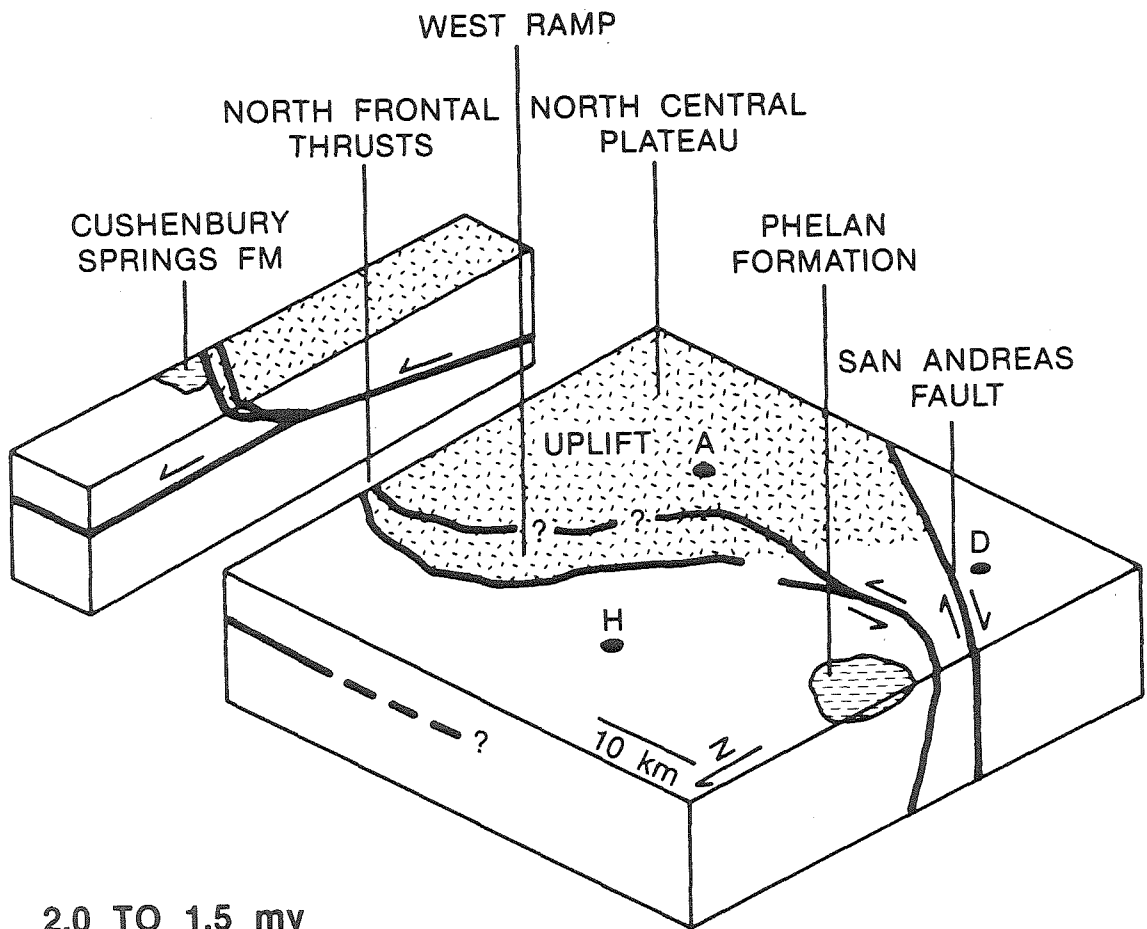


Figure 6-7

the range, near Pipes Wash.

The system becomes quite complex between Deep Creek and Silverwood Lake (Figure 2). At Deep Creek, a reverse fault exposed in the abutment of Deep Creek Dam (U.S. Army Corps of Engineers, 1982; Leighton and Associates, 1984) juxtaposes basement and Phelan formation, and dips 45° to the east. Although the range front system is cut by a later system of high-angle east-west trending faults just south of Deep Creek, range front relief decreases from a few hundred meters to nothing as the thrust system turns west through another 90° bend and dies out at Silverwood Lake. No north-block-down faults are evident west of the Cedar Springs Dam. Although the geometry and timing of this complex knot is not well understood, it appears that major Quaternary reverse faulting did not extend beyond Deep Creek.

Range-front warping followed the first phase of range front thrusting. In Blackhawk Canyon, the Santa Fe and Voorheis thrusts are deformed into a northeast-block down, northwest-trending monocline, with dips reaching 85° NE in the Old Woman Sandstone (Shreve, 1968). Although thrusts generally dip south along the range front (Shreve, 1968, pl. 1), surfaces are commonly observed to roll over and dip northward (Meisling, 1984; Sadler, 1981). Large landslides are common where thrusts have been warped and are dipping parallel to range-front slope (Shreve, 1959, 1968). The Miocene(?) surface is warped into a range-front monocline at Arrastre Canyon (Figure 2), Grapevine Canyon, and east of Lovelace Canyon (Meisling, 1984). Range-front warping is observed at Grass Valley, south of Deep Creek (Meisling, 1984), and warping may simply not be recognized in other areas due to the lack of suitable reference horizons. This warping is an important part of the

range-front relief and needs to be addressed in any model for uplift of the mountains.

Constraints on Timing of Thrusting

Thrusting on the northern range front began in early Pleistocene time (Vaughan, 1922, Woodford and Harris, 1928; Shreve, 1968; Sadler, 1981, 1982b), as deduced from the dramatic change in provenance, texture, and sorting from the Plio-Pleistocene Old Woman Sandstone to early Pleistocene marble conglomerates (Cushenbury Springs Formation of Shreve, 1968; o2 of Sadler, 1981), both of which are overridden by the range-front thrusts (Richmond, 1960; Sadler, 1981). The youngest facies of the Old Woman Sandstone has been dated at about 2.0 Ma by May and Repenning (1982), based on mammalian fauna.

At the foot of the Ord Mountains, early range-front sediments (Ord River Gravels of Meisling, 1984) also display an abrupt textural change and influx of distinctive range front lithologies, signaling the presence of range-front relief reflecting local uplift. The fluvial sand and conglomerate of the Ord River Gravels contain gneiss, quartz-monzonite, and occasional volcanic porphyries derived from the west-central San Bernardino Mountains, while the conformably overlying coarser and more angular conglomerates are almost exclusively composed of quartzite clasts derived from the immediately adjacent Ord Mountains metamorphic pendant (Figure 3; Meisling, 1984).

The Ord River Gravels are paleomagnetically reversed (Meisling, 1984). The sequence was therefore deposited prior to the Brunhes/Matuyama polarity reversal of 0.73 Ma. Furthermore, the sequence unconformably overlies the Pliocene Phelan formation at Deep

Creek Dam (U.S. Army Corps of Engineers, 1982), limiting the age to be less than 3.8 ± 0.4 Ma. While the Phelan formation consistently dips 25° northward on the north flank of the western San Bernardino Arch (Figure 2), the Ord River Gravels in Summit Valley dip 10° or less, indicating that they largely postdate arch development, estimated at ~ 1.5 Ma. We therefore postulate that range-front uplift in the Ord Mountains began in early-to-middle Pleistocene time, concurrent with thrusting on the northern range front to the east.

Late Pleistocene alluvial fans at the foot of the Ord Mountains and along the northern range front were apparently deposited in the waning stages of uplift, since they are either undisturbed or only slightly displaced by thrusts (Qf2 and Qf3 of Meisling, 1984). Although the precise age of these fans is not known, incision, surface weathering, range-front embayment, and offset on later strike-slip faults argue for deposition during the late Pleistocene (Meisling, 1984). It appears that thrusting and uplift on the northern range front occurred in a sudden pulse in early-to-middle Pleistocene time (Meisling, 1984, Fig. 2), and has since decreased dramatically.

The Pleistocene Victorville Fan Complex

Quaternary sedimentary rocks on the north flank of the westernmost San Bernardino Mountains signal yet another fundamental change in drainage regimen. The Harold Formation, Shoemaker Gravel, and Older Alluvium, known informally as the "Victorville Fan Complex" (Figure 8), contain the first appearance of distinctive clasts of the San Gabriel Mountains crystalline basement lithologies in the stratigraphy of the western San Bernardino Mountains and western Mojave blocks (Noble,

Figure 6-8. Interpretive paleotectonic reconstruction of the western San Bernardino Mountains: 1.5 to 0.7 Ma (Middle-to-Late Pleistocene). A dramatic decrease in rates of uplift on the northern range front accompanied a shift of the locus of uplift to the south and west side of the range. New deformational patterns include the northwestwardly migrating San Bernardino Arch, interpreted to be the result of deformation of the San Andreas fault at depth by the San Jacinto/Cucamonga structural knot, and the rapid uplift of the San Gorgonio massif on a steep north-dipping ramp that overrode the San Andreas fault in San Gorgonio Pass (see Figure 9d). The San Gabriel Mountains crystalline terrane, brought in along the San Andreas fault, becomes a dominant sediment source, depositing the Harold Formation and Shoemaker Gravel of the Victorville Fan Complex, while the Ord River Gravel records uplift on the western San Bernardino Mountains.

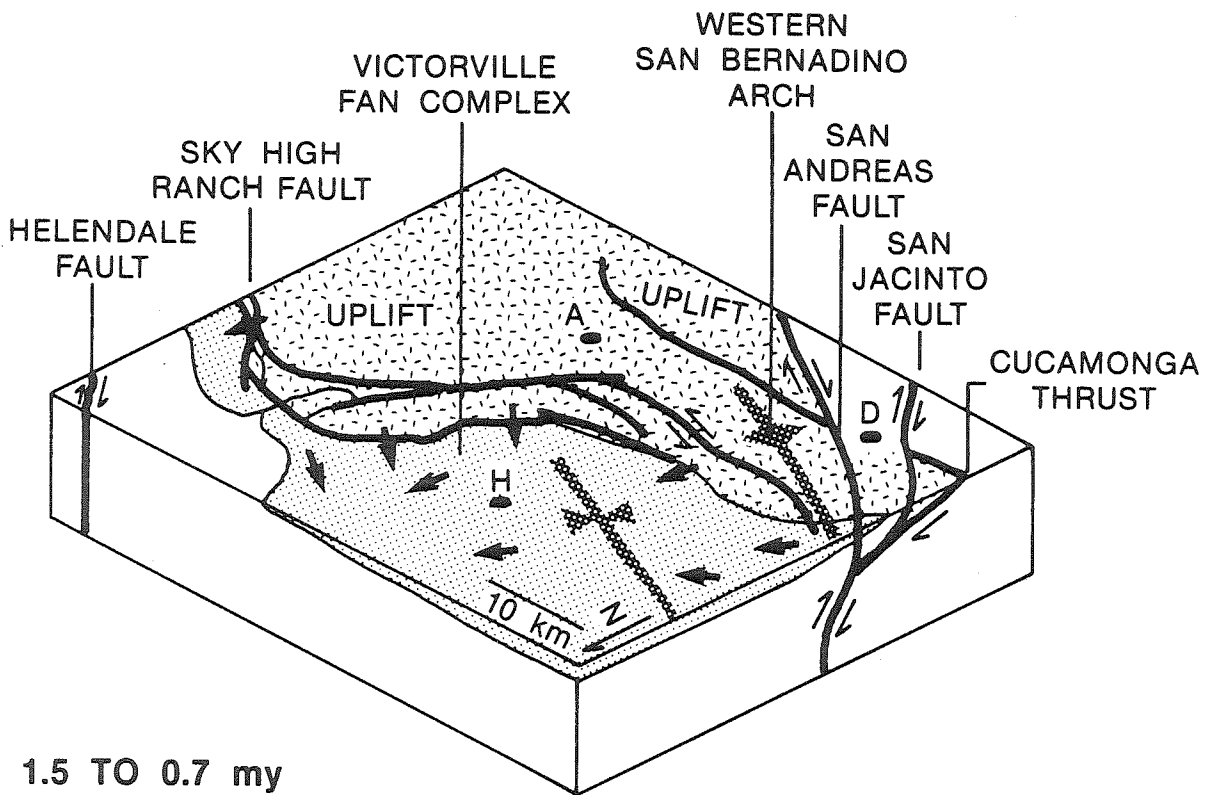


Figure 6-8

1954b; Foster, 1980). Sharp and Silver (1971) and Weldon (1984) have discussed the slip on the San Andreas fault necessary to explain the distribution of these clasts.

The Harold Formation overlies the Crowder Formation in Cajon Pass (Foster, 1980), extending northwest along the San Andreas fault to Littlerock from whence it is correlated with deposits in the Palmdale area (Noble, 1953, 1954a; Foster, 1980). The Harold Formation grades up into the Shoemaker Gravel. In Cajon Valley these units are recognized on the basis of clast lithologies; the Harold Formation contains clasts of Pelona Schist and the Shoemaker Gravel contains clasts of Mt. Lowe Granodiorite and other distinctive lithologies derived from the adjacent San Gabriel Mountains (Noble, 1954b; Foster, 1980). As the units are followed to the east, source changes render lithologic criteria for distinguishing them useless (Figure 3). This depositional package is correlated magnetostratigraphically to the Ord River Gravels in Summit Valley which contain clasts derived from stripping of the Crowder Formation from the western San Bernardino Mountains (Figure 3; Meisling, 1984). A veneer of Older Alluvium capping the Shoemaker Gravel in Cajon Pass contains clasts of Pelona Schist lithologies unique to the eastern San Gabriel Mountains.

The Harold Formation, Shoemaker Gravel, and Older Alluvium are time-transgressive units (Meisling, 1984; Weldon 1984), representing a trail of sediment shed across the San Andreas fault from distinctive basement terranes within the San Gabriel Mountains as they moved northwest along the fault zone. Thus depositional centers in the Victorville Fan migrated northwestward along with their source areas to the southwest of the San Andreas fault. The southern flank of the

Victorville Fan was derived from stripping of the western San Bernardino Arch, which began about 1.5 Ma. Thus, the eastern facies of these units are contemporaneous, but of somewhat different origin.

Pleistocene Arching

Uplift of the westernmost San Bernardino Mountains was accomplished by arching in early-to-late Pleistocene time (Figure 8; Meisling and Weldon, 1982b; Weldon and Meisling, 1982; Weldon, 1984). This arching, which tilted sediments in the western San Bernardino Mountains northward about 20° to 30°, began west of Lake Arrowhead about 1.5 Ma and migrated northwestward (Weldon, 1984). Deformation is concentrated in the interval of time represented by the unconformity between the Shoemaker Gravel and the Older Alluvium (Figure 3). In Summit Valley, the Ord River Gravel largely postdates arch formation. In Cajon Pass, the Harold Formation and Shoemaker Gravel were deposited between ~1.6 and ~1.0 Ma based on magnetostratigraphic data (Weldon, 1984), indicating that most of the tilting has occurred since ~1.0 Ma. The Harold Formation and Shoemaker Gravel become progressively younger to the northwest, as does the overlying unconformity and arching event. Contacts within the Victorville Fan Complex represent migrating areas of nondeposition or erosion, and as such are time-transgressive features.

The Pleistocene Cleghorn Fault System

Dynamic exploitation of the pre-existing Mio-Pliocene reverse fault system characterizes the complex development and evolution of the Cleghorn fault zone in the westernmost San Bernardino Mountains (Figure

2; Meisling and Weldon, 1982a, 1982b; Weldon et al., 1981; Meisling, 1984). The trace of the Cleghorn fault zone clearly reflects the trend of older faults of the reverse fault system. The integration of these earlier faults into the Pleistocene Cleghorn fault system is discussed by Weldon et al. (1981). The Cleghorn fault cannot be traced with any certainty west of the Squaw Peak fault (Woodburne and Golz, 1972; Weldon et al., 1981) and it merges with the Tunnel Ridge lineament at its eastern end (Meisling, 1984).

Between 3.5 and 4.0 km of cumulative left-lateral motion on the Cleghorn fault is proposed on the basis of (1) the offset eastern limit of the Punchbowl Formation and western limit of the Crowder Formation, (2) offset traces of north-plunging monoclines in the Crowder Formation and Miocene weathering surface, and (3) the restoration of the pre-existing Cedar Springs reverse fault system (Meisling and Weldon, 1982). Additional evidence for left-lateral offset is found in late Quaternary terrace deposits, stream courses, and a bedrock scarp (Meisling and Weldon, 1982b). One kilometer of left-lateral motion on the Cleghorn fault has occurred since about 0.5 Ma, based on crude correlation of terraces in Cleghorn Valley, Miller Canyon, and Cajon Creek (Weldon et al., 1981; Meisling and Weldon, 1982a). These offsets yield an average slip-rate for the Cleghorn fault of 2 to 3 mm/yr (Meisling, 1984; Meisling and Weldon, 1982a, 1982b; Weldon et al., 1981), depending on assumptions. The most recent scarps are best explained by a combination of left-lateral and normal (north-block-down) motion on the Cleghorn fault.

Based on the above slip-rate estimates, lateral motion must have occurred on the Cleghorn fault during the early Pleistocene.

Therefore, lateral motion must have been, in part, contemporaneous with the major thrusting on the northern range front (Figure 7) as well as the development of relief in the western San Bernardino Mountains recorded in the Shoemaker Gravel and Harold Formation (Figure 8).

Late Pleistocene Faults

At its east end the Cleghorn fault turns northward and merges with the Tunnel Ridge lineament, a prominent northeast-trending fault zone that is largely unstudied (Figure 2; Meisling, 1984). The Tunnel Ridge lineament crosses the western ramp of the San Bernardino Mountains and turns east to join the northern range front east of Arrastre Canyon (Figure 8). The straight trace of the Tunnel Ridge lineament, which trends parallel to the Ord Mountains frontal fault system, suggests high-angle faulting, while an inconsistent sense of dip displacement on the Miocene weathering surface hints at lateral or scissors motion. A close match of basement lithologies (MacColl, 1964) and continuity of the Miocene(?) erosion surface across the lineament precludes large-scale late Cenozoic displacement. Although displacement history on the Tunnel Ridge lineament is unknown, the feature defines an important structural trend that once connected the left-lateral Cleghorn fault with the north frontal thrust system.

Displacements on high-angle faults at the north end of the Tunnel Ridge lineament define a shallow structural graben which has been a site of deposition since middle-to-late Pleistocene time (Figure 2; Meisling, 1984). This graben can be understood as the product of extension related to strike-slip motion on the Cleghorn and Sky High Ranch faults (Meisling, 1984).

Northeast-trending dip-slip faults along the western and northern front of the Ord Mountains have continued to move since early Pleistocene time (Figure 8). Faceted spurs, steeply westward-dipping conglomerate-basement contacts, and sudden changes in fault strike are suggestive of high-angle dip-slip faulting. Clast lithologies rule out any significant lateral component of motion on these range-front faults (Meisling, 1984).

Pleistocene uplift rates on the west flank of the Ord Mountains, crudely estimated from scarp heights in alluvial fans and the distribution of early Quaternary deposits, indicate a dramatic decrease in deformation in late Pleistocene time. Scarps averaging about 50 m in height displace fans graded to the level of the Old Alluvium and estimated to be ~0.7 Ma in age, yielding a late Pleistocene uplift rate of 0.07 mm/yr (50 m in 0.7 Ma). The 400 m high western escarpment of the Ord Mountains largely developed since deposition of the Ord River Gravel, which contains few clasts of Ord Mountain affinity, about 1.5 Ma. This suggests an uplift rate of nearly 0.3 mm/yr (400 m in 1.5 Ma). If 50 m of uplift since 0.7 Ma are removed, middle Pleistocene uplift rates exceed 0.4 mm/yr (350 m in 0.8 Ma). The ~1000 m high escarpment in Lucerne Valley has developed since deposition of the Old Woman Sandstone about 2 Ma, which requires an uplift rate of 0.5 mm/yr (1 km in 2 Ma). Taking the negligible displacement of ~0.5 Ma old alluvial fans into account, early-to-middle Pleistocene range-front uplift rates approach 0.7 mm/yr (1 km in 1.5 Ma). These estimates reflect an order of magnitude decrease in rates in the late Pleistocene, suggesting a pulse of uplift in early to middle Pleistocene time after which deformation on the northern range front

has waned. Field observations confirm this conclusion (Meisling, 1984).

Waning deformation on the north frontal thrust systems has been accompanied by modification of the range-front by high-angle faulting. The northern range front thrusts both cut (Shreve, 1968, p. 19; Sadler, 1981, p. 22), and are cut by (Sadler, 1981, p. 22, Fawnskin Quadrangle; Meisling, 1984, p. 209), northwest trending high-angle faults, interpreted as pre-existing structural features of the pre-uplift Mojave-San Bernardino Mountains block. This suggests reactivation of pre-existing high-angle fault trends in the late Pleistocene. One such fault in our map area is the Sky High Ranch fault (Figures 2 and 8) a northwest-trending, right-lateral fault which cuts both range-front thrusts and Pleistocene fans east of Arrastre Canyon. Clast lithologies in the range front fans show about 0.5 km of right-lateral displacement (Meisling, 1984). Both the Ord Mountains frontal fault zone and the Tunnel Ridge lineament appear to merge with the Sky High Ranch fault at its northwestern end. The Sky High Ranch fault resembles the Helendale and Old Woman Springs faults in trend and displacement.

Thus, during late Pleistocene time the northwestern San Bernardino Mountains have been modified by a complex system of high-angle lateral, reverse, and normal faults which have extensively exploited pre-existing weaknesses. Although the relationship between these various structural elements is somewhat obscure, the late Pleistocene can be characterized by a decrease in activity and an increase in diversity of structural styles. We believe that this change is due to a shift in the locus of north-south convergence from the northern to

the southern range front. While motion continues on the northern range front, rates are roughly an order of magnitude less than in the early Pleistocene.

DISCUSSION

In this section we will propose a mechanism for uplift of the San Bernardino Mountain and discuss its regional implications for the style and timing of deformation for the Transverse Ranges and San Andreas fault system. Key observations which must be explained by any mechanism for uplift of the San Bernardino Mountains include: (1) The presence of relief in early Pliocene time which acted both as an impediment to drainage and a source for local sedimentation long before Quaternary uplift of the range, (2) the relatively undeformed planar state of the uplifted early Miocene weathering surface over much of the northern range, (3) the spatial coincidence of the plateau with complexities in the trend of the San Andreas fault zone, (4) the existence of both warping and thrusting on the northern range front, and (5) the large panels of uniform dip in the early Miocene weathering surface and overlying Miocene sediments in the westernmost San Bernardino Mountains and the San Gorgonio Massif.

Sadler (1981, 1982b; Sadler and Reeder, 1983) proposes that the San Bernardino Mountains are a transpressional uplift. This uplift is thought to be rooted either at the San Andreas fault (Sadler, 1981) or beneath the long axis of the range (Sadler and Reeder, 1983). Sadler and Reeder (1983) cite (1) the depositional trends of the Santa Ana Sandstone, Old Woman Sandstone, and Phelan formation as evidence for an echelon warping during the early stages of transpressional uplift in

Pliocene time, (2) the opposing frontal thrusts north and south of the range and elongate "welt" as evidence of the symmetrical upthrusting characteristic of advanced transpression, and (3) the oblique orientation of the long axis of uplift relative to the trend of the San Andreas fault, consistent with the relationship predicted for transpression along a major wrench zone.

If the Mio-Pliocene basins developed in an echelon troughs characteristic of the of the early stages of transpression, they should be roughly contemporaneous (Harland, 1971; Lowell, 1972; Wilcox et al., 1973). However, Late Miocene basalts in the Santa Ana Sandstone predate uplift of the northern range front by 4 Ma and deposition of the Old Woman Sandstone by almost 3 Ma. It is difficult to reconcile this discrepancy in timing with the inherently symmetric evolution of well documented transpressional uplifts (Sadler, 1982b; Bartlett et al., 1981; Sylvester and Smith, 1976; Lowell, 1972; Wilcox et al., 1973).

Based on our field observations, we submit that the wide range in age of the Santa Ana, Phelan, and Old Woman depositional systems is better explained by the infilling of elongate troughs associated with relief due to south-directed thrusting in late Miocene through late Pliocene time, prior to Quaternary uplift of the range. The evidence presented in this paper suggests that south-directed thrusting on the Santa Ana thrust was a late-Miocene or early Pliocene event contemporaneous with motion on the Squaw Peak fault system, and is unrelated to the Quaternary uplift of the mountains. Furthermore, it appears that thrusting on the south range front is very young (Matti, et al., 1985), and likely postdates the main phase of thrusting on the

north range front. Our evidence supports three phases of late Cenozoic deformation in the San Bernardino Mountains: (1) late Miocene to early Pliocene south-directed motion on the Squaw Peak thrust, (2) early-to-middle Pleistocene north-directed motion on the north frontal thrust system leading to uplift of the plateau, and (3) late Pleistocene south-directed motion on the Banning and related thrusts giving rise to rapid uplift of the San Gorgonio massif and westernmost part of the range. These three deformational episodes are illustrated in Figure 9, and discussed in detail below. The various structures cited as evidence for transpressional uplift are not contemporaneous. We therefore propose that long-term north-south compression due to the change in trend of the San Andreas fault in San Gorgonio Pass has instead been accommodated by three discrete episodes of thrusting and uplift. Structure, timing, and topography point to the existence of deep-seated low-angle structures beneath the entire San Bernardino Mountains that are involved in upper crustal compression across the San Andreas fault.

The existence of deep-seated, low-angle faults beneath the Mojave Desert has been proposed by many workers. Yeats (1980) and Powell (1981) suggest that the upper five to ten kilometers of the crust in the Mojave block are behaving mechanically as a brittle sheet over a ductile substrate. Several workers conclude that the Mojave block is underlain by Pelona Schist, which is exposed around the margins of the Mojave along major strike-slip faults (Yeats, 1980; Powell, 1981; Silver, 1983; Crowell, 1981). Pelona Schist would behave much more ductily than the overlying thin sheet of batholithic rocks. In our map area, the surface expression of the Squaw Peak thrust coincides with

Figure 6-9. Schematic block diagrams across the central San Bernardino Mountains. This series of diagrams illustrates the proposed interaction of low-angle fault systems and San Andreas fault zone along the southwestern margin of the San Bernardino Mountains, and their role in uplifting the range. Faults are shown trending roughly east-west; however, detailed restoration and reconstruction of structural elements will require considerable further study. [Faults shown in black are active; those shown in gray are inactive.]

(a) Mio-Pliocene south-directed thrusting on the Squaw Peak/Wilson Creek/Liebre Mountain thrust system overrode the inactive north branch of the San Andreas fault. During this period of time, the San Gabriel fault was the active strand of the San Andreas transform system. Timing of motion on the Liebre Mountain and Squaw Peak thrust systems coincides with deposition of the Ridge Route Formation in the Ridge Basin, which is thought to have been derived from the San Bernardino Mountains across the San Andreas fault.

(b) Following early Pliocene cessation of activity on the San Gabriel fault, the north branch of the San Andreas again became active, severing and offsetting the toe of the Squaw Peak thrust system along the Mill Creek fault. The offset toe is now represented by the Liebre Mountain crystalline terrane.

(c) The development of a bend in the San Andreas fault in San Geronimo Pass resulted in upper crustal compression, which was accommodated by northward motion on a deep, south-dipping ramp beneath the San Bernardino Mountains. This early Pleistocene northward motion uplifted the north central plateau of the range, spawned the north frontal thrust system, and gave rise to warping along the northern range front.

It also shunted the upper crustal trace of the San Andreas fault (Mill Creek fault) northward (1), until mechanical conditions favored the establishment of a new upper crustal trace (Mission Creek fault) to the south (2). Documented displacement on the north frontal system is insufficient to account for all of the motion required on the deep ramp; we therefore postulate that some motion is taken up on low-angle surfaces beneath the Mojave block.

(d) In late Pleistocene time, a steep, north-dipping backthrust ramp developed beneath the San Gorgonio massif, and activity virtually ceased on the north frontal system. The south-directed ramp overrode the active trace of the San Andreas fault, breaking the surface along the central segment of the Banning fault. The steep dip of the southern ramp has led to extremely high uplift rates in the San Gorgonio massif. We interpret the final geometry of opposing thrust systems as the product of three distinct episodes of low-angle faulting along the San Andreas fault.

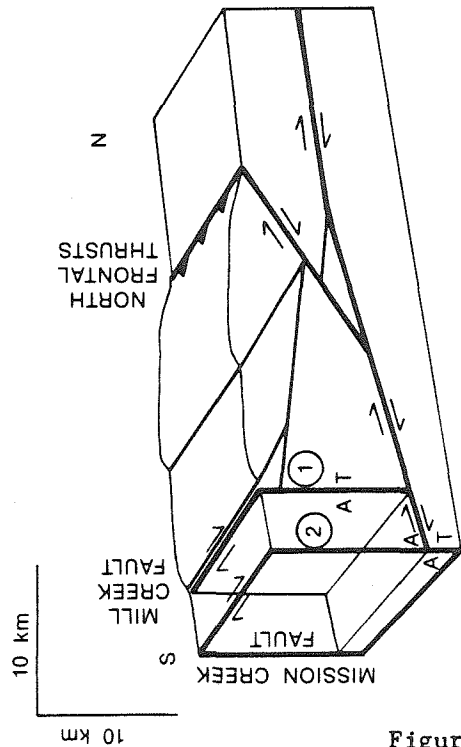
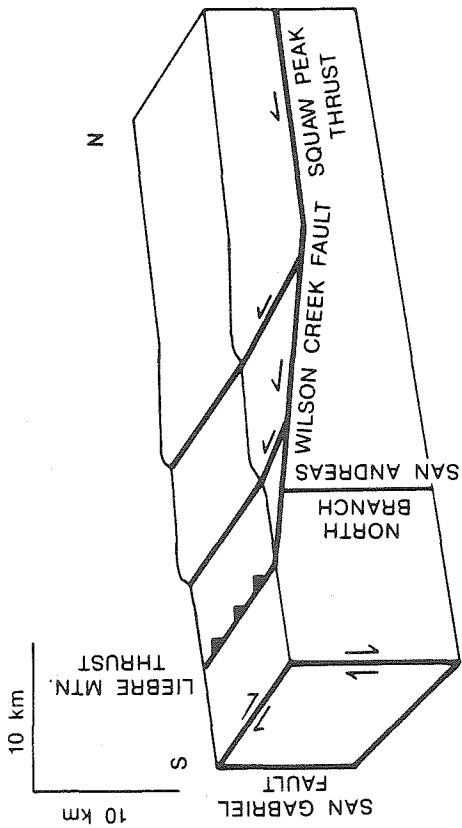
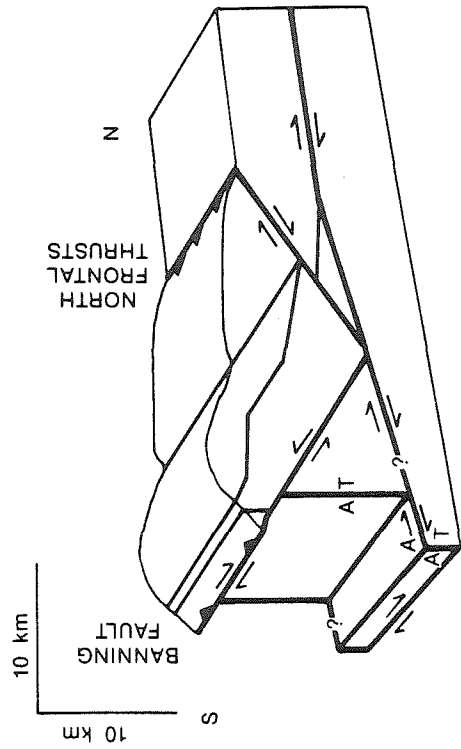
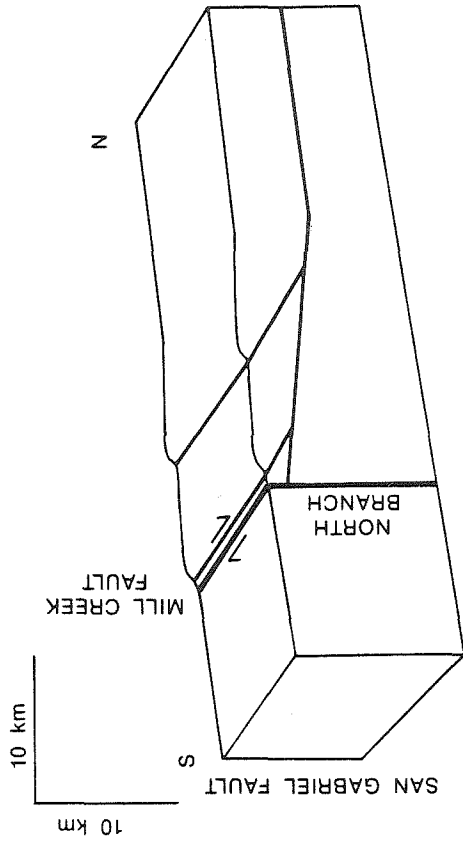


Figure 6-9

early Cenozoic zones of cataclasis in the western San Bernardino Mountains (Weldon et al., 1981). Cataclastic units of unknown protolith are also extensively exposed along the northern range front east of White Mountain (Meisling, 1984). If these cataclastic zones are associated with the deformation internal to a Mojave "flake", they might serve as pre-existing zones of weakness facilitating the development of low-angle thrusting in the San Bernardino Mountains.

Seismicity provides the only direct evidence of low-angle structures at depth beneath the San Bernardino Mountains. The lower limit of microseismicity beneath the San Bernardino Mountains closely approximates a south-dipping plane descending from 5 km beneath the Mojave Desert to about 12 km beneath the San Geronio Massif (Figure 10; Corbett, 1984), suggesting a decoupling or contrast in mechanical behavior of the crust beneath the San Bernardino Mountains. The plane has a dip of about 10° , projecting to the surface in the Mojave Desert, 20 to 30 km north of the range front. It appears to steepen and abruptly shift southward to the San Andreas fault under the Ord Mountains to the west. It shallows and loses definition as relief disappears at the east end of the range. Northward motion on a detachment surface coincident with the south-dipping plane defined by the seismicity offers a means of lifting the entire San Bernardino Mountains block intact. We propose that the early-to-middle Pleistocene uplift of the San Bernardino Mountains is the surface manifestation of northward movement on structures coincident with this ramp at depth.

If the south-dipping seismicity floor represents a detachment ramp, about 6 kilometers of northward motion are required to uplift the

Figure 6-10. Microseismicity beneath the central San Bernardino Mountains. Cross section shows depth of seismic events of quality A from October, 1981 to August, 1983, projected to longitude -117 from the region between $-116^{\circ} 45'$ and $-117^{\circ} 15'$. (SA) and (SJ) indicate the location of the San Andreas and San Jacinto faults, respectively. Seismic events do not occur below a "floor" which rises from about 12 km beneath San Gorgonio Pass to less than 5 km beneath the Mojave Desert. The proposed early Pleistocene detachment ramp coincides with the seismicity "floor", which presumably reflects a contrast in mechanical behavior or decoupling in the upper crust. The seismicity ramp would project to the surface 20 to 30 km north of the north frontal thrusts; we postulate that it actually flattens and merges with a horizontal detachment plane at about 5 km beneath the Mojave block (Figure from Corbett, 1984).

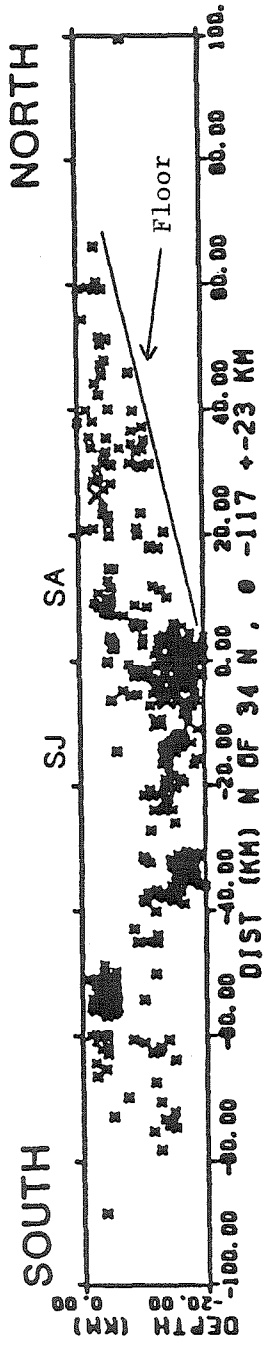


Figure 6-10

plateau about 1 kilometer. Because the range front does not appear to be offset more than about 3 kilometers (Shreve, 1968; Woodford and Harris, 1928; Baird et al., 1974), we infer that the remaining displacement is accommodated on a sub-horizontal surface under the Mojave Desert. Range-front warping is a geometric consequence of northward movement of the San Bernardino Mountains block over the change in dip of the detachment surface where it flattens beneath the Mojave block. The compression that drives motion up the ramp is a consequence of the step in the San Andreas fault in San Gorgonio Pass. We therefore predict that displacement on the detachment beneath the Mojave Desert should decrease and die out both east and west of the zone of convergence in San Gorgonio Pass (Figure 7).

Following about six kilometers of early to middle Pleistocene northward motion on the ramp, continued convergence has been taken up on steep north-dipping faults close to the San Andreas fault. On the basis of the V-shaped seismicity distribution, we speculate that these north-dipping faults are backthrusts that terminate against the south-dipping ramp at depth. Movement up the plane of the steeper north-dipping faults is responsible for the rapid uplift and northward tilting that is occurring in the San Gorgonio Mountain area. The surface expression of this latest phase of south-directed range-bounding thrusts is the Banning thrust.

Implications for Thrusting across the San Andreas Fault

The Squaw Peak thrust juxtaposes what appears to be the hearts of the Cajon-Punchbowl and Crowder basins. Because these basins are contemporaneous and laterally consistent over tens of kilometers we

feel that an offset on the order of tens of kilometers is necessary to explain their current positions. This hypothesis is consistent with the observed upper plate deformation that includes many reverse faults with individual offsets ranging up to a kilometer. Details of the deformation associated with the Squaw Peak thrust and the orientation of the upper plate reverse faults suggest a south to southwest transport direction for the upper plate of the Squaw Peak thrust. The Squaw Peak thrust can be traced right up to the San Andreas fault, and the characteristic internal deformation and lithologies of the upper plate extend throughout the southwestern San Bernardino Mountains (Figure 2). This implies that a strip of San Bernardino Mountains rocks up to sixty kilometers long and several tens of kilometers wide once extended across the current trace of the San Andreas fault.

There is a wedge of San Bernardino Mountains basement that lies between the Wilson Creek, Mission Creek, and Mill Creek faults (Figure 1), which has been displaced less than 16 kilometers (Matti et al., 1985) based on petrologic affinity with San Bernardino Mountains lithologies. Unnamed Tertiary gravels (Figure 1; Morton and Miller, 1975; Weldon, unpublished data) that lie between the Mill Creek (north branch San Andreas of Dibblee, 1964), Wilson Creek, and San Bernardino strand of the San Andreas fault (south branch San Andreas of Dibblee, 1964) are thought to be offset less than 16 kilometers on the Mill Creek fault, on the basis of clast affinities (Matti et al., 1985). The Mill Creek Formation (Figure 1), on the southwest side of the Wilson Creek fault, is postulated to be offset a distance of ~120 kilometers (Gibson, 1971). These observations lead Matti et al. (1985) to propose that the Wilson Creek fault is a major early strand of the

San Andreas fault. Unpublished mapping by Weldon (Devore Quadrangle) shows that the unnamed Tertiary unit does not contain clasts of San Bernardino Mountains affinity, and is locally depositional on a quartz-monzonite basement unlike the rocks in this part of the San Bernardino Mountains. In fact, the contact between the unnamed Tertiary unit and the San Bernardino Mountains (Mill Creek fault of Matti et al., 1985) is low angle, with the San Bernardino Mountains basement on top.

Based on these observations, we propose that the sliver of rocks between the Mill Creek fault and San Bernardino strand of the San Andreas fault were first offset about 120 kilometers on a northern strand of the San Andreas fault, as proposed by Gibson (1971). The trace of this fault was then thrust over and concealed by San Bernardino Mountains basement rocks, as revealed in relationships near Cajon Pass (Weldon, unpublished mapping). We infer a similar relationship between the wedge of San Bernardino Mountains basement bounded by the Mill Creek, Mission Creek, and Wilson Creek faults, and the far-travelled block containing the Mill Creek Formation. Although this may seem to be a major departure from the scenario put forward by Matti et al. (1985), they do map the Mill Creek fault near Cajon Pass and the southernmost part of the Mission Creek/Wilson Creek fault as a thrusts. We argue that the observed relationships are better explained by alternating periods of lateral and thrust faulting, rather than a sequence of cross-cutting lateral faults alone.

While there are few data to constrain the timing of thrusting, the spatial association of thrusting along the San Andreas with the distribution of "upper-plate" deformation in the San Bernardino

Mountains leads us to attribute all of these features to the Squaw Peak thrust system (Figure 9a). Since the time of overthrusting, the San Andreas fault has passed south of the north branch, except for a brief period of reactivation that produced the ~16 kilometers of offset on the Mill Creek fault (Figure 9b; Matti et al., 1985) and an undetermined amount of dip slip near Cajon Pass (Weldon, unpublished mapping) required to expose the unnamed Tertiary unit beneath the thrust flap.

The Squaw Peak Thrust West of the San Andreas Fault

Matti et al. (1985, 1986) and Silver (pers. comm., 1984) have noted the similarity between the rocks in the Liebre Mountain area (Figure 1) and the San Bernardino Mountains. Matti et al. (1985, 1986) propose that the two masses have been offset by the San Andreas fault about 160 km. If this is the case, the Liebre Mountain area may be the missing strip of San Bernardino Mountains rocks southwest of the San Andreas fault. The Liebre Mountain thrust, which bounds the Liebre Mountain block to the south and southwest, could be the offset toe of the Squaw Peak thrust. While published cross sections of the Ridge Basin show the Liebre Mountain fault steepening with depth (e.g., Crowell and Link, 1982), we are not aware of any data to rule out the shallow projection of this low-angle structure all the way to the San Andreas fault. In fact, if the Liebre Mountain area is correlative with the San Bernardino Mountains as Matti suggests, overthrusting of the San Andreas fault provides a means of reconciling Matti's 160 km offset with the total offset of 270 km proposed for the San Andreas fault system by Crowell (1982, p. 38).

If the above inferences are valid, the 160 kilometers of cumulative offset documented by Matti et al. (1985, 1986) only represent the motion on the San Andreas fault since Squaw Peak thrusting. To this must be added 120 kilometers of offset on the North Branch proposed by Gibson (1971), yielding the total offset of ~280 kilometers, essentially the number put forward by Crowell (1982). Even considering the large errors associated with the above offset estimates and the uncertainty in extent and distribution of thrusting, our hypothesis seems worthy of serious consideration in that it allows all previous correlations to be essentially correct.

Thrusting on the Squaw Peak system is firmly constrained to have occurred between 9.5 and 4 Ma, and probably occurred between 6 and 4 Ma. This timing indicates that Mio-Pliocene thrusting overlapped with motion on the San Andreas system, which began at least 10 Ma (Crowell, 1982) and perhaps as early as 20 Ma ago (e.g., Huffman, 1972) in central California. The timing of movement on the Liebre Mountain thrust between 8 and 4 Ma (Ensley and Verosub, 1982) is consistent with motion on the Squaw Peak system. Our hypothesis not only explains the origin of Mio-Pliocene relief in the ancestral San Bernardino Mountains, but also places this relief northeast of the Ridge Basin. This provides a ready source for the bulk of the Ridge Route sediments postulated to have San Bernardino Mountains clast affinities and inferred to have come from the northeast across the San Andreas fault (Crowell, 1982). Thrusting in the San Bernardino Mountains was contemporaneous with activity on the San Gabriel fault, which occurred between 12 and 5 Ma (Crowell, 1982).

It is not clear whether the San Andreas fault was active either

during or before Mio-Pliocene movement on the San Gabriel fault. Crowell (1982) argues that motion on the San Andreas fault started as motion ceased on the San Gabriel fault. He proposes, however, that the upper Ridge Route Formation and the Hungry Valley Formation were derived from the San Bernardino Mountains, indicating an offset of about 150 kilometers (Crowell, 1982, p. 40). He concludes that the remaining 120 kilometers of motion on the San Andreas fault must have predated these deposits. An offset of 120 kilometers would take 2 Ma at the full plate rate of 6 cm/yr, which seems unlikely if motion was contemporaneous with movement on the San Gabriel fault. Crowell (1982, p. 38) implies that the Liebre Mountain thrust and San Andreas fault may have overlapped somewhat, producing the complicated structure of the bounding faults of Liebre Mountain. However, as the toe of the thrust (in our model) remains in about the same place for at least 1 Ma (Ensley and Verosub, 1982), large amounts of contemporaneous motion seems unlikely. Therefore, the missing offset on the San Andreas fault probably predated the Squaw Peak fault, perhaps preceding or overlapping early motion on the San Gabriel fault.

Quaternary Uplift of the San Bernardino Mountains

Field data show that the San Bernardino Mountains have experienced two discrete phases of uplift in the Quaternary: (1) Uplift of the central plateau in early-to-middle Pleistocene time, and (2) uplift of the San Gorgonio massif in late Pleistocene time. Lack of contemporaneity of north- and south-directed thrusting, coupled with the observed flatness of the plateau, are incompatible with a "flower structure" style of transpressional welt mechanism for uplift of the

range. We propose an alternative means of uplift involving deep-seated, low-angle thrusts.

Early-to-middle Pleistocene uplift of the plateau reflects northward movement of the San Bernardino Mountains block up a detachment ramp at a depth of 5-12 km beneath the range. Observations supporting this hypothesis include: (1) The gentle southward-dipping "floor" to microseismicity beneath the range, (2) the widespread occurrence of warping coincident with the northern topographic escarpment, (3) the remarkable planar geometry of the northwestern plateau, and (4) the close spatial coincidence of the extent and displacement on northern range front thrusts with the extent and elevation of the uplifted plateau. We interpret range-front warping as a geometric consequence of northward shallowing of the deep seated master thrust system where it merges with the detachment horizon beneath the Mojave Desert. Range front shortening appears insufficient to account for uplift of the central plateau on the proposed microseismicity "ramp", suggesting that some slip may be transferred to low-angle structure within or beneath the Mojave block. Alternatively, range-front shortening may be greater than heretofore recognized. The Ord Mountains frontal faults and Tunnel Ridge lineament are the surface expression of a lateral ramp in the detachment surface. The role of the ancestral Cleghorn fault in the early Quaternary deformation is not clear, but it may be a continuation of the lateral ramp and probably was an oblique left-lateral reverse structure accommodating regional shortening.

Late Pleistocene uplift of the San Geronio area and the westernmost San Bernardino Mountains ("western wing") reflects motion

on a steep north-dipping ramp which may, in part, coincide with the San Andreas fault itself. Evidence for this conclusion includes: (1) The large regions of uniform northward dip on the Miocene weathering surface and late Cenozoic sediments, (2) the lack of a through-going trace of the San Andreas fault in San Gorgonio Pass, (3) the rapid rates of late Pleistocene uplift proposed for the San Gorgonio block (Morton and Herd, 1980), and (4) the documented northwestward migration of uplift in the western wing (Weldon et al., in preparation). We attribute the uplift of the western wing and San Gorgonio block to two different, but related, mechanisms.

Stratal attitudes in the western wing define a narrow (<5 km wide) panel of uniform (30°) northward dip, suggesting southwestward movement up a north-dipping ramp at depth. Well-documented northward migration of the locus of uplift in the western wing indicates that the causative ramp may be attached to the southwestern side of the San Andreas fault, with northward dips reflecting motion parallel rather than perpendicular to the San Andreas fault. These observations suggest that the causative ramp is actually the surface of the San Andreas fault, which is deformed at a depth of several kilometers (Figure 8). We envision a northward bulging or step in the San Andreas surface at depth. Motion of the Mojave block over this bulge in the San Andreas fault would account for the rapid, migratory uplift of the western wing, generating the observed northward dips. Material opposite the bulge at depth might wedge out eastward, perhaps resulting in late Pleistocene left-lateral motion on the Cleghorn fault.

The depth at which the San Andreas steps northeastward is not known, but we speculate that it may coincide with the intersection of

the Cucamonga thrust and the San Andreas surface. The northwestern point of initiation of the proposed ramp coincides with the region in which the southwestern side of the San Jacinto fault is being moving northward beneath the Cucamonga upper plate and impinging on the San Andreas fault at depth. Northeastward stepping of the San Andreas surface is intuitively reasonable, since it served to shift the fault into better alignment with the trace south of San Gorgonio Pass. The proposed geometry is remarkably similar, but opposite in sense, to the geometry visualized for northward overthrusting of the San Andreas fault during early-to-middle Pleistocene plateau uplift.

Consistent northward dips also characterize the San Gorgonio massif, which has a latest Pleistocene uplift rate of 18 to 36 mm/yr (Morton and Herd, 1980) based on a study of Wisconsin glacial deposits. Late Quaternary thrusting on the central segment of the Banning fault leaves little doubt that the San Gorgonio block is being uplifted on north-dipping thrusts. Based on the distribution of microseismicity (Figure 10) we interpret the Banning fault as a back-thrust that terminates against the master ramp. Scarps on the northern range front provide evidence of continued activity there, albeit at a greatly reduced rate. Thus, it appears that northward thrusting has given way to southward thrusting with the development of the backthrusts of the Banning system. We conclude that the Banning fault has overrun and concealed the middle Pleistocene trace of the San Andreas fault. The compression driving this thrust system is clearly the result of the change in trend of the San Andreas fault in San Gorgonio Pass.

There are numerous similarities between the late Pleistocene deformation in Cajon Pass and San Gorgonio Pass: (1) Panels of

consistent northward dip, (2) north dipping structures, (3) a narrow zone of uplift parallel and adjacent to the San Andreas fault, and (4) extremely rapid uplift, 5 mm/yr in the western wing; 18 to 36 mm/yr in the San Gorgonio block (Morton and Herd, 1980). When motion on the San Andreas fault for this time period is restored, the San Jacinto fault is positioned opposite the western end of the San Gorgonio massif, suggesting that the San Jacinto fault was part of the early Pleistocene complications along the San Andreas fault that gave rise to its change in trend, and the uplift of the San Bernardino Mountains. Since then, compression has continued in San Gorgonio Pass, while the San Jacinto fault has migrated northwestward along the San Andreas fault producing its own separate wake of deformation.

CONCLUSIONS

The field data presented in this paper provide a critical test of tectonic models for the geometry and evolution of the Transverse Ranges and their relation to the history of the San Andreas fault in southern California. Our work provides a structural and stratigraphic framework for the late Cenozoic development of the western San Bernardino Mountains. New fossil, magnetostratigraphic, and radiometric age data permit the correlation of late Cenozoic sedimentary rocks in the northwestern San Bernardino Mountains. Our detailed mapping, integration, and characterization of structural geometries provide the basis for a series of paleotectonic block diagrams outlining the history of sedimentation and deformation in the study area. The field data suggest three distinct phases of late Cenozoic deformation in the San Bernardino Mountains and lead us to propose a new mechanism for

uplift of the San Bernardino Mountains on a series of closely related low-angle structures. Our proposition has a direct bearing on the mechanism by which upper crustal compression is accommodated along the San Andreas fault in southern California.

We have identified and characterized a Mio-Pliocene thrust system (Squaw Peak thrust system) which accounts for the postulated existence of an ancestral San Bernardino Mountains that disrupted Miocene drainage patterns and led to the deposition of a distinctive suite of Pliocene sedimentary rocks in a structurally controlled hinterland trough. Field relationships indicate that the Squaw Peak thrust system extended across the present site of the San Andreas fault, suggesting that the results of our study may contribute to the understanding of other areas along the San Andreas fault. We propose a correlation of the Squaw Peak thrust with thrusts exposed along the San Andreas fault in San Gorgonio Pass, parts of the Mill Creek, Wilson Creek, and Mission Creek faults of Matti et al., (1985), and on the northeast flank of the Ridge basin (Liebre Mountain thrust). This correlation implies that the San Andreas fault was overthrust by the Squaw Peak system during a period of inactivity coincident with the time-span proposed for the San Gabriel fault. We suggest that the upper plate of the Liebre Mountain thrust is the offset toe of the Squaw Peak thrust, and therefore its position does not record the full amount of offset on the San Andreas fault since its inception.

We propose a two-phase history of Quaternary uplift of the San Bernardino Mountains: (1) Early-to-middle Pleistocene uplift of the entire plateau by northward motion up a gentle north-directed ramp, and (2) late Pleistocene uplift of the westernmost San Bernardino Mountains

and San Gorgonio massif on steep south-directed ramps. Each phase of uplift is characterized by a distinctive pattern of deformation. North-directed ramping is expressed in the broad undeformed north-central plateau bordered by thrusts and large monoclinical warps. The south-directed ramping is characterized by large panels of consistent northerly dips in Pliocene and older rocks, high uplift rates, and north-dipping faults.

The ramp under the westernmost San Bernardino Mountains is inferred to be, in part, a step or bulge in the surface of the San Andreas fault at its intersection the Cucamonga and San Jacinto faults at depth. Uplift in the westernmost part of the range has migrated steadily northwestward, as documented in the Plio-Pleistocene sedimentary record. The steep ramp on which the San Gorgonio block is being uplifted overrides and conceals the active trace of the San Andreas fault, reaching the surface as the Banning fault.

Our field evidence points to underthrusting, overthrusting, and deformation of the San Andreas fault on low-angle structures. Thus rocks thrust across and sliced off by the San Andreas fault can be transferred across the fault at any time in its history. This offers an explanation correlated packages of rocks that show less than the total offset on the San Andreas fault. Strand switching on the San Andreas fault can also be understood in terms of a stable deeper fault zone that must become reestablished following a shift in the surface trace of the fault on low-angle structures. This process could be considered a mechanism for accretion of thin slivers of upper crustal material from one plate to another along a transform boundary.

REFERENCES CITED

- Allen, C. R., 1957, San Andreas fault zone in San Geronio Pass, southern California: *Geol. Soc. Amer. Bull.*, v. 68, p. 315-350.
- Allen, C. R., 1968, The tectonic environments of seismically active and inactive areas along the San Andreas fault system: in Dickinson, W. R., and Grantz, A., eds., Proceedings of conference on geologic problems of San Andreas fault system, Stanford University Publications in Geological Sciences, v. 11, p. 70-82.
- Baird, A. K., Morton, D. M., Woodford, A. O., and Baird, K. W., 1974, Transverse Ranges province: A unique structural-petrochemical belt across the San Andreas fault system: *Geol. Soc. America Bull.*, v. 85, p. 163-174.
- Barrows, K. J., and Barrows, A. G., 1975, Comparison of lithology and provenance of cobbles in the western and type facies of the Punchbowl Formation: *Geol. Soc. America Abs. with Programs*, v. 7, no. 3, p. 295-296.
- Bartlett, W. L., Friedman, M., and Logan, T.M., 1981, Experimental folding and faulting of rocks under confining pressure: Part IX. Wrench faults in limestone layers: *Tectonophysics*, v. 79, p. 255-277.
- Bird, P., and Rosenstock, R. W., 1984, Kinematics of present crust and mantle flow in southern California: *Geol. Soc. Am. Bull.*, v. 95, p. 946-957.
- Blackwelder, E., 1925, Exfoliation as a phase of rock weathering: *Jour. Geol.*, v. 33, p. 789-806.
- Chinnery, M. A., 1965, The vertical displacements associated with

transcurrent faulting: Jour. Geophys Res., v. 70, no. 18, p. 4627-4632.

Corbett, E. J., 1984, Seismicity and crustal structure of southern California: Tectonic implications from improved earthquake locations: Ph.D. Dissert., Calif. Inst. of Technology, Pasadena, Calif., 231 p.

Crowell, J. C., 1981, An outline of the tectonic history of southeastern California: in Ernst, W. G., ed., The geotectonic development of California, Rubey Volume 1, Englewood Cliffs, NJ, Prentice-Hall, p. 583-600.

Crowell, J. C., 1982, The tectonics of the Ridge Basin, southern California: in Crowell, J. C., and Link, M. H., eds., Geologic History of Ridge Basin, southern California, Pacific Section, SEPM, p. 25-42.

Crowell, J. C., and Link, M. H., 1982, Geologic history of Ridge Basin, southern California: Pacific Section S. E. P. M., Los Angeles, California, 304 p.

Dibblee, T. W., Jr., 1964a, Geologic map of the Lucerne Valley Quadrangle, San Bernardino County, California: U. S. Geol. Survey, Misc. Geol. Invest. Map I-426, 1:62,500.

Dibblee, T. W., Jr., 1964b, Geologic map of the San Geronio Mountain Quadrangle, San Bernardino and Riverside Counties, California: U. S. Geol. Survey, Misc. Geol. Invest. Map I-431, 1:62,500.

Dibblee, T. W., Jr., 1965a, Geologic map of the Cajon 7 1/2 minute Quadrangle, San Bernardino County, California: U. S. Geol. Survey Open-File map 65-42, 1:24,000.

Dibblee, T. W., Jr., 1965b, Geologic map of the the Hesperia 15 minute

- Quadrangle, San Bernardino County, California: U. S. Geol. Survey open-file map 65-43, 1:62,500.
- Dibblee, T. W., Jr., 1967, Areal Geology of the western Mojave Desert, California: U. S. Geol. Survey, Prof. Paper 522, 153 p.
- Dibblee, T. W., Jr., 1975, Tectonics of the western Mojave Desert near the San Andreas fault, in Crowell, J. C., ed., San Andreas fault in southern California, Cal. Div. Mines and Geol., Spec. Rept. 118, p. 155-161.
- Ensley, R. A., and Verosub, K. L., 1982, Biostratigraphy and magnetostratigraphy of the southern Ridge Basin, central Transverse Ranges, California: in Crowell, J. C., and Link, M. H., eds., Geologic history of Ridge Basin, southern California, Pacific Section S. E. P. M., p. 13-24.
- Foster, J. H., 1979, Quaternary tectonism in Cajon Valley, California and its relation to the southern California uplift: Geol. Soc. Amer. Abs. with Programs, v. 11, no. 3, p. 78.
- Foster, J. H., 1980, Late Cenozoic tectonic evolution of Cajon Valley, southern California: Ph. D. Dissert., Univ. Calif. Riverside, Riverside, Calif., 235 p.
- Foster, J. H., 1982, Late Cenozoic tectonic evolution of Cajon Valley, southern California: in Sadler, P. M., and Kooser, M. A., eds., Late Cenozoic stratigraphy and structure of the San Bernardino Mountains: Geol. Soc. Amer., Cordilleran Section Field Trip Guide, 6, p. 67-73.
- Garfunkel, Z, 1974, Model for the late Cenozoic Tectonic history of the Mojave Desert, California, and for its relation to adjacent regions: Geol. Soc. Amer. Bull., v. 86, p. 1931-1944.

- Gibson, R. C., 1971, Non-marine turbidites and the San Andreas fault, San Bernardino Mountains, California: in Geological Excursions in southern California, W. A. Elders, ed., University of California, Riverside, Campus Museum Contributions, no. 1, p. 167-181.
- Hadley, D., and Kanamori, H., 1977, Seismic structure of the Transverse Ranges, California: Geol. Soc. America Bull., v. 88, p. 1469-1478.
- Harland, W. B., 1971, Tectonic transpression in Caledonian Spitsbergen. Geol. Mag., v. 108, no. 1, p. 27-42.
- Hill, D. P., 1982, Contemporary block tectonics: California and Nevada: Jour. Geophys. Res., v. 87, no. B7, p. 5433-5450.
- Huffman, O. F., 1972, Lateral displacement of upper Miocene rocks and the Neogene history of offset along the San Andreas fault in central California, Geol. Soc. Amer. Bull., v. 83, p. 2913-2946.
- Jones, D. L., and Irwin, G. A., 1975, Rotated Jurassic rocks in the Transverse Ranges, California: Geol. Soc. Amer. Abs. with Programs, v. 7, no. 3, p. 330.
- Kamerling, M. J., and Luyendyk, B. P., 1979, Tectonic rotations of the Santa Monica Mountains region, western Transverse Ranges, California, suggested by paleomagnetic vectors: Geol. Soc. Amer. Bull., v. 90, p. 331-337.
- Kamerling, M. J., and Luyendyk, B. P., 1985, Paleomagnetism and Neogene tectonics of the northern Channel Islands, California, Jour. Geophys. Res., v. 90, p. 12,485-12,502.
- Leighton and Associates, 1984, Geological, geophysical, and seismic investigation, Mojave River Dam, northern San Bernardino Mountains, California: Report to the U. S. Army Corps of

- Engineers, Geotechnical Branch, Los Angeles, California, 32 p.
- Lowell, J. D., 1972, Spitsbergen Tertiary orogenic belt and the Spitsbergen fracture zone: *Geol. Soc. Am. Bull.*, v. 83, p. 3091-3102.
- Luyendyk, B. P., Kamerling, M. J., and Terres, R. R., 1980, Geometric models for Neogene crustal rotations in southern California, *Geol. Soc. Amer. Bull.*, v. 91, p. 211-217.
- Luyendyk, B. P., Kamerling, M. J., Terres, R. R., and Hornafius, J. S., 1985, Simple shear of southern California during Neogene time suggested by paleomagnetic declinations, *Jour. Geophys. Res.*, v. 90, p. 12, 454-12,466.
- MacColl, R. S., 1964, Geochemical and structural studies in batholithic rocks of southern California: Part 1, Structural geology of the Rattlesnake Mountain Pluton: *Geol. Soc. Am. Bull.*, v. 75, no. 9, p. 805-822.
- Matti, J. C., Morton, D. M., and Cox, B. F., 1985, Distribution and geologic relations of fault systems in the vicinity of the central Transverse Ranges, southern California, U. S. Geol. Surv. Open File Rept. 85-365, 37 p.
- Matti, J. C., Frizzell, V. A., and Mattinson, J. M., 1986, Distinctive Triassic megaporphyritic monzogranite displaced 160 ± 10 km by the San Andreas fault, southern California: A new constraint for palinspastic reconstructions, *Geol. Soc. Amer. Abs. with Programs*, v. 18, p. 154.
- May, S. R., and Repenning, C. A., 1982, New evidence for the age of the Old Woman Sandstone, Mojave Desert, California: in Sadler, P. M., and Kooser, M. A., eds., Late Cenozoic stratigraphy and structure

of the San Bernardino Mountains: Geol. Soc. Am., Cordilleran Section Field Trip Guide, 6, p. 93-96.

Meisling, K. E., 1984, Neotectonics of the north frontal fault system of the San Bernardino Mountains: Cajon Pass to Lucerne Valley, California: Ph.D. Dissert., Calif. Inst. of Technology, Pasadena, Calif.

Meisling, K. E., and Weldon, R. J., 1982a, Slip-rate, offset, and history of the Cleghorn fault, western San Bernardino Mountains, southern California: Geol. Soc. America Abs. with Programs, v. 11, no. 3, p. 215.

Meisling, K. E., and Weldon, R. J., 1982b, The late-Cenozoic structure and stratigraphy of the western San Bernardino Mountains: in Geologic Excursions in the Transverse Ranges, J. D. Cooper ed., Cal. State Univ. Fullerton, Fullerton, Calif., p. 75-81

Mendenhall, W. C., 1905, The hydrology of the San Bernardino Valley, California: U. S. Geol. Survey Water Supply Paper 142.

Miller, C. F., and Morton, D. M., 1975, K-Ar geochronology for the eastern Transverse Ranges: Geol. Soc. Am. Abstr. with Prog., v. 7, no. 3, p. 348.

Morton, D. M., and Herd, D. G., 1980, Earthquake hazard studies, Upper Santa Ana Valley and adjacent areas, southern California, in Summaries of Technical Reports, v. IX, NEHRP, U. S. Geol. Surv. Open File Rept., 80-6, p. 1-15.

Morton, D. M., and Miller, F. K., 1975, Geology of the San Andreas fault zone north of San Bernardino between Cajon Canyon and the Santa Ana Wash, in Crowell, J. C., ed., San Andreas fault in southern California, Cal. Div. Mines and Geol. Spec. Rept. 118, p.

136-146.

- Neville, S. L., and Chambers, J. M., 1982, Late Miocene alkaline volcanism, northeastern San Bernardino Mountains and adjacent Mojave Desert: in Geologic excursions in the Transverse Ranges, J. D. Cooper, ed., Cal. State University, Fullerton, Fullerton, California, p. 103-106.
- Noble, L. F., 1932, The San Andreas rift in the desert region of southeastern California: Carnegie Inst. Washington Yearbook 31, p. 355-363.
- Noble, L. F., 1953, Geology of the Pearland Quadrangle, California: U. S. Geol. Survey Quadrangle Map GQ-24, scale 1:24,000
- Noble, L. F., 1954a, Geology of the Valyermo Quadrangle and vicinity, California: U. S. Geol. Survey Quad. Map GQ-50.
- Noble, L. F., 1954b, The San Andreas fault zone from Soledad Pass to Cajon Pass, California: Cal. Div. Mines and Geol. Bull. 170, Ch. 4, p. 32-48.
- Oberlander, T. M., 1972, Morphogenesis of granitic boulder slopes in the Mojave Desert, California: Jour. Geol., v. 80, p. 1-20.
- Ramirez, V. R., 1982, Hungry Valley Formation: Evidence for 220 km of post Miocene offset on the San Andreas fault, in Anderson, D. W., and Rymer, M. J., eds., Tectonics and sedimentation along the San Andreas fault, Pac. Sect. S. E. P. M., p. 33-44.
- Powell, R. E., 1981, Geology of the crystalline basement complex, eastern Transverse Ranges, southern California: Constraints on regional tectonic interpretation: Ph.D. thesis, California Institute of Technology, 441 p.
- Reynolds, R. E., 1984, Miocene faunas in the lower Crowder Formation,

- Cajon Pass, California: A preliminary discussion: in San Andreas fault - Cajon Pass to Wrightwood, Hester, R. L., and Hallinger, D. E., eds., Pacific Section, AAPG, Volume and Guidebook, 55, p. 17-21.
- Richmond, J. F., 1960, Geology of the San Bernardino Mountains north of Big Bear Lake, California: Cal. Div. Mines Geol. Special Report 65, 68 p.
- Robinson, P. T., and Woodburne, M. O., 1971, Source of volcanic clasts in the Punchbowl Formation, Valyermo and Cajon Valley, California: Geol. Soc. America Abs. with Programs, 67th Annual Meeting, Cordilleran Section, p. 185-186.
- Sadler, P. M., 1981, Structure of the northeast San Bernardino Mountains: Report and Open File Maps submitted to Cal. Div. Mines and Geology in response to RFP-SMPI.
- Sadler, P. M., 1982a, Late Cenozoic stratigraphy and structure of the San Bernardino Mountains: Geol. Soc. America Field Trip Guidebook 6, P. M. Sadler and M. A. Kooser eds., in Geologic Excursions in the Transverse Ranges, J. D. Cooper ed., Cal. State Univ. Fullerton, Fullerton, Calif., p. 55-106.
- Sadler, P. M., 1982b, Provenance and structure of late Cenozoic sediments in the northeast San Bernardino Mountains: in Geologic Excursions in the Transverse Ranges, J. D. Cooper ed., Cal. State Univ. Fullerton, Fullerton, Calif., p. 83-91.
- Sadler, P. M., and Reeder, W. A., 1983, Upper Cenozoic, quartzite-bearing gravels of the San Bernardino Mountains, southern California; recycling and mixing as a result of transpressional uplift: in Tectonics and sedimentation along

- faults of the San Andreas system, Anderson, D. W., and Rymer, M. J., eds., Pacific Section, SEPM, Los Angeles, California, p. 45-57.
- Sharp, R. V., and Silver, L. T., 1971, Quaternary displacement on the San Andreas and Punchbowl faults at the San Gabriel Mountains, southern California: Geol. Soc. Am. Abstr. with Prog., v. 3, no. 2, p. 191.
- Shreve, R. L., 1959, Geology and mechanics of the Blackhawk landslide: Ph.D. Dissert., Calif, Inst. of Technology, Pasadena, Calif.
- Shreve, R. L., 1968, The Blackhawk landslide: Geol. Soc. America Special Paper 108, 47p.
- Silver, L. T., 1982, Evidence and a model for west-directed early-to-mid Cenozoic basement overthrusting in southern California, Geol. Soc. Amer. Abs. with Programs, v. 14, p. 617.
- Stout, M. L., 1979, A cyclist's view of the internal structure within the upper plate of the Bear Creek thrust, San Bernardino Mountains, California: Geol. Soc. America Abs. with Programs, v. 11, no. 3, p. 130-131 .
- Strathouse, E. C., 1982, The Santa Ana Sandstone (Miocene in part) and evidence for late Cenozoic orogenesis in the San Bernardino Mountains: in Geologic Excursions in the Transverse Ranges, J. D, Cooper ed., Cal. State Univ. Fullerton, Fullerton, Calif., p. 97-102.
- Strathouse, E. C., 1983, Late Cenozoic fluvial sediments in Barton Flats and evidence for orogenesis, San Bernardino Mountains, San Bernardino County, southern California: M.S. Thesis, Univ. Cal. Riverside, Riverside, Calif., 127 p.

- Sylvester, A. G., and Smith, R. R., 1976, Tectonic transpression and basement-controlled deformation in San Andreas fault zone, Salton trough, California: Amer. Assoc. Petrol. Geol. Bull, v. 60, no. 12, p. 2081-2102.
- U. S. Army Corps of Engineers, 1982, Mojave River Dam foundation report: U. S. Army Engineer District, Los Angeles, Corps of Engineers, C. W. Orvis, Project Geologist, 66 p, 13 Figs., 11 tables, 53 Dwgs.
- Vaughan, F. E., 1922, Geology of the San Bernardino Mountains north of San Gorgonio Pass: Univ. Cal., Dept. Geol. Sci. Bull., v. 13, p. 319-411.
- Weldon, R. J., 1984, Implications of the age and distribution of the late Cenozoic stratigraphy in Cajon Pass, southern California: in San Andreas fault - Cajon Pass to Wrightwood, Hester, R. L., and Hallinger, D. E., eds., Pacific Section, AAPG, Volume and Guidebook, 55, p. 9-15.
- Weldon, R. J., Meisling, K. E., Sieh, K. E., and Allen, C. R., 1981, Neotectonics of the Silverwood Lake area, San Bernardino County: Report to the California Department of Water Resources, 22 p., 11 Figs., 1 map.
- Weldon, R. J., and Meisling, K. E., 1982, Late Cenozoic tectonics in the western San Bernardino Mountains: Implications for the uplift and offset of the central Transverse Ranges, Geol. Soc. Amer. Abs. with Programs, v. 14, p. 243-244.
- Weldon, R. J., Winston, D. S., Kirschvink, J. L., Burbank, D. W., 1984, Magnetic stratigraphy of the Crowder Formation, Cajon Pass, southern California: Geol. Soc. Am. Abstr. with Prog., v. 16, no.

6, p. 689.

Weldon, R. J., and Humphreys, E., 1986, A kinematic model of southern California: *Tectonics*, v. 5, p. 33-48.

Wilcox, R. E., Harding, T. P., and Seely, D. R., 1973, Basic wrench tectonics: *Amer. Assoc. Petrol. Geol. Bull.*, v. 57, no. 1, p. 74-96.

Woodburne, M. O., 1975, Cenozoic stratigraphy of the Transverse Ranges and adjacent areas, southern California: *Geol. Soc. America Special Paper 162*, 91 p.

Woodburne, M. O., and Golz, D. J., 1972, Stratigraphy of the Punchbowl Formation, Cajon Valley, southern California: *Univ. Calif. Publ. Geol. Sci.*, v. 92, 57 p.

Woodford, A. O., and Harris, T. F., 1928, Geology of Blackhawk Canyon, San Bernardino Mountains, California: *Calif. Univ. Dept. Geol. Sci. Bull.*, v. 17, no. 8, p. 265-304.

Yeats, R. S., 1980, Quaternary flake tectonics of the California Transverse Ranges: *Geol. Soc. America Abs. with Programs*, v. 11, no. 3, p. 160.

Yeats, R. S., 1981, Quaternary flake tectonics of the California Transverse Ranges: *Geology*, v. 9, p. 16-20.

CHAPTER SEVEN

CONCLUSION:

A SPECULATIVE HISTORY OF THE SAN ANDREAS FAULT
IN SOUTHERN CALIFORNIA

Introduction

The late Cenozoic geology of Cajon Pass provides an excellent record of the evolution of the tectonic and sedimentary depositional styles associated with the San Andreas fault system. In this chapter I will trace a speculative development of the San Andreas system, based mainly on the geology of the Transverse Ranges. Inferences are drawn from other published work, but the history presented here is not meant to be a complete summary of the work in the area, just a selection of observations that bear on the story presented here.

The early San Andreas fault

An early branch of the San Andreas fault system is believed to have been active in Cajon Pass during the Middle Miocene (the Middle Miocene is approximately 15 to 11 my ago, Harland et al., 1982). The earliest phase of activity was coincident with the development of the extensive system of Middle Miocene sedimentary basins that characterized the Transverse Ranges at that time. The assertion that the San Andreas system was active by the Middle Miocene is based on several lines of evidence.

First, the Squaw Peak thrust system displaced San Bernardino Mountains rocks across the future trace of the modern San Andreas fault during the late Miocene (Chapter 6). Subsequently, these rocks have been offset to Liebre Mountain, a distance of about 160 km (Matti, in review; this thesis, Chapter 6). Because the thrusting occurred between 9.5 and 4.2 my ago, and may have been limited to 6 to 8 my ago (Chapter 6), the value of 160 km probably represents the total offset across the San Andreas and San Jacinto faults since the opening of the Gulf of California about 5 my ago (Larson et al., 1968; Curry and Moore, 1984). The extra 80 to 100 km necessary to account for the 240-260 km of total offsets across the San

Andreas fault in southern California (e.g., Crowell, 1962; 1981; Bohannon, 1975; Powell, 1981) must have occurred before the Pliocene (Pliocene is approximately 5 to 2 my ago, Harland et al., 1982).

A second line of evidence may be the existence of several rift or pull-apart basins along the San Andreas fault that are older than the generally accepted Pliocene onset of faulting along the San Andreas fault. These long narrow, northwest-trending, structural basins include the Mill Creek (Gibson, 1971; Sadler, personal communication, 1985) and the Devil's Punchbowl (Noble, 1954; Barrows, 1979) basins, and may include enigmatic slivers of Tertiary sediment in the fault zone like the unnamed Tertiary between the North and South Branches of the San Andreas near San Bernardino (see Chapter 6 and Plates 4 and 7) and the Anaverde Formation (Barrows, 1980). Despite having outcrop belts up to tens of kilometers long these rocks show evidence of being limited to the narrow strips preserved today and do not appear to be slices from larger basins as do the Crowder or Cajon-Punchbowl outcrops. The existence of these northwest-trending structurally-controlled basins in the Miocene requires activity on early faults of the San Andreas system.

The third line of evidence is the slip rate on the San Andreas fault system (Chapter 4). The modern San Andreas system (which includes both the San Andreas and San Jacinto faults south of their junction) has been accumulating slip at 37.5 ± 2 mm/yr throughout the Quaternary (Chapter 4). This rate is indistinguishable from the 30 to 40 mm/yr rate calculated for the 160 km offset of Liebre Mountain from the San Bernardino Mountains in the last 5 ± 1 my. This agreement strengthens the correlation and has several important implications for the evolution of the San Andreas system that are discussed below. Unfortunately, there are no well-established

Pliocene offsets across the San Andreas fault with which to test this agreement.

If the Plio-Pleistocene San Andreas fault cannot account for the total displacement, the rest of the offset must have been contemporaneous with or predated activity on the San Gabriel fault. There is no evidence of contemporaneous activity on the San Andreas and Squaw Peak faults (Chapter 6) or on the San Andreas and San Gabriel faults (Crowell, 1982b). Matti (in review) suggests that the Cajon Valley fault is the offset extension of the San Gabriel fault. They are the same age (see Chapter 4 for the constraints on the Cajon Valley fault; Crowell, 1982b for the San Gabriel fault) and are offset the appropriate amount for the Liebre Moun-San Bernardino Mountains correlation. If this is the case, the modern San Andreas could not have been contemporaneous with the San Gabriel fault. For these reasons I place the extra 80-100 km of offset on the San Andreas before the San Gabriel fault's period of activity (11 to 5 my, Crowell, 1982).

The ages of the two most likely candidates for this early activity support this age assignment. One candidate is the North Branch of the San Andreas fault (note that this fault has subsequently been reactivated: Chapter 6). Gibson (1971) and Dibblee (1968, 1975) have suggested that this fault has accumulated about 100 km of slip. In Chapter 6 evidence is presented supporting the hypothesis that the North Branch predated the Squaw Peak fault and, therefore, the San Gabriel fault as well. If these observations are correctly interpreted, the North Branch has the correct timing and offset to be the earliest branch of the San Andreas fault. Another likely candidate is the San Francisquito-Fenner-Clemens Well fault. Powell (1981) proposed about 90 km of middle Miocene activity to

account for the bedrock distribution before the onset of activity on the San Gabriel and San Andreas faults. If his hypothesis is correct, and offset is part of the offset across the San Andreas system, the modern San Andreas fault must have had less than 200 km of offset, consistent with the Liebre Mountain-San Bernardino Mountains offset presented above.

In summary, the San Andreas system is proposed to have accumulated about 160 km during the Pliocene and Quaternary (the last 5 my), 60 km on the San Gabriel fault during the late Miocene (11 to 5 my), and 80 to 100 km during the middle Miocene. The exact timing of the earliest branch (and even the exact fault) is unclear; however, an argument for the age can be made from the sedimentary record. Each well-documented switching of strands in the San Andreas system was accompanied by profound changes in the depositional style in Cajon Pass. The onset of activity on the San Gabriel fault, about 11 my ago approximately corresponds to the end of the Middle Miocene basins in the Cajon Pass area; deposition of the Crowder Formation ended about 9.5 my ago (Weldon, 1984, Weldon et al., 1984) and deposition in the Cajon-Punchbowl basin probably ended at about the same time (extrapolating the Middle Miocene fossil ages through the uppermost portion of the formation that has not yet been dated, Woodburne and Golz, 1972; Reynolds, 1985). Deposition in the Mint Canyon-Caliente basin, which Matti (in review) infers to have been south of the San Bernardino Mountains at the time, also ended at this time (Ehlig et al., 1975; Crowell, 1982b). The onset of activity on the San Gabriel fault was also coincident with the beginning of deposition in the Ridge Basin (Crowell, 1982b) and the onset of uplift and erosion associated with the proto San Bernardino Mountains, discussed in Chapter 6. The return of the activity from the San Gabriel to the San

Andreas fault apparently ended the uplift of the proto-San Bernardino Mountains and began the Plio-Pleistocene deposition in the Cajon Pass area (Chapters 4 and 6).

The most obvious turning point in the tectonics to associate with the onset of the earliest activity on the San Andreas system is the onset of the Middle Miocene basin system, following the profound earliest Miocene unconformity. The Cajon Punchbowl, Crowder, and possibly, the western Santa Ana basins all began to accumulate sediments within a few million years of each other, during the latest Early Miocene.

This speculative history is presented in Figure 1. The slip rate is inferred to be constant for the last 5 my, based on the Quaternary offsets and the age and offset of the Liebre Mountains from the San Bernardino Mountains. The difference between the average slip rate for the San Gabriel fault and the pre-San Gabriel strand cannot be determined accurately because of the uncertainty in the age of that structure. The three points for the Miocene could fall on a line, within the limits of the data. The data could also be representing a smoothly increasing slip rate, such as similar plots for the history in central California appear to require (Hill, 1971; Dickinson, et al., 1972; Huffman, 1972). However, the data from the Quaternary do not record any systematic change in southern California (Chapter 4). Also, the long periods of constant depositional and structural styles, separated by relatively brief transitions from one strand to another, suggest major periodic reorganizations of the tectonic regime that are likely to produce discrete changes in the slip rates.

The history presented here specifically violates several proposed offsets across the San Andreas fault in southern California, and requires that the simple relationship between the modern San Andreas fault and

Figure 7-1 - Accumulation of slip on the San Andreas system in southern California. The lower box summarizes the slip data for the San Andreas fault southeast of its junction with the San Jacinto fault during the last 15,000 years (Chapter 2). The middle box summarizes the Quaternary slip data for the San Andreas fault (Chapter 4), NW of its junction with the San Jacinto fault (6 square points) and SE of the junction (2 round points). For comparison, the small box in the lower left corner represents about four times the record presented in the lowest box. The upper box represents the long-term history of the system: 160 km of offset on the modern San Andreas fault in the last 5 my, 60 km of offset on the San Gabriel fault between 11 and 5 my, about 100 km of offset on either the North Branch or the San Francisquito-Fenner-Clemens Well fault during the Middle Miocene. The box in the lower left corner of the uppermost box represents the portion of the record presented in the middle box. The data are inferred to be the result of an initially slow period of activity, followed by a 37 mm/yr since the opening of the Gulf of California 5 my ago. During the Quaternary, the San Andreas SE of its junction with the San Jacinto fault has accommodated about 25 mm/yr and the San Jacinto fault has been slipping at about 12 mm/yr.

the opening of the Gulf of California be reevaluated (a discussion of this latter issue is presented below). The approximately 240 km of offset of the Middle Miocene Mint Canyon Formation from its inferred source in the Chocolate Mountains (Ehlig et al., 1975) is violated by the story presented here. However, both Powell (1981) and Matti (in review) have questioned the uniqueness of the inferred source terrain.

This story also violates the 220 km offset of the Pliocene Hungry Valley Formation from its inferred source southeast of the San Bernardino Mountains (Ramirez, 1982). Ramirez notes that the clasts in the Hungry Valley Formation have general Mojave Desert affinity and are not particularly distinctive. However, the presence of an undated olivine basalt and marble-rich megaconglomerate on Liebre Mountain, that is inferred to be younger than the Hungry Valley Formation and is proposed to have been shed off the San Bernardino Mountains as they passed by across the San Andreas fault, indicates a source for the dated Hungry Valley southeast of the San Bernardino Mountains. Ramirez does not address the question of why the younger megaconglomerates are only on Liebre Mountain and not on the Hungry Valley Formation in the physically lower Ridge Basin. Ramirez (1982) and Crowell (1982a) both state that Liebre Mountain was high at the time of Hungry Valley deposition and that little or none of the Hungry Valley Formation has been eroded off the top; so the Hungry Valley area should have also received debris off the inferred high source of the San Bernardino Mountains as it passed by. The solution is that the megaconglomerates are syntectonic deposits associated with the late Miocene deformational event represented by the thrusting in the San Bernardino Mountains, of which Liebre Mountain was a part. The fact that they are on the upper plate of the thrust explains their abundance on Liebre

Mountain and their absence in the Hungry Valley Formation, which never passed by the San Bernardino Mountains.

This example illustrates the problem of using offset source terranes of rocks old enough to involve major assumptions about the geology and the paleogeography. A widely cited offset by the San Andreas fault in southern California that does not involve questionable source terranes is the latest Oligocene to earliest Miocene Vasquez Rocks-Diligencia Basin offset (Bohannon, 1975). This correlation is based on rock types, similar bounding structures of identical ages and matching paleogeographies across the fault. This offset is essentially the same as the proposed offset of the Mint Canyon from its inferred source. Therefore, if the Mint Canyon offset were correct there could be no activity across the San Andreas fault until the late Miocene, and the San Gabriel fault would have to be the first strand of the San Andreas fault system. However, both Powell (1981) and Silver (1982) have proposed other solutions to this "iron-clad" offset. Silver takes the Vasquez Rocks off the top of the Diligencia basin and moves them west with a thrust before being offset by the San Andreas fault; Powell first offsets the basins along the San Francisquito-Fenner-Clemons Well fault and then offsets them less than 200 km along the modern San Andreas fault.

The final piece of evidence for an early San Andreas fault is the record in central California; if the San Andreas was active during the Middle Miocene in southern California it must also have been active in central California and vice versa. Tertiary rocks older than late Early Miocene consistently record about 315 km of offset across the fault zone (e. g. Hill and Dibblee, 1953; Matthews, 1973). Progressively less offset across the San Andreas fault, beginning at some time during the late

Early Miocene, is inferred to indicate Middle Miocene activity on the San Andreas system (Hill and Dibblee, 1953; Hill, 1971; Dickinson et al., 1972; Huffman, 1972; Huffman et al., 1973). The timing of the Middle Miocene offsets are particularly important because the early offsets may have been contemporaneous with the San Gabriel fault and not an early San Andreas fault in southern California. Hill and Dibblee (1953), Hill (1971), Huffman (1972) and Dickinson et al. (1972) document up to 50 km less than the total offset across the San Andreas fault in rocks that are clearly Middle Miocene in age. The age assignments are based on benthic forams (early Mohnian) and molluscs (Santa Margaritian) and are correlated with the latest Barstovian or earliest Clarendonian in the vertebrate scale. These rocks correlate with the Mint Canyon Formation in the Ridge Basin, which predates the San Gabriel fault's activity (Crowell, 1982b). Even if the faunal time scales are stretched to allow the central California offsets to be contemporary with the Castaic Formation, which marks the onset of activity on the San Gabriel fault, the rocks in central California were already offset the amount of the total displacement across the San Gabriel fault (about 60 kms) by the time the San Gabriel fault started. However, the San Gabriel fault did not accumulate its total offset until the Pliocene. Even within the errors of the various relative time scales, there can be little doubt that the San Andreas fault in central California started well before the San Gabriel fault to the south.

Crowell himself (1973) acknowledged the discrepancy and suggested that earlier faults, such as the Clemens Well fault could account for the difference. Powell (1981) was the first to completely elucidate the possibility that the Clemens Well-Fenner-San Francisquito fault was the earliest branch of the San Andreas system. While I inferred, from the

relationships in the San Bernardino Mountains, that the North Branch could have served this role, the evidence for a Middle Miocene San Andreas fault, whichever fault it was, is strong.

Surprisingly, the issue of the early San Andreas activity becomes crucial to the understanding of the modern San Andreas fault, its relationship to the opening of the Gulf of California, and the coastal system proposed in Chapter 5. If the pre-San Gabriel San Andreas fault did not exist, and the total 240 to 260 km of offset across the San Andreas fault have occurred during the last 5 my, the activity on the San Andreas during the Pliocene must have been extremely high. Only about 75 km of offset have occurred across the combined San Andreas and San Jacinto faults in the last 2 million years (Fig. 1, see Chapter 4 for details). Therefore, the San Andreas fault between 5 and 2 my ago must have had a slip rate of about 60 mm/yr, far greater than the rate at any other time during its history, and barely within the errors of the slip rate across the total plate margin (Minster and Jordan, 1978; 1984). The San Andreas fault would have briefly assumed the total plate motion and has since returned some of it to other structures. While this scenario is extremely unlikely, until unquestionable offsets between the earliest Miocene and the Quaternary are found it must be considered. Possible support for this alternative is discussed below, after the discussion of the modern San Andreas fault.

Uplift associated with the San Gabriel phase of the San Andreas system

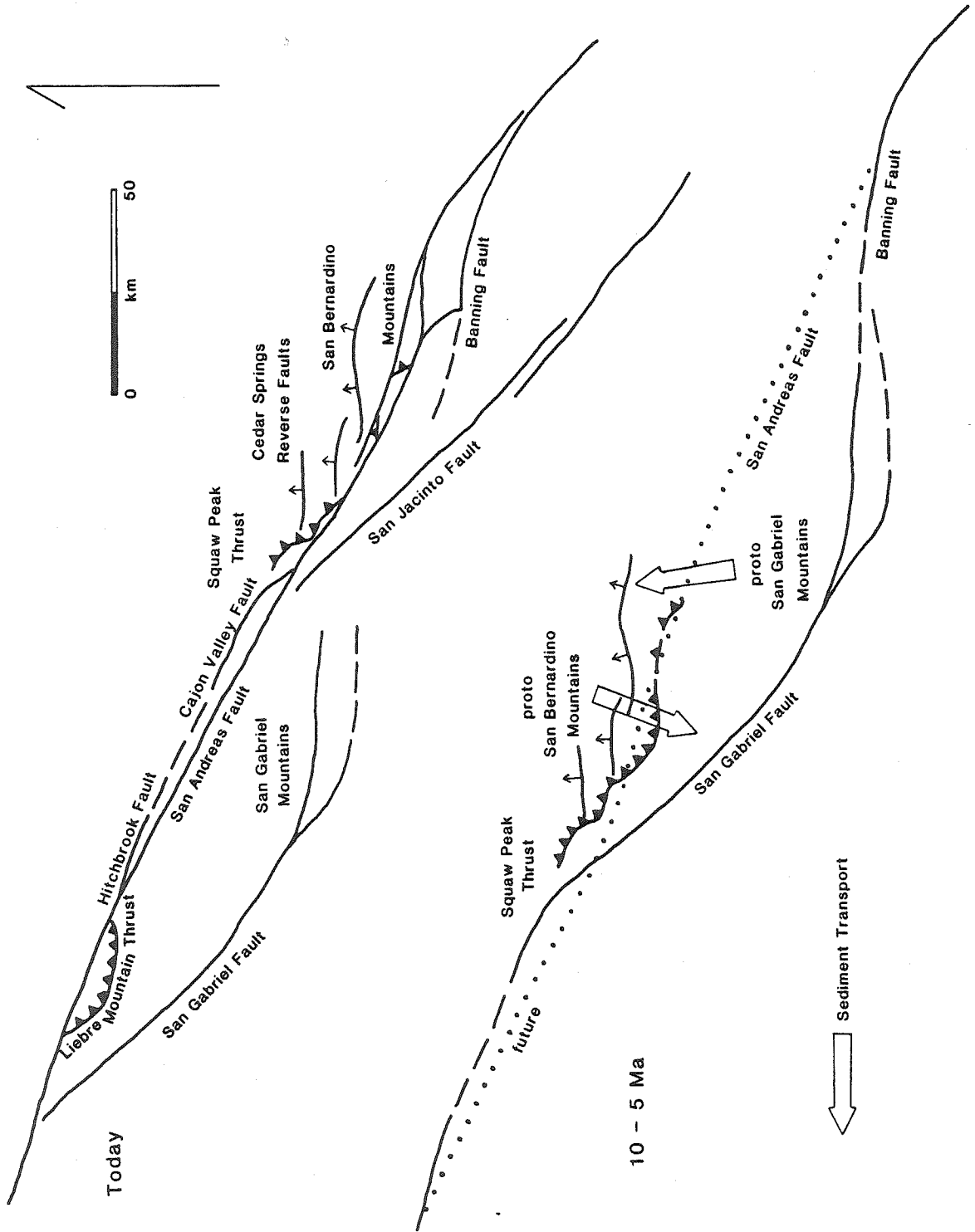
Deposition in both the Cajon Punchbowl and the Crowder Formations ended at the beginning of the Late Miocene. No sediments are preserved in Cajon Pass from that time until the deposition of the Phelan formation (beginning about 4.2 my ago in its type area, Chapter 4). Within this

unconformity the proto-San Bernardino Mountains were uplifted in the Cajon Pass-southwestern San Bernardino Mountains area, and much of the Crowder Basin and significant amounts of bedrock were eroded and the debris was shed to the south. The uplift was due to thrusting and reverse faulting associated with the Squaw Peak thrust system discussed in Chapter 6. To the east, deposition occurred during this time period in the Santa Ana Sandstone basin. In fact, during the late Miocene it was a syntectonic intermontane basin receiving sedimentary debris from both the north and south, and, locally basaltic volcanism (Sadler, 1985). Sadler (1985) has found clasts from the Sierra Pelona in these Late Miocene sediments, suggesting that the central San Gabriel Mountains were a high source at that time.

The relatively high western San Bernardino Mountains, according to the story developed above, were in the appropriate place to shed debris into the Ridge Basin during the Middle Miocene. Crowell (1982b) notes that most of the Ridge Route Formation, filling the Ridge Basin, was derived from the northeast across the San Andreas fault. If the western San Bernardino Mountains were north of the Ridge Basin, as the proposed Liebre Mountain-San Bernardino Mountains correlation requires, the Santa Ana Sandstone also would have been in the correct place to receive material from the central San Gabriel Mountains, including the Sierra Pelona, as proposed by Sadler (1985). These tentative correlations of likely source terranes lend additional credence to the Liebre Mountains-San Bernardino Mountains offset and are summarized in Figure 2.

Deposition in these basins was contemporaneous with the activity on the San Gabriel fault (Crowell, 1982b) and Squaw Peak thrust system (Chapter 6). There could not have been significant activity on the San Andreas

Figure 7-2 Paleogeography of the "proto" Transverse Ranges and their inferred offset across the modern San Andreas fault. This reconstruction is derived from the proposed offset of the San Bernardino Mountains area from the Ridge Basin - Liebre Mountain area, and the distribution of upland areas and basins receiving sediments during the Late Miocene.



fault or any other fault north of the Ridge Basin because the thrusting remained in the same place northeast of Ridge Basin for at least several million years (Ensley and Verosub, 1982). The thrusting in the San Bernardino Mountains and at the base of Liebre Mountain, which was at that time part of the San Bernardino Mountains, was very similar to the later Quaternary deformation (Chapter 6). The evidence suggests a N-S or NNE-SSW axis of convergence, essentially the same as the Quaternary deformation across the Transverse Ranges. This observation raises several important questions about the Transverse Ranges before the opening of the Gulf of California and the beginning of the modern San Andreas system.

First, the San Gabriel fault was contemporaneous with significant thrusting and uplift to the northeast (the Squaw Peak-Liebre Mountain system), the southwest in the Ventura Basin (e.g., Canton fault Crowell, 1982b), and uplift to the northwest, in the source area of the Violin Breccia (Crowell, 1974). All of this compressional deformation can be viewed in the context of the more easterly trend of the San Gabriel fault through the Transverse Ranges, with respect to the motion between the North American and Pacific plates and the trend of the fault in central California to the north (Fig. 2). The geometry of the situation appears to have been very similar to that existing for the San Andreas through the Transverse Ranges today. In this context, it is worth considering whether the Ridge Basin is an extensional feature at all.

Crowell (1974) explains the compression to the northwest and the opening of the Ridge Basin as related features caused by an S-shaped bend in the San Gabriel-San Andreas fault. Compression occurred within the bend and extension outside of it. This model cannot include the Liebre Mountain thrust, which is outside the bend bounding the eastern margin

of the basin. Link (1982) extends this model to include the Liebre Mountain thrust, but it is clear from Crowell (1974) that the Liebre Mountain thrust is not part of the compression in the bend, but is located where the basin pulls away on the northeastern side (Crowell, 1974, Fig. 5; also, 1982b, Fig. 8).

While Crowell maps the Liebre Mountain fault as a thrust (e.g., Crowell, 1982b), in cross sections he shows it steepening at depth and apparently views it as a minor feature in forming the basin. The correlation of the Liebre Mountain thrust with the Squaw Peak system in the San Bernardino Mountains suggests that the fault does not steepen at depth and is not a minor feature. A possible alternative to the pulling away and stretching of the basin may be that the basin formed in a compressional setting, perhaps by flexural downwarping in front of the Squaw Peak-Liebre Mountain thrust. This would make the style of deformation similar to the contemporaneous and nearly adjacent eastern Ventura and Santa Ana Sandstone (Sadler, 1982; 1985; this thesis, Chapter 6) basins.

This mechanism is consistent with the formation of basins throughout the Transverse Ranges today. In fact, Crowell (1974) used the San Bernardino basin as a modern example of this mechanism. I suggest that a similar mechanism may have formed the Ridge Basin. Just as the strike slip San Andreas fault traverses the modern Transverse Ranges, the San Gabriel fault could have traversed the actively compressing late Miocene Transverse Ranges. Also, like the San Andreas fault today, the San Gabriel fault was essentially strike slip and compression took place on secondary thrusts and across downwarping basins, like the those in the Transverse Ranges province today.

The inferred cause of the N-S convergence was the "anomalous" trend

of the San Gabriel fault through southern California, just as the current Transverse Ranges are related to the "anomalous" trend of the San Andreas through the Transverse Ranges. This similarity motivates the second point about the Transverse Ranges during the late Miocene: does the similarity of structural style indicate that the relatively E-W trend of the San Andreas system through the Transverse Ranges existed at this time, or was there some other reason for the compression occurring then?

Many workers have suggested that the San Andreas fault was once straight and has since been bent or deformed into its trend through the Transverse Ranges (e.g., Hill and Dibblee, 1953; Garfunkle, 1974; Bohannon and Howell, 1982). If this were the case, the similarity in the deformation of the late Miocene Transverse Ranges with the current tectonics would be coincidence, because everything was oriented differently at that time.

Paleomagnetic data from the Ridge Basin (Ensley and Verosub, 1982) and Cajon Pass (Weldon et al., 1984) effectively rules out the rotation hypothesis for the central and eastern Transverse Ranges. The late Early through early Late Miocene Crowder Formation (Fig. 3) have not been rotated more than a few degrees (Fig. 4). The Late Miocene Ridge Route sediments have not been rotated either (Ensley and Verosub, 1982). The Pliocene and Pleistocene sediments in Cajon Pass (Chapter 4) contain no evidence of significant rotations either, so scenarios involving counteracting rotations to return the Middle or Late Miocene sediments back to a position of no net rotation (e.g., Ehlig, pers. comm., 1984) are also ruled out. The lack of rotation of sediments at both ends of the "anomalously" trending section of the San Andreas system effectively pins it into its current geometry since the late Miocene, and probably

Figure 7-3 Magnetic stratigraphy of the type Crowder Formation. Units 1-3 were collected and analysed by Doug Winston of USC and units 4-5 were collected and analysed by Ray Weldon, Joe Kirschvink and colleagues at Caltech (Weldon et al., 1984). The match with the absolute polarity scale is based on the ages of vertebrate fossils (Reynolds, 1984) at the two localities indicated. Regardless of the details of the match, there can be little doubt that the sediments span a significant portion of the Middle Miocene.

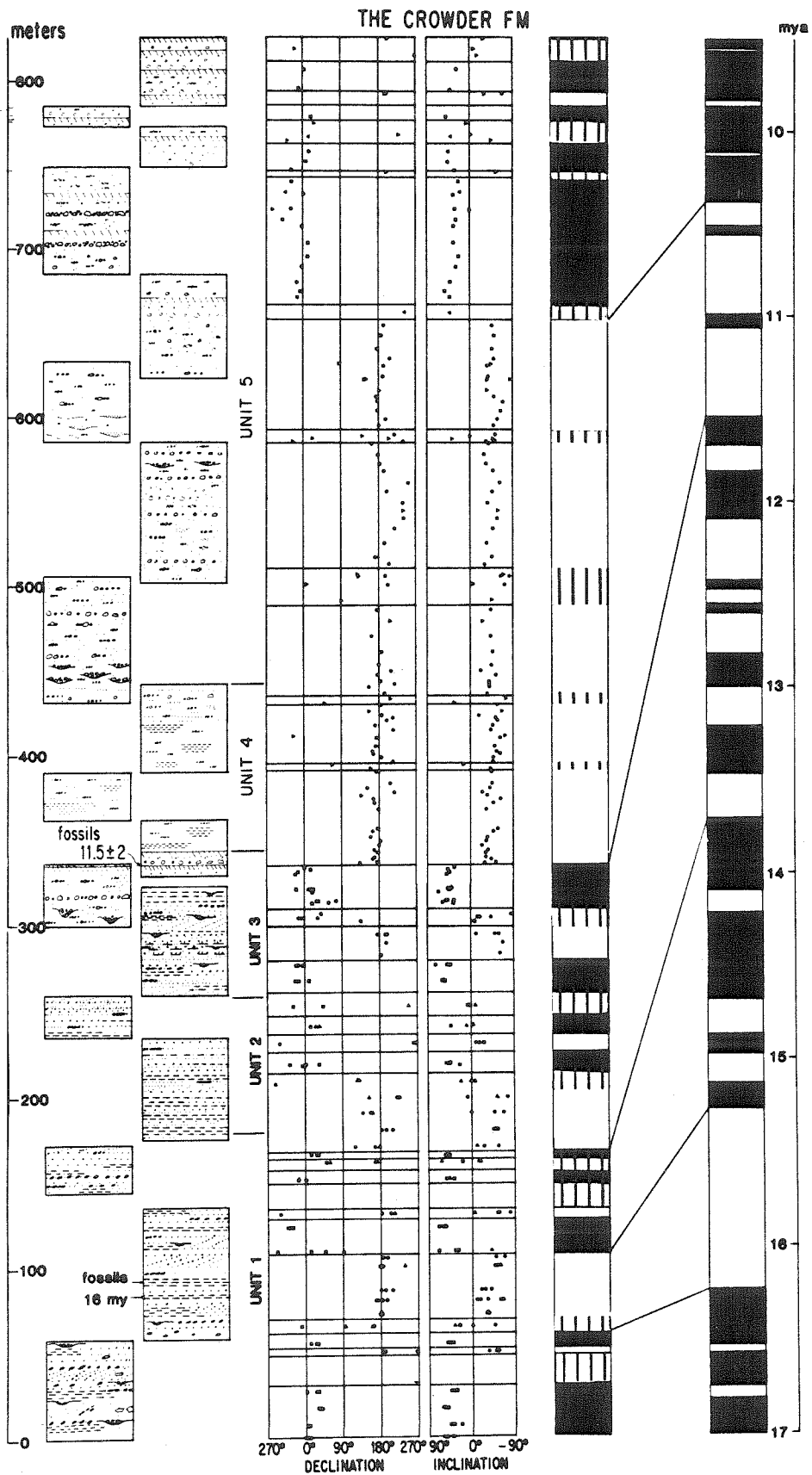
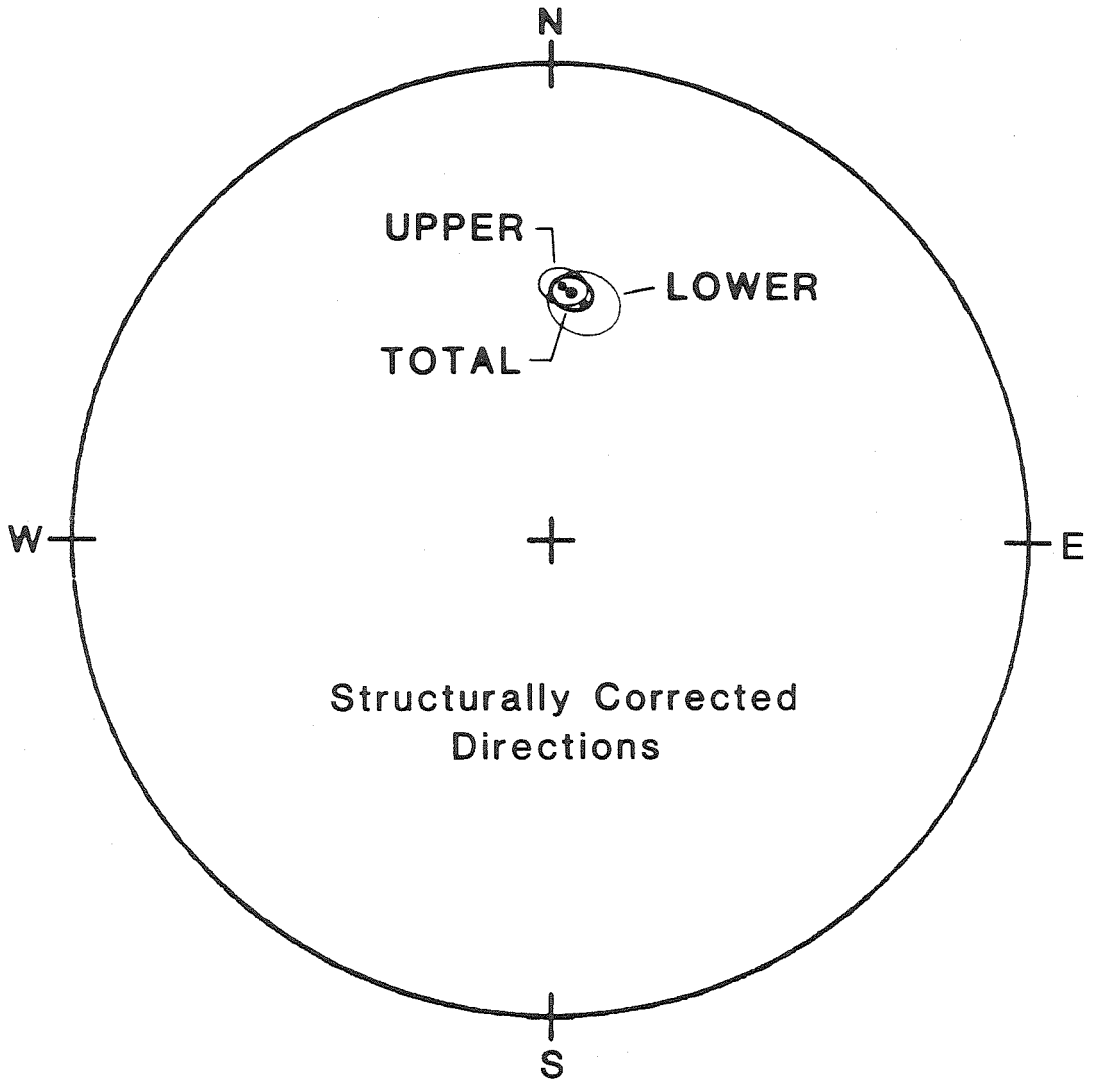


Figure 7-2

Figure 7-4 Declination and inclination of the Crowder Formation based on 199 samples that preserve stable primary remanence (based on the criteria described in Chapter 4). The upper and lower Crowder sediments preserve indistinguishable remanent magnetization directions and indicate little or no rotation since the Middle Miocene. The low inclination is probably due to depositional inclination error in these fluvial sediments.

CROWDER FORMATION



	<u>DECLINATION</u>	<u>INCLINATION</u>	<u>BINGHAM 95% ANGLE</u>	<u>OVAL AZIMUTH</u>	<u>NUMBER OF SAMPLES</u>
UPPER	2.6	45.6	3.2 , 4.0	71.1	100
LOWER	7.6	48.4	5.3 , 6.0	58.5	99
TOTAL	4.7	46.8	3.0 , 3.5	63.3	199

throughout the total span of its activity. In other words, the trend of the San Andreas fault system through the Transverse Ranges is a primary feature of the San Andreas system and has certainly existed since the late Miocene. The left-lateral activity on the Garlock, near the northern end of the Transverse Ranges, and the Pinto Mountain and related faults, near the southern end, has locally lengthened and modified the "anomolous" segment through time, but left-lateral activity has not been of sufficient magnitude to have created it, and inferred rotations have not occurred. The implications of the later modifications are discussed below.

The Pliocene San Andreas fault

Based on the record in the Ridge Valley (e.g., Crowell, 1962; 1982b) and the Gulf of California (Larson, et al., 1968; Atwater, 1970; Curry and Moore, 1984) the modern San Andreas fault is generally believed to have originated at about the Mio-Pliocene boundary, about 5 my ago. In Cajon Pass the Mio-Pliocene boundary is associated with the end of the late Miocene thrusting and the beginning of Plio-Pleistocene deposition (Chapters 4 and 6). There is very little record of vertical tectonic activity along the San Andreas fault or in the San Bernardino Mountains during the Pliocene. Deposition was localized to several narrow east-west trending basins, probably created by the Late Miocene thrusting.

There are few (if any) recognized offsets across the San Andreas fault involving Pliocene rocks. Also, with the exception of relatively minor deposits of coarse debris in the Hungry Valley Formation in the Ridge Basin (Crowell, 1982a; Ramirez, 1982), locally in the Phelan formation in the Cajon Pass area (Foster, 1980; this thesis), and deposition in the San Timoteo Formation (Matti and Morton, 1975; Morton and Matti, 1979) south of the Transverse Ranges, there is little evidence of major

uplift in the central Transverse Ranges along the San Andreas fault during the Pliocene. This is surprising, in light of the observation that the San Andreas must have had its "anomalous" trend and was accumulating slip at least as fast as it did during the Quaternary.

It appears that the switch from the San Gabriel to the San Andreas fault "relieved" much of the compression contemporaneous with the San Gabriel fault. It is tempting to suggest that "relieving" the compressional stress associated with the late Miocene San Gabriel phase of the San Andreas system was the reason for the activity switching from the San Gabriel to the San Andreas fault. However, this is hard to understand in the context of N-S regional shortening because relative to the plate motion the San Andreas is only slightly more favorably oriented than the San Gabriel fault. Also, a marked increase in slip rate accompanied the switch, but there appears to have been a decrease in vertical deformation. It is possible that the counterclockwise rotation of southern California, that currently "relieves" most of the convergence across the central Transverse Ranges (discussed in Chapter 5), began at this time and the local geometric complexities that are currently uplifting different parts of the central and eastern Transverse Ranges (Chapter 5) had not yet developed.

The Quaternary San Andreas fault

The tectonic and depositional styles in Cajon Pass changed again during the early Quaternary, with the beginning of the uplift of the San Bernardino Mountains and, perhaps, renewed uplift in the San Gabriel Mountains (Chapters 4 and 6). Convergent activity and uplift appears to have increased throughout the Transverse Ranges at that time. The San Bernardino and eastern San Gabriel Mountains rapidly became sources of

coarse debris during the early Quaternary (Chapters 4 and 6), the convergence in the western Transverse Ranges accelerated (Yeats, 1983), the Ridge Basin began uplifting (Crowell, 1982b), and activity along the south margin of the San Gabriel Mountains may have accelerated. This pulse of compressional deformation has been called the Pasadenan Orogeny (Stille, 1936). The change from the relatively quiet Pliocene to the Quaternary may be related to an actual strand-switching event in the San Andreas system (Matti, in review); at least several elements have changed in relative importance.

The San Jacinto fault probably has been more active in the Quaternary than the Pliocene. The data presented on Figure 1 suggest that the combined slip rate of the San Andreas and San Jacinto faults did not change significantly during the last 5 my. However, extrapolating the Quaternary rate on the San Jacinto fault (10 mm/yr, Sharp, 1981; Chapter 4) back 5 my would produce far more offset than the 29 km (Hill, 1984) that the fault has accumulated. This observation suggests that the San Jacinto fault may not have been as active during the Pliocene or that it originated during the late Pliocene. Evidence presented by Hill (1984) suggests that deposition began in valleys formed by the San Jacinto fault at about 4 to 5 my ago, essentially coincident with the modern San Andreas fault; so, the fault must have begun very slow and has since speeded up.

The increase in activity on the San Jacinto fault is almost certainly associated with the rapid uplift of the eastern San Gabriel Mountains. As discussed in Chapters 4 and 5, the San Andreas and San Jacinto faults converge at a 15° angle (Fig. 5). Because the motion on the San Jacinto fault is not parallel to the San Andreas, compression must occur where the slip is added to the San Andreas fault to the northwest, uplifting the eastern

Figure 7-5 - Active deformation near the junction of the San Jacinto and San Andreas faults. Secondary deformation north of the San Andreas fault can be broken into zones of normal faulting (north of Devore) and reverse faulting and active folding (between Valyermo and Wrightwood and southeast of Lake Arrowhead). These zones correspond to changes in trend of the San Andreas fault that are related to right lateral activity on the San Jacinto fault. As discussed in Chapter 4, these zones move with the San Jacinto fault at the slip rate on the San Andreas fault.

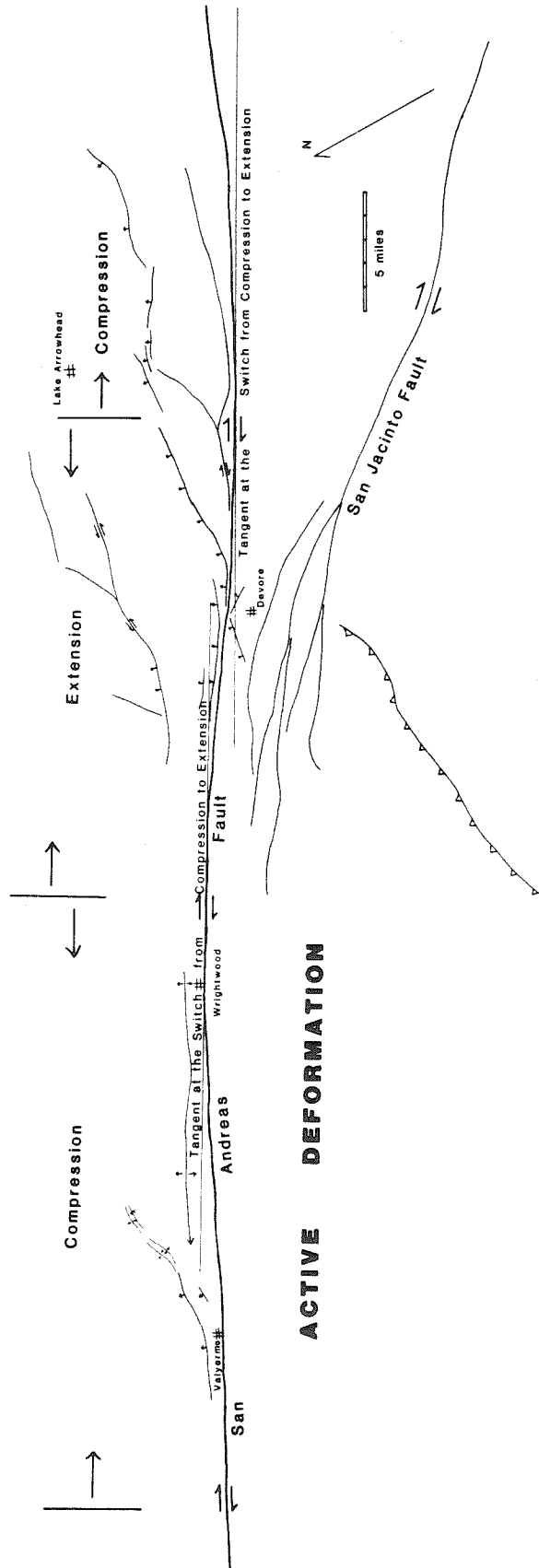


Figure 7-3 (Also Plate 10)

San Gabriel Mountains in the southwest elbow of the junction. The San Jacinto is also deforming the San Andreas fault where its motion is added to the San Andreas (Fig. 5). The deformed San Andreas fault apparently then causes deformation north of the fault.

Active minor faults and folds, mapped north of the San Andreas fault, exactly reflect the trend of the San Andreas fault (Fig. 5). Compression occurs northwest of the junction with the San Jacinto (note that the exact junction cannot be found on the ground, Morton, 1975), compression occurs southeast of the junction and compression begins again at about Lake Arrowhead, as the San Andreas turns more easterly and approaches San Geronimo Pass. Tangents to the San Andreas fault, where the secondary deformation switches from extension to compression, are parallel and match the broad arcuate trend of the San Andreas discussed in Chapter 5 (Fig. 5-3).

As discussed in Chapter 4, the location of the San Jacinto moves, relative to the north side of the San Andreas fault, at the rate of slip of the San Andreas fault southeast of their junction. Therefore, the deformation caused by the San Jacinto migrates northwest, north of the fault. At the moment it is uplifting the area between Wrightwood and Valyermo; a million years ago it was uplifting the area between Lake Arrowhead and Cajon Pass, that is now being extended. The deformation along the San Andreas fault can be interpreted as occurring above a north-dipping lateral ramp (Chapter 6). The deformation of the surface expression of the San Andreas fault reflects a broad north dipping ramp or "keel" under the Mojave Desert north of the junction with the San Andreas fault (Chapter 6). The movement of this "keel" progressively uplifts the San Bernardino and San Gabriel Mountains, north of the San Andreas fault, as they move across the lateral ramp of the deformed San

Andreas fault, much like a snowplow lifts and overturns snow by lateral motion across the sloping blade.

This style of deformation began during the early or middle Pleistocene and appears to be contemporaneous with a decrease in activity along the North Frontal fault system of the San Bernardino Mountains (Chapter 6) and the beginning of the very rapid convergence in the Banning Pass area and uplift of the San Gorgonio Massif (Fig. 1-1). Because the uplift in the San Gorgonio Pass area has not migrated through the San Bernardino Mountains, its cause must be "attached" to the north side of the San Andreas fault. The deformation associated with the San Jacinto is on the south side of the San Andreas fault because it moves on the north side. The two areas of most active uplift were essentially across the San Andreas fault from each other when they started, suggesting a related cause. The earliest phase of this pulse of deformation was the northward thrusting of the San Bernardino Mountains, uplifting the central plateau and creating its northern escarpment (Chapter 6).

The uplift of the high central Transverse Ranges (includes the San Bernardino and eastern San Gabriel Mountains) appears to have been due to left lateral faulting near San Gorgonio Pass, that modified the smooth arcuate trace of the San Andreas fault, that was the solution to the late Miocene compressional event. The arcuate traces of the San Andreas fault north and south of San Gorgonio Pass are offset about 30 km left laterally. If the Pinto Mountain and other left lateral faults near San Gorgonio Pass experienced significant activity during the Pliocene, the trace of the San Andreas would have been progressively "offset", causing compression across the discontinuity, just as the San Jacinto causes compression north of the San Andreas today (Fig. 5). The first evidence of large-scale com-

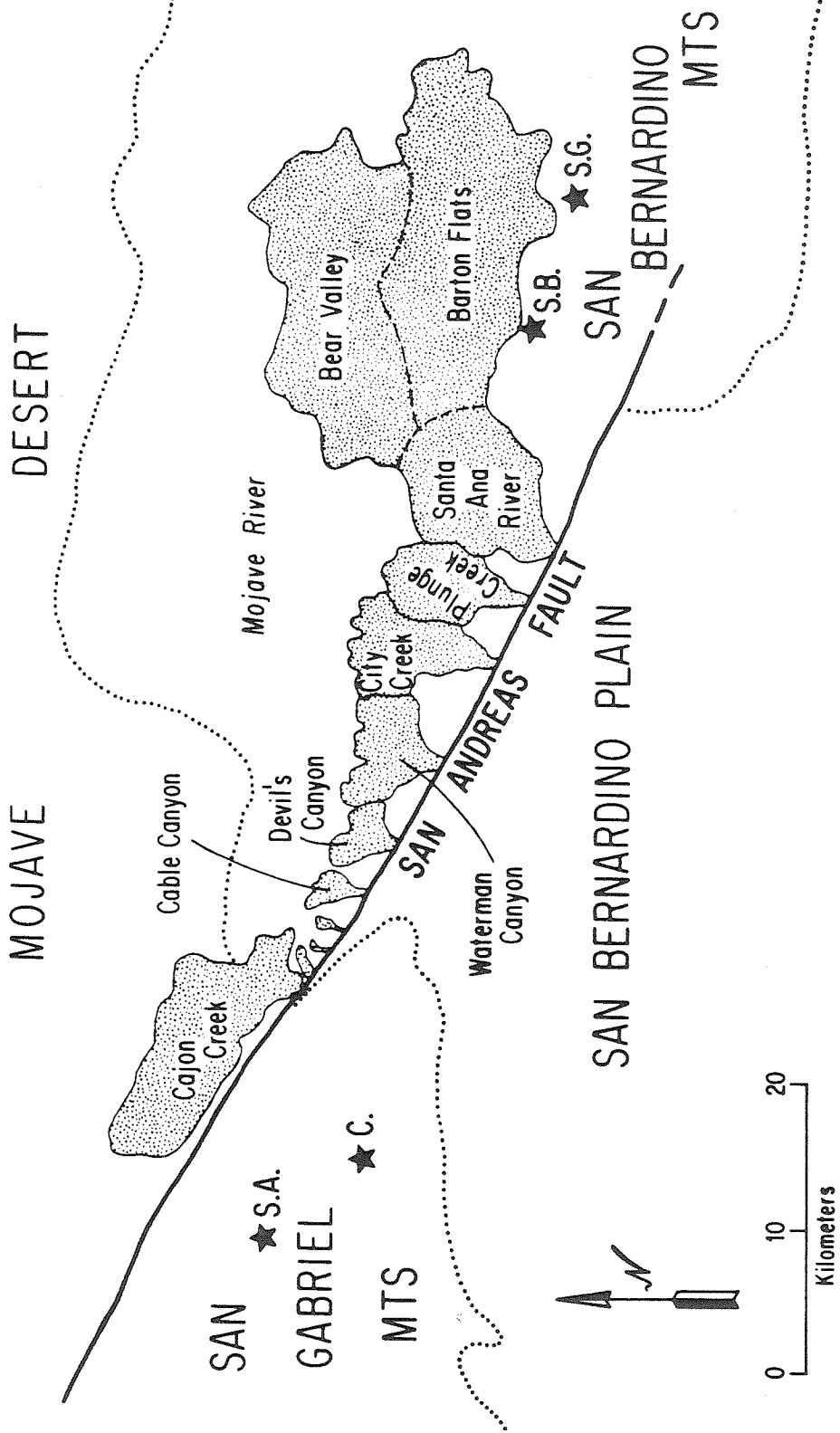
pression due to this deformation outside the fault zone is the uplift of the central plateau of the San Bernardino Mountains and the creation of the North Frontal fault system (Meisling, 1984; this thesis, Chapter 6). Soon thereafter, in the early or middle Pleistocene, activity decreased on the northern front and the area of most active deformation shifted to the south (Chapter 6).

Since the shift to the south, deformation has broken into two parts, one portion remaining at the step in the San Andreas fault at San Geronio Pass and the other migrating with the San Jacinto fault, as described above. In effect the structural knot is being offset. The broad uplift of the early Quaternary central Transverse Ranges became localized and the mass has since been offset about 50 km. The lateral offset produced the steep northern escarpment of the San Gabriel Mountains (Chapter 4) and the steep southwestern escarpment of the San Bernardino Mountains.

The progressive nature of this offset can be seen in the progressive offset of alluvial fans off the northern San Gabriel Mountains (Chapter 4) and the geomorphology of the streams eroding into the southwestern escarpment of the San Bernardino Mountains (Fig. 6). The drainages become progressively more mature to the southeast because that portion of the San Bernardino Mountains was offset from behind the San Gabriel Mountains first. If the ranges are restored at the slip rate of the San Andreas fault, that is offsetting them, this style of deformation can be estimated to have begun during the early Pleistocene, as determined independently above. The central Transverse Ranges are now essentially two different ranges, despite their having a common origin. As noted in Chapter 4, in another million years they will be completely separated, and a common origin would be difficult to infer.

Figure 7-6 - Major drainages developed into the southwestern escarpment of the San Bernardino Mountains. Cajon Creek and upper Santa Ana River are anomalously large due to capture of preexisting drainages and erosion into poorly consolidated late Cenozoic sediments. The drainages expanding into bedrock are progressively more mature to the southeast, indicating progressive development of the escarpment by lateral displacement of the San Bernardino Mountains from behind the San Gabriel Mountains to face the San Bernardino Plain. The high eastern San Gabriel Mountains are inferred to have been adjacent to the high southern San Bernardino Mountains when uplift began in the early Quaternary.

Major Drainages of the San Bernardino Mountains



The change from broad uplift to localized deformation along the San Andreas fault may be associated with the increase in the activity of the San Jacinto fault. While increasing the activity on the San Jacinto fault increases compressional deformation near its junction with the San Andreas fault, it decreases compressional activity across the step in the San Andreas fault in San Gorgonio Pass by reducing the slip rate on the San Andreas fault. Perhaps the 2.5 to 1 ratio of activity between the San Andreas and the San Jacinto faults, that has existed for the last 700,000 years (Chapters 2 and 3), is the "balance" that allows the strike slip motion of the San Andreas system to occur across the step with the least compression.

The step in the San Andreas fault in San Gorgonio Pass, and its relation to the San Jacinto fault, apparently caused most of the compressional tectonics in the high central Transverse Ranges. Other areas in the Transverse Ranges have also experienced higher rates of deformation during the Quaternary. As noted in Chapter 5, the western Transverse Ranges and the area near the northern Big Bend are currently loci of very active compressional deformation. Both of these areas have experienced accelerating deformation during the Quaternary (Big Bend: Davis, 1984; western Transverse Ranges: Yeats, 1983).

Left-lateral activity on the Garlock fault or rotation of the Sierra-San Joaquin block (see Chapter 5) may be making it progressively more difficult for motion on the San Andreas fault to "turn the corner" of the Big Bend. Increasing activity in the western Transverse Ranges may be due to the growth of the step in the coastal system that is compressing the area (Chapter 5). As southern California translates northwest about the arcuate trace of the San Andreas, and the Great Basin opens, moving cen-

tral California farther west, the step in the coastal system grows and increasing compression occurs as the right lateral faults to the north and south of the western Transverse Ranges become more misaligned.

In conclusion, it appears that the San Andreas system has maintained an essentially constant rate since it became active during the early Pliocene. However, compressional deformation associated with the system has increased dramatically, particularly during the Quaternary. It appears that the compressional activity is a consequence of the fact that the solution to the late Miocene compressional event, the reactivation or initiation of the modern San Andreas through the Transverse Ranges, is encountering increasing problems accommodating the strike slip activity through the system. All of the areas of very active uplift in the Transverse Ranges and the greater importance of the San Jacinto fault can be explained in this context.

The relationship of the San Andreas system to the Gulf of California

The two most widely believed "facts" about the San Andreas fault are its 300 km of offset and its association with the opening of the Gulf of California, which also has about 300 km of offset. However, the clear physical connection and similarity of total offsets must be balanced against the apparent conflict in their timing. It is very important to resolve the fact that the opening of the Gulf is reported to have begun only 5.5 my ago (Curry and Moore, 1984) with the fact that the San Andreas fault system began at least 11 my ago and perhaps as early as 20 my ago.

The most obvious solution is that the similarity in offset is simply a coincidence. The fact that the San Andreas fault system currently only accommodates about 2/3 of the plate motion (Chapters 2), and has done so throughout the Quaternary (Chapter 4) and probably throughout the whole

history of the Gulf of California, as discussed above, supports this possibility. Earlier activity, however, must have gone somewhere, and some mechanism must be found to remove some of the activity at the mouth of the Gulf before it reaches the San Andreas fault. While the former objection cannot be addressed until more work is done on the Miocene history of the Gulf area, part of the current activity at the mouth of the Gulf of California has to cross the Baja Peninsula to the coastal system in southern California (Chapter 5). This activity may be documented by the high activity on the Aqua Blanca and other faults in northern Baja California (Allen et al., 1960). However, the Aqua Blanca has not been mapped completely across the peninsula and, despite its high rate of Quaternary activity, does not appear to have enough cumulative displacement to have accommodated 1/3 of the plate motion since the beginning of the opening of the Gulf (Allen, et al., 1960; Lee Silver, pers. comm. 1985). Also, the continuity of the Cretaceous batholith and its geochemical and geochronological zonation down most of the Baja Peninsula may rule out large cumulative offsets (Lee Silver, pers. comm., 1985).

The improbability of large cumulative offsets across the Baja Peninsula may be evidence for an alternative model mentioned in the first section of this chapter. If the Liebre Mountain - San Bernardino Mountains correlation is not valid, and the evidence for an early San Andreas is misinterpreted, the Pliocene San Andreas must have accommodated the total plate motion for the period between 5.5 and 2 million years ago, and slowed at the beginning of the Quaternary to its current value. Perhaps geometric complexities that led to the Quaternary uplift in the Transverse Ranges also forced a fraction of the plate motion back offshore. In this case the high activity in Baja and the low cumulative offset would be ex-

plained, as would the extremely high rates of convergence in the western Transverse Ranges during the Quaternary discussed above. Only unquestionable offsets of Pliocene rocks across the San Andreas, the discovery of more cumulative displacement than expected across Baja, or an earlier history of activity in the Gulf can resolve these two possibilities.

Implications of the model for seismic hazards

Seismic hazards are related to the instantaneous tectonic setting, which is unlikely to change rapidly enough to affect the location or timing of seismicity in time frames of human interest. However, much of what we believe about the active San Andreas fault system is based on extrapolations of the past to the present. So consistency between geologic observations and our tectonic framework is very important. The primary importance of the San Andreas fault is based, to a large degree, on its inferred role as the principal fault in the plate boundary. The proposed coastal system (Chapter 5), which implies a far greater seismic hazard associated with the offshore region than previously believed, is based on the refinement in our understanding of the overall system. The history presented here also implies that different portions of the Transverse Ranges have very different levels and styles of tectonic activity which can help understand their associated seismic hazard. Also, the history of the San Andreas presented here places compressional tectonics in a far more important role than usually inferred.

As a specific example it may be possible, by locating the portions of major strike slip faults that are deformed or affected by compressional tectonics, to focus study on areas that may be relatively strong portions of the fault plane that may control the origin and propagation of the rupture that causes major earthquakes. For example, the last 2 earthquakes

on the San Andreas fault show an interesting relationship to areas that are currently experiencing compression across the fault. As discussed in Chapter 2, the 1857 rupture stopped between Wrightwood and Cajon Pass, near the junction between the San Andreas and the San Jacinto faults, and was centered at the junction between the San Andreas and the Garlock fault, where very active compressional deformation is occurring (Chapter 5). The previous earthquake is believed to have stopped near the junction of the San Andreas and the Garlock faults and was centered in the structurally complex region between Cajon and San Gorgonio Passes, that contains the locus of Quaternary uplift and compressional deformation in the central Transverse Ranges. The recognition of these key areas and their characterization can only be carried out in the broader context of our understanding of the entire system.

References Cited

- Allen, C. R., Siver, L. T., and Stehli, F. G., 1960, Agua Blanca fault—a major transverse structure on northern Baja California, Mexico, *Geol. Soc. Amer. Bull.*, v. 71, p. 457-482.
- Atwater, T., 1970, Implications of plate tectonics for the Cenozoic tectonic evolution of western North America, *Geol. Soc. Amer. Bull.*, v. 81, p. 3513-3536.
- Barrows, A. G., 1980, Geologic map of the San Andreas fault zone and adjoining terrane, Juniper Hills and vicinity, Los Angeles County, California, *Cal. Div. Mines and Geology*, OFR - 80-2 LA.
- Barrows, A. G., 1979, Geology and fault activity of the Valyermo segment of the San Andreas fault zone, Los Angeles County, California, *Cal. Div. Mines and Geology*, OFR - 79-1 LA, 49 p.
- Bohannon, R. G., 1975, Mid-Tertiary conglomerates and their bearing on Transverse Range tectonics, southern California, in *San Andreas fault in southern California: A guide to San Andreas fault from Mexico to Carrizo Plain*, ed. Crowell, J. C., *Cal. Div. of Mines and Geology*, Spec. Rpt. 118, p. 75-82.
- Bohannon, R. G. and Howell, D. B., 1982, Kinematic evolution of the junction of the San Andreas, Garlock and Big Pine faults, California, *Geology*, v. 10, p. 358-363.
- Crowell, J. C., 1982a, Pliocene Hungry Valley Formation, Ridge Basin, southern California, in *Geologic history of Ridge Basin, southern California*, eds. Crowell, J. C. and Link, M. H., *Pac Sect. S. E. P. M.*, Guidebook, p. 143-149.
- Crowell, J. C., 1982b, The tectonics of Ridge Basin, southern California, in *Geologic history of Ridge Basin, southern California*, eds. Crowell,

- J. C. and Link, M. H., Pac. Sect. S. E. P. M. Guidebook, p. 25-41.
- Crowell, J. C., 1981, An outline of the tectonic history of southeastern California, in The geotectonic development of California, ed. Ernst, W. G., Rubey Volume 1, Prentice-Hall, Englewood Cliffs, N. J., p. 583-600.
- Crowell, J. C., 1974, Sedimentation along the San Andreas fault, California, in Modern and ancient geosynclinal sedimentation, eds. Dott, R. H. S. E. P. M. Spec. Pub. # 19, p. 292-303.
- Crowell, J. C., 1973, Problems concerning the San Andreas fault system in southern California, in Proceedings of the conference on tectonic problems of the San Andreas fault system, Stanford Univ. Pubs. Geol. Sci., v. 13, p. 368-373.
- Crowell, J. C., 1962, Displacement along the San Andreas fault, California, Geol. Soc. Amer. Spec. Paper 71, 62 p.
- Curry, J. R. and Moore, D. G., 1984, Geologic history of the mouth of the Gulf of California, in Tectonics and sedimentation along the California margin, eds. Crough, J. K., and Bachman, S. B., Pac. Sect. S. E. P. M., v. 38, p. 17-35.
- Davis, T., 1984, Cenozoic structural development of the north-central Transverse Ranges and southern margin of the San Joaquin Valley, Geol. Soc. Amer., 97th Annual Meeting, Abstracts with Programs, v. 16, p. 484.
- Dibblee, T. W., Jr., 1975, Late Quaternary uplift of the San Bernardino Mountains on the San Andreas and related faults, in San Andreas fault in southern California: A guide to San Andreas fault from Mexico to Carrizo Plain, ed., Crowell, J. C., Cal. Div. of Mines and Geology, Spec. Rpt. 118, p. 127-135.
- Dibblee, T. W., Jr., 1968, Displacements on the San Andreas fault system

- in San Gabriel, San Bernardino, and San Jacinto Mountains, southern California, in Proceedings of Conference on geologic problems of the San Andreas fault system, Stanford Uni. Pubs. Geol. Sci., v. 11, p. 260-278.
- Dickinson, W. R., Cowan, D. S., and Schweickert, R. A., 1972, Test of the new global tectonics: Discussion, A. A. P. G. Bull., v. 56, p. 375-384.
- Ehlig, P. L., Ehlert, K. W., Crowe, B. M., 1975, Offset of the upper Miocene Caliente and Mint Canyon Formations along the San Gabriel and San Andreas faults, in San Andreas fault in southern California: A guide to San Andreas fault from Mexico to Carrizo Plain, ed. Crowell, J. C., Cal. Div. of Mines and Geology, Spec. Rpt. 118, p. 83-92.
- Ensley, R. A. and Verosub, K. L., 1982, Biostratigraphy and magnetostratigraphy of southern Ridge Basin, central Transverse Ranges, California, in Geologic history of Ridge Basin, southern California, eds. Crowell, J. C. and Link, M. H., Pac. Sect. S. E. P. M. Guidebook, p. 13-24.
- Foster, J. H., 1980, Late Cenozoic tectonic evolution of Cajon Valley, Ph. D. Dissertation, Univ. of California, Riverside, CA, 242 p.
- Garfunkel, Z., 1974, Model for the late Cenozoic tectonic history of the Mojave Desert, California, and its relation to adjacent regions, Geol. Soc. of Amer. Bull., v. 85, p. 1931-1944.
- Gibson, R. C., 1971, Non-marine turbidites and the San Andreas fault, San Bernardino Mountains, California, in Geological excursions in southern California, ed., Elders, W. A., University of California Riverside, Campus Museum Contributions, #1, p. 167-181
- Harland, W. B., Cox, A. V., Llewellyn, P. G., Pickton, C. A. G., Smith, A. G., and Walters, R., 1982, A geologic time scale, Cambridge University Press, 131 p.

- Hill, M. L., 1971, A test of new global tectonics: Comparisons of north-east Pacific and California structures, *A. A. P. G., Bull.*, v. 55, p. 3-9.
- Hill, M. L. and Dibblee, T. W. Jr., 1953, San Andreas, Garlock, and Big Pine faults, California - A study of the character, history, and tectonic significance of their displacement, *Geol. Soc. Amer. Bull.*, v. 64, p. 443-458.
- Hill, R. I., 1984, Petrology and petrogenesis of batholithic rocks, San Jacinto Mountains, southern California, Ph. D. Dissertation, Caltech, Pasadena, CA, 660 p.
- Huffman, O. F., 1972, Lateral displacement of upper Miocene rocks and the Neogene history of offset along the San Andreas fault in central California, *Geol. Soc. Amer. Bull.*, v. 83, p. 2913-2946.
- Huffman, O. F., Turner, D. L., and Jack, R. N., 1973, Offset of late Oligocene - Early Miocene volcanic rocks along the San Andreas fault in central California, in *Proceedings of the conference on tectonic problems of the San Andreas fault system*, Stanford Univ. Pubs. Geol. Sci., v. 13, p. 368-373.
- Larson, R. L., Menard, H. W., and Smith, S. M., 1968, Gulf of California: a result of ocean floor spreading and transform faulting, *Science*, v. 73, p. 3361-3397.
- Link, M. H., 1982, Sedimentation, tectonics, and offset of Miocene - Pliocene Ridge Basin, California, in *Tectonics and sedimentation along faults of the San Andreas system*, ed. Andresen, D. W. and Rymer, M. J., Pac. Sec., S. E. P. M., p. 17-31.
- Matthews, V., 1973, Pinnacles - Neenach correlation: A restriction for models of the origin of the Transverse Ranges and the Big Bend in the

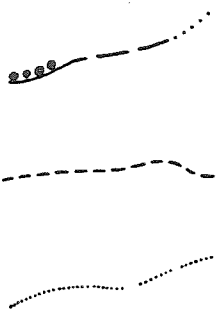
- San Andreas fault, Geol. Soc. Amer. Bull., v. 84, p. 683-688.
- Matti, J. C., in review, Distinctive megaporphyritic monzogranite offset 160 km by the San Andreas fault, southern California: A new constraint for palenospastic reconstructions, sub Geology 1985.
- Matti, J. C. and Morton, D. M., 1975, Geologic history of the San Timoteo badlands, southern California, Abstracts with Programs, Cordilleran Section, Geological Society of America, v. 7, p. 344.
- Meisling, K. E., 1984, Neotectonics of the North Frontal fault system of the San Bernardino Mountains: Cajon Pass to Lucerne Valley, California, Ph. D. Dissertation, Caltech, Pasadena, CA.
- Minster, J. B. and Jordan, T. H., 1984, Vector constraints on Quaternary deformation of the western United States east and west of the San Andreas fault, in Tectonics and sedimentation along the California margin, eds, Crough, J. K. and Bachman, S. B., Pac. Sect. S.E.P.M., v. 38, p. 1-16.
- Minster, J. B. and Jordan, T. H., 1978, Present-day plate motions, Jour. Geophys. Res., v. 83, p. 5331-5354.
- Morton, D. M., 1975, Synopsis of the geology of the eastern San Gabriel Mountains, southern California, in San Andreas fault in southern California: A guide to San Andreas fault from Mexico to Carrizo Plain, ed. Crowell, J. C., Cal. Div. Mines and Geology, Spec. Rpt. 118, p. 170-176.
- Morton, D. M. and Matti, J. C., 1979, Evidence for a vanished post-middle Miocene pre-late Pleistocene alluvial-fan complex in the northern Peris block, southern California, Abstracts with Programs, Cordilleran Section Geological Society of America, v. 11, p. 118.
- Noble, L. F., 1954, Geology of the Valyermo Quadrangle and vicinity,

- California, U. S. Geol. Surv. Quad. Map GQ-50.
- Powell, R. E., 1981, Geology of the crystalline basement complex, eastern Transverse Ranges, southern California: Constraints on regional tectonic interpretations, Ph. D. Dissertation, Caltech, 441 p.
- Ramirez, V. R., 1982, Hungry Valley Formation: Evidence for 220 km of post Miocene offset on the San Andreas fault, in Tectonics and sedimentation along the San Andreas system, eds. Andersen, D. W. and Rymer, M. J., Pac. Sect. S. E. P. M., p. 33-44.
- Reynolds, R. E., 1985, Tertiary small mammals in the Cajon Valley, San Bernardino County, California, in Geologic investigations along Interstate 15 - Cajon Pass to Manix Lake, California, ed., Reynolds, R. E., Field Trip Guide for the 60th meeting, western Assoc. Verte. Paleon., p. 49-58.
- Reynolds, R. E., 1984, Miocene faunas in the lower Crowder Formation, Cajon Pass, California: A preliminary discussion, in San Andreas fault Cajon Pass to Wrightwood, eds., Hester, R. L., and Hallinger, D. E., Pac. Sect. A. A. P. G., volume and guidebook 55, p. 17-21.
- Sadler, P. M., 1985, Provenance of the Santa Ana sandstone, San Bernardino Mountains, in Geologic investigations along Interstate 15 - Cajon Pass to Manix Lake, California, ed., Reynolds, R. E., Field Trip Guide for the 60th meeting, western Assoc. Verte. Paleon., preprint.
- Sadler, P. M., 1982, Provenance and structure of late Cenozoic sediments in the northeast San Bernardino Mountains, in Late Cenozoic stratigraphy and structure of the San Bernardino Mountains, eds. Sadler, P. M. and Kooser, M. A., in Geologic excursions in the Transverse Ranges, ed. Cooper, J. D., Cal. State Fullerton, California, p. 83-91.
- Sharp, R. V., 1981, Variable rates of late Quaternary strike slip on the

- San Jacinto fault zone, Southern California, *Jour. Geophys. Res.*, v. 86, p. 1754-1762.
- Silver, L. T., 1982, Evidence and a model for west-directed early-to-mid-Cenozoic basement overthrusting in southern California, *Abstracts with Programs, Geol. Soc. Amer.*, v. 14, p. 617.
- Stille, H., 1936, The present tectonic state of the earth, *A. A. P. G. Bull.*, v. 20, p. 849-880.
- Weldon, R. J., 1984, Implications of the age and distribution of late Cenozoic stratigraphy in Cajon Pass, southern California, in *San Andreas fault - Cajon Pass to Wrightwood*, eds. Hester, R. L. and Hallinger, D. E., *Pac. Sect., A. A. P. G., Guidebook 55*, p. 9-16.
- Weldon, R. J., Winston, D. S., Kirschvink, J. L., and Burbank, D. W., 1984, Magnetic stratigraphy of the Crowder Formation, Cajon Pass, southern California, *Abstracts with Programs, 97th Annual Meeting, Geological Society of America*, v. 16, p. 689.
- Woodburne, M. O. and Golz, D. J., 1972, Stratigraphy of the Punchbowl Formation, Cajon Valley, southern California, *Univ. Cal. Pubs. in Geol. Sci.*, v. 92, 73 p.
- Yeats, R. S., 1983, Large-scale Quaternary detachments in Ventura Basin, southern California, *Jour. Geophys. Res.*, v. 88, p. 569-583.

PLATES

LEGEND FOR PLATES 1 - 7



-- Depositional contact; solid where certain, dashed where inferred or uncertain and dotted where buried; contains circles for a distinct basal conglomerate.

-- Limit of present drainage.

-- Geomorphic contact, dashed where inferred or uncertain; designates the edge of a surface where it is not a geologic contact; where two surfaces meet it is the edge of the upper one (top of riser). Note that a geomorphic contact can cross a geologic contact where a geomorphic surface is developed across more than one geologic unit.



-- Fault, solid where certain, dashed where inferred and dotted where buried.



-- Fold hinge, with direction of plunge; arrows indicate syncline or anticline.

QUATERNARY UNITS

1982 A.D.

- Qal -- Current alluvium.
- Qhs -- Active swamp; underlain by sediments that span most of the Holocene.
- Qhf -- Fanglomerates; locally includes material deposited continuously since the Pleistocene.
- Qc -- Colluvium (where distinguished), commonly transitional into Qhf or Qoa.
- Qm -- Man-made fill (where distinguished).

QUATERNARY UNITS (Continued)

1938 A.D.	Qal-0	-- Alluvium deposited by the 1938 flood (where distinguished).
~ 200 B.P.	Qt-7	-- Youngest strath mapped.
275 - 1705 B.P.	Qoa-a (Qt-6)	-- Holocene alluvium; Qt6 is the surface formed by the top of the Qoa-a deposit.
5900 B.P.	Qt-5	-- Youngest strath recognized above the Qoa-a fill.
	Qt-4	-- Strath terrace, probably underlies Lost Lake.
8350 B.P.	Qt-3	-- Only Holocene strath widely recognized outside the Lost Lake area; Qt3 underlies most of Lost Swamp.
	Qt-2	-- Oldest strath between Qoa-a and Qoa-c.
12.4 to 14.8 ka	Qoa-c (Qt-1)	-- Latest Pleistocene alluvium; Qt1 is the surface of the deposit.
	Qls	-- Landslide.
53 - 57 ka	Qoa-d	-- Mid-Wisconsin alluvium.
~ 500 ka	Qoa-e	-- Old red alluvium; deeply weathered with, locally, several meters of brick red soil.
700 ka	Qoa-N	-- Noble's Older Alluvium; coarse, poorly sorted fanglomerates and fluvial gravels, mainly Pelona Schist debris from near Wrightwood.
1.3 to 1.0 my	Qs	-- Shoemaker Gravels; coarse, poorly sorted fanglomerates and fluvial gravels, contain a variety of distinctive clasts from the San Gabriel Mountains
1.6 to 1.3 my	Qh	-- Harold Formation; conglomeratic sandstone and siltstones, derived from the San Gabriel Mountains.

PRE-QUATERNARY UNITS

4.2 to 1.7 my	QTp	-- Phelan formation, pebbly sands, with locally coarse conglomerates, tuffs, lacustrine clays
17 to 9.5 my ago	Tc	-- Crowder Formation, undifferentiated, tan to white sandstones, conglomerates and siltstones. In Crowder Canyon the formation is divided into 5 members; members 1, 3, and 5 are arkosic fluvial sands and conglomerates; 2 and 4 are siltstones.
<u>></u> 18 to <u><</u> 13 my	Tp	-- Punchbowl Formation (Cajon beds) - buff to pink, continental arkosic sandstone and conglomerate. Locally subdivided into 6 members (after Woodburne and Golz, 1972).
Tertiary (?)	Tu	-- Tertiary unnamed unit, usually subdivided into Tur (red) and Tub (buff), immature arkosic sandstones and conglomerates, generally overlies a distinctive quartz monzonite; only occurs between the North and South Branches of the San Andreas fault.
Late Cretaceous to Eocene (?)	KTsf	-- San Francisquito Formation. Marine sand and siltstone overlying gn. Has a coarse basal conglomerate of mainly local clasts (indicated by small circles).
<u>></u> Mid Tertiary	Psb	-- Blue facies, Pelona Schist; low grade metasedimentary marine (?) rocks; only occurs southwest of the Punchbowl fault.
<u>></u> Mid Tertiary	Psg	-- Green facies, Pelona Schist; low to medium grade metavolcanic (?) rocks; only occurs between the Punchbowl and San Andreas faults.

- > Late Cretaceous gr -- Undifferentiated granitic rocks; includes porphyritic Permo-Triassic monzonites; Cretaceous tonalites to quartz monzonites.
- > Late Cretaceous gn -- Undifferentiated gneiss. Heterogeneous, generally tonalitic, foliated and locally banded rocks. Locally subdivided into gn-c, cataclastic gneiss, and gn-s, a distinctive red and green weathering gneiss under the San Francisquito Fm.
- > Late Cretaceous m -- Metasedimentary pendants; generally marbles, but locally quartzites, calc-silicates and garnet-mica schists.